Appendix 6: Modeling the Fate and Transport of Nutrients Using DSM2: Calibration/Validation Report

Prepared by:

Marianne Guerin

Resource Management Associates
1756 Picasso Ave, Suite G
Davis, CA 95618

Modeling the Fate and Transport of Nutrients Using DSM2: Calibration/Validation Report

December 2015

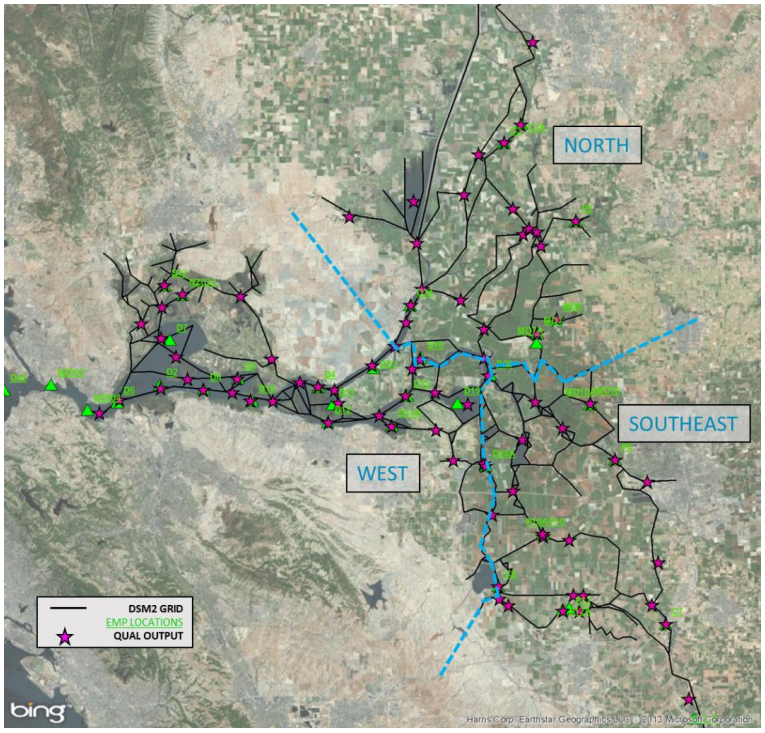

Prepared For:
San Francisco Estuary Institute
4911 Central Ave
Richmond, CA 94804
Representative: David Senn
Email:davids@sfei.org

Funded By
State of California
Department of Water Resources
Representative: Karen Gehrts
Email: Karen.Gehrts@water.ca.gov

Prepared By:
Resource Management Associates
1756 Picasso Ave, Suite G
Davis, CA 95618

Contact:
Dr. Marianne Guerin
530-564-7043

RMA Resource Management Associates

CONTENTS

FIGURES

TABLES

6 Chapter 6 – DSM2 Information

6.1 Calibrating the DSM2-QUAL Nutrient Model

6.1.1 Project Background

6.1.1.1 Objective

The main objective of this portion of the project was to recalibrate the water quality model DSM2-QUAL model for temperature and nutrients, extending the end previous model calibration period (1990 – 2008) to March 2012. Because of changes in Delta bathymetry implemented in the base hydrodynamic module, DSM2-HYDRO, the start of the simulation period was changed to January 2000. Once calibrated, the output of the model was supplied to Project PI's to use as supplementary information to nutrient measurement data with the goal of improving the understanding of nutrient dynamics in the Delta. QUAL volumetric model output, which is independent of the nutrient model calibration, was also supplied to project members.

6.1.1.2 Calibration Summary

QUAL's conceptual model for nutrient dynamics is a mixed model, with greater detail in some aspects of nutrient dynamics than in others. On the plus side, this results in a relatively simple nutrient model with the advantage that there is generally some data available for setting or estimating most boundary model conditions for nutrients and water temperature. On the negative side, there are processes that would have been valuable to include, such as more complete representation of sediment interactions or multiple avenues to depict primary production.

However, the ultimate determination of a successful application of the nutrient model to the Delta is data availability which determines the useful extent of model complexity. In other words, if there is no data with which to either check the models results or to develop parameters for specific reactions or processes, then that the inclusion of that reaction will generally not increase the accuracy of the overall model results and will generally decrease the predictive power of forecast model simulations.

Model calibration was assessed in several ways, ranging from time series plots comparing model results to data, to the calculation of several model statistics and histograms in a model residual analysis, to an assessment of Model Skill for each constituent with sufficient data. Residual statistics were calculated in a variety of ways depending both on water year type and for separate calibration and validation ranges. The most comprehensive set used All model years. There was not striking difference between the calibration and validations results for Wet and Dry water years.

Three statistics, NSE, PBIAS and RSR (discussed in Section 6.7.5) were used to assess Model Skill over the entire simulation time frame. Model Skill is loosely defined herein as a summary measure of the model capabilities to accurately simulate nutrient dynamics. Model Skill ranged from Very Good to Satisfactory over the model domain for the model constituents with sufficient calibration data.

Not surprisingly, those model constituents with the most data, Algae (from chlorophyll-a) and DO, had the best Model Skill ratings – ranging from Very Good to Good. There were a few locations that were modeled poorly for all constituents, and these locations tended to be in areas with less calibration data

in their vicinity, in areas with many agricultural influences, or that were further from the main inflow boundaries. Of the N-bearing constituents, NO_3-N had the best model skill, and there was an apparent trade-off between getting one or the other of these constituents calibrated accurately. One possible reason for the apparent trade-off was that NH_3-N had the largest source terms from wastewater treatment plants and the model parameterization was not flexible or detailed enough to satisfactorily calibrate for both of these constituents.

6.1.2 DSM2 – General Information

DSM2 is a set of one-dimensional (1-D) hydrodynamic and water quality simulation models for hydrodynamics, water quality and particle tracking used to represent conditions in the Sacramento-San Joaquin Delta. The model is frequently used to model impacts associated with projects in the Delta, such as changes in exports, diversions, or channel geometries associated with dredging in Delta channels. It is frequently considered the official Delta water quality model, and as such it has been used extensively to model hydrodynamics and salinity as well as dissolved organic carbon (DOC). Both salinity and DOC are modeled as conservative constituents in QUAL. The capability to simulate nutrient dynamics and primary production in QUAL was developed by Rajbhandari (1995a, 1995b) – nutrients are modeled as non-conservative constituents. The formulation of the nutrient model equations is covered in Section 6.3.2.

The simplification of the Delta to a one-dimensional (1-D) model domain means that DSM2 can simulate the entire Delta region rapidly in comparison with many higher dimensional models. Although many channels in the Delta are modeled well in 1-D, the loss of spatial detail in areas that are clearly multi-dimensional limit DSM2's accuracy in those areas.

DSM2 contains three separate modules: a hydrodynamics module HYDRO; a water quality module QUAL; and, a particle tracking module PTM. HYDRO was developed from the USGS FOURPT model (USGS, 2008). DWR adapted the model to the Delta, accounting for such features as operable gates, open water areas, and export pumps. The water quality module, QUAL, is based on the Branched Lagrangian Transport Model (Jobson, 1997), also developed by the USGS. QUAL uses the hydrodynamics simulated in HYDRO as the basis for its transport calculations. The third module in the DSM2 suite is PTM, which simulates the fate and transport of neutrally buoyant particles. PTM also uses hydrodynamic results from HYDRO to track the fate of particles released at user-defined points in space and in time.

HYDRO, QUAL and PTM are maintained and upgraded regularly by the Delta Modeling Section in the Department of Water Resources (DWR-DMS). The version of the DSM2 model suite used in the current project is V.8.1.2. HYDRO was recalibrated in 2009[1], and this project accepts the current calibration of the hydrodynamics as sufficient for the purposes of this project. Additional changes to HYDRO and QUAL since 2009 are discussed at the DWR-DMS website[2] - all of those changes current as of this report are implemented in V.8.1.2 for HYDRO and V.8.1.3 for QUAL.

Detailed descriptions of the mathematical formulation implemented in the hydrodynamic module, DSM2-HYDRO and for salinity in the water quality module, DSM2-QUAL, the data required for

[1] See: http://baydeltaoffice.water.ca.gov/modeling/deltamodeling/DSM2UsersGroup/DSM2_Recalibration_102709.pdf
[2] http://baydeltaoffice.water.ca.gov/modeling/deltamodeling/models/dsm2/dsm2.cfm

simulation, calibration of HYDRO and QUAL, and past applications of the DSM2 Historical model are documented in a series of reports available at:

http://baydeltaoffice.water.ca.gov/modeling/deltamodeling/annualreports.cfm.

6.1.2.1 Previous DSM2-QUAL nutrient model calibrations

The nutrient model in QUAL was initially calibrated for DO on the San Joaquin River, approximately between Vernalis and Prisoner's Point for the period 1996 – 2000 (Rajbhandari, 2001). The most extensive calibration of the DSM2-QUAL nutrient model, Version 8.0.4, for all model constituents is documented in (Guerin, 2011) in detail – most of that detail will only be referenced herein and only essential or new information are included in this document. The DSM2-QUAL nutrient model formulation and numerical solution has since been revised several times since DSM2 Version 8.0.4 – those changes are incorporated in the current Version 8.1.3 of QUAL. As a consequence of these revisions, the QUAL nutrient model has recalibrated several times after the initial documentation in (Guerin, 2011) was written.

6.1.2.2 Previous DSM2-QUAL nutrient simulations and analyses

Previous uses of QUAL to simulate nutrient dynamics in the Delta focused on dissolved oxygen (DO). Rajbhandari (2000, 2001, 2003, 2004, and 2005) used QUAL to model DO dynamics on the San Joaquin River, addressing concerns about low DO in the vicinity of Stockton. Subsequently, the application and area of calibration were extended to the San Joaquin Deep Water Ship Channel. Another application focusing on DO extended model development to a wider region of the Delta to support technical studies for the In-Delta Storage Project Feasibility Study - this model study assessed the potential impact of the project on temperature and DO levels using CALSIM II (Rajbhandari, 2004) output for the hydrological conditions in 16-year hypothetical scenarios (1975 – 1991). The latter type of study is an example of a Planning Study in which DSM2 is used to quantify the effects that a modification in the Delta water regime may have on hydrodynamics and water quality.

In addition, the QUAL nutrient model was used in Bay-Delta Conservation Plan (BDCP) analyses. The documents written for the BDCP are not available as they are subject to non-disclosure agreements.

6.2 DSM2 Model Configuration

The implementation of the DSM2 modules HYDRO and QUAL discussed in this report extends the standard configuration of the DSM2 "Historical Model", which simulates historical conditions in the Delta from 2000 – 3/2012, by including effluent flows and constituent concentrations from the wastewater treatment plants (WWTPs) with outfalls within DSM2's model domain in the Delta. Although the volume of these effluent inflows is small and variable in comparison with other inflows to the Delta, they are important sources of the nutrients modeled in QUAL. In addition, the Jones Tract levee breach flows and nutrient transport, June – December 2004, are included as boundary conditions (Swift et al., 2009). The nutrient loads into and out of the Delta of this levee breach are small when considering the entire model domain. In addition, monthly-averaged, annually-repeating time series of DICU inflow nutrient model concentrations (Modeling Support Branch, 1995) have been implemented in favor of the previous constant values.

6.2.1 Model Grid

The DSM2 model grid is shown in Figure 6-1. The grid consists of one-dimensional channels, indicated by red lines, linked by nodes, indicated by black symbols, and open water areas whose approximate locations are indicated by blue numbers. Open water areas are modeled as zero-dimensional well-mixed reservoirs of water.

With the inclusion of the flooded Liberty Island in Version 8 of DSM2, HYDRO underwent a "Mini-recalibration"[3] (Chilmakuri, 2010). The bathymetry of the upstream section of the Sacramento River was included as a grid extension and the open water area at Liberty Island was included as a reservoir (see Figure 6-2).

6.2.2 Numerical Solution Parameters

The user can specify the computational time step of the solution algorithms used in HYDRO and QUAL. The standard time step for HYDRO and QUAL simulations is 15 minutes – this was the computational step used in the nutrient model simulations discussed in this report.

6.2.3 Model Boundaries

6.2.3.1 Flow and Stage Boundaries

Boundaries that define the movement of water into and out of the Delta consist of inflow boundaries, outflow boundaries and a stage boundary set at Martinez (Figure 6-3). Exports and diversions remove water from the model – water also flows out of the model at its downstream stage boundary at Martinez. In addition, there are structures in the model, such as gates and weirs, that are operated to control flow, stage or the transport of salinity that simulate the operation of these physical structures in the Delta. All of the standard DSM2 Historical model boundary conditions for flow and salinity were used in the application discussed in this report as developed by DWR-DMS, with the exception of flows at the Yolo inflow boundary.

In Figure 6-3 the main inflow boundaries are denoted by blue stars. These boundaries are found at the each of the major rivers (Sacramento, San Joaquin, Calaveras, Mokelumne and Cosumnes), and at the Yolo Bypass and the Lisbon Toe Drain (in the Yolo region). The Yolo Bypass only has inflow during periods of high Sacramento River inflow which can occur in the late fall through early spring. Flows at the Lisbon Toe Drain near Liberty Island on the north western edge of the Delta were added when available in the modeled time frame.

Figure 6-3 also shows Delta export locations, denoted by red stars. The greatest (combined) volume of export occurs at the State Water Project (SWP) and the federal Central Valley Project (CVP). Contra Costa Water District (CCWD) maintains three export/diversion locations, at Rock Slough, in Old River, and in Victoria Canal. Figure 6-3 shows the location of effluent inflow boundaries discussed in this report.

Information on the main boundary conditions for flow and stage is covered in Section6.12.3.

[3] http://baydeltaoffice.water.ca.gov/modeling/deltamodeling/DSM2UsersGroup/DSM2_Recalibration_102709.pdf

The effects of evaporation, precipitation, and channel depletions and additions ascribed to agricultural influences are modeled using the Delta Island Consumptive Use (DICU) model[4]. This model is used to set boundary conditions at 258 locations throughout the Delta. DICU flow boundary conditions vary monthly (DWR 1995a, 1995b.). The uncertainty in the estimates of DICU inflow, outflow and constituent concentrations is unknown, but can be high. During periods of low inflow, volumes ascribed to DICU boundaries may dominate model results at some locations.

6.2.3.2 WWTP Boundary Flows

Figure 6-4 identifies the approximate location of the effluent inflow boundaries in the DSM2 model domain. At these boundaries, effluent inflow rates were identified from data or from a combination of data and publically available information sources.

6.2.4 Transport Model Boundaries

6.2.4.1 Transport Model Boundary Conditions – General Information

Each flow boundary type, including river, stage, DICU and effluent boundaries, is also a boundary for transported constituents. There are eleven equations in the transport model, nine of which are referred to as "nutrient model constituents" in this report, plus one equation for salinity and one equation for water temperature. Water temperature plays an important role in nutrient dynamics but (clearly) has no mass, while each of the other ten equations in the model represents a constituent with mass. Salinity is important in modeling dissolved oxygen saturation, as an increase in salinity can decrease DO saturation. Salinity generally only plays an important role near the Martinez boundary but otherwise does not significantly influence nutrient dynamics in the model domain. Salinity boundary conditions at the main model boundaries and DCU inflows were accepted as defined by DWR-DMS. For effluent boundaries, salinity concentrations were other derived from data or developed based on web-accessible data.

Time series plots for the main inflow and outflow boundaries are documented in Section 6.12.3.

6.2.4.2 Water Temperature Boundary Conditions

The formulation used for the heat transport equation requires data for barometric pressure, air temperature, wet bulb temperature, wind speed and cloud cover. Meteorological conditions are used in modeling the exchange of heat at the air-water interface. Modeled water temperature plays a role in the rate of each constituent reaction (except salinity). Atmospheric pressure is used in modeling the saturation of dissolved oxygen in water, along with other conditions such as water temperature, salinity and reaeration. QUAL can be run to simulate water temperature alone, as water temperature is independent of the other constituents in the nutrient model. The current model formulation only allows for a single meteorological region for the entire model domain. As discussed in Section 6.6, this has proved to be a disadvantage in the simulation of modeled water temperature in DSM2.

Meteorological boundary conditions were extended through March 2012. Wet bulb temperature was not available directly, so instead was calculated using relative humidity and air temperature data (Stull, 2011).

[4] http://www.iep.ca.gov/dsm2pwt/reports/DSM2FinalReport_v07-19-02.pdf, http://baydeltaoffice.water.ca.gov/modeling/deltamodeling/models/dicu/DICU_Dec2000.pdf

6.2.4.3 Nutrient Boundary Conditions

Detailed information on nutrient concentrations and concentration time series plots for each model boundary is too extensive to be covered in the body of this report – instead, readers should consult the DSM2 input files as documentation. The Yolo Bypass/Toe Drain model boundary had no data available to set it's boundary condition, and the data at the Mokelumne and Cosumnes Rivers was limited to grab sample measurements for a couple of years. There was only very limited data to use for setting the Sacramento River model boundary – instead boundary conditions at this boundary were set using data from downstream locations, sometimes shifted in time and at other times multiplied by a factor in order to match the concentrations recorded at the downstream location.

Table 6-1 Constant concentration nutrients at the main model boundaries.

Location	Nutrient	Constant Value (mg/L)
Calaveras	NO_2	0.005
	DO	7.0
	CBOD	1.5
	EC	125
Cosumnes	NO_2	0.005
	DO	9.0
	CBOD	1.5
	EC	125
Mokelumne	NO_2	0.004
	DO	9.0
	CBOD	1.1
	EC	125
Martinez	Organic-P	0.01
	CBOD	2.8
	NO_2	0.008
Sacramento/Freeport	NO_2	0.004
	CBOD	1.2
San Joaquin/Vernalis	NO_2	0.15
	CBOD	2.8
Yolo Bypass/Toe Drain	Organic-N	0.85
	Organic-P	0.35
	CBOD	1.5
	NH_3	0.04
	NO_2	0.004
	NO_3	0.08
	PO_4	0.2
	DO	9.0
	ALGAE	0.2

6.2.5 Volumetric Model Set-up

QUAL boundary conditions for the volumetric simulation are set by setting the inflow concentration at each inflow boundary at 100 units – this includes river inflow locations, DICU flow sources as well as effluent inflow sources. The initial concentration for the model domain is set by the user – additional detail is described in (Anderson, 2002). Generally, it takes several months to two years for the model domain to reach a good initial condition – the amount of time depends on the location in the model domain and the inflow conditions during the run-up period. Locations that receive higher rates of flow, particularly from the Sacramento River, generally takes one to two month to complete the run-up period, while low flow regions, particularly near dead end channels, can take much longer.

Volumetric model output at any location in the model domain can be defined for any or all of the flow input sources. When the model set-up is successful the sum of the volumes from all sources at any output point in the model domain should equal 100 units. Model output was specified on a daily average basis at numerous locations in the model domain.

Note that these are hypothetical model volumes – they do not contain information on the actual flow at any location. So, the individual source volumes at a given point in space can theoretically be equal under very high or very low total inflow conditions.

To reduce the number of individual output time series, some inflow locations were combined at be named as a single source. The Mokelumne and Cosumnes River inflows were combined, along with individual WWTP plants along the San Joaquin River, in the West region, and in the South region.

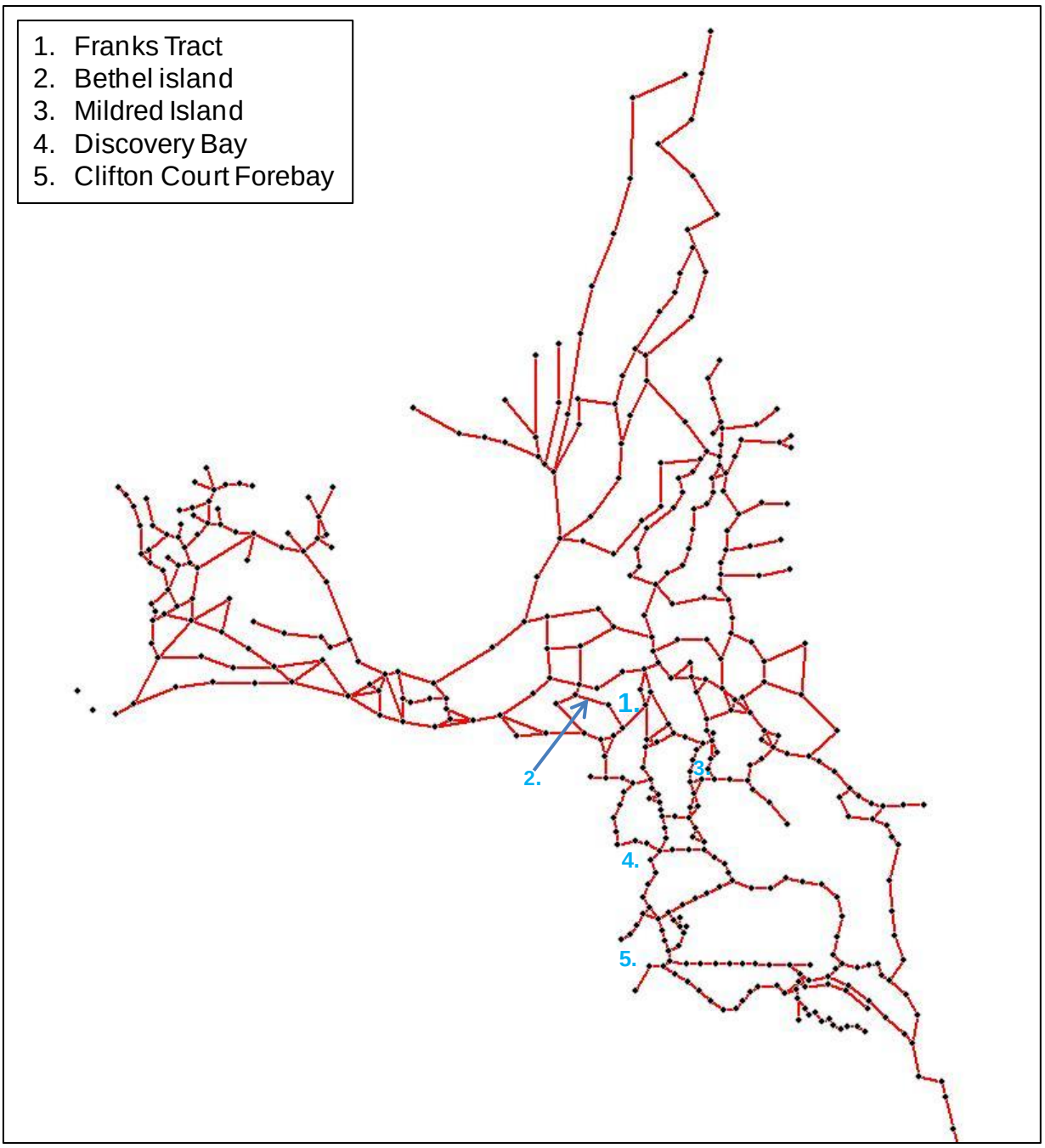

Figure 6-1 Channels (red), reservoirs (blue numbers), and nodes (black) in the DSM2 model grid.

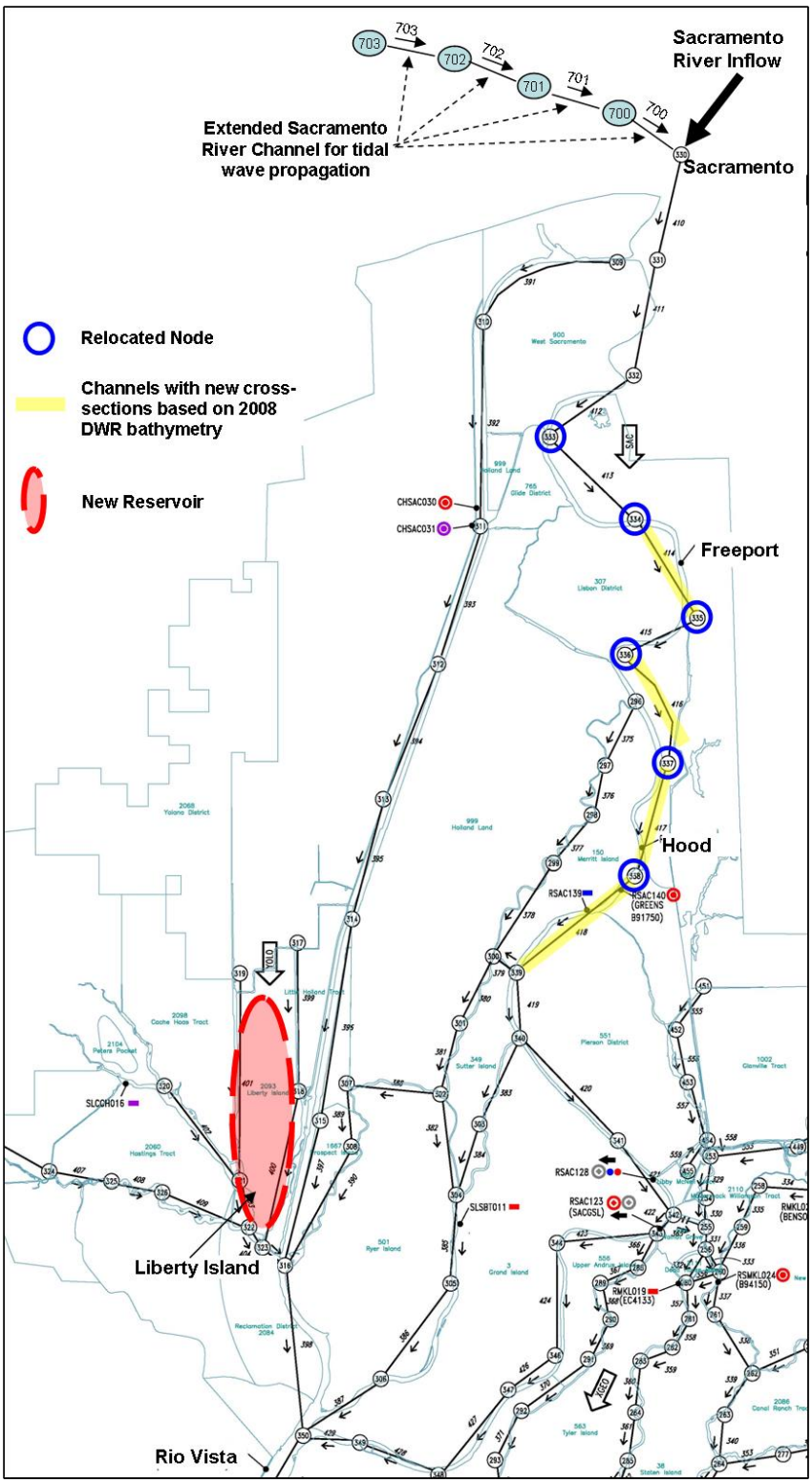

Figure 6-2 Changes implemented in the DSM2 Version 8 model grid include the new Liberty Island "reservoir" location (red oval), and changes to the grid and nodes along the upstream portion of the Sacramento River (blue circles).

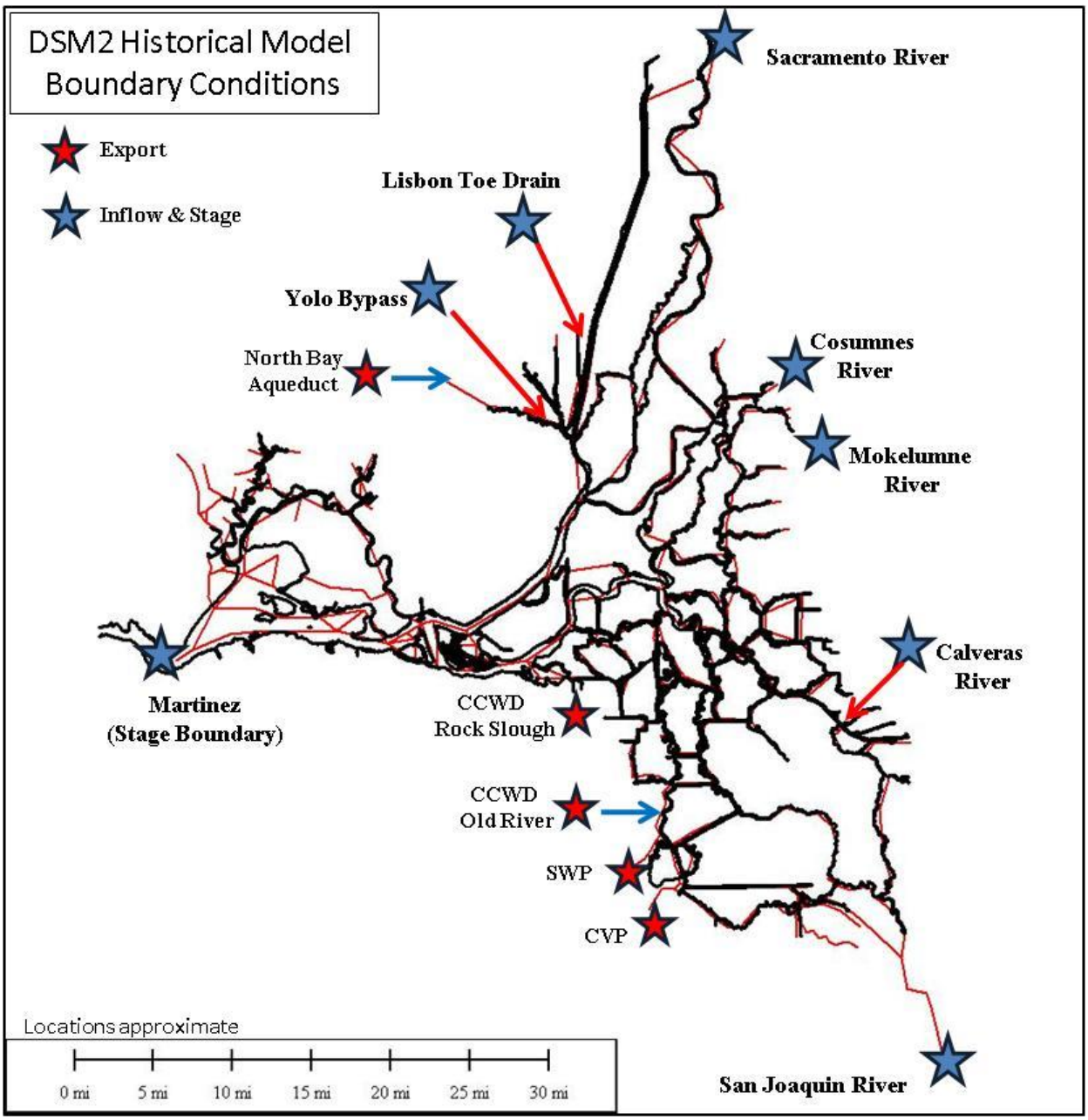

Figure 6-3 Approximate location of the model inflow boundaries and the stage boundary is at Martinez (blue stars). Export locations are indicated by red stars.

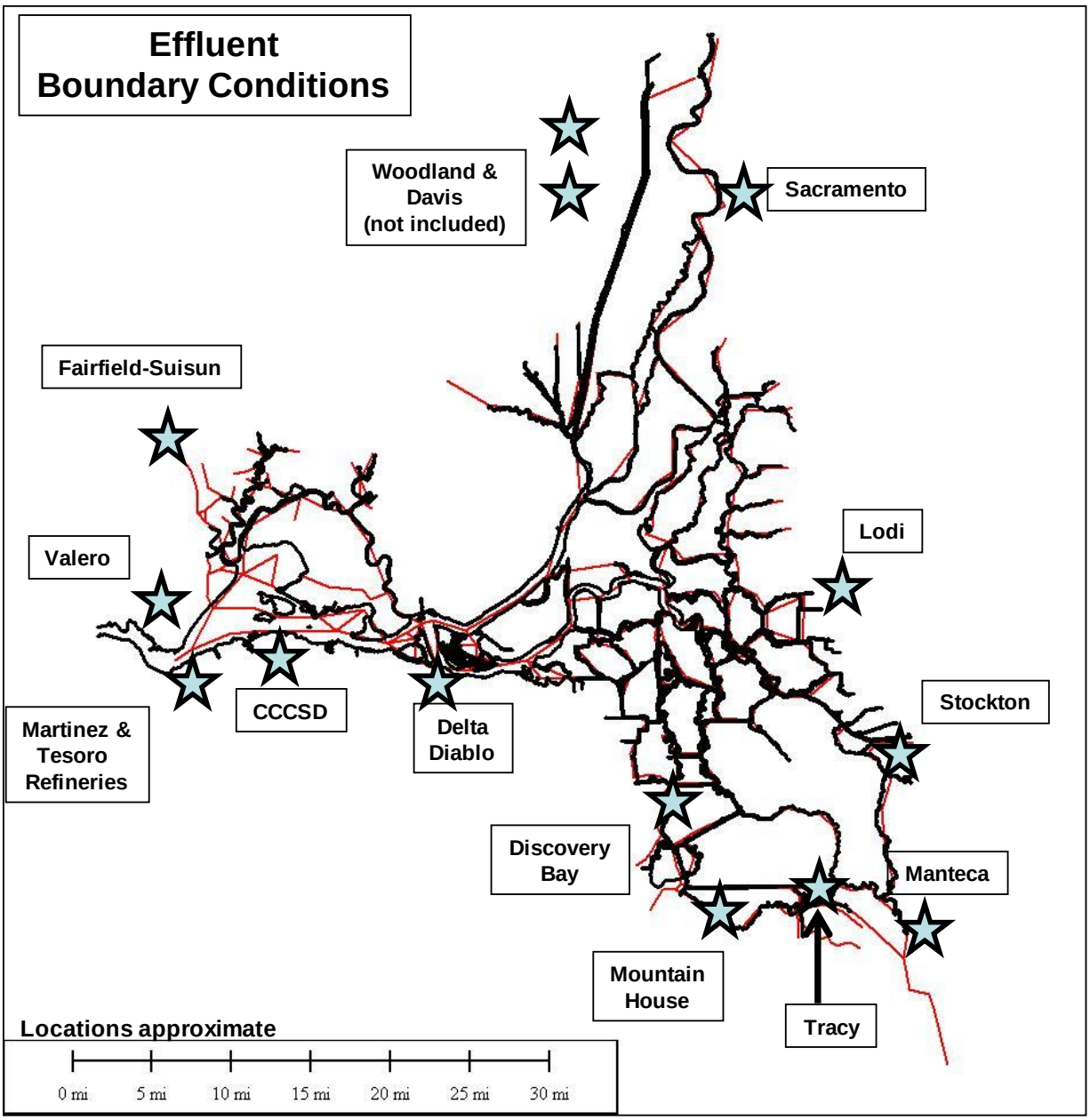

Figure 6-4 Approximate locations of effluent boundary conditions for waste water treatment plants considered in this report.

6.3 QUAL's Model for Nutrient Dynamics

6.3.1 QUAL Conceptual Background

Figure 6-5 is a conceptualization of the interactions between the main constituents used to model nutrient dynamics in the QUAL mass transport model - this figure is an adaptation of figures shown in (Rajbhandari, 2003). Each box (or oval) in the blue region (water) symbolizes one of the nine equations for non-conservative constituents in the transport model. There are equations for simulating the transport and reaction of dissolved oxygen (DO), nitrate (NO_3), nitrite (NO_2), ammonia (NH_3), organic-N, carbonaceous biochemical oxygen demand (CBOD), orthophosphate (PO_4, dissolved-P in the Figure), organic-P, and algae. Chlorophyll a (chl-a) measurements are used to calculate the biomass of algae in the model. Salinity is modeled as a conservative constituent - it is not included in Figure 6-5.

Arrows in Figure 6-5 indicate a relationship modeled as a temperature-dependent reaction rate between two variables for adding mass into or removing mass out of the model calculation for a given constituent. Water temperature influences the dynamics of the constituent interactions as a factor in the rate of reactions - an increase in water temperature results in a change, generally an increase, in reaction rates. Conversely, modeled DO saturation decreases with increased temperature. The reactions themselves do not influence the temperature of the water in QUAL.

Although each of the constituents occurs in an ionized form in aqueous solutions, charges on the constituents are not used in the model – they are used in this report only where specifically indicated. In reality, each modeled nutrient constituent occurs as a suite of chemical sub-species in solution with variable charge and potentially associated with many other aqueous species. As this level of interaction is not explicitly accounted for QUAL, no single charge can be legitimately assigned. This brings up the need for a distinction between term "ammonia" and the concentrations of each of the chemical species NH_3 and NH_4^+. NH_3 occurs naturally as a gas that is dissolved in the aqueous phase, but the gas is also ionized to NH_4^+, *i.e.* ammonium, in a pH-dependent reaction in solution. At neutral pH (pH = 7.0), the majority of the "ammonia" in solution occurs in its ionized form as NH_4^+. Because QUAL does not explicitly model pH and cannot distinguish between the unionized and ionized forms, the term "ammonia" is used in this report to indicate the total concentration[5] of $[NH_3] + [NH_4^+]$. A simplifying assumption in interpreting model results is that the majority of the "ammonia" concentration reported in calculations is occurring in the ionized "ammonium" form. Measured data collected for setting boundary conditions and as calibration/validation data is generally reported by the collecting agency as "ammonia", and is actually reporting the total $[NH_3] + [NH_4^+]$.

The equation expressing the conceptual model for each constituent is discussed in greater detail in the following sections.

6.3.2 Nutrient Model formulation

The ten equations that comprise the nine non-conservative constituents in the nutrient model plus temperature are discussed individually below. The equation for salinity, the conservative constituent, is

[5] Unlike the convention in aqueous chemistry, square brackets are used to symbolize the concentration of an aqueous species (not the activity) in solution. The units of concentration are understood to be the units in the model, mg/L, unless specifically stated otherwise.

not discussed. Each mass balance equation represents the mass per unit volume of water. The transport of the constituent due to advection is not shown due to the assumption of a Lagrangian reference frame that moves through the domain at the mean velocity of the water - additional information can be found in (Rajbhandari, 1995a and 1995b).

Table 6-2 defines the model variables, while Table 6-3 and Table 6-4 detail the adjustable parameters that are used in the equations. Parameters that appear in the equations that are not listed in the Tables are defined at their initial appearance in the text.

There are sixteen temperature coefficients for reaction rates shown in Table 6-4. Temperature coefficients are defined by the relationships $k(T) = k(20)\Theta^{(T-20)}$, where k(T) is the reaction rate day^{-1} at temperature T in °C and Θ is the user-defined temperature coefficient for the reaction shown in the Table. The values used for these coefficients were set at standard literature values, although there was minor variation in the values during calibration

Table 6-2 Definitions for variables appearing in equations 1 – 10.

Variable Symbol	Modeled Constituent	Measurement Unit
O	DO	mg/L
L	CBOD	mg/L
NH_3	Total ammonia as N	mg/L
NO_2	Nitrite as N	mg/L
NO_3	Nitrate as N	mg/L
A	Phytoplankton biomass	mg/L[1]
N-org	Organic nitrogen as N	mg/L
P-org	Organic phosphorus as P	mg/L
PO_4	Orthophosphate as P	mg/L
T	Water Temperature	° C

1. This is the dry weight as estimated from Chl-a concentration.

6.3.2.1 Temperature

The formulation for the transport of temperature in the model, equation (1) was adapted from the QUAL2E model (Brown and Barnwell, 1987), with several changes documented in (Rajbhandari, 1995b). Water temperature influences the interactions between the modeled constituents as discussed in above, but is independent of the other constituents.

The net transfer of energy, Q_n, across the air-water interface is formulated as a function of net short wave radiation flux, net long wave atmospheric radiation flux, water surface back radiation flux, evaporative heat flux and sensible heat flux. The expressions accounting for this energy transfer are functions of the meteorological inputs (not shown). In equation (1), p is the density of water, c is the specific heat of water and d is the hydraulic depth of the water. E_x is the longitudinal dispersion coefficient.

$$\frac{\partial[T]}{\partial t} = \frac{\partial}{\partial \xi}\left[E_x \frac{\partial T}{\partial \xi}\right] + Q_n \Big/ pcd \qquad (1)$$

Diffusion **Energy**

6.3.2.2 *Dissolved Oxygen (DO)*

DO concentration is a critical indicator of the general health of an aquatic ecosystem (Rajbhandari, 1995a; Cole and Wells, 2008). Equation (2) specifies the rate of change in DO concentration due to dispersion, sources (reaeration and photosynthesis), and sinks (CBOD, oxidation of NH_3 and NO_2, algal respiration and benthic demand). The expressions used to model DO saturation and reaeration are discussed in detail in (Rajbhandari, 1995a).

Benthic oxygen demand represents a generic expression encompassing several processes in the sediment that remove oxygen from the water column, including the decay of organic matter and utilization of dissolved oxygen by benthic species (such as clams) and macrophytes.

$$\frac{\partial[O]}{\partial t} = \frac{\partial}{\partial \xi}\left[E_x \frac{\partial[O]}{\partial \xi}\right] - (k_1 + k_3) L + k_2 (O_s - [O]) - \alpha_5 k_n [NH_3] - \alpha_6 k_{ni} [NO_2] + \alpha_3 \mu [A] - \alpha_4 \rho [A] - {K_4}/{d}$$

Diffusion **CBOD** **Reaeration** **Ammonia ox.** **Nitrite ox.** **Photosyn.** **Respir.** **Benthic** (2)

6.3.2.3 *Carbonaceous Biochemical Oxygen Demand (CBOD)*

Carbonaceous biochemical oxygen demand (CBOD) refers to the potential for microorganisms to consume oxygen as they utilize organic-carbon substrates. A related measurement is nitrogenous BOD (NBOD) – this refers to the oxygen consumed by nitrifying bacteria as they consume organic and inorganic materials that contain a reduced form of nitrogen. Collectively, CBOD+NBOD is called BOD, and tests that measure any of the three forms occur over a number of days, typically five or twenty days (Brake, 1998). For the purposes of this project, we utilized $CBOD_5$, a five-day test for CBOD when available. Further detail is found in (Guerin, 2011).

Equation (3) accounts for the sinks and sources of CBOD due to oxidation and settling, and the contribution to CBOD from the death of algae, respectively.

$$\frac{\partial[L]}{\partial t} = \frac{\partial}{\partial \xi}\left[E_x \frac{\partial[L]}{\partial \xi}\right] - (k_1 + k_3) L + \sigma_7 [A]$$

Diffusion **Oxidize/Settle** **Algal death** (3)

6.3.2.4 Algae (Phytoplankton)

Equation (4) accounts for the biomass of algae in the model. Algae utilize chlorophyll pigments to convert solar radiation to energy, and chl-a (a particular form of pigment) measurements are typically used as an indicator of algal biomass. A conversion factor is used to convert chl-a concentrations to algal biomass. For this project, we used a conversion factor of 67 g algae/mg chl-a (dry weight of algae) (Clesceri et al., 1999). Although there are many different algal species (Cole and Wells, 2008) with variable characteristics including growth rates, preferred nutrient sources, and levels of chlorophyll per unit of mass, in QUAL a single equation is used to estimate a generic algal species.

$$\frac{\partial [A]}{\partial t} = \frac{\partial}{\partial \xi}\left[E_x \frac{\partial [A]}{\partial \xi} \right] + (\mu - \rho)[A] - \sigma_1 [A]/d - \sigma_6 [A] \quad (4)$$

Diffusion Algae Grow Settle Die

Algal growth is a function of the difference between the respiration rate, ρ, and the growth rate, μ, of this generic algal population. The growth in algal biomass is assumed to be limited by availability of light, F_L, inorganic nitrogen, *N,* as the sum of the concentrations of NH_3 and NO_3, and inorganic phosphorus, *P*, as expressed in the following equation (4a):

$$\mu = \mu_{MAX}\ F_L\ Min\left(\frac{N}{K_N + N}, \frac{P}{K_P + P} \right) \quad (4a)$$

where K_N and K_P are the half-saturation constants of nitrogen and phosphorus, respectively. F_L is further expressed as a Monod equation as a function of light intensity at a given depth (Rajbhandari, 1995a). When algae die, their decomposition contributes to CBOD. Algae settle out from the water column and themass is lost from the system.

The generic algal biomass is assumed to be composed of a ratio of N:P concentrations. Although this ratio is known to vary between different algal species, only a single generic algal species is modeled and the parameters defining this ratio are set globally in the model domain.

6.3.2.5 Organic nitrogen (Org-N)

Organic nitrogen dynamics (as N) are represented by equation (5):

$$\frac{\partial [N-org]}{\partial t} = \frac{\partial}{\partial \xi}\left[E_x \frac{\partial [N-org]}{\partial \xi} \right] + \alpha_1 \rho [A] - k_{N-org}[N-org] - \sigma_4 [N-org] \quad (5)$$

Diffusion Algae Decay to NH3 Settle

The only source of nitrogen due to nutrient dynamics occurs as a result of algal respiration as a fraction of the algal biomass assumed to be nitrogen. Org-N is lost from the system as it decays and settles.

When organic-N measurements are unavailable, Total Kjeldahl Nitrogen (TKN) can be used to estimate organic-N if ammonia measurements are also available, as TKN = organic-N + ammonia.

6.3.2.6 Ammonia (NH_3)

Ammonia (as N) dynamics are represented by equation (6):

$$\frac{\partial[NH_3]}{\partial t} = \frac{\partial}{\partial \xi}\left[E_x \frac{\partial[NH_3]}{\partial \xi}\right] - f\,\alpha_1 \mu[A] + k_{N-org}[N-org] - k_n[NH_3] + {}^{\sigma_3}\!/_{d} \quad (6)$$

Diffusion **Algae** **Org – N Decay** **NH3 Decay** **Sediment Source**

Although ammonia concentration is represented in this equation by the formula NH_3, in fact the concentration of ammonia is assumed implicitly to be the total of aqueous NH_3 (g) and NH_4^+, as discussed previously. NH_3 is a nutrient source for algae as is NO_3, and the preferential consumption of these two sources of nitrogen is given by a preference factor, $0.0 \le p \le 1.0$, in the following expression:

$$f = \frac{p[NH_3]}{p[NH_3] + (1-p)[NO_3]} \quad (6a)$$

where the square brackets indicate modeled concentration. For example, a preference factor set at p=0.5 indicates no algal preference for either nutrient, so at equal concentrations equal amounts of NH_3 and NO_3 would be consumed for algal growth.

6.3.2.7 Nitrite (NO_2)

Sources and sinks of NO_2 (as N) are shown in equation (7). In equation (6), NH_3 is seen to decay at a set rate – in equation 7 we see that that the NH_3 has decayed into NO_2, and that NO_2 decays to NO_3:

$$\frac{\partial[NO_2]}{\partial t} = \frac{\partial}{\partial \xi}\left[E_x \frac{\partial[NO_2]}{\partial \xi}\right] - k_{ni}[NO_2] + k_n[NH_3] \quad (7)$$

Diffusion **Decay to NO3** **NH3 Decay**

6.3.2.8 Nitrate (NO_3)

Nitrate dynamics are given by equation (8). Here we see that NO_2 has decayed into NO_3 (as N):

$$\frac{\partial[NO_3]}{\partial t} = \frac{\partial}{\partial \xi}\left[E_x \frac{\partial[NO_3]}{\partial \xi}\right] - (1-f)\alpha_1 \mu[A] + k_{ni}[NO_2] \quad (8)$$

Difusion **Algae** **NO2 Decay**

Nitrate is consumed by algae, where the rate is assumed to be governed by the preference of algae for NH_3 or NO_3 (see equation (6a)).

6.3.2.9 Organic Phosphorus (Org-P)

Equation (9) shows the sources (algal biomass) and sinks (decay and settling) for org-P (as P) in the nutrient dynamics:

$$\frac{\partial[P-org]}{\partial t}=\frac{\partial}{\partial \xi}\left[E_x\frac{\partial[P-org]}{\partial \xi}\right]+\alpha_2\,\rho[A]-k_{P-org}[P-org]-\sigma_5[P-org]$$

Diffuson Algae Decay Settling (9)

6.3.2.10 Dissolved Phosphorus (PO_4)

The final equation. (10), represents the sources (decay of organic-P, benthic source) and sinks (algal growth) of inorganic phosphorus, which is assumed to the concentration of ortho-phosphate (as P), PO_4:

$$\frac{\partial[PO_4]}{\partial t}=\frac{\partial}{\partial \xi}\left[E_x\frac{\partial[PO_4]}{\partial \xi}\right]-\alpha_2\,\mu[A]+k_{P-org}[PO_4]+{}^{\sigma_2}\!/_{d}$$

Diffusion Algae grow Org – P Decay Benthic (10)

6.3.3 Reaction Rates and Parameters

There are 15 Regional Reaction Rate parameters (Table 6-3 and Table 6-4) that can that can be varied by channel in the grid as well as in each open water body (DSM2 reservoir). There are 31 Global Reaction Parameters that are set for the entire model domain, sixteen of which are temperature coefficients for reaction rates (Table 6-4). The values listed in the "Calibrated Values" column give the ranges set in the model. The values for regionally-set rate parameters may differ among channels within a region (regions are defined in Section 6.4.2) or in a reservoir within a region. The parameter values are generally consistent with the ranges used by the Department of Water Resources in the applications of DSM2-QUAL for modeling DO in the Delta (Rajbhandari, 2001; Rajbhandari, 2003; Rajbhandari, 2004). The parameter specifying SOD was utilized as a fitting parameter to calibrate DO in the original DO simulations (Rajbhandari, 2001).

Many of the parameter ranges shown in these Tables were obtained from Cole and Wells (2008), the CE-QUAL-W2 manual. CE-QUAL-W2 is routinely applied by the U.S. Army Corps of Engineers (USACE), and was developed under the auspices of the USACE (Cole, 1994).

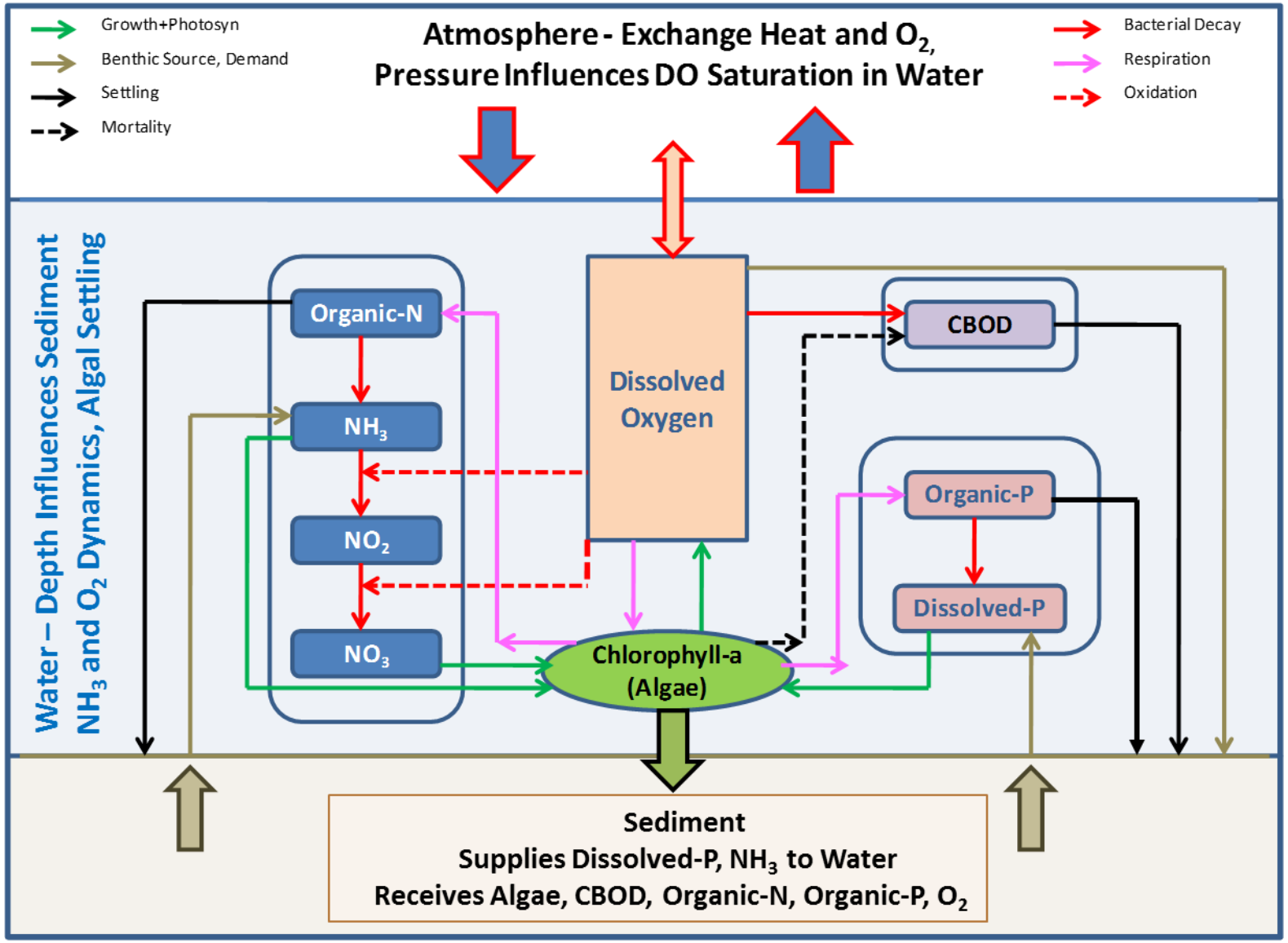

Figure 6-5 The figure depicts interactions among the main constituents, and external influences (figure adapted from original DWR references). Water temperature) influences reaction rates, denoted by arrows.

Table 6-3 Parameters used in the model. Some parameters do not appear explicitly in the equations as discussed in this report.

Symbols	Description	Lit. Range Min/Max	Calibrated Value	Units	Source
Global Reaction Parameters					
α_5	Amount of oxygen consumed in conversion of ammonia to nitrite	3.0-4.0	3.0	-	Rajbhandari (1995)
α_6	Amount of oxygen consumed in conversion of nitrite to nitrate	1.0-1.14	1.14	-	Rajbhandari (1995)
p	Preference factor for ammonia nitrogen	0-1.0	0.5	-	Rajbhandari (1995)
α_7	Conversion factor Chlorophyll-a *vs.* algal biomass	10-100	14.9	µg-Chl-a mg^{-1}	Rajbhandari (1995)
α_1	Fraction of algal biomass, which is nitrogen	0.07-0.09 0.02-0.11	0.09	-	Rajbhandari (1995) Chapra (2008)
α_2	Fraction of algal biomass, which is phosphorus	0.01-0.02 0.001-0.03	0.03	-	Rajbhandari (1995) Chapra (2008)
α_3	Amount of oxygen produced per unit of algal photosynthesis	1.4-4.8	1.60	-	Rajbhandari (1995)
α_4	Amount of oxygen consumed per unit of algal respired	1.6-2.3	2.0	-	Rajbhandari (1995)
-	Dust attenuation coefficient (not shown)	0.04	0.04	-	Rajbhandari (1995)
k_2	Rearation rate at the ambient temperature	0.02-3.4 0.01 – 0.06	0.12	day^{-1}	Rajbhandari (1995) Chapra (2008)
κ_L	Half saturation constant for light (not shown)	0.02-0.1	0.085	Kcal m^{-2} s^{-1}	Rajbhandari (1995)
κ_N	Half saturation constant for nitrogen	0.01-0.3 0.01–4.3	0.05	mg L^{-1}	Rajbhandari (1995) Chapra (2008)
κ_P	Half saturation constant for phosphorus	0.001-0.05 0.001-1.5	0.02	mg L^{-1}	Rajbhandari (1995) Chapra (2008)
λ_0	Non-algal portion of the light extinction coefficient (not shown)	0.116	0.26	ft^{-1}	Rajbhandari (1995)
λ_1	Linear algal self shading coefficient (not shown)	0.002-0.02	0.003	ft^{-1} (µg-Chla L^{-1}) $^{-1}$	Rajbhandari (1995)
λ_2	Nonlinear algal self shading coefficient (not shown)	0.0165	0.0165	ft^{-1} (µg-Chla L^{-1}) $^{-2/3}$	Rajbhandari (1995)
σ_7	Algal mortality contribution to CBOD	1.0	1.0	mg (m^2 day)$^{-1}$	Rajbhandari (2002)
Regional Reaction Parameters					
k_1	CBOD decay rate at the ambient temperature	0.02-3.4 0.01 – 0.06	0.12	day^{-1}	Rajbhandari (1995) Chapra (2008)
k_3	Rate of loss of CBOD due to settling at the ambient temperature	-0.36-0.36	0.1	day^{-1}	Rajbhandari (1995)
μ_{max}	Maximum algal growth rate at the ambient temperature	1.0-3.0	1.2 - 3.0	day^{-1}	Rajbhandari (1995)
ρ	Phytoplankton respiration rate at the ambient temperature	0.05-0.5 0.01-0.04	0.15	day^{-1}	Rajbhandari (1995) Chapra (2008)
σ_1	Phytoplankton settling rate at the ambient temperature	0.5-6.0 0.06-33.0	0.1 – 1.5	ft day^{-1}	Rajbhandari (1995) Chapra (2008)
σ_6	Phytoplankton death rate at the ambient temperature	0.2 0.03-0.3	0.11 – 1.0	ft day^{-1}	Rajbhandari (2002) Chapra (2008)

Table 6-4 Model parameters, continued. Some parameters do not appear explicitly in the equations as discussed in this report.

Symbols	Description	Lit. Range Min/Max	Calibrated Values	Symbols	Source
k_n	Ammonia decay rate at the ambient temperature Ammonium decay rate	0.1-1.0 0.001 – 0.95	0.2 - 0.6	day^{-1}	Rajbhandari (1995) Chapra (2008)
k_{ni}	Nitrite decay rate at the ambient temperature	0.2-2.0	1.0 – 4.0	day^{-1}	Rajbhandari (1995)
$k_{N\text{-}org}$	Rate constant for hydrolysis of organic nitrogen to ammonia nitrogen at the ambient temperature	0.02-0.4	0.02 - 0.1	day^{-1}	Rajbhandari (1995)
σ_4	Organic nitrogen settling rate at the ambient temperature	0.001-0.1	0 - 0.005	day^{-1}	Rajbhandari (1995)
$k_{P\text{-}org}$	Organic phosphorus decay rate at the ambient temperature	0.01-0.7	0.005	day^{-1}	Rajbhandari (1995)
σ_5	Organic phosphorus settling rate at the ambient temperature	0.001-0.1	0.00 – 0.1	day^{-1}	Rajbhandari (1995)
σ_2	Benthic release rate for orthophosphate at the ambient temperature (mass transfer rate of $PO4$ in the sediment)	1.0 0.0816 0.057–21.0	0.001 - 0.3	mg m^{-2} day^{-1} m day^{-1} mg m^{-2} day^{-1}	Rajbhandari (1995) Sanford and Crawford(2000) Chapra (2008)
σ_3	Benthic release rate for ammonia-N at the ambient temperature (mass transfer rate of $NH3$ in the sediment)	4.0 0.06-0.1464	0.0 – 0.4	mg m^{-2} day^{-1} m day^{-1}	Rajbhandari (1995) Sanford and Crawford (2000)
k_4	Benthic oxygen demand	30 – 300 0.3 – 5.8	30 - 250	g m^{-2} day^{-1}	Rajbhandari (1995) Chapra (2008)
Global Temperature Coefficients for Reaction Rates (not explicitly shown)					
θ(1)	BOD decay	1.047 1.02	1.047		Wilson et al. (1998) Chapra (2008)
θ(2)	BOD settling	1.024	1.024		Wilson et al. (1998)
θ(3)	DO Reaeration	1.024	1.0		Wilson et al. (1998); Chapra (2008)
θ(4)	DO SOD	1.060 1.04-1.13	1.06		Wilson et al. (1998) Chapra (2008)
θ(5)	Organic-N decay	1.047	1.000		Wilson et al. (1998)
θ(6)	Organic-N settling	1.024	1.074		Wilson et al. (1998)
θ(7)	Ammonia-N decay	1.083	1.047		Wilson et al. (1998)
θ(8)	Ammonia-N benthic source	1.074	1.0		Wilson et al. (1998)
θ(9)	Nitrite-N decay	1.047	1.047		Wilson et al. (1998)
θ(10)	Organic-P decay	1.047	1.047		Wilson et al. (1998)
θ(11)	Organic-P settling	1.024	1.024		Wilson et al. (1998)
θ(12)	Dissolved-P benthic source	1.074	1.074		Wilson et al. (1998)
θ(13)	Algae growth	1.047	1.024		Wilson et al. (1998)
θ(14)	Algae respiration	1.047	1.047		Wilson et al. (1998)
θ(15)	Algae settling	1.024	1.024		Wilson et al. (1998)
θ(16)	Algae death	1.047	1.024		Wilson et al. (1998)

6.4 Conceptual Model of the Delta Used in QUAL's Nutrient Model

QUAL's conceptual model of nutrient dynamics is general enough for application in many surface water bodies. However, in its implementation within DSM2-QUAL, this conceptual model is applied specifically in the Delta, a geographically large and physically diverse estuary. Figure 6-6 shows several aspects of the Delta from a flooded island in Franks Tract, to a remnant of functioning tidal marsh in Suisun Marsh, to the channels of water in the central and southern Delta which have been altered by the introduction of a system of levees that channelize flow. Thus, the parameterization of the nutrient model (i.e., the way model parameter values are set in each channel in the model grid) needs to be varied to account for differences in nutrient dynamics that can be influenced by differences in hydrology, bathymetry and other physical characteristics. Parameter values were set in the nutrient model within five parameterization regions that in large part reflect regional differences in Delta hydrology and other characteristics that have been observed in specific regions. This section discusses the assumptions behind the regionalization applied in this implementation of the QUAL nutrient model.

6.4.1 A Very Brief Description of Delta Hydrodynamics

Figure 6-3 shows the general location of the DSM2 river inflow boundaries and the major export locations in the south and central Delta. Inflow, outflow, exports and diversions in the Delta vary seasonally and regionally. Similarly, net outflow volumes moderate the tidal influence represented in DSM2 *via* the stage boundary at Martinez. Figure 6-7 is a cartoon illustrating the major hydrologic influences in the Delta. In DSM2, tidal influences introduced at Martinez produce variations in stage (water level) that can be felt throughout much of the model domain (double-ended arrows in Figure 6-7), although the extent of tidal influence within the Delta depends on the volume of outflow and the timing of the spring-neap cycle. Inflow volume to the Delta (single-ended arrows) varies by source locations and the season. The largest volume of inflow comes from the Sacramento River in the winter wet season – during exceptionally high flow years, flooding in the Yolo Bypass distributes some of this flow further downstream. Large volumes of water are exchanged between the Sacramento and San Joaquin Rivers through Threemile Slough and at the confluence of these two rivers (see: curved, partially transparent arrows in Figure 6-7). Exports and diversions -including agricultural diversions- can strongly influence Delta flow patterns, with the majority of exports removed in the south of the Delta.

6.4.2 QUAL-Nutrient Parameterization Regions

Figure 6-8 through Figure 6-10 illustrate the areas defining the five general "parameterization regions", as defined below, applied in the current application of the QUAL nutrient model. Note that the open water areas in DSM2, called "reservoirs" in DSM2 terminology, were parameterized separately as their nutrient dynamics is considered to be different from dynamics in Delta channels. DSM2 "reservoirs" are treated numerically as single fully mixed volumes in DSM2.

A *parameterization region* in the QUAL nutrient model consists of those channels in DSM2 in which each Regional Reaction Parameter in Table 6-3 and Table 6-4 was set at the same value at the start of the calibration process. The region boundaries are set to define hydrodynamically similar areas in the Delta. As the iterative calibration process proceeded, parameters were varied by region, but not within the regions. In the final calibration iterations refining parameter values, the value for given parameter could be varied within a region. For example, in the region denoted "Confluence to Martinez", the channels

defining Grizzly Bay and Honker Bay were found to have quite different characteristics, so parameters were varied within the Confluence to Martinez region for each of these bays. Note that this region includes the (stage) boundary at Martinez. Although they are both close, given their differing proximity to Martinez the two bays are affected differently by the Martinez boundary conditions.

The five parameterization regions specified for this project in large part reflect regional differences in hydrology. However, there are large variations in hydrology even within these regions as their characteristics will change not only with Delta inflow but also with tidal cycle and with season. For example, in January 1994 the combined inflow from the Sacramento River and the Yolo Bypass was 14,218 cfs (cubic feet per second), inflow from the San Joaquin River was 1773 cfs and combined SWP+CVP exports was 5735 cfs on a monthly average basis, but these flows were, respectively, 210,006 cfs, 33,122 cfs and 2757 cfs in January 1997. These values reflect more than an order of magnitude difference in inflow and only a factor of two difference in export levels. As a consequence, in these two examples, tidal influences within the parameterization regions will vary significantly.

Figure 6-8 (Upper) illustrates the "Confluence to Martinez" region. This region is dominated during lower flow periods by high salinity (ocean salinity). Previous work (for the Franks Tract project[6]) has shown that salinity intrusion further upstream on the Sacramento River out of this region occurs primarily under extremely low flow conditions. Water flowing through Montezuma Slough, the main channel in Suisun Marsh, reverses direction tidally and is influenced not only by water flowing through the lower Sacramento River but also by mixing of waters from the smaller side channels and sloughs. The area roughly bounded by the dashed triangle in the lower left corner of Figure 6-8 could be considered a sub-region on its own, as it is strongly influenced by both the Sacramento and San Joaquin Rivers and by ocean influences during periods of very low inflow. However, for simplicity, this area was instead incorporated in the Confluence to Martinez region.

Figure 6-8 (Lower) illustrates the Sacramento River Region. This region includes the main stem of the Sacramento River from the confluence with the San Joaquin River to the model boundary for the Sacramento River, as well as the area which includes the tributaries in the Yolo Basin and Cache Slough. It does not include Liberty Island which is geographically within this portion of the model domain – as discussed above, open water areas like Liberty Island are dealt with separately. This region is dominated by Sacramento River water.

Figure 6-9, the Stockton Region, is mainly influenced by the San Joaquin River. This section of the San Joaquin River, particularly near the Stockton Ship Channel, has experienced problems with low DO during low flow periods. The San Joaquin River has higher nutrient concentrations than the Sacramento River during the model simulation time span.

Figure 6-10 (Upper), the Central Delta parameterization region, encompasses the central and southern portion of the Delta including the downstream section of the San Joaquin River. This region is tidally influenced. The parameterization of the reservoirs within the boundary of this region – Franks Tract, Mildred Island, Clifton Court Forebay and Discovery Bay – was considered separately. The flow in these channels is strongly affected by export volumes, and the channels can experience low flow during the

[6] http://www.water.ca.gov/frankstract/

summer months. Invasive water weeds can clog and overwhelm some of these channels, severely restricting flow and altering nutrient dynamics particularly in the summer months.

Figure 6-10 (Lower), the East Delta parameterization region, encompasses the eastern portions of the Delta. This region is heavily influenced by the Sacramento River when the Delta Cross Channel (DCC) is open, but mainly by the Cosumnes and Mokelumne Rivers when the DCC is closed. There are also many agricultural influences in this region, and the flow volume in some of the outer channels is low particularly in the warmer months.

Reservoirs Franks Tract, Mildred Island, Clifton Court Forebay and Discovery Bay were given identical parameter values initially as no nutrient data was available. Additional nutrient data (Lehman *et al*., 2010) identified for Liberty Island allowed this open water area to be parameterized to better represent Liberty Island nutrient dynamics.

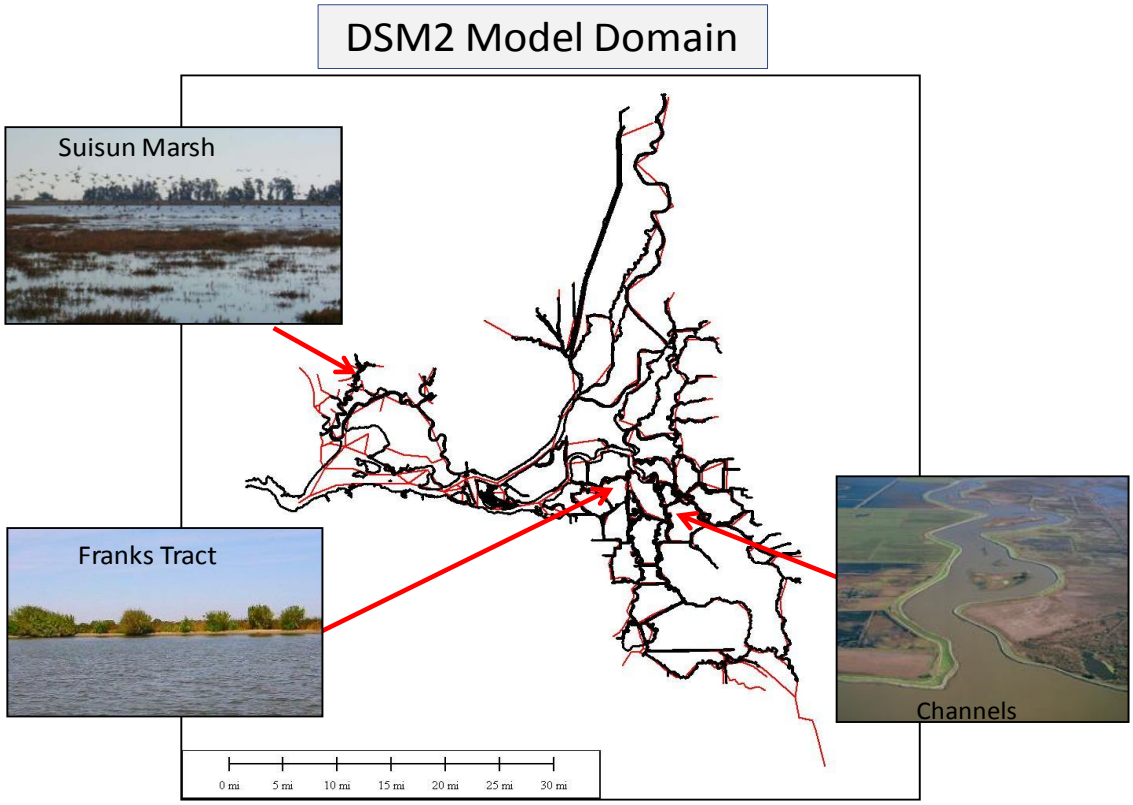

Figure 6-6 The Delta is a physically diverse system, as illustrated at several locations within the DSM2 model domain.

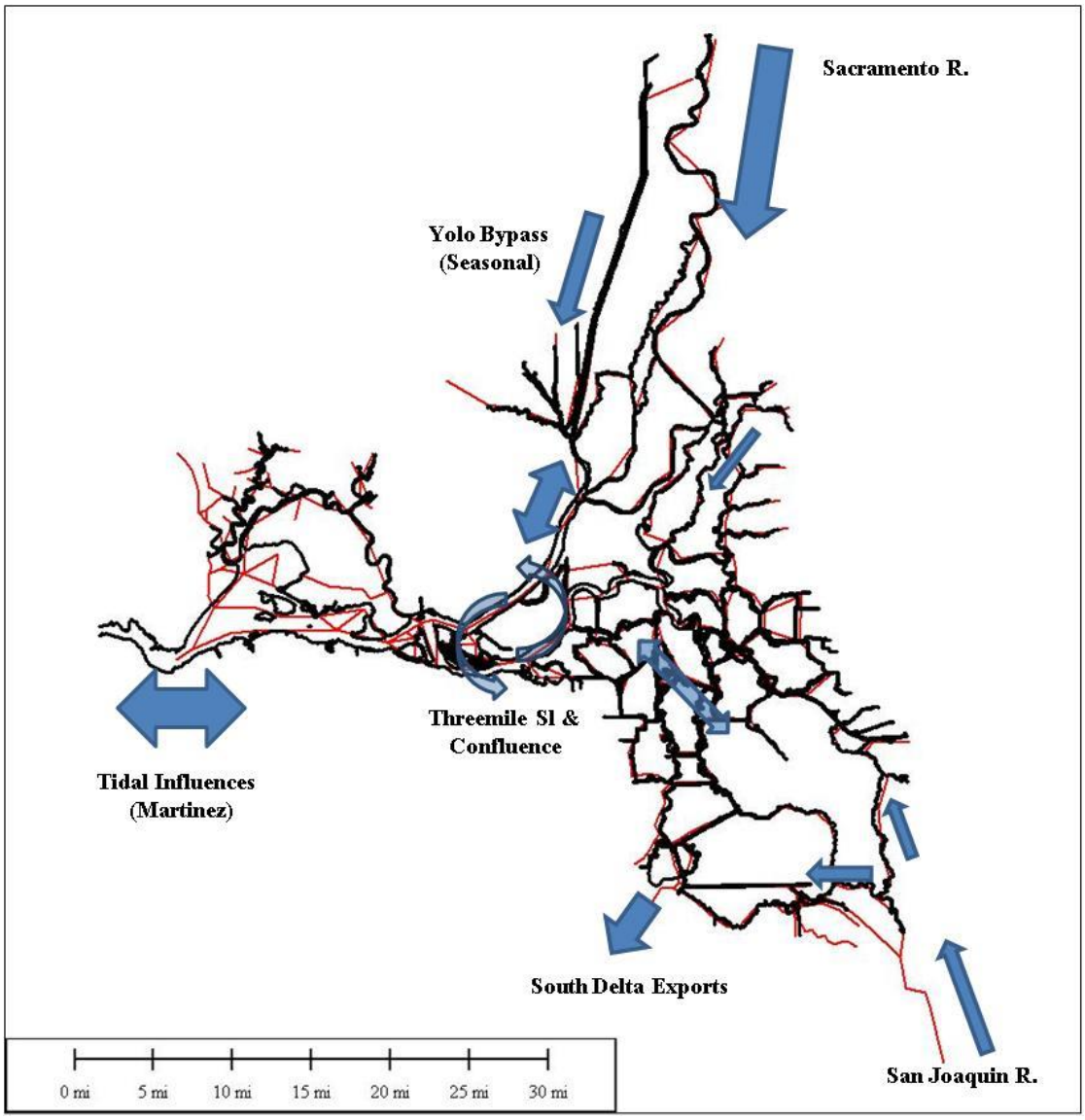

Figure 6-7 Overview figure of some major influences on Delta hydrodynamics – river inflow, exports, and tidal influences. Large volumes of water are exchanged between Threemile Slough and at the confluence of the Sacramento and San Joaquin Rivers.

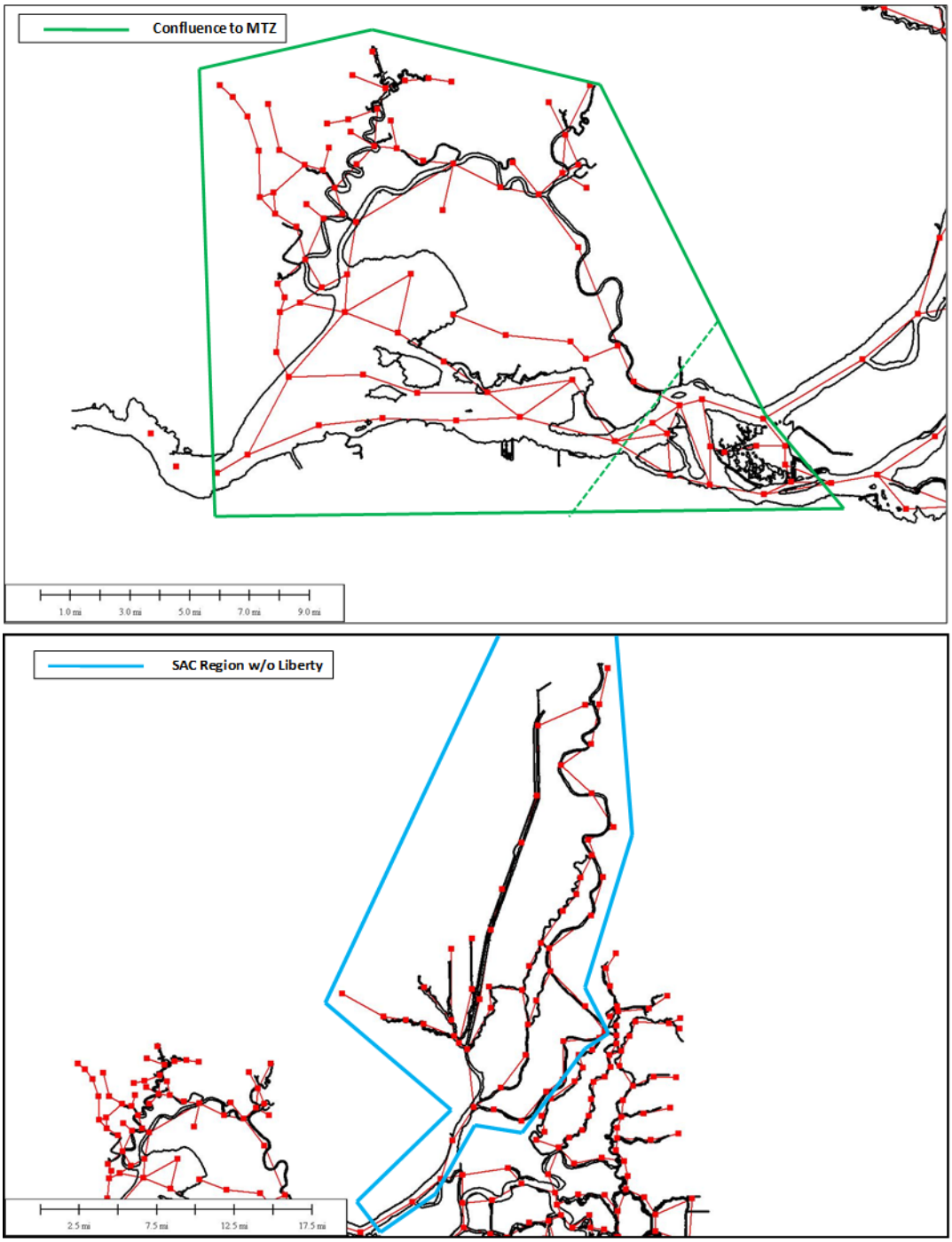

Figure 6-8 (Upper) Parameterization region extending from the confluence west to the model boundary at Martinez, including Suisun Marsh. Dashed line indicates the confluence region of the Sacramento and San Joaquin Rivers.

(Lower) Parameterization region extending north from the confluence to the Sacramento River inflow model boundary, and incorporating the Liberty Island, Yolo Basin and Cache Slough.

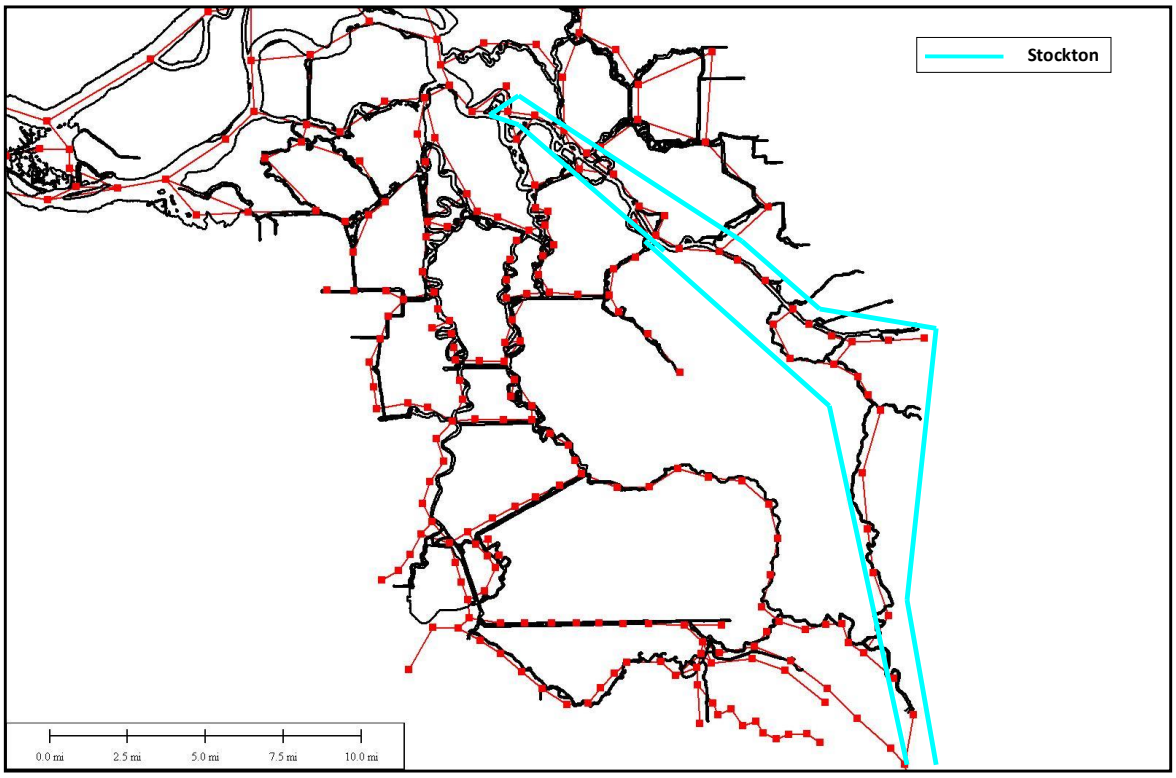

Figure 6-9 The parameterization region for the upstream portion of the San Joaquin River.

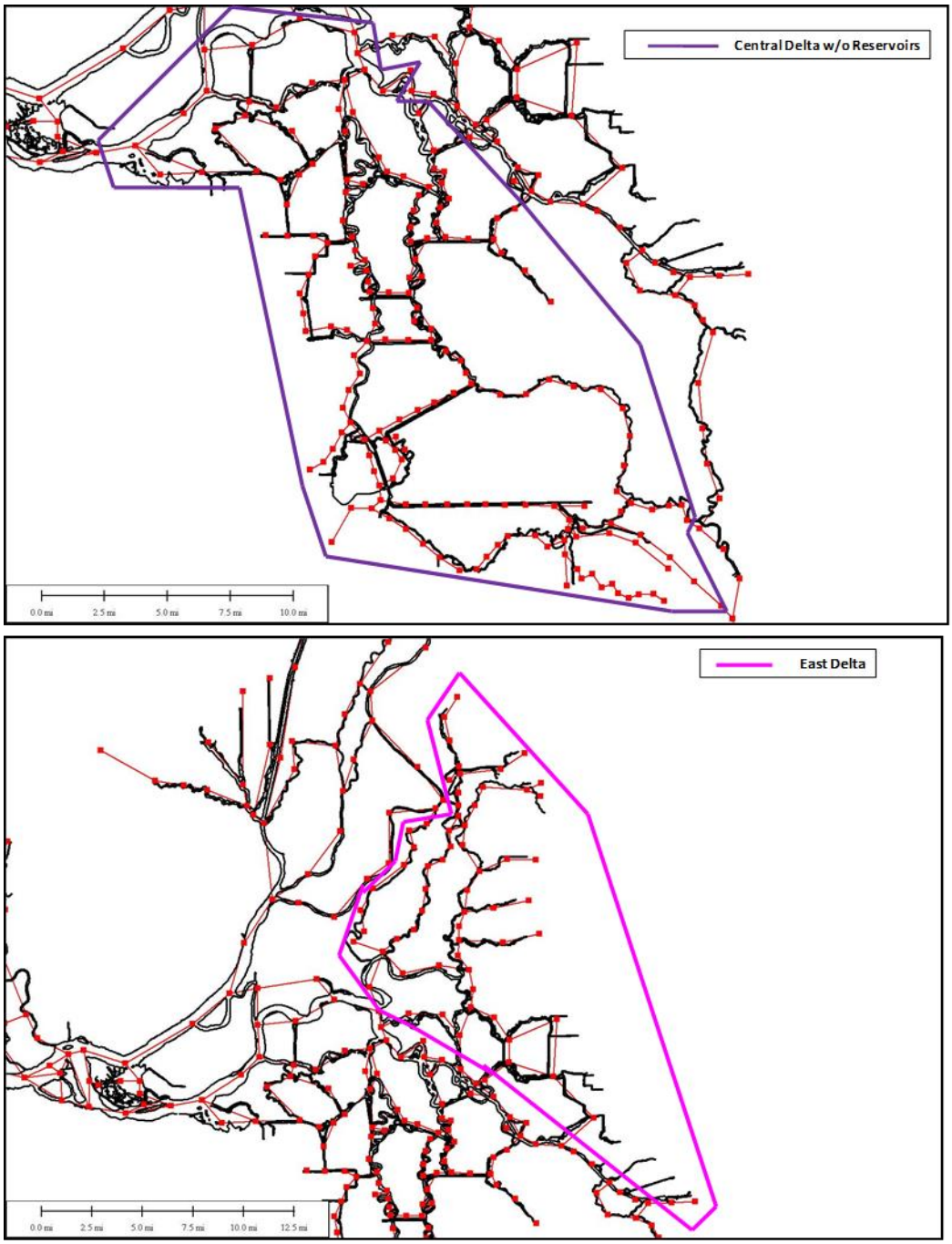

Figure 6-10 (Upper) Parameterization region for the central and south Delta. The reservoirs within this region were parameterized separately. The area is affected by exports and low flow during the summer months. Invasive water weeds can severely restrict flow and alter nutrient dynamics.

(Lower) Parameterization region for the East Delta. The region is heavily influenced by the Sacramento River when the Delta Cross Channel (DCC) is open, and from the Cosumnes and Mokelumne Rivers when the DCC is closed. There are also many agricultural influences in this region.

6.5 Data: Sources and Refinement

Several sources were identified for data needed in the development of boundary conditions and for the model calibration and validation effort. Data quality was assessed and several approaches were used to improve the quality of the data or render the representation to match model characteristics. The final set of data was made available to DWR-DMS along with the model set-up.

Constituent concentration data were originally reported in a variety of measurement units depending on data source. Reported concentrations were converted to units of mg L^{-1}, the measurement unit used in QUAL, in terms of the molecular weight the atom characterizing the chemical species. For example, the concentration of orthophosphate, PO_4, is calculated as milligrams of PO_4-P, not in terms of the molecular weight of the entire chemical species *(i.e.,* without accounting for the weight of the oxygen atoms in the chemical species).

Additional detail on the setting of boundary conditions is found in (Guerin, 2011).

6.5.1 Data Sources

Raw data for the previous calibration (Guerin, 2011) were downloaded from BDAT7, DWR's Water Data library8 (WDL), IEP9, CDEC10 and USGS11 website. Nutrient data measurements available through BDAT ceased at many in-Delta locations in 1995. Note that data found on the BDAT website was no longer web-accessible as of December, 2015. EMP data has metadata information available (see Table 6-5). For the current calibration, raw data were downloaded from DWR's Water Data Library, IEP's Environmental Monitoring Program (EMP), CDEC, CIMIS and USGS websites. Additional data were obtained directly from individual researchers or from individuals identified as representing an organization. Effluent data were obtained directly from contacts at the individual WWTPs or downloaded from publically available sources and new data were combined with previous compilations of effluent data. Measurements upstream and downstream of effluent outfalls, called receiving water measurements, were collected when available. Stockton WWTP had a very complete set of receiving water measurements – their locations are shown in Figure 6-11. Meteorological data were downloaded from the CIMIS[12] website (see Table 6-6 and Figure 6-12). Access to NOAA meteorological data for the 2011 QUAL nutrient model calibration was purchased and downloaded from a NOAA website (NNDC Online Store, NOAA Data Center).

A new initiative for the current recalibration of QUAL-nutrient was to improve the representation of DICU nutrient inflow concentrations, as DICU nutrient data were set as constant values in the previous DO-models (Rajbhandari 1995a, 2000, 2001, 2003). Monthly averaged, annually repeating DICU inflow concentrations had been compiled in a 1995 report document[13] prepared by DWR. In that report three

[7]http://bdat.ca.gov/
[8]http://www.water.ca.gov/waterdatalibrary/
[9]http://www.iep.ca.gov/data.html
[10]http://cdec.water.ca.gov/
[11]http://sfbay.wr.usgs.gov/access/wqdata/
[12]http://wwwcimis.water.ca.gov/cimis/welcome.jsp
[13] Modeling Support Branch, Representative Delta Island Return Flow Quality for Use in DSM2: Memorandum Report May 1995, Division of Planning, Department of Water Resources

subregions were identified in the Delta – the concentration time series of each nutrient was the same for each DICU location within a region. In addition, to test the DICU time series concentrations against recent data, nutrient data from agricultural return flows was downloaded from the DWR-WDL. Figure 6-13 shows the three DICU regions along with EMP data locations in the Delta – black lines are the channel locations in the DSM2 model grid.

Figure 6-14 shows the net DICU flows – drain, seepage and diversion – for the three regions. Figure 6-15, Figure 6-16, and Figure 6-17 illustrate the comparison between the previous constant values used for DICU concentration inflow and the monthly averaged, annually repeating time series for the three DICU parameter regions.

6.5.2 Data processing methodology

Measurement units and data measurement methodology were checked in each data set for consistency with DSM2 model assumptions. Latitude-longitude (lat-long) co-ordinates were used to verify the position of the data acquisition location and to ensure appropriate placement in the model. Raw data were converted to DSS format for use in the program HEC-DSSVue[14]. MATLAB codes and other data processing tools were developed to automate some of the transfer to DSS format. Irregular time series data were further processed into regular time series data for use in setting boundary conditions, typically as daily or monthly time series with linear interpolation between the irregularly-spaced data points. Processing irregular data into regular time series was not necessary for plotting or for residual calculations in the calibration/validation process.

6.5.2.1 Data Quality

Data quality was mixed, depending on the constituent. All data were assessed visually (by plotting) to check for unreasonable values (*e.g.,* negative numbers) and in comparison with data at nearby locations. When problems with data quality clearly occurred (*e.g.,* all nearby stations had significantly different magnitudes), suspect data were deleted from the time series.

Continuous time series (15-minute or hourly) of temperature and DO data were available at or near the main model boundaries on the Sacramento River, the San Joaquin River and at Martinez at well as at several other locations within the model domain. There were frequently large gaps in the data during the modeled period for each of these data types (see Figure 6-20).

The quality of grab sample data from EMP and USGS sources for the nutrients was good, as assessed by comparison with data at nearby locations and comparisons between the agencies, although it was generally only available at approximately monthly or bi-monthly intervals and the time span was variable. Figure 6-20 through Figure 6-27 show comparisons of Environmental Monitoring Program (EMP) and USGS measurements at Rio Vista and Point Sacramento (chl-a measurements were converted to algal biomass as described in Section 6.3.2.4). The chl-a measurements from the two agencies are within the same range of magnitude in most months, and although measurements could vary by factors of 2 – 5 particularly when a peak occurred, the general patterns are similar. A similar comparison for DO data at the same locations shows that the measurements generally track both in magnitude and pattern. For NO_3+NO_2 measurements we see again they track fairly closely in magnitude when taken at similar

[14]http://www.hec.usace.army.mil/software/hec-dss/hecdssvue-dssvue.htm

times. The situation for PO_4 is quite different. The inter-agency data comparison at Point Sacramento is not very good for this constituent, with differences in magnitude of up to a factor of two between the agencies, with no apparent similarity in pattern. On the other hand, measurements by the same agency at nearby locations are more consistent. Thus, the constituent comparisons are good between the USGS and EMP measurements except for PO_4.

6.5.2.2 Missing Data

Although some boundary conditions required that data gaps be filled in some manner prior to application to supply a regular time series of data to HYDRO and QUAL, data for calibration and validation required no further modification after removal of suspect data. Several methods were used to fill gaps in time series of data used for boundary conditions – this process is covered in detail in (Guerin, 2011). Linear interpolation was used on irregular time series when converted to regular interval data – this is the default methodology used in HEC-DSSVue for conversion to regular time series.

When data values were below instrument detection limits, the value was set at the half the stated value of the detection limit or at zero as specified by some data sources, for both boundary condition data and for plotting. Measurements recorded as below detection limits were excluded from statistical (residual) calculations for model calibration and validation.

6.5.3 Data Availability: Time Spans and Locations

Data were needed to set concentrations for each of the eleven constituents at each river boundary, at each effluent boundary, and at the 258 DICU boundaries for the modeled time period, 2000 – 3/2012. As this project was an extension of a previous calibration project (Guerin, 2011), additional data was acquired for the period 1/2009 – 3/2012 for setting boundary conditions and for calibration of the model. Flow and salinity data was available from DWR Historical model at all the standard inflow boundaries (rivers, stage and DICU), but not for effluent boundaries.

6.5.3.1 WWTP Receiving Water Measurements and Effluent Data

An important set of long-term measurements on the San Joaquin River supplied by the Stockton WWTP are measurements for receiving waters (*i.e.*, Delta waters that the effluent flows into, Figure 6-11). Grab sample measurements were taken for chl-a, nitrite, nitrate, ammonia, DO (bottom and mid-depth), organic-N and BOD-10 or BOD-5 (the frequency of the last two data types is very limited). These BOD data was compared with modeled CBOD measurements, merely for trend comparison.

Additional data were also obtained for the effluent flow and nutrient composition, and at a few locations for receiving waters, for the other WWTPs included in the model domain. Data to extend the previous model boundary conditions for the period 1/2009 – 3/2012 was obtained from publically available sources on the web, generally 2011 – 2012. Missing data was filled in using professional judgment.

6.5.3.2 Lehman Data for Liberty Island

P. Lehman supplied data collected in Liberty Island from a study on Liberty Island nutrient dynamics - the background for this data is discussed in (Lehman *et al.,* 2010). In brief, measurements were collected monthly from February 2004 to July 2005 from 4 locations within Liberty Island (See Figure 1 in the Lehman paper). Data from water samples that were analyzed included several modeled constituents,

NH_3, NO_3, chlorophyll-a and PO_4 (called soluble-P in the Lehman data set). On each sample date, data for these constituents from the four locations (labeled north, south, east and west in Figure 1 in Lehman's paper) were averaged for comparison with QUAL nutrient model output.

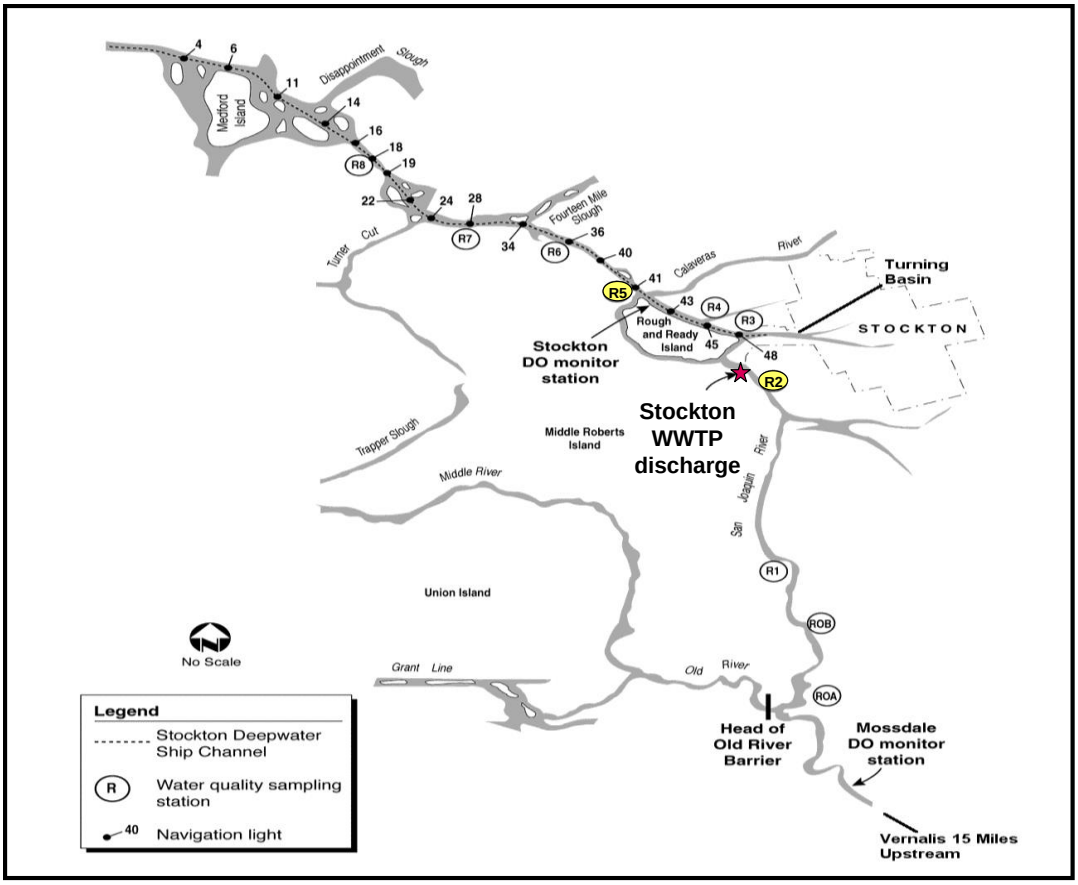

Figure 6-11 Location of the Stockton WWTP receiving water measurement locations (Figure from C. Kendall, personal communication).

Table 6-5 Metadata for the EMP-DWR measurements.

Metadata for EMP-DWR Measurements - List of Lab Constituents								
Group	**Matrix**	**Fraction**	**Analyte**	**Units**	**Method**	**Data from**	**Data to**	**Comments**
Nutrients	Water	Dissolved	Ammonia	mg/L as N	EPA 350.1	1/16/1979	Ongoing	1979-ongoing
Nutrients	Water	Total	Kjeldahl Nitrogen	mg/L as N	EPA 351.2	5/1/1978	Ongoing	1978-ongoing
Nutrients	Water	Dissolved	Nitrite + Nitrate	mg/L as N	Std Method 4500-NO3-F Modified	7/19/1996	Ongoing	1996-ongoing
Nutrients	Water	Dissolved	Organic Nitrogen	mg/L as N	EPA 351.2 (Dissolved)	5/2/1978	Ongoing	1978-ongoing
Nutrients	Water	Dissolved	Ortho-phosphate	mg/L as P	EPA 365.1 (DWR Modified)	1/16/1979	Ongoing	1979-ongoing
Nutrients	*Water*	*Total*	*Phosphorus - Not Used*	*mg/L*	*EPA 365.4*	*5/2/1978*	*Ongoing*	*1978-ongoing*
Biological	Water			µg/L	Std Method 10200 H	2/2/1998	Ongoing	1998-ongoing

Table 6-6 Meteorological data – the difference between CIMIS and NOAA measurements, such as measurement height above ground, timing (instantaneous vs. average).

	CIMIS	NOAA
Measure height	2 m	10 m
Frequency	Hourly/Daily averaged	Hourly
Constituents	Solar Radiation Air Temperature Soil Temperature Dew Point Relative Humidity Wind Speed Wind Direction Wind Gust Vapor Pressure Precipitation Evapotranspiration	Sky Condition Visibility Weather Type Dry Bulb Wet Bulb Dew Point Relative Humidity Wind Speed Wind Direction Value For Wind Character Station Pressure Pressure Tendency Pressure Change Sea Level Pressure Hourly Precipitation Altimeter
Stations in Delta	Brentwood (Jan98 - Dec05) Concord (Apr01 - present) Hasting Tract (Jan98 - present) Lodi (Jan98 - Dec00) Lodi West (Sep00 - present) Manteca (Jan98 - present) Tracy (Sep01 - present) Twitchell Island (Jan98 - present)	Stockton (88-present)

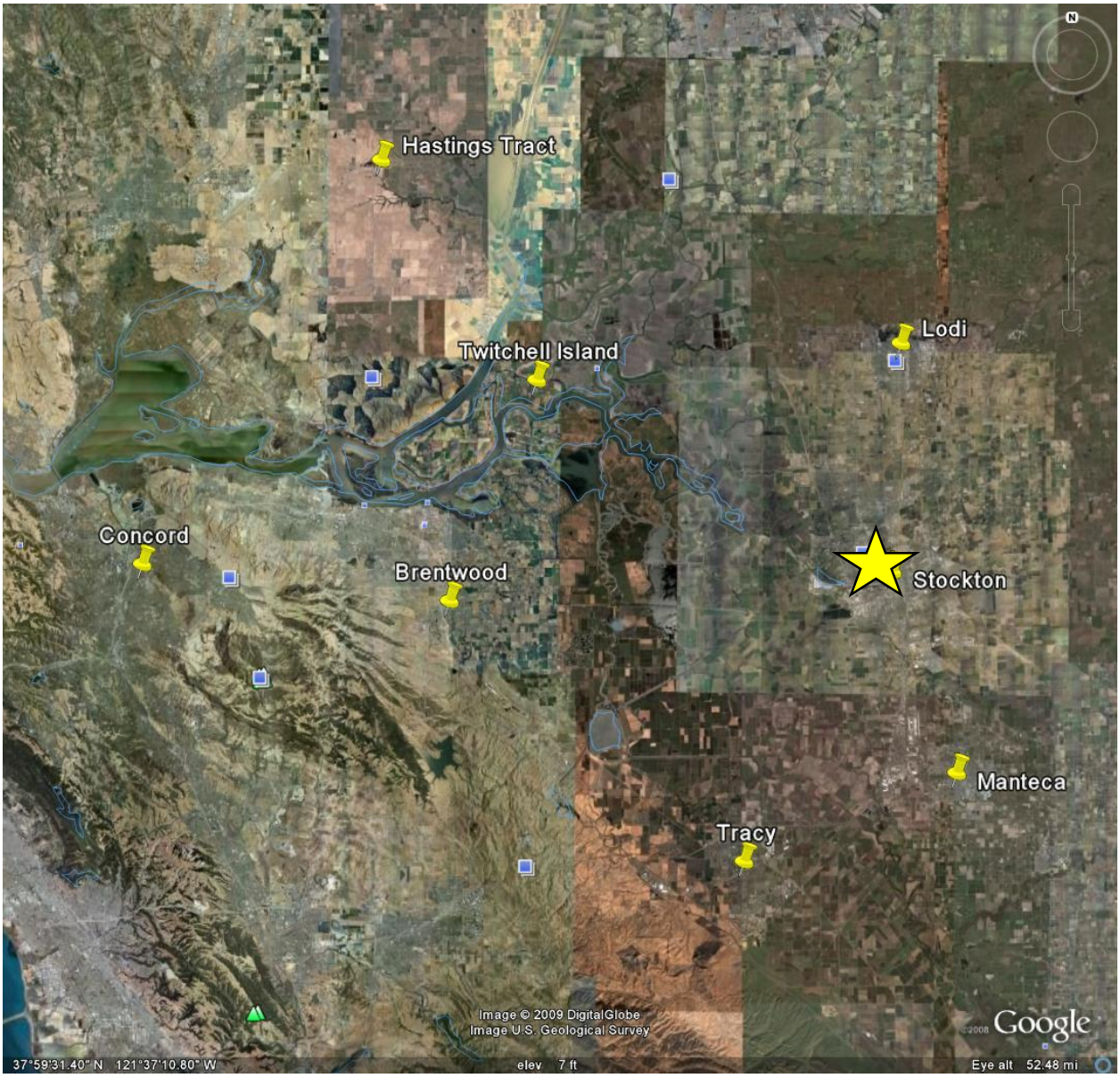

Figure 6-12 Meteorological measurements from NOAA at the Stockton airport (yellow star), and CIMIS measurements, indicated by yellow Google Earth push-pins.

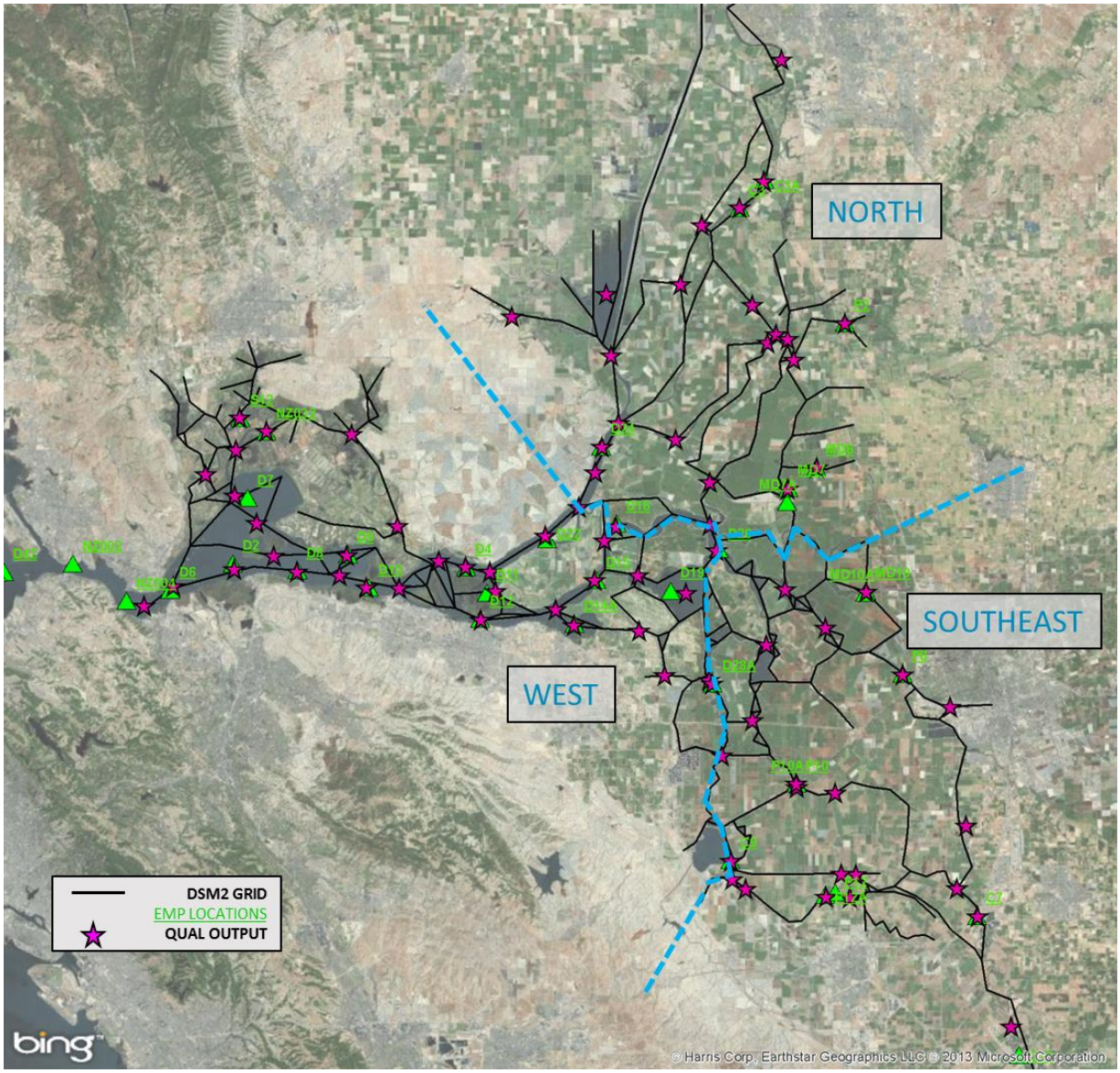

Figure 6-13 This figure documents the three DICU nutrient concentration regions and the EMP data locations in the Delta along with the outline of the DSM2 grid (black lines).

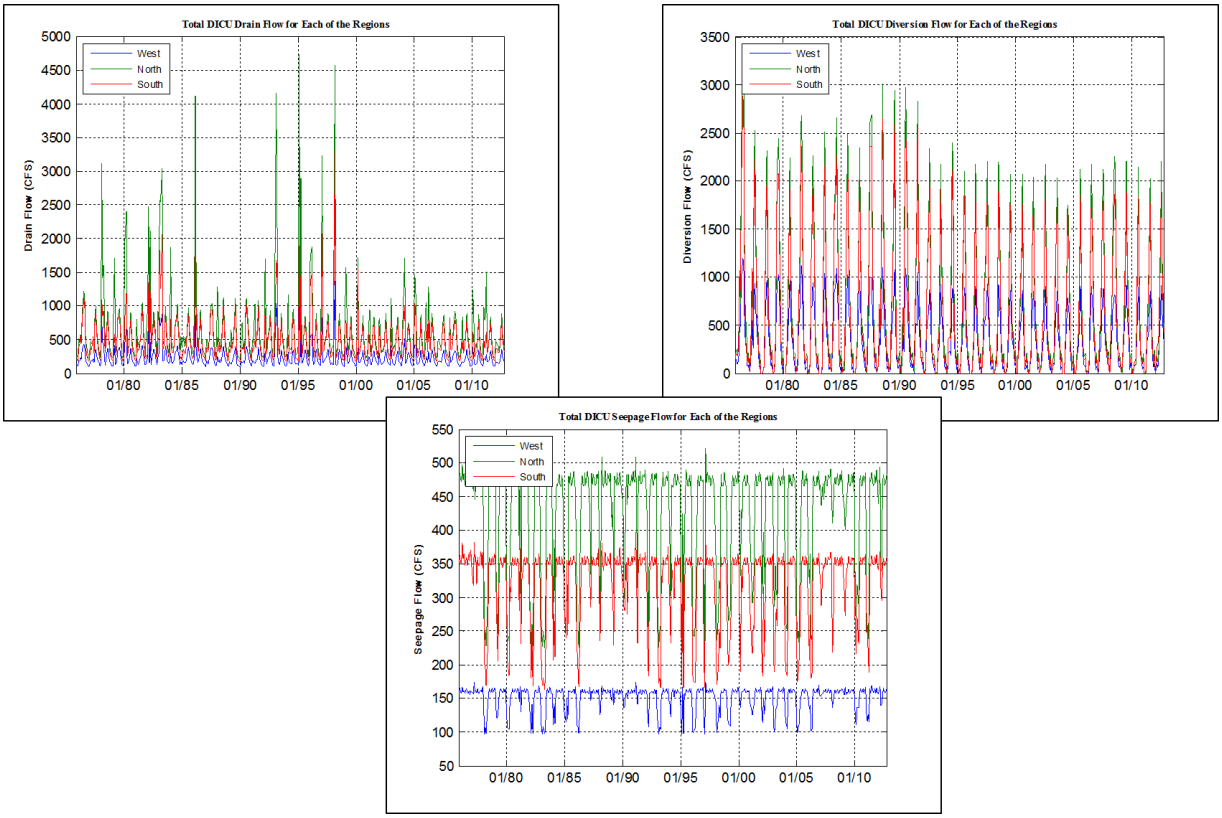

Figure 6-14 This figure shows the net DICU flows in the three DICU regions – the Drain flow is an inflow to the model domain, while Seepage and Diversion flows are net outflows from the model.

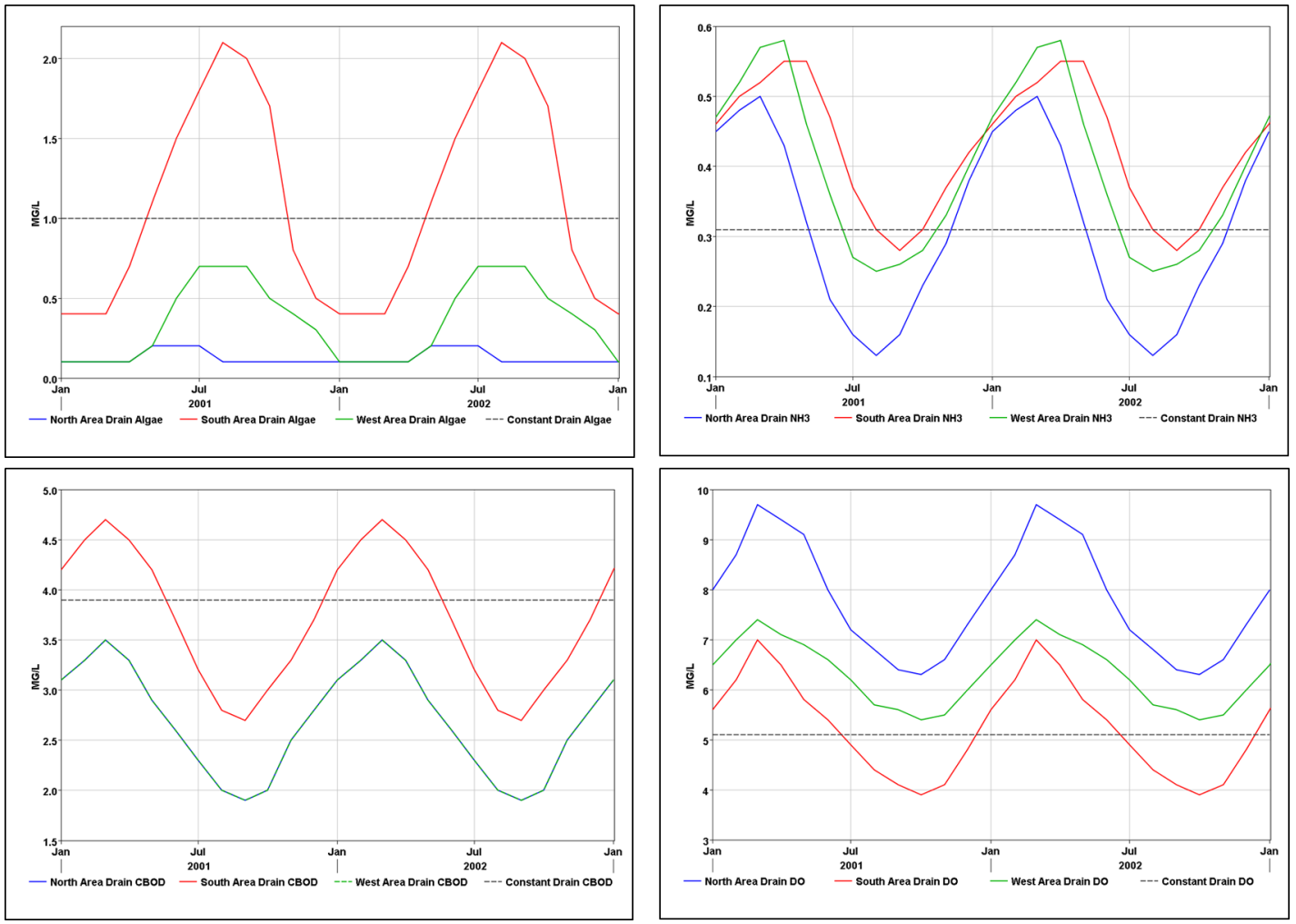

Figure 6-15 This figure shows the concentrations of Algae, NH3, CBOD and DO in the three DICU regions. Dashed black lines show the previously implemented constant concentrations.

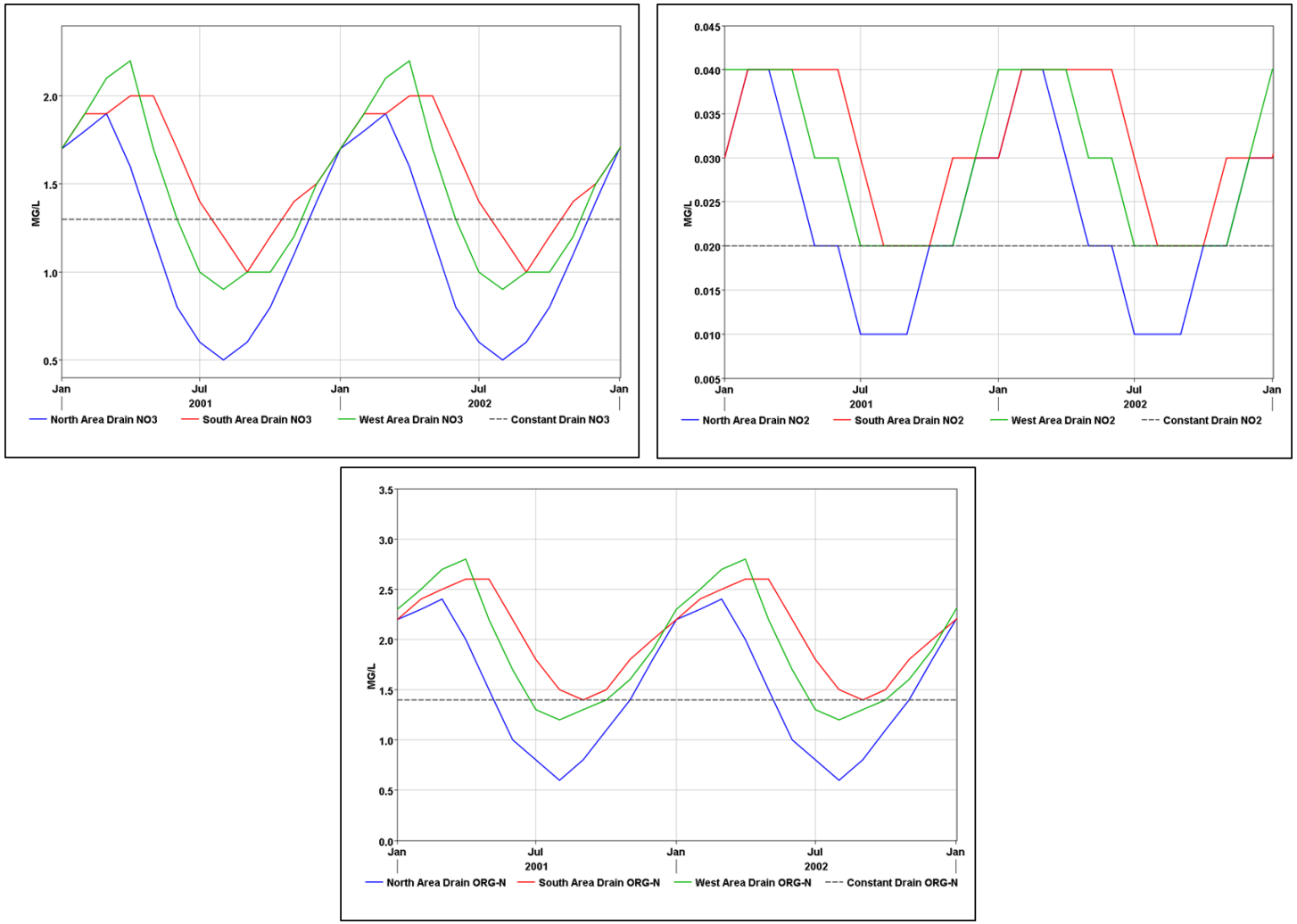

Figure 6-16 This figure shows the concentrations of NO3, NO2, and Organic-N in the three DICU regions. Dashed black lines show the previously implemented constant concentrations.

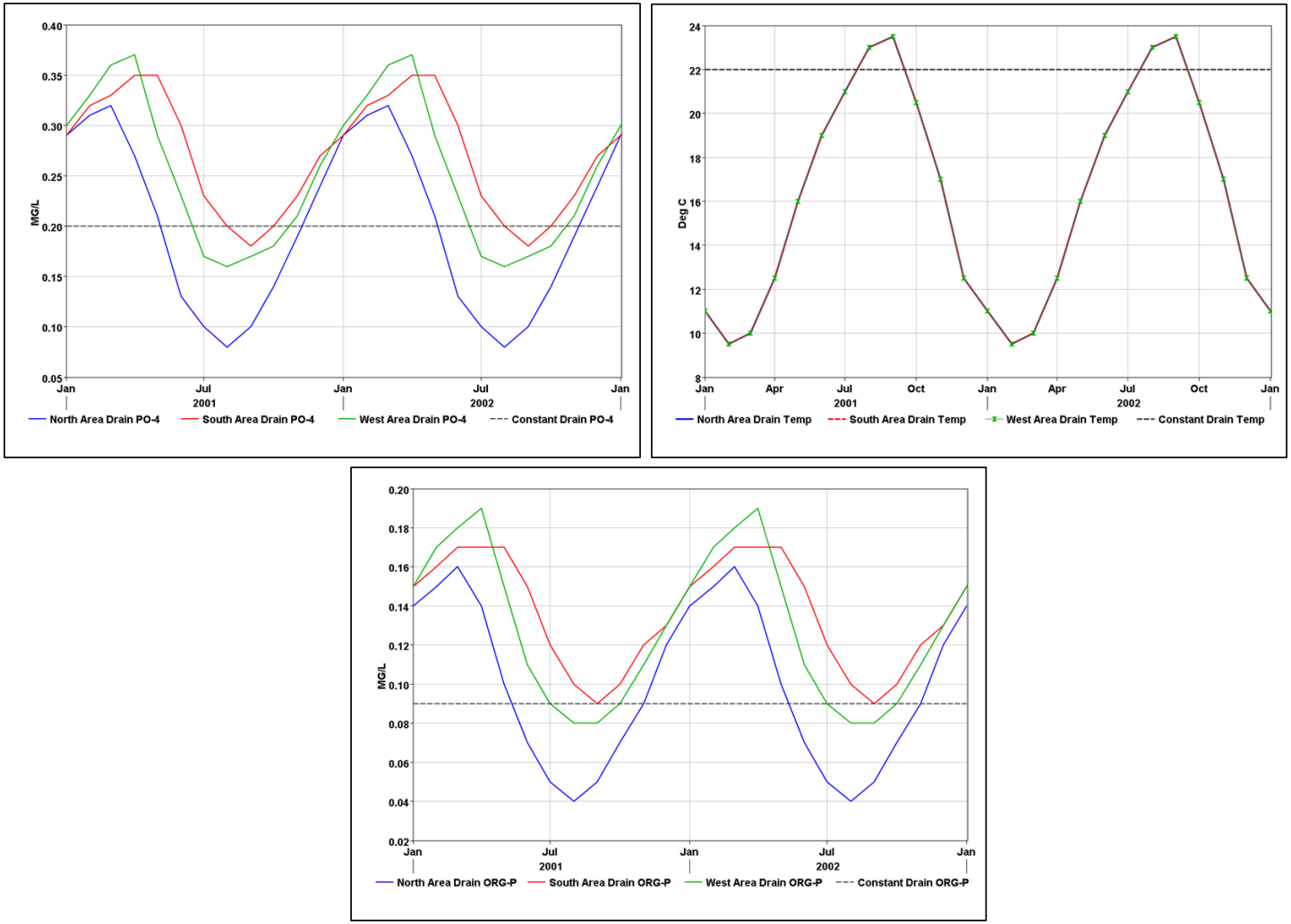

Figure 6-17 This figure shows the concentrations of PO4, Water Temperature, and Organic-P in the three DICU regions. Dashed black lines show the previously implemented constant concentrations. Note that the water temperature time series is constant across the 3 regions.

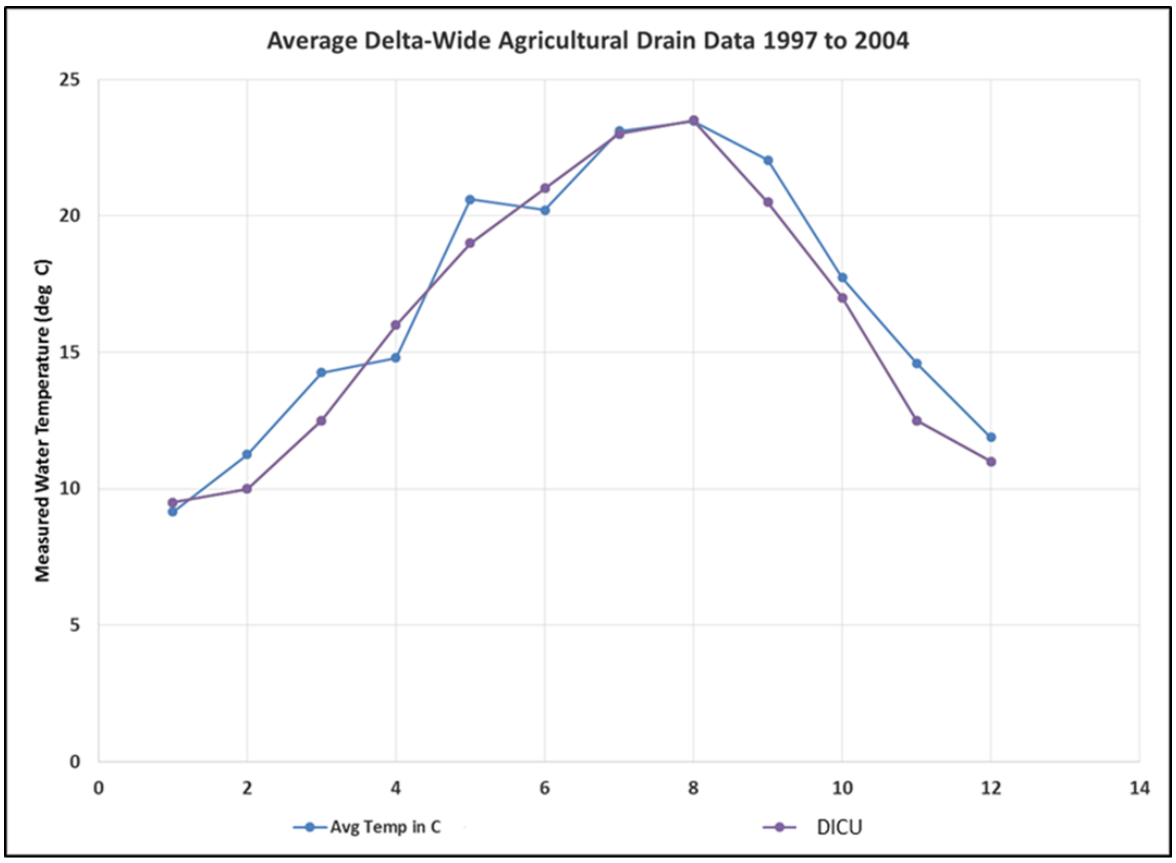

	Jan	Feb	Mar	Apr	May	Jun	Jul	Aug	Sep	Oct	Nov	Dec
Avg	9.15	11.26	14.26	14.80	20.60	20.21	23.11	23.47	22.04	17.73	14.60	11.89
Count	8	5	7	9	8	8	8	7	5	7	8	7

Figure 6-18 This figure documents a comparison between the DWR-1995 3-region estimated water temperatures (purple line) and the monthly average of agricultural Drain data, 1997 – 2004, from the DWR-WDL website (Blue line). Count in the lower table signifies the number of data points in the Delta-wide average.

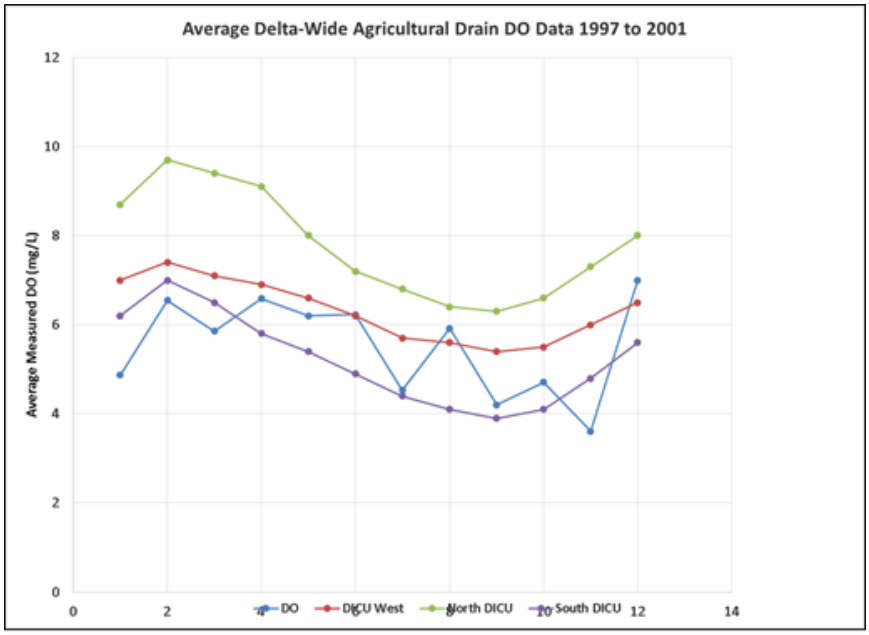

	Jan	Feb	Mar	Apr	May	Jun	Jul	Aug	Sep	Oct	Nov	Dec
Avg	4.87	6.54	5.86	6.58	6.20	6.23	4.53	5.92	4.20	4.71	3.61	6.60
Count	8	5	7	8	8	7	8	7	5	5	4	7

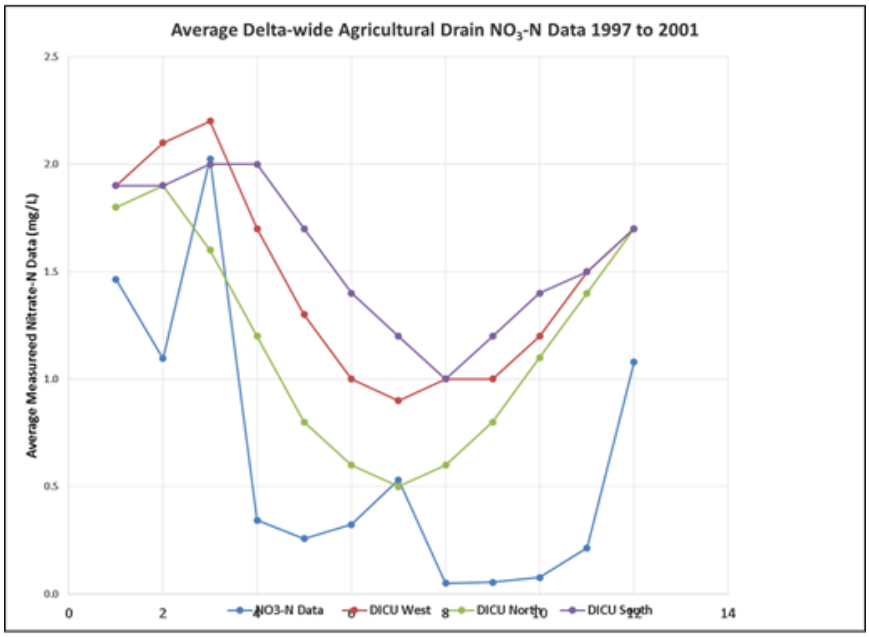

	Jan	Feb	Mar	Apr	May	Jun	Jul	Aug	Sep	Oct	Nov	Dec
Avg	1.46	1.10	2.03	0.34	0.26	0.32	0.53	0.05	0.05	0.08	0.21	1.08
Count	6	4	6	7	6	7	6	5	5	4	4	4

Figure 6-19 This figure documents a comparison between the DWR-1995 3-region DO and NO3 concentrations and the monthly average of agricultural Drain data, 1997 – 2001, from the DWR-WDL website. Count in the lower table signifies the number of data points in the Delta-wide average. Blue lines are the WDL data.

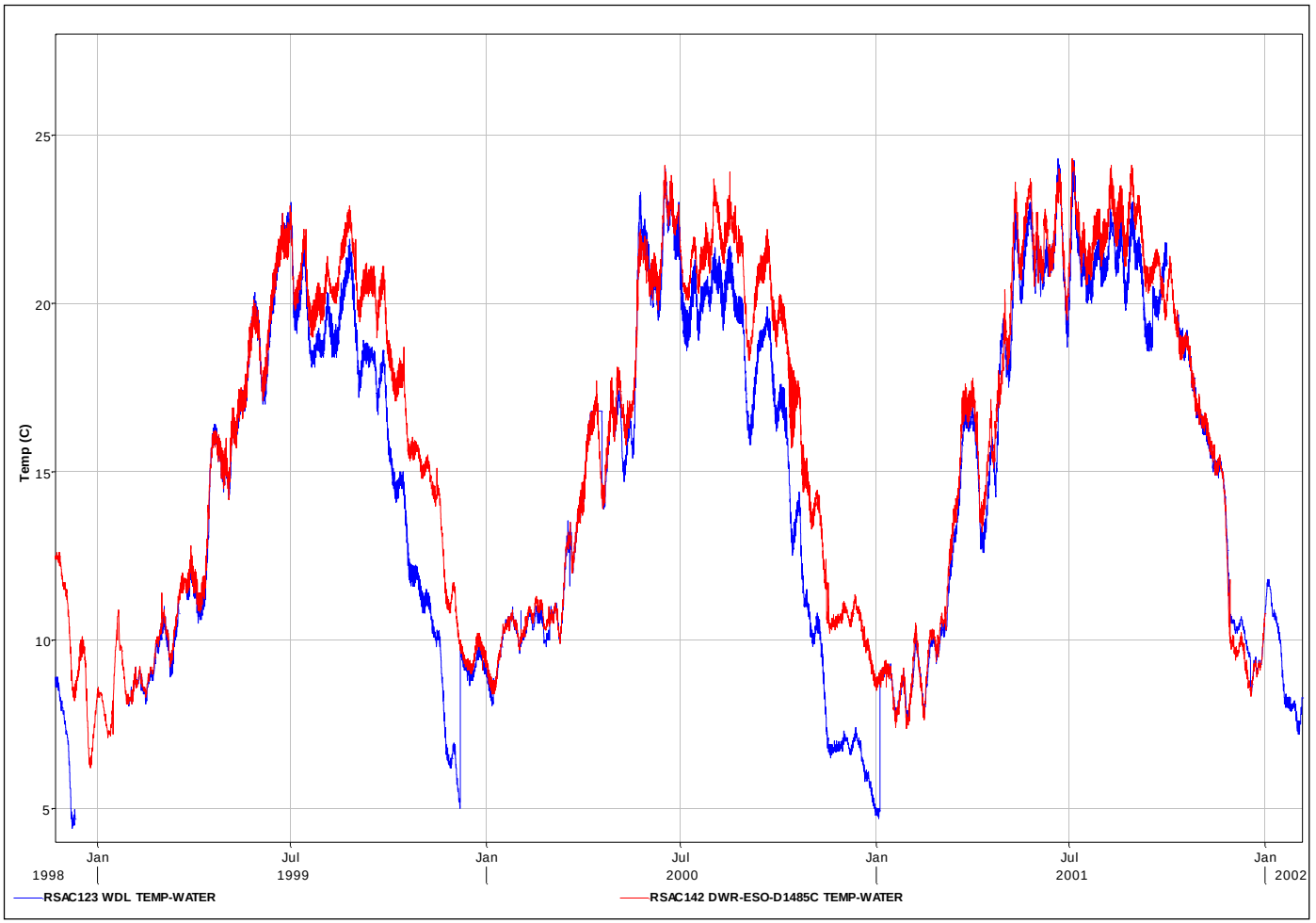

Figure 6-20 Suspect data were identified at RSAC123 (blue line) by large jumps in value at low temperatures in comparison with water temperature data at RSAC142 (red line). These locations are on the Sacramento River.

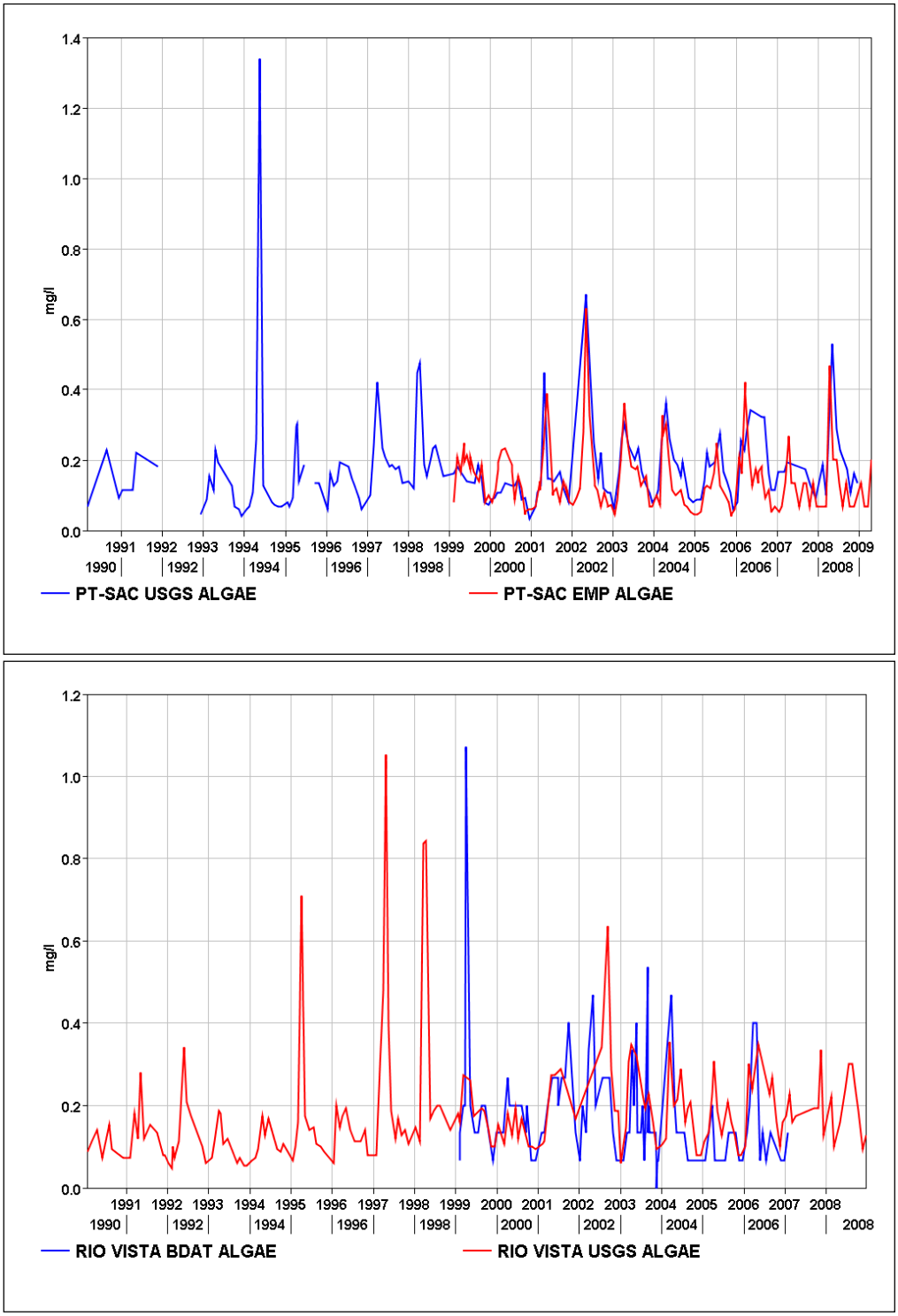

Figure 6-21 Comparison of EMP and USGS measurements at Point Sacramento (upper) Rio Vista (lower) – chlorophyll a measurements were converted to biomass of algae which is shown in the plots above.

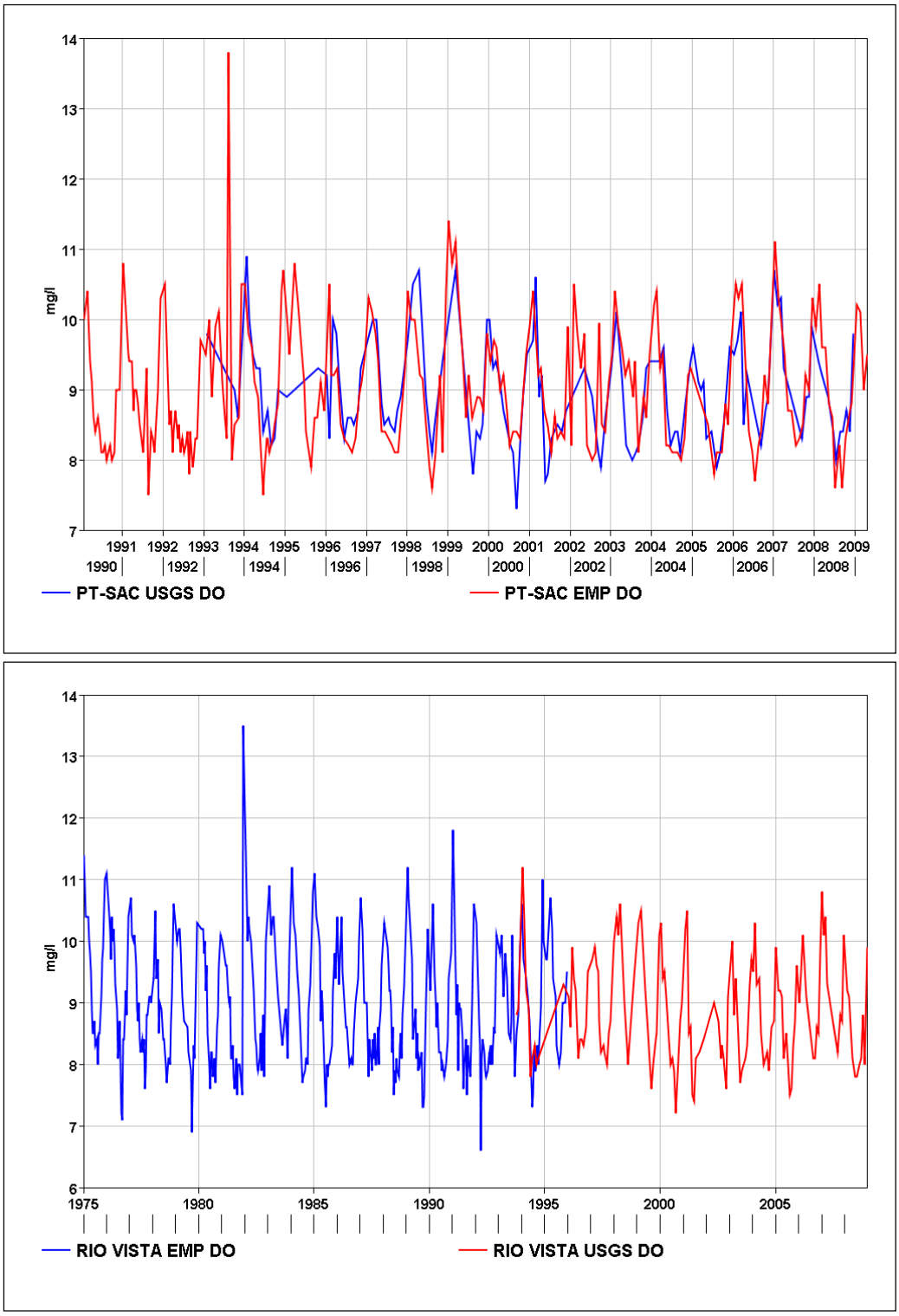

Figure 6-22 Comparison of EMP and USGS DO measurements at Point Sacramento (upper) Rio Vista (lower).

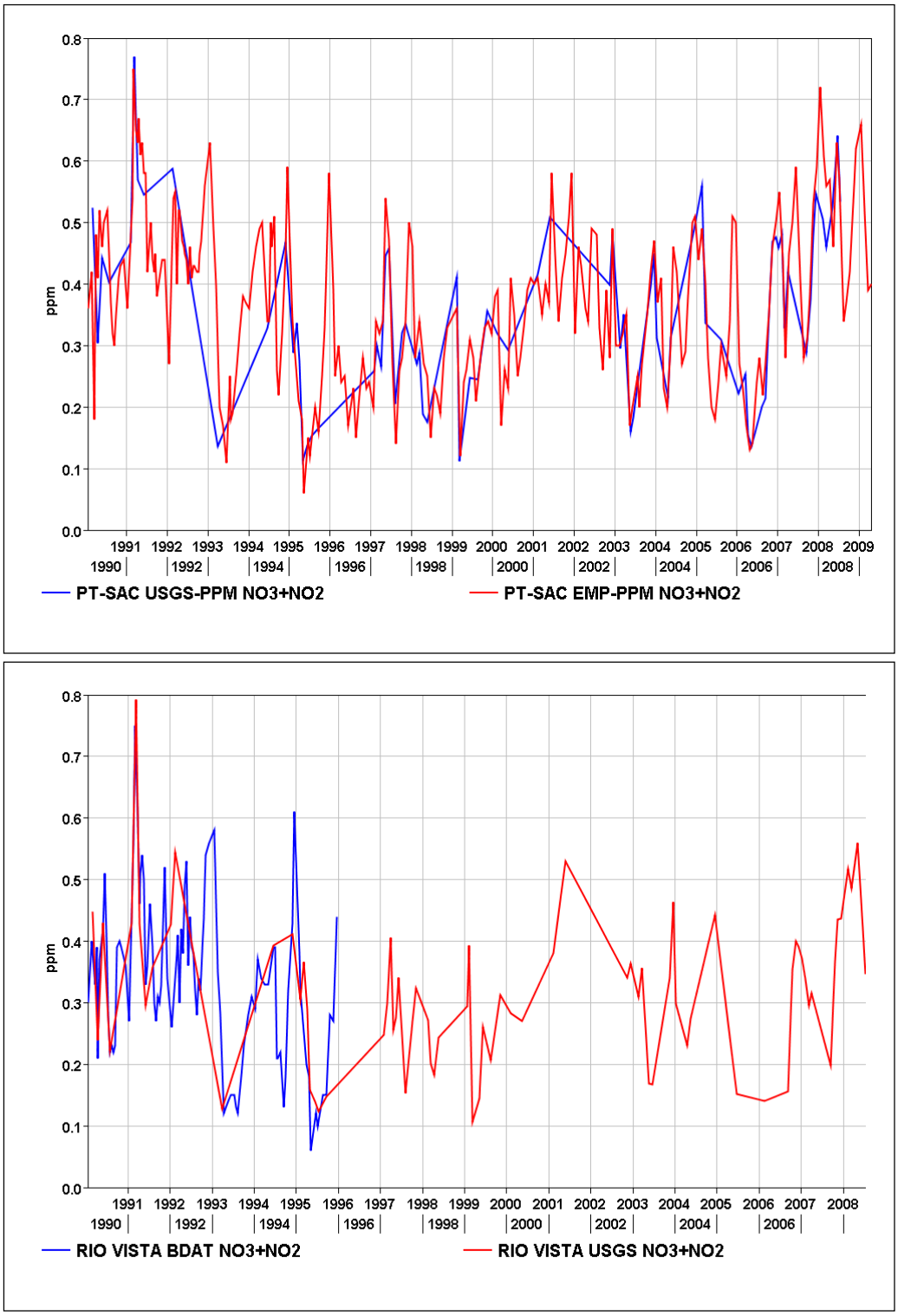

Figure 6-23 Comparison of EMP and USGS Nitrate+Nitrite (NO3+NO2) measurements at Point Sacramento (upper) Rio Vista (lower).

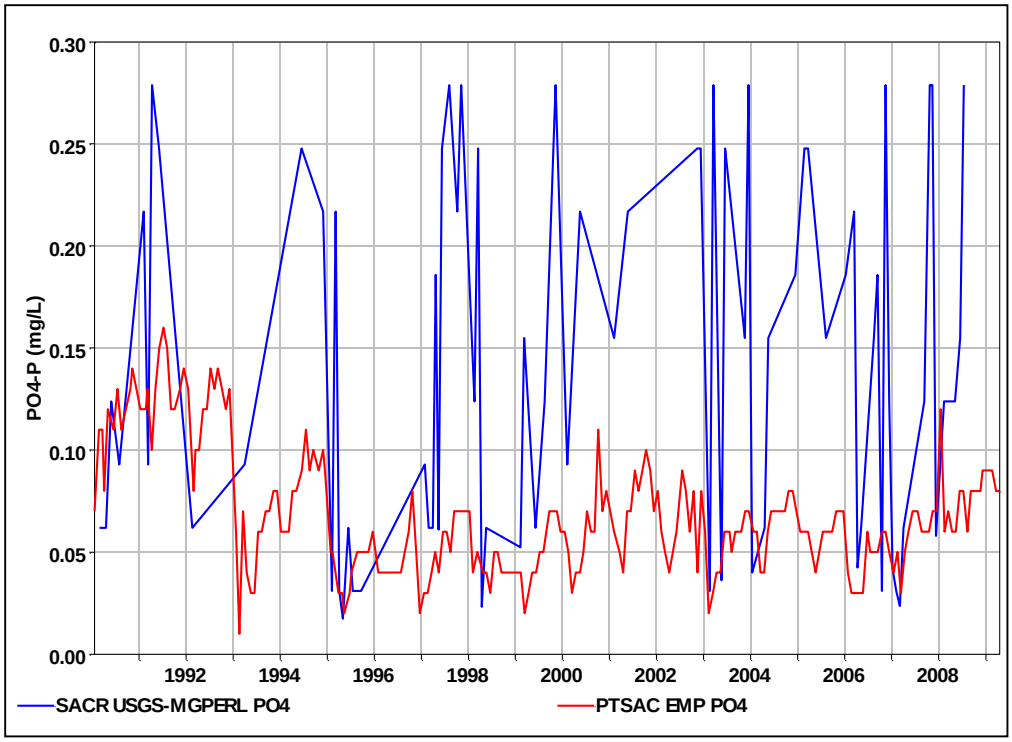

Figure 6-24 Comparison of EMP and USGS ortho-phosphate (PO_4) measurements at Point Sacramento.

Figure 6-25 Comparison of EMP and USGS Nitrate+Nitrite measurements near Martinez (upper) and near Chipps and Pittsburg (lower).

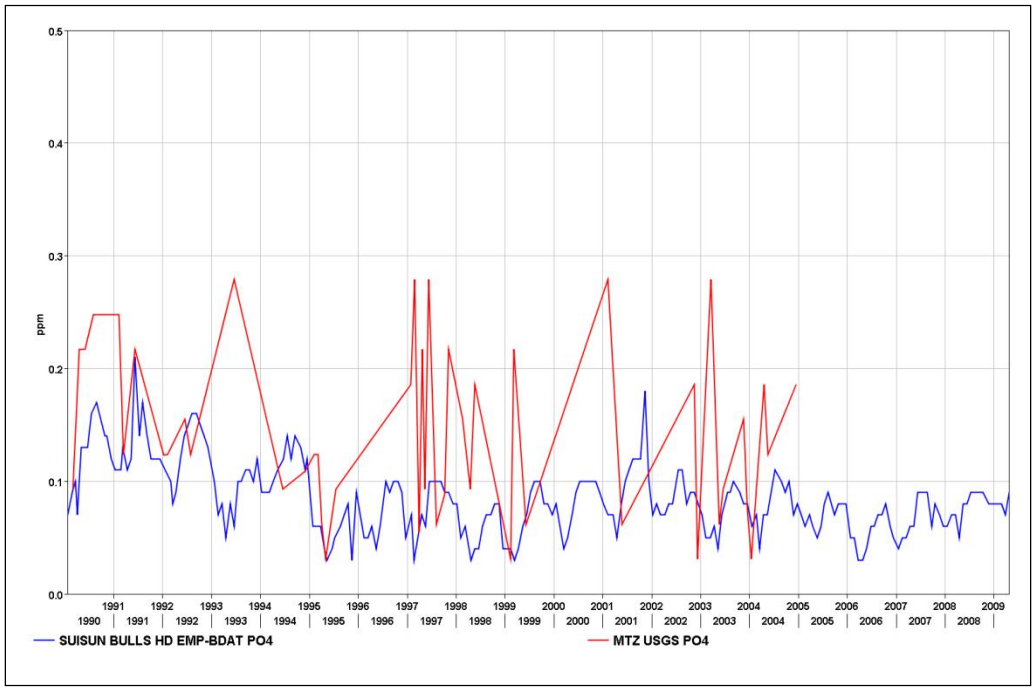

Figure 6-26 Comparison of EMP and USGS PO_4 measurements near Martinez.

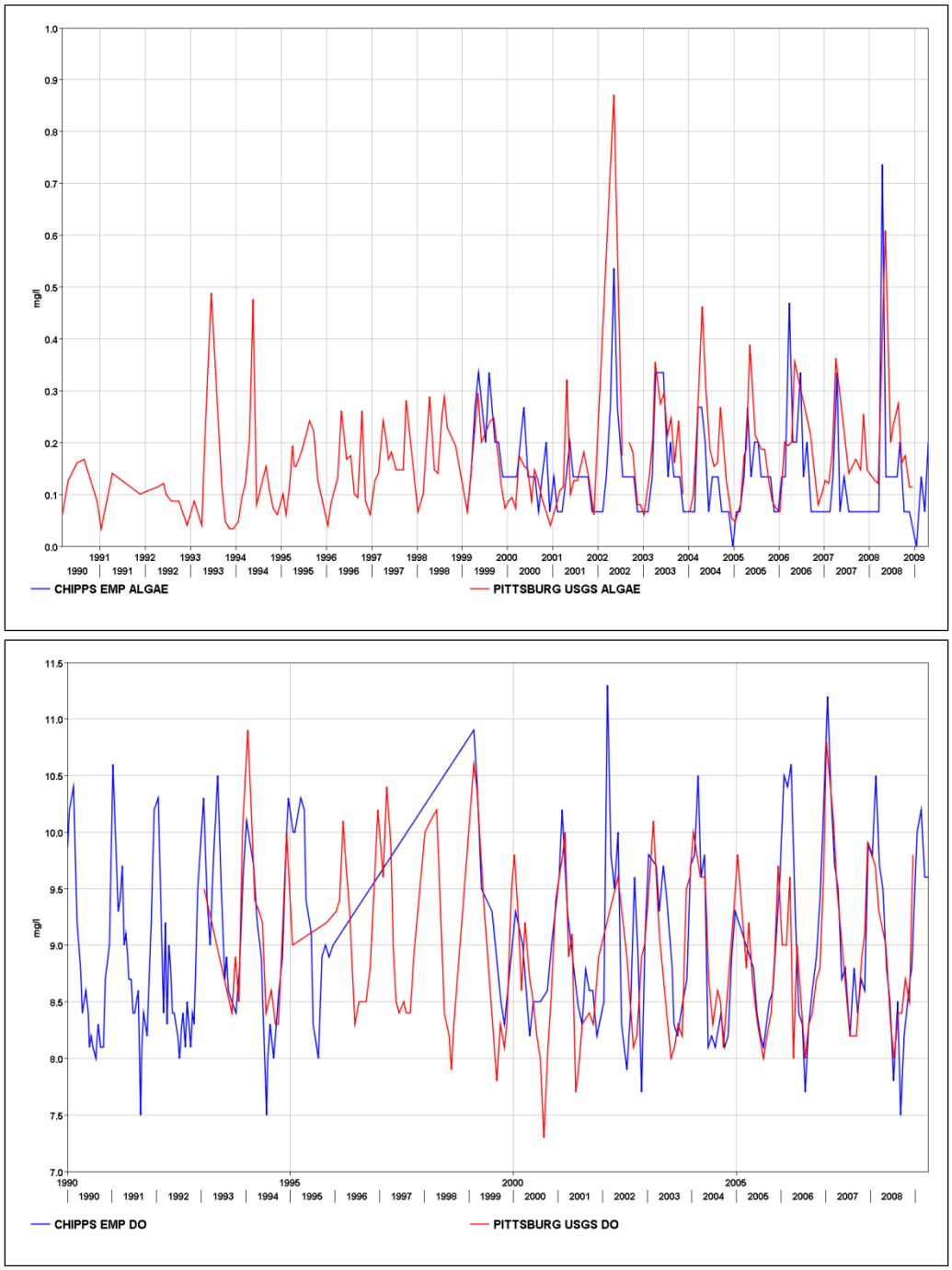

Figure 6-27 Comparison of EMP and USGS algae (upper) and DO (lower) measurements near Chipps and Pittsburg.

6.6 DSM2-QUAL: Re-Calibration of the Water Temperature Model

6.6.1 Background

The necessary first step in the process of recalibrating the DSM2-QUAL nutrient model was recalibrating the water temperature model. The water temperature transport equation can be calculated independently of the other constituents in the nutrient model. On the other hand, most of the equations in the nutrient model depend on the water temperature calculation. In previous nutrient model calibration simulation periods started in January, 2000 and ended December, 2008. The current project extends the end of the simulation period to March, 2012.

6.6.2 Regions in DSM2-QUAL Recalibration for Water Temperature

Although QUAL is limited to one meteorological region, previous model development and application have shown that at least two meteorological regions are needed for a good Delta-wide simulation of water temperature. For practical purposes, the meteorological data from the CIMIS stations near Lodi was used as the extensions of the nutrient model build upon previous work done in DWR using these stations – the initial DWR focus was on the San Joaquin River and dissolved oxygen concentration. In addition, the CIMIS meteorological data set near Lodi is relatively complete. Although the Lodi-area meteorological station set worked well for the south Delta and the San Joaquin River, water temperatures in the Sacramento River were too warm in the summer. The 2011 recalibration of QUAL-nutrient (Guerin, 2011) focused on the Sacramento River area, so modeled water temperature was recalibrated to favor accuracy in that region. To correct the temperatures in the Sacramento River area, an increase in summer wind speed by a factor of 2.0 (i.e., 2.0*summer wind speed) gave an acceptable fit for that region. The results that the south Delta and the San Joaquin River were then biased too cold during the summer.

The current project is Delta-wide – i.e., without a regional focus – so the previous wind speed factor was modified to improve water temperature calibration in other areas of the Delta. To this end, the meteorology was updated to run a series of simulations with the summer wind speed set as follows:

- Base case - no increase in summer wind speed
- Increase summer wind speed by a factor of 1.3
- Increase summer wind speed by a factor of 1.5
- Increase summer wind speed by a factor of 1.6
- Increase summer wind speed by a factor of 2.0 (2011 calibration value)

Using a data set of CDEC water temperature data (with clearly bad or suspect data removed), a residual analysis (Model – data) with several statistical measures to assess model goodness of fit were calculated at each data location for each of these simulations. The main statistics used were:

- Mean of the residual
- Standard deviation of the residual
- Root-mean-square-error
- Percent Bias

Locations in the Delta were categorized for each of the simulations by the minimum of the absolute value of the percent bias. Typically, the other three statistical measures followed the trend of the

percent bias to indicate which simulation was “the best” out of the five simulations at each location. The simulation increasing summer wind by a factor of 1.5 generally gave the best results for the entire set of data locations. The following plots are color-coded to show the spatial distribution of the locations where water temperature residuals were calculated – residuals were not calculated at light blue dot data locations. Not surprisingly, the locations where bias was minimized are grouped spatially – so, the green dots show locations were the “best” simulation used the Base Case wind speed, while the locations with the red dots had a minimum bias when summer wind was increased by a factor of 2.0.

The simulation with (wind speed)*1.5 in the summer was selected for the current calibration – in this simulation, half of the data locations have a positive bias, and half have a negative bias. Table 6-7 documents the resulting statistics recorded from the various water temperature test simulations.

6.6.2.1 Constituents Sensitive to Water Temperature Recalibration

Comparing the constituent concentration results for the simulation before recalibration (“Original”) with the simulation after recalibration (Summer Wind *1.5), the modeled concentrations of DO and NH3 saw the largest percent change during the summer period. At most locations, the percent change was on the order of 5 – 10%, while at some locations it was much greater. Figure 6-29 shows that percent changes in DO could reach upwards of 50% at EMP location P8, near Buckley Cove on the San Joaquin River.

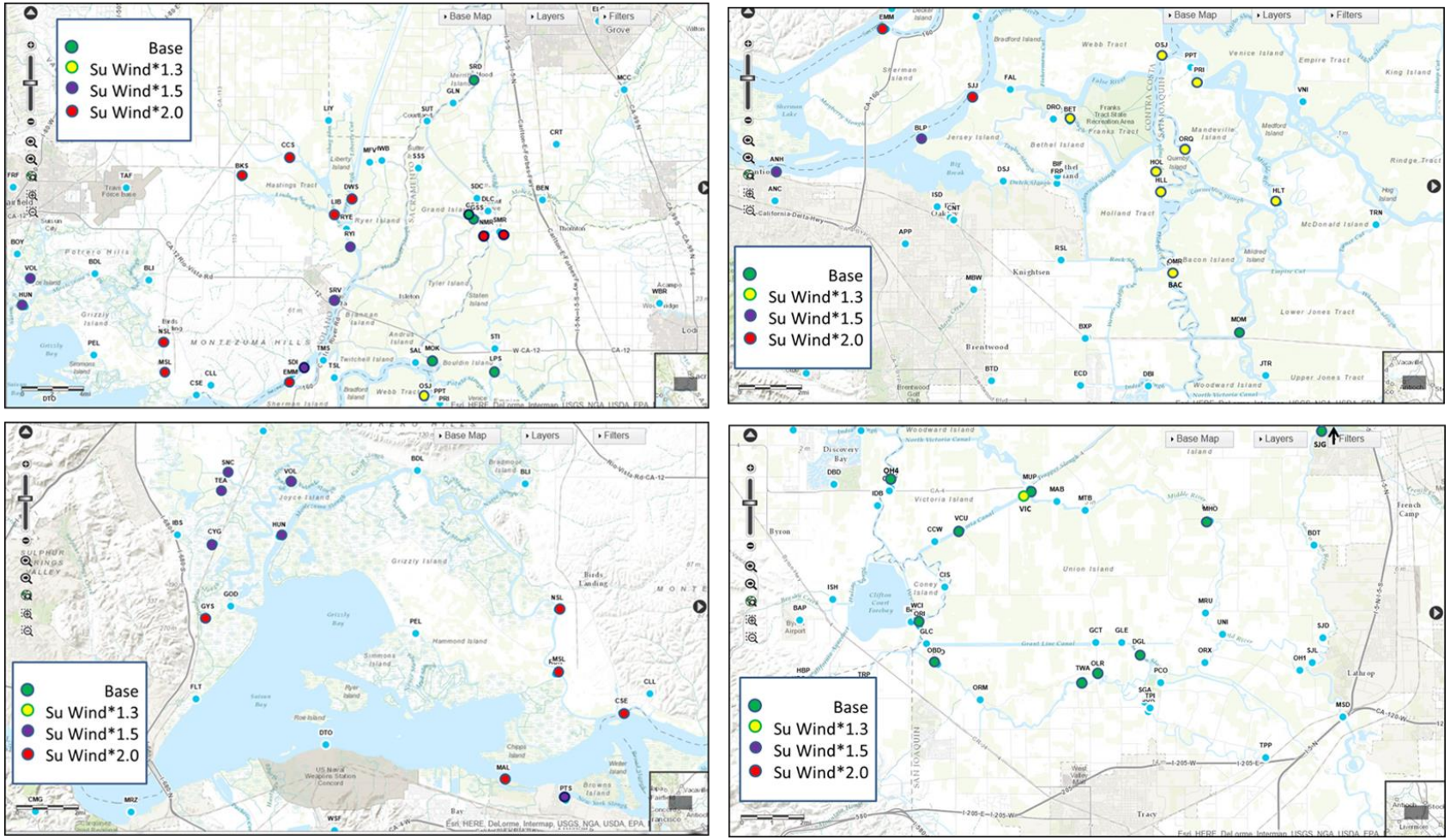

Figure 6-28 Spatial distribution of the locations where model residuals of Percent Bias (Model – CDEC water temperature data) were minimized for each of the four indicated simulations. Residuals were NOT calculated at locations with light blue dots.

Table 6-7 Locations and statistics used in water calibration. Entries are sorted and color-coded by the best statistical results for a given simulation factor (e.g. 1.50, second line in this table, increased summer wind speed by a factor of 1.5*velocity).

MODELNAME	CDEC	Region	N	mean resid	st dev resid	rmse	pbias	mean resid	st dev resid	rmse	pbias	mean resid	st dev resid	rmse	pbias	mean resid	st dev resid	rmse	pbias	mean resid	st dev resid	rmse	pbias
Simulation factor				**Base**				**1.3**				**1.50**				**1.6**				**2**			
RSAC092	EMM	Sac	4403	1.1	1.3	1.7	7.1	0.74	1	1.2	4.7	0.55	0.95	1.10	3.50	0.48	0.85	0.98	3	0.15	0.75	0.76	0.95
RSAC081	CSE	Sac	4413	1.3	1.5	2	8.2	0.86	1.2	1.4	5.4	0.65	1.10	1.30	4.10	0.56	1	1.1	3.5	0.2	0.86	0.89	1.3
RSAC075-MALLARD	MAL	Sac	4382	1.1	1.9	2.2	6.8	0.68	1.7	1.8	4.3	0.49	1.70	1.70	3.10	0.41	1.6	1.7	2.6	0.081	1.5	1.5	0.5
BARKER-SL	BKS	Cache/Yolo	370	1.8	2	2.7	11	1.1	1.6	2	6.8	0.83	1.50	1.70	5.00	0.67	1.4	1.6	4.1	0.15	1.3	1.3	0.92
SLCCH016	CCS	Cache/Yolo	4376	1.4	2	2.5	8.8	0.82	1.6	1.8	5	0.55	1.50	1.60	3.40	0.43	1.4	1.5	2.6	-0.037	1.3	1.3	-0.23
LIBERTY-D	LIB	Cache/Yolo	467	0.66	1.4	1.5	4.7	0.38	1.1	1.2	2.7	0.25	1.00	1.00	1.80	0.19	0.95	0.96	1.3	-0.027	0.8	0.8	-0.19
DWSC-DWS	DWS	Cache/Yolo	440	0.76	1.3	1.5	5.3	0.42	1	1.1	2.9	0.27	0.90	0.94	1.90	0.19	0.84	0.86	1.3	-0.061	0.7	0.7	-0.42
GOODYEAR-SL	GYS	SM	4269	0.94	1.7	1.9	5.8	0.49	1.4	1.5	3	0.29	1.40	1.40	1.80	0.2	1.3	1.3	1.2	-0.16	1.2	1.2	-1
RORR_512_MONTEZUMA	MSL	SM	1034	1.1	1.7	2	7.1	0.66	1.4	1.5	4.3	0.47	1.20	1.30	3.00	0.37	1.2	1.2	2.4	0.013	0.97	0.97	0.086
MONTEZUMA-NURSE	NSL	SM	1045	1.5	1.6	2.2	9.6	0.96	1.2	1.6	6.2	0.74	1.10	1.40	4.80	0.62	1.1	1.3	4	0.22	1	1	1.4
RSAN018	SJJ	SJR	4462	1.1	1.3	1.6	6.5	0.57	0.95	1.1	3.5	0.35	0.92	0.98	2.10	0.25	0.81	0.85	1.6	-0.13	0.75	0.76	-0.83
RSMKL024_SFMOKE	SMR	ED	467	0.39	0.83	0.92	2.9	0.37	0.82	0.9	2.7	0.36	0.82	0.90	2.70	0.35	0.82	0.89	2.6	0.34	0.81	0.88	2.5
NMR-RMKL019	NMR	ED	472	0.16	1.2	1.2	1.2	0.15	1.2	1.2	1.1	0.14	1.20	1.20	0.99	0.13	1.2	1.2	0.95	0.11	1.3	1.3	0.82
CACHE_RYER-RYI	RYI	Cache/Yolo	845	0.48	0.97	1.1	3.3	0.24	0.76	0.79	1.6	0.13	0.68	0.69	0.88	0.07	0.64	0.65	0.48	-0.13	0.55	0.56	-0.87
RSAC101	SRV	Sac	1576	0.57	0.9	1.1	3.7	0.27	0.68	0.73	1.7	0.14	0.61	0.63	0.88	0.062	0.58	0.59	0.4	-0.19	0.56	0.6	-1.2
DECKER	SDI	Sac	784	0.52	1.1	1.2	3.5	0.27	0.84	0.89	1.8	0.16	0.76	0.77	1.10	0.1	0.71	0.72	0.68	-0.1	0.6	0.6	-0.7
RSAC077-PITTSBURG	PTS	Sac	1547	0.63	1.4	1.5	4	0.23	1.1	1.1	1.5	0.06	1.00	1.00	0.38	-0.035	0.95	0.95	-0.22	-0.35	0.82	0.89	-2.2
CORDELIA	CYG	SM	702	0.86	1.7	1.9	5.4	0.35	1.4	1.5	2.2	0.14	1.30	1.30	0.85	0.019	1.3	1.3	0.12	-0.36	1.2	1.2	-2.3
SLMZU003-HUNTER	HUN	SM	723	0.88	1.5	1.7	5.6	0.45	1.2	1.3	2.8	0.26	1.10	1.10	1.70	0.16	1.1	1.1	1	-0.17	0.97	0.99	-1.1
SUNRISE-CLUB	SNC	SM	1580	1	1.6	1.9	6.6	0.48	1.3	1.4	3.1	0.25	1.20	1.30	1.60	0.13	1.2	1.2	0.84	-0.27	1.2	1.2	-1.7
TEAL-CLUB	TEA	SM	661	0.86	2	2.2	5.4	0.28	1.7	1.7	1.8	0.05	1.50	1.50	0.30	-0.079	1.5	1.5	-0.5	-0.48	1.3	1.4	-3
SLSUS012-VOLANTI	VOL	SM	4101	0.97	1.5	1.8	5.9	0.46	1.2	1.3	2.8	0.25	1.10	1.10	1.50	0.13	1	1	0.8	-0.26	0.97	1	-1.6
BLIND-POINT-BLP	BLP	SJR	756	0.74	1.3	1.4	4.7	0.3	1.1	1.1	1.9	0.12	1.00	1.00	0.77	0.017	0.98	0.98	0.11	-0.32	0.98	1	-2
RSAN007	ANH	SJR	4424	0.8	1.4	1.6	4.9	0.31	1.1	1.1	1.9	0.08	1.00	1.00	0.50	-0.008	0.91	0.91	-0.049	-0.4	0.8	0.9	-2.4
HOLLAND-TRACT	HLL	SD	4453	0.6	0.96	1.1	3.6	0.11	0.79	0.79	0.67	-0.11	0.81	0.82	-0.66	-0.2	0.78	0.81	-1.2	-0.59	0.89	1.1	-3.5
SLPPR003-BETHEL	BET	SD	1583	0.51	1.2	1.3	3.1	0.021	0.95	0.95	0.13	-0.18	0.88	0.90	-1.10	-0.3	0.86	0.91	-1.8	-0.68	0.89	1.1	-4.2
HOLLAND-CUT	HOL	SD	1492	0.31	1.1	1.1	2	-0.13	0.86	0.87	-0.8	-0.32	0.83	0.89	-2.00	-0.42	0.83	0.93	2.6	-0.77	0.93	1.2	-4.8
RMID005-HOLT	HLT	SD	2059	0.31	0.75	0.81	1.9	-0.14	0.58	0.6	-0.86	-0.34	0.59	0.68	-2.00	-0.45	0.62	0.77	-2.7	-0.82	0.81	1.2	-4.9
OLD-AT-FRANKS	OSJ	SD	1563	-0.38	0.99	1.1	2.4	0.019	0.79	0.79	0.12	-0.14	0.74	0.75	-0.86	-0.22	0.73	0.76	-1.4	-0.52	0.76	0.92	-3.3
OLD-R-QUIMBLY	ORQ	SD	1557	0.32	0.99	1	2	-0.12	0.8	0.81	-0.77	-0.31	0.78	0.84	-1.90	-0.41	0.78	0.88	-2.6	-0.76	0.89	1.2	-4.7
ROLD024	BAC	SD	3615	0.35	0.88	0.95	2.1	-0.12	0.73	0.74	-0.72	-0.32	0.73	0.80	-1.90	-0.43	0.75	0.87	-2.6	-0.8	0.9	1.2	-4.8
RMID023-VIC-ISLE	VIC	SD	4468	*0.24*	*0.66*	*0.71*	*1.4*	*-0.25*	*0.55*	*0.6*	*-1.4*	-0.47	0.66	0.81	-2.70	-0.56	0.65	0.86	-3.2	-0.95	0.89	1.3	-5.5
PRIS-PT-TERM	PRI	SJR	1568	0.22	0.79	0.82	1.4	-0.13	0.61	0.62	-0.79	-0.28	0.58	0.64	-1.70	-0.36	0.57	0.68	-2.3	-0.65	0.65	0.92	-4.1
RSAC123-BLW-DCC	GES	Sac	849	-0.2	0.29	0.35	-1.4	-0.23	0.28	0.36	-1.6	-0.25	0.28	0.37	-1.70	-0.26	0.28	0.38	-1.8	-0.3	0.28	0.42	-2.1
SLGEO-GEORG-SAC	GSS	Sac	847	-0.14	0.29	0.32	-0.94	-0.17	0.28	0.33	-1.2	-0.19	0.28	0.33	-1.30	-0.2	0.27	0.34	-1.4	-0.24	0.28	0.36	-1.7
RSAC142	SRD	Sac	4441	-0.17	0.4	0.43	-1.1	-0.22	0.41	0.46	-1.4	-0.24	0.42	0.49	-1.50	-0.25	0.42	0.49	-1.6	-0.3	0.44	0.53	-1.9
MOKEATSJR	MOK	SJR	1371	-0.04	0.47	0.47	-0.25	-0.19	0.4	0.45	-1.2	-0.26	0.39	0.47	-1.60	-0.3	0.4	0.49	-1.9	-0.44	0.44	0.62	-2.8
RSAN063-GARWOOD	SJG	SJR	851	-0.71	0.5	0.87	-4.5	-0.83	0.6	1	-5.3	-0.88	0.66	1.10	-5.70	-0.92	0.7	1.2	-5.9	-1	0.86	1.3	-6.6
LIT-POT-SL-TERM	LPS	ED	850	-0.17	0.53	0.56	-1.1	-0.31	0.46	0.56	-2.1	-0.38	0.45	0.59	-2.50	-0.42	0.45	0.61	-2.8	-0.56	0.49	0.74	-3.7
DOUGHTY-CUT	DGL	SD	1581	-0.35	0.66	0.75	-2.2	-0.61	0.65	0.89	-3.7	-0.72	0.70	1.00	-4.40	-0.79	0.75	1.1	-4.8	-1	0.95	1.4	-6.2
RMID015_144_MIDATMID	MDM	SD	850	-0.14	0.7	0.71	-0.88	-0.5	0.55	0.74	-3.1	-0.65	0.56	0.86	-4.10	-0.74	0.59	0.94	-4.6	-1	0.76	1.3	-6.4
RMID041-UNION	MUP	SD	711	-1.2	1.7	2.1	-6.9	-1.3	1.7	2.1	-7.5	-1.30	1.60	2.10	-7.80	-1.3	1.6	2.1	-7.9	-1.4	1.6	2.2	-8.6
MIDDLE-R-HOWARD	MHO	SD	511	-0.41	0.42	0.59	-2.8	-0.45	0.43	0.63	-3.2	-0.48	0.44	0.65	-3.30	-0.49	0.45	0.66	-3.4	-0.53	0.49	0.72	-3.7
ROLD040-CCFB	ORI	SD	393	-0.79	0.36	0.87	-4.9	-0.97	0.38	1	-6	-1.00	0.42	1.10	-6.50	-1.1	0.45	1.2	-6.8	-1.2	0.6	1.4	-7.6
ROLD046-DMC	OBD	SD	821	-0.12	0.75	0.76	-0.79	-0.39	0.51	0.64	-2.5	-0.50	0.45	-0.67	-3.20	-0.57	0.43	0.71	-3.6	-0.79	0.49	0.95	-5
ROLD034	OH4	SD	848	-0.19	0.72	0.75	-1.2	-0.53	0.59	0.79	-3.3	-0.68	0.60	0.90	-4.30	-0.76	0.62	0.98	-4.8	-1	0.78	1.3	-6.5
ROLD059-TRACY	OLR	SD	2551	0.082	0.94	0.94	0.49	-0.26	0.93	0.97	-1.5	-0.40	0.98	1.10	-2.40	-0.48	1	1.1	-2.9	-0.77	1.2	1.4	-4.6
OLD-R-TWA	TWA	SD	441	-0.46	-0.36	0.58	-3.1	-0.53	0.33	0.62	-3.6	-0.56	0.33	0.65	-3.80	-0.58	0.33	0.66	-3.9	-0.64	0.35	0.73	-4.3
AIP_229-VICT-BYRON	VCU	SD	1923	0.2	0.7	0.73	1.2	-0.29	0.54	0.61	-1.7	-0.49	0.57	0.76	-2.90	-0.6	0.62	0.87	-3.6	-0.99	0.87	1.3	-6.6

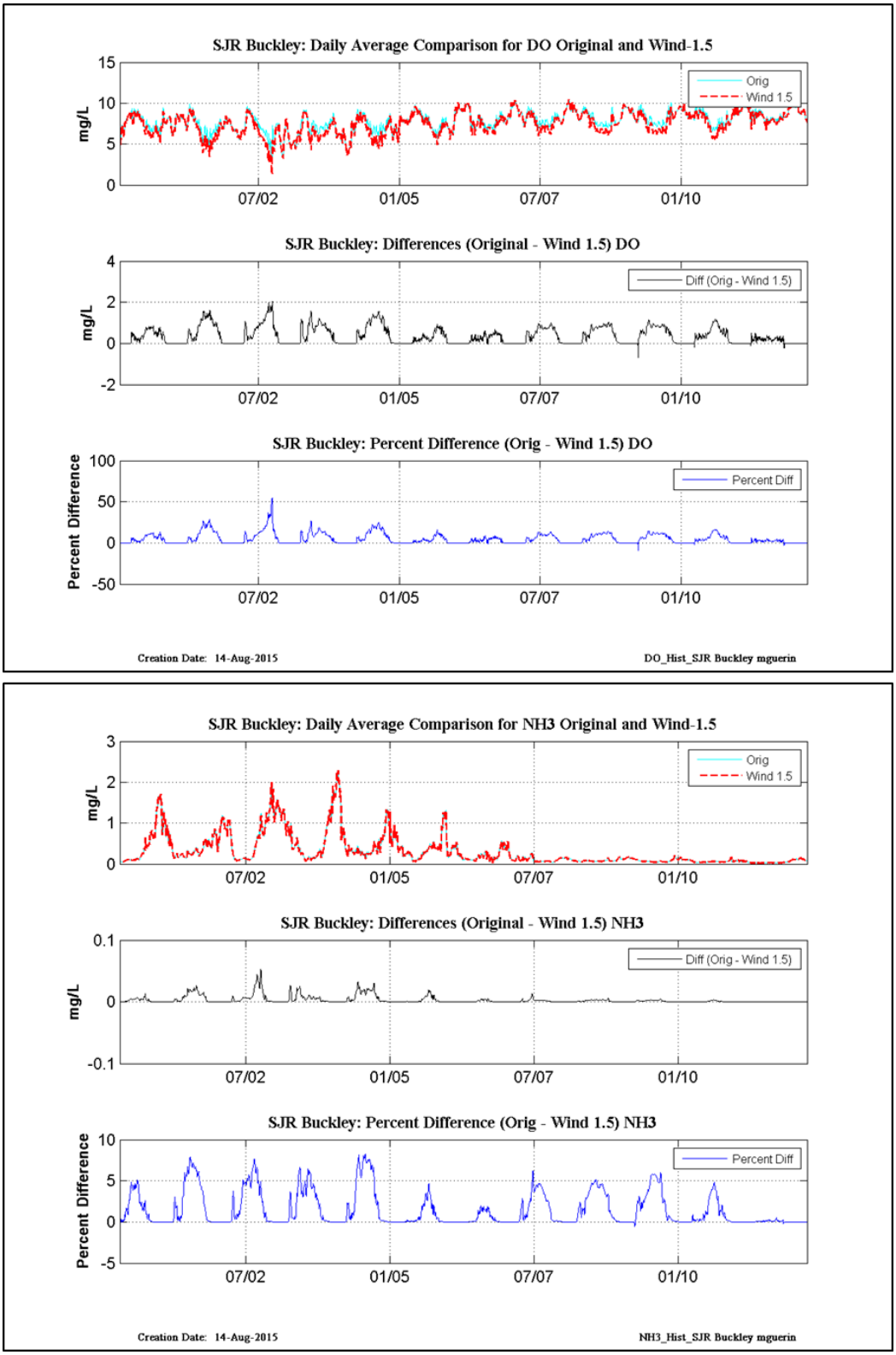

Figure 6-29 This figure documents the changes in DO and NH3 concentration at site P8, Buckley Cove on the San Joaquin River, solely due to changes in meteorology – the previous calibration values are denoted 'Orig' (for: Original Simulation) and the updated meteorology is denoted 'Wind 1.5' (for: summer wind increased by a factor of 1.5)

6.7 Recalibrating the DSM2-QUAL Nutrient Model

At the outset, it is important to note that a model calibration is not unique – there are an infinite number of ways to calibrate a model. For example, the objective for a particular project may focus more intensively on some constituents or in some subregions more than others. For the calibration in this project, the nitrogen-bearing constituents are the focus, although all model constituents were subject to calibration constraints (with the proviso that there was calibration data available). Since the nutrient model equations are not mutually independent, changes in the calibration of one constituent can result in less than desirable changes in another constituent. For example, improving the NH_3 calibration can easily results in change in the calibration status of NO_3 and of algae. In particular, the calibration process will invariably require judgment decisions to be made by the modeler.

There are two types of parameters that were used to recalibrate the nutrient model to better fit calibration data, global parameters and channel-specific parameters. Global parameters, as the name suggests, apply to the entire model domain – i.e., changing the value of the parameter will influence model calculations everywhere. Channel-specific parameters in DSM2 are applied individually to user-specified channels in the grid, *i.e*., they spatially-variable (NOTE: the DSM2 grid is composed of channels of variable length connected by nodes).

As mentioned in Section 6.4, the calibration update began by setting all channel-specific parameters to region-specific values. Global parameter values were varied to make minor adjustments that would help model domain-wide. Then multiple calibration runs were employed to modify channel-specific parameters to bring the model as close to calibration as possible in as many data locations as possible, where calibration is defined herein minimizing the difference between the set of data values and the modeled values.

The EMP dataset of nutrient concentrations and locations was the primary data source used for calibration, although some USGS data was also used as well as receiving water data for several wastewater treatment plants with outflows in the Delta. Of these wastewater facilities, the Stockton facility on the San Joaquin River had supplied an extensive data set to the project which proved invaluable for calibrating that portion on the model domain. For a few of the other WWTP facilities, some limited receiving water data was available for the period 2011 – 2012.

6.7.1 Global Parameters

After the water temperature recalibration was complete, nutrient model global parameters were used for calibration. Global model parameters are set in a QUAL input file - the nutrient conditions they influence are varied. Those parameters that affect only the water temperature equation, such as meteorological parameters, were not considered in this part of the calibration process. For the purposes of this nutrient model recalibration, those parameters that effect light availability for algal growth were not varied – note that in reality, these conditions will vary both in time and in space within the Delta. For each global parameter change, the model effects for specific nutrients were assessed at EMP locations with available data.

There are numerous parameters that influence the temperature dependence of constituent rate parameters. Those parameters dealing with the temperature dependence of the CBOD equation were

not varied (i.e., were held within previous literature values) as there is a lack of CBOD data to assess the change in parameter value. For the oxygen equation, the only parameter that was varied was the "reaeration parameter". For the algae equation, several temperature dependence coefficients were varied, for: algal growth; algal death; algal fraction N; algal fraction P; and, algal preference for NH3 over NO_3. For the ammonia equation, the temperature dependence parameters for benthic sources and for decay were varied. For the NO_2 equation, the only global parameter was varied – that for NO_2 decay. There were no global parameters dealing with the NO_3 equation. For organic-N and organic-P, the temperature dependence parameters for decay and settling were varied. In addition for organic-P, the temperature dependence parameter for benthic sources was varied. Although there is no EMP data for organic-P, changing the parameters for this constituent can change the concentration of PO_4 (dissolved-P).

Global model parameters apply to the entire model domain, so, as mentioned above, when altered the effects of the parameter change will be felt everywhere. For some global parameters this is a good assumption, for others a problem arises for a model with as many diverse conditions as DSM2 conceptualizes in the Delta. An example of the latter is the oxygen equation for reaeration temperature dependence –when varied the effects were quite diverse over the Delta. This is an example of a parameter that would benefit from being a spatially variable parameter, as there is evidence that values should vary dependent on local conditions (Langbein *et al*., 1967). The effects of global parameter variation influenced not only the magnitude of the nutrient concentrations affected, but sometimes also the timing, as a parameter change could advance or delay the onset of a nutrient concentration change.

Details on the final global parameter values can be found in the associated DSM2 input file.

6.7.2 Spatially –Variable Parameters

The fine-tuning of the constituent concentrations was accomplished in numerous model simulations – parameter values within individual channels were sometimes changed, at other times all the parameter values within a region were changed to a single value. Parameter values for the reservoirs were for the most part held at the initial values, except for Liberty Island which had the benefit of a short time span of measurement data (Lehman *et al*., 2010).

This portion of the calibration process began by working with parameters influencing the NH_3 and NO_3 concentrations, working regionally but leaving the San Joaquin Region (SJR) untouched initially as the downstream influences of San Joaquin River concentrations is relatively small. Concentrations of algae were then calibrated, followed by Organic-N, PO_4 and DO. There was insufficient NO_2 data to calibrate for NO_2, but changes in the parameter values for NO_2 were used to impart a minor effect on NO_3 concentrations. Similarly, Organic-P parameters were varied to influence PO_4 concentrations. Using the available data for constituent concentrations in Liberty Island, the calibration for that reservoir consisted of a combination of variation in constituent parameters and boundary condition concentrations for the Yolo/Lisbon Toe Drain inflow (there was no data available for setting inflow concentrations there).

The San Joaquin Region was calibrated after the initial round of calibration for the other regions, The Stockton wastewater facility had supplied an extensive dataset of concentrations for their receiving water locations were used to calibrate that portion of the model domain.

The results from the initial channel-specific parameter tuning process was then reviewed, and multiple changes were then implemented. In particular, the concentration boundary condition for NO_3 on the

Sacramento River was reduced as the modeled NO_3 concentrations were high at all locations heavily influenced by Sacramento River waters. Note that the concentrations at the Sacramento River boundary were set in order to match downstream locations as there was not sufficient data to use for setting these concentrations using a primary data source (details are found in (Guerin, 2011)).

The full set of calibration statistics using methodology described in the following section are found in Section 6.12.4 in this document.

6.7.3 Nutrient Model Calibration Evaluation

6.7.3.1 Background

Both graphical and statistical model evaluation techniques were used in the analysis of calibration and validation results. EMP data was used at all locations, with the exception that along the San Joaquin River, Stockton WWTP receiving water data was used.

6.7.3.2 Methodology

Nutrient calibration results were grouped for the calculation of calibration statistics for the entire calibration/validation period (all years). These years were also subdivided into calibration and validation ranges, shown in Table 6-8, and grouped into Dry Years and Wet Years.

Because nutrient data was only available on a monthly basis and the number of data points was limited, only two types of hydrologic conditions[15] were considered is assessing the quality of the calibration by inflow conditions. The Wet type is composed of Wet and Above Average Water Year types, while the Dry type is composed of Critically Dry and Dry Water Year types:

Table 6-8 Calibration and validation years used in calculating residual statistics

	Calibration Years	Validation Years
DRY	2001, 2002, 2009	2007, 2008
WET	2000, 2003, 2011	2005, 2006

Several statistics were calculated along with residual histograms for All Years, Dry Years and Wet Years, but only three statistical measures are used to calculate measures of Model Skill and discussed herein – Nash-Sutcliffe Efficiency (NSE), RMSE-Standard deviation Ratio (RSR), and Percent Bias (PBIAS). These statistics give an overall view of the quality of the calibration – the statistical measures are discussed in Section 6.7.5.1. At each location where calibration data was available, model statistics were calculated and ranked categorically as Very Good, Good, Satisfactory or Unsatisfactory using ranges of the statistics to perform the rankings. Ranges for model calibration performance ratings for the NSE, RSR and PBIAS statistics are discussed in (Moriasi *et al*., 2007).

6.7.4 Definition of the statistical calibration/validation measures

The following methodology and statistics adapted from (Moriasi *et al*., 2007) were used:

[15] See: http://cdec.water.ca.gov/cgi-progs/iodir/wsihist for a discussion of water year type.

Mean Residual – The mean of the residual values gives an indication of the magnitude of model under-prediction (positive residuals) or over-prediction in a region. The optimal value is zero, which occurs in the unlikely situation that the model is a perfect fit for the data.

Standard Deviation of Residual – The standard deviation of the residual values gives an indication of the variability in model under-prediction and over-prediction in a region.

Residual Histogram – The histogram documents the shape of the residual distribution. Along with the mean and standard deviation, this gives a first-order view of the goodness of model fit. The ideal histogram would have an approximately normal shape centered at zero with a small spread. Histograms were prepared using all year, wet year and dry year ranges for calibration and validation calculations at each location.

MSE – The Mean Squared Error is a standard statistic that measures the quality of the prediction. The optimal value is zero:

$$MSE = \left[\frac{\sum_{i=1}^{n} \left(Y_i^{Obs} - Y_i^{Sim} \right)^2}{n} \right] \quad \text{(A3)}$$

RMSE – The Root Mean Squared Error is a standard statistic used to indicate the accuracy of the simulation. It is the square root of the MSE. The optimal value is zero.

NSE – The Nash-Sutcliffe Efficiency is a normalized statistic that measures the relative magnitude of the residual variance compared to the data variance. NSE indicates how well the measured vs. modeled data fit the 1:1 line (Moriasi et al., 2007). A value of 1 of optimal, values between 0 and 1 are acceptable, and negative values indicate that the data mean is a better predictor of the data than the model:

$$NSE = 1 - \left[\frac{\sum_{i=1}^{n} \left(Y_i^{Obs} - Y_i^{Sim} \right)^2}{\sum_{i=1}^{n} \left(Y_i^{Obs} - Y_i^{Mean} \right)^2} \right] \quad \text{(A4)}$$

PBIAS – Percent bias measures the average tendency of the simulated data to be larger or smaller than the measured data. A value of 0 is optimal – a positive value indicates underestimation bias and a negative value indicate overestimation bias:

$$PBIAS = \left[\frac{\sum_{i=1}^{n} \left(Y_i^{Obs} - Y_i^{Sim} \right) * 100}{\sum_{i=1}^{n} \left(Y_i^{Obs} \right)} \right] \quad \text{(A5)}$$

RSR – The RMSE-observation standard deviation ratio is a statistic that normalizes the RMSE using the standard deviation of the observations. Because it is normalized, it can be used to compare errors among various constituents (Moriasi et al., 2007). A value of 0 is optimal:

$$RSR = \frac{\left[\sqrt{\sum_{i=1}^{n}\left(Y_i^{Obs} - Y_i^{Sim}\right)^2}\right]}{\left[\sqrt{\sum_{i=1}^{n}\left(Y_i^{Obs} - Y_i^{Mean}\right)^2}\right]} \quad \text{(A6)}$$

6.7.5 Calibration/validation statistics and residual analysis

6.7.5.1 Nutrient Calibration – Use of Model Monthly Max-and-Min

The methodology for assessing the calibration of nutrients and DO required special development. Because nutrient model boundary conditions for each month are generally composed of grab samples taken on a (approximately) monthly basis, data for different nutrients are generally sampled at different times on different days, and calibration data is also composed of grab samples, comparing average monthly model output values (the appropriate time scale given the boundary condition time scale) with an instantaneous data measurement did not make sense.

Instead, calibration data measurements were compared with modeled monthly maximum and minimum values – this is denoted the modeled monthly nutrient "envelope". If the calibration data fell within the envelope (i.e., was less than the maximum and greater than the minimum), the residual was calculated as zero. Otherwise, the residual was calculated as the difference between the data value and the nearest envelope value. So, for example, if the data was lower than the modeled monthly minimum, the residual (data – model minimum) would be negative.

Conceptually, the nutrient calibration is thus interpreted to be accurate if the data falls within the model envelope, and then the residual is zero. Calculations of residual statistics use these zero values and the positive and negative residual values for data points that fall outside the envelope.

Model bias, i.e., the underestimation or overestimation of data by the model, was calculated but should be interpreted with the following provisos: when data was listed as "Below Detection limit" (BDL), data point was excluded from the residual calculation. When many values were BDL, the number of data points used to calculate model statistics could be very small. Thus, although calibration or validation statistics were calculated for all relevant years and also split into wet and dry year types, the quality of the statistics may be dominated by a few measurements.

Note that using the method of model Max-and-Min for calculating residual statistics generally will overestimate the residual value in comparison with a residual calculated using average monthly model value. Previous nutrient model calibration (Guerin, 2011) were calculated using a reduced model envelope widths (*e.g.*, 95%, 90%80% and 75% of the full width) in addition to the full width envelope. Generally speaking, the sign of the Bias (positive or negative) did not change at any location – in general almost no change was noted in the assessment of the model calibration.

6.7.5.2 Residual Analysis of the Nutrient Model

All statistics mentioned above were calculated in the calibration and validation of the nutrients. In addition, residuals were assessed by plotting residual histograms. The majority of the calibration data were from EMP locations. There was no CBOD or Organic-P data available for calibration and validation over the simulation time span. BOD measurements were lacking except in the upstream reach along the San Joaquin River, and these were limited in the temporal frame. The measurements for NO_2 individually were sparse.

Only RSR, PBIAS and NSE were used to categorically evaluate the results as discussed in (Moriasi et al., 2007). The recommendations in that paper were followed with one modification. Unlike the ranges used in Moriasi (2007), NSE was ruled unsatisfactory only when negative, so the satisfactory range was essentially extended to all positive values. Thus, the following categories were used to evaluate the quality of the nutrient constituent calibration:

Table 6-9 Categories used to rate the quality of the nutrient calibration/validation.

Performance Rating	RSR	NSE	PBIAS (%)	Categorical Rating
Very Good	0.00 ≤ RSR ≤ 0.50	0.75 < NSE ≤ 1.00	PBIAS < +/- 25	**1**
Good	0.50 < RSR ≤ 0.60	0.65 < NSE ≤ 0.75	+/- 25 ≤ PBIAS < +/- 40	**2**
Satisfactory	0.60 < RSR ≤ 0.70	0.00 ≤ NSE ≤ 0.65	+/- 40 ≤ PBIAS < +/- 70	**3**
Unsatisfactory	RSR > 0.7	NSE < 0.0	PBIAS ≥ +/- 70	**4**

The PBIAS ranges are specific to N- and P-nutrients, the ranges for RSR and NSE are not constituent-specific in the general performance ratings presented in (Moriasi et al, 2007). PBIAS ranges for constituents tend to be more lenient than those listed for streamflow or sediment transport. Thus, we can expect that the ratings for RSR and NSE are quite strict when applied to constituent calibration/validation statistics. To accommodate this observation somewhat, the NSE range for "Satisfactory" was extended to all positive values. The range for RSR was not altered.

An assessment of "Model Skill" for each calibrated constituent was made for the model domain using the categories and numerical values shown in Table 6-9. Model Skill is defined loosely as a summary measure of the model capabilities to simulate nutrient dynamics. The Model Skill assessment is discussed in Section 6.10.

6.7.6 Calibration Plots

6.7.6.1 Types of Calibration Information

Three types of information on the QUAL nutrient model calibration are presented in this section - regional representation of model bias by calibrated constituent (Figure 6-32, Figure 6-36, Figure 6-42, Figure 6-46, Figure 6-55, Figure 6-56), selected time series plots comparing calibration data with modeled monthly Max and Min of constituents, and tables of categorical statistics of the calibration measures by location and constituent. There are no striking differences between Dry or Wet water year types for either calibration or validation periods, so they won't be discussed further.

Additional time series plots of WWTP data vs. Model Max and Min are found in Section 6.12.2. Detailed calibration and validation histograms along with the full set of calibration and validation statistics defined in Section 6.7.4 for All, Dry and Wet Historical periods is found in Section 6.12.4.

6.7.6.2 Discussion of Calibration Information

Figure 6-33 and Figure 6-43 illustrates the comparison of Algae data and monthly Max-Min model output at EMP data locations, while Figure 6-57and Figure 6-58 illustrates the Stockton WWTP Algae data *vs.* model output on the San Joaquin River.

At several EMP locations (Figure 6-33), for example at D4, the model output captures the data trends, but misses the peak concentrations. At a number of other locations, for example at D7, the model overestimates the peaks as the data at these locations decreases substantially during periods that otherwise facilitate algal growth, possible due to grazing by clams. On the San Joaquin River, the data is

more numerous and the measurements are frequently below detection limits, but modeled peak values generally match data peaks.

Figure 6-34 and Figure 6-44 illustrates the comparison of DO data and monthly Max-Min model output at EMP data locations, while Figure 6-65 and Figure 6-66 illustrates the Stockton WWTP DO data *vs.* model output on the San Joaquin River. In general, the model captures DO trends and values very well in the model domain, although Suisun Marsh model results (and a few other locations) were not captured within reasonable parameter values.

Figure 6-35 and Figure 6-45 illustrates the comparison of PO_4-P data and monthly Max-Min model output at EMP data locations, while the Stockton WWTP did not collect PO_4-P data on the San Joaquin River. In general, the model captures PO_4-P trends quite well in the model domain, although the number of locations is very limited which certainly resulted in overall results being less acceptable in comparison with DO data.

Figure 6-37 and Figure 6-47 illustrates the comparison of NH_3-N data and monthly Max-Min model output at EMP data locations, while Figure 6-59 and Figure 6-60 illustrates the Stockton WWTP NH_3-N data *vs.* model output on the San Joaquin River. The model follows EMP data trends fairly well except along the San Joaquin River, and the Stockton WWTP model-data comparisons are better at upstream data locations than at downstream data locations, Figure 6-59 and Figure 6-60 respectively. The results on the San Joaquin River are difficult to explain, as the boundary condition data sets are comparatively very good along the river.

Figure 6-37 and Figure 6-48 illustrates the comparison of NO_3+NO_2-N data and monthly Max-Min model output at EMP data locations, while Figure 6-61 and Figure 6-62 illustrates the Stockton WWTP NO_3-N or NO_3+NO_2-N data *vs.* model output on the San Joaquin River. The model results for these constituents are generally very good both in capturing trend and values. Note that there was a trade-off for capturing these constituents *vs*. NH_3-N data.

Figure 6-37 and Figure 6-49 illustrates the comparison of Organic-N data and monthly Max-Min model output at EMP data locations, the Stockton WWTP Organic-N data was sparse at measurement locations, so calibration statistics are not included herein. Figure 6-63 and Figure 6-64 illustrate the Stockton WWTP data *vs.* model output on the San Joaquin River. The model results for these constituents are generally very good in capturing EMP trends – data values were frequently at EMP stated detection limits. For the Stockton WWTP Organic-N data, the model results generally captured values better before the WWTP switched to tertiary treatment.

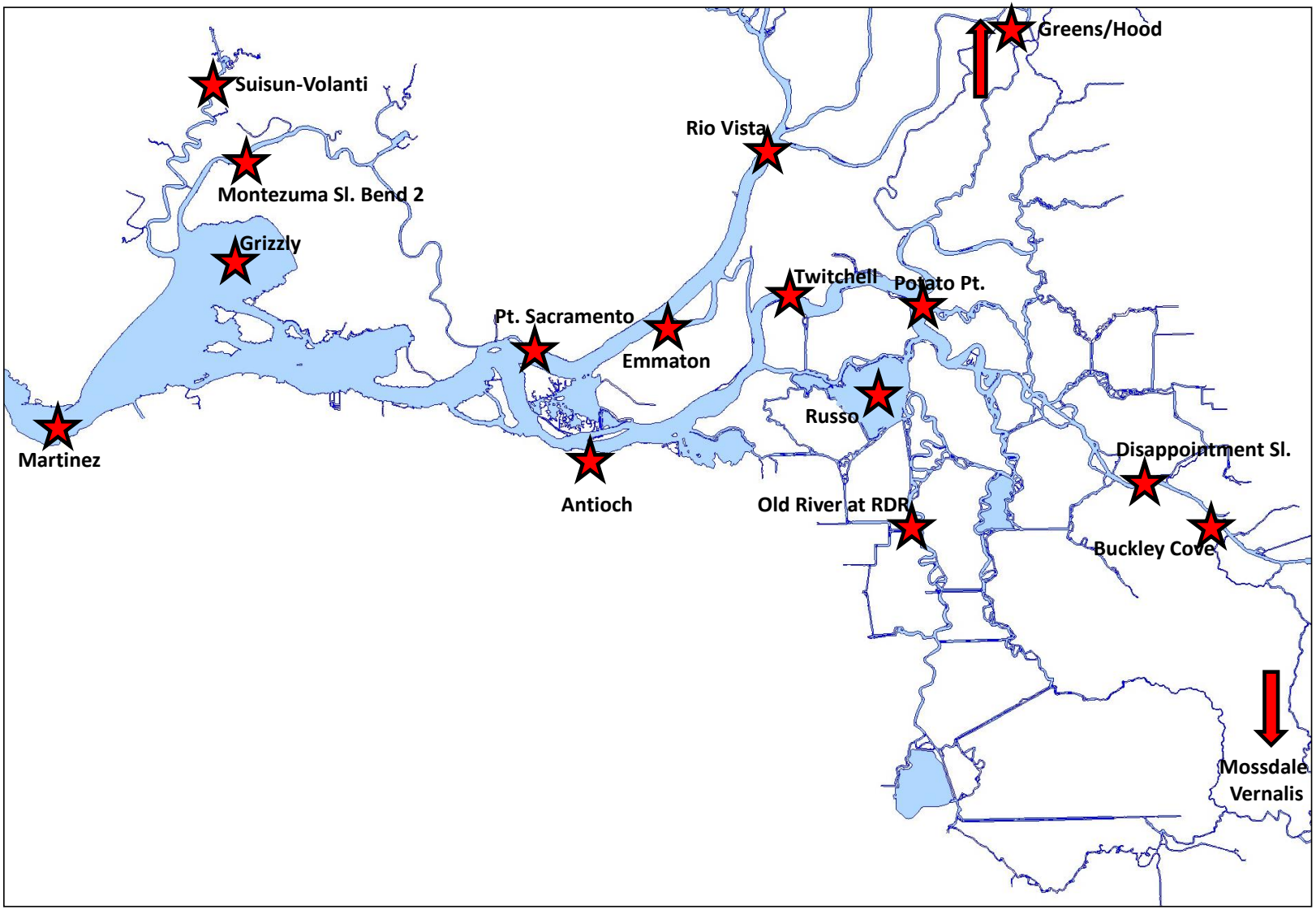

Figure 6-30 This figure shows the locations (with the exception of boundary conditions) where EMP data was used to calculate residual statistics used in the model calibration/validation. Only a few locations had measurements for the majority of the constituents.

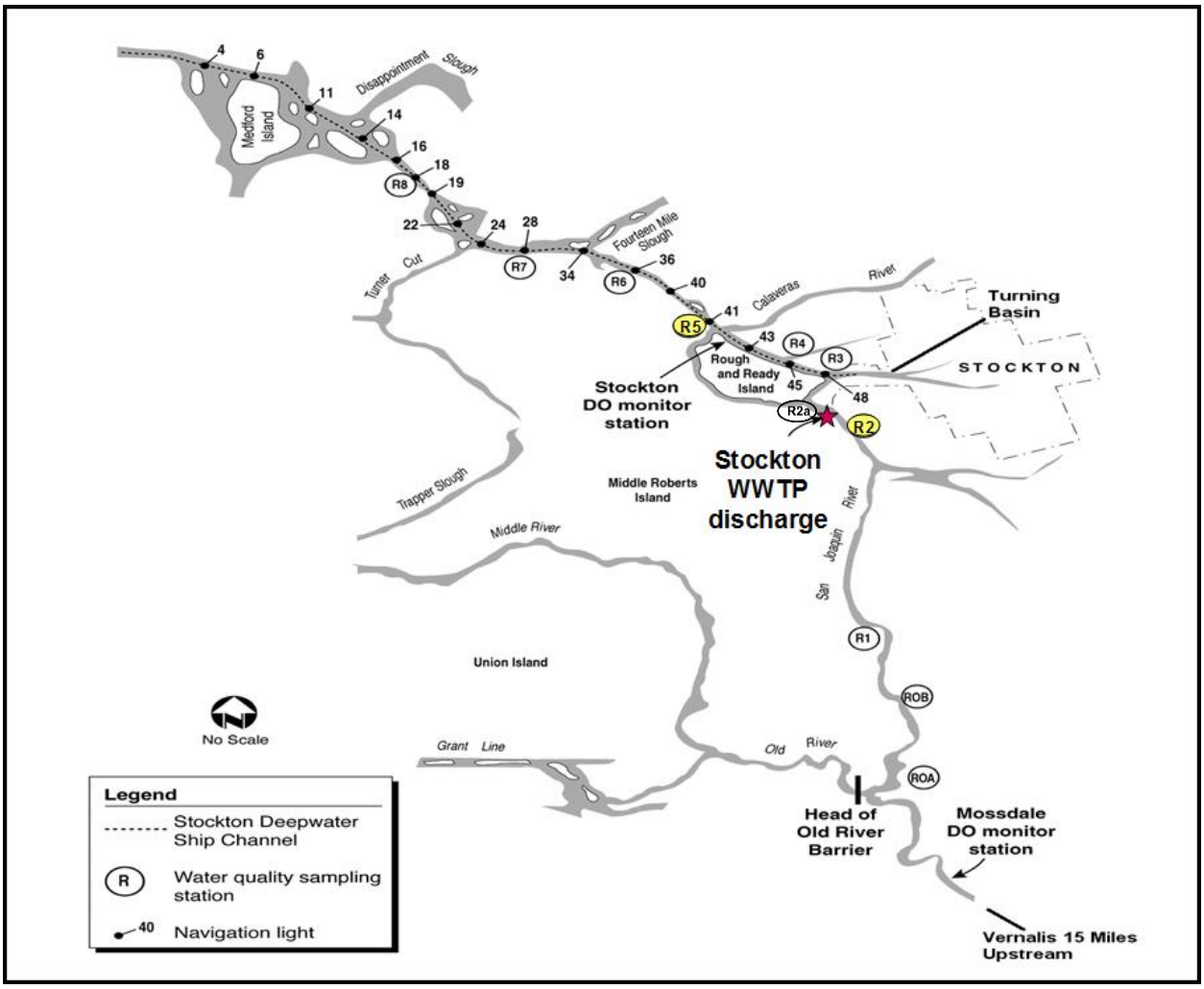

Figure 6-31 This figure shows the locations of the Stockton WWTP receiving water locations used for model calibration along the San Joaquin River.

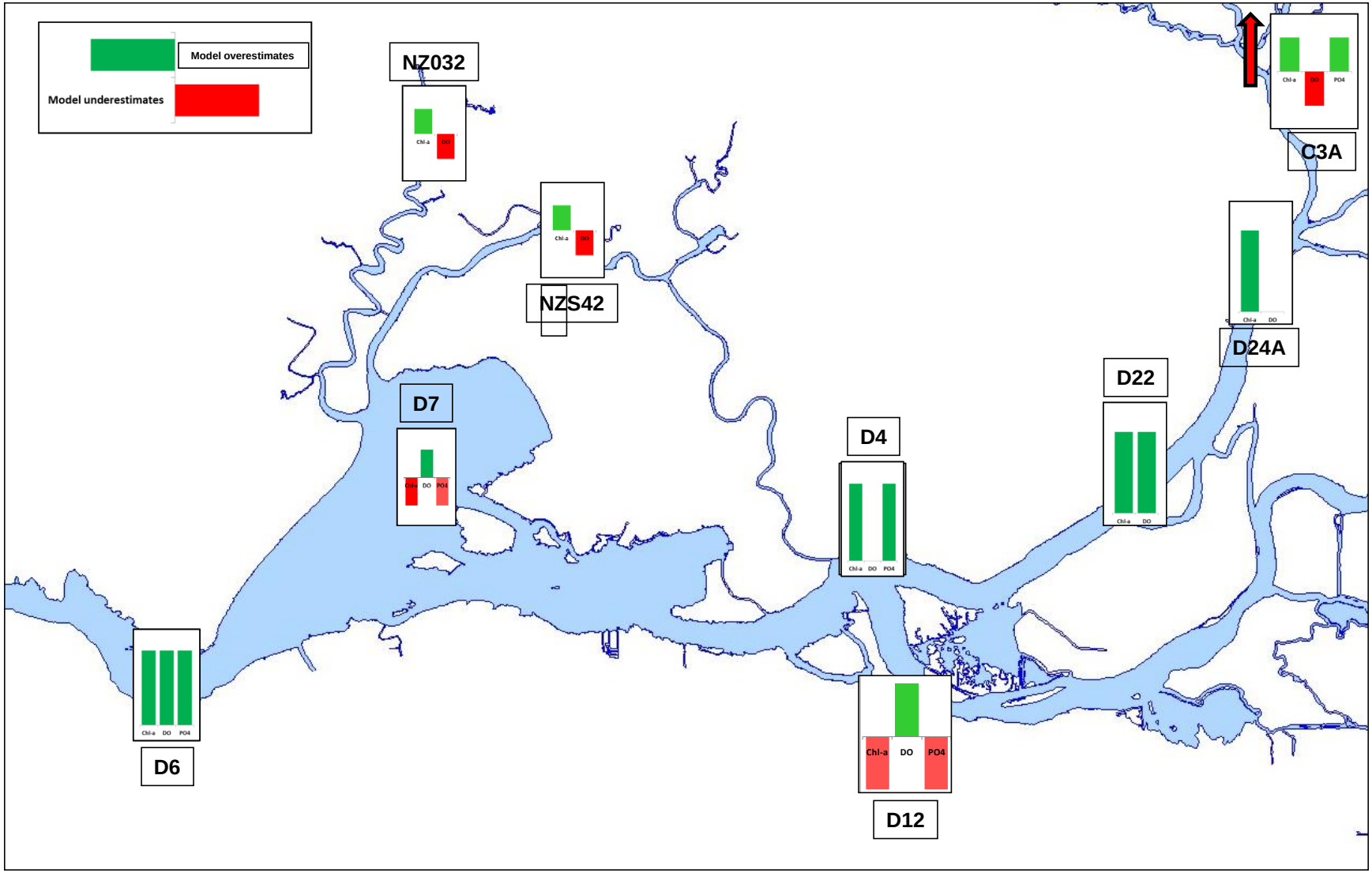

Figure 6-32 This graphical representation of model results shows the over- or under-estimation BIAS of three constituents – Algae (measured as Chlorophyll-a, Chl-a), DO and PO4-P. The bar height represents the values shown in the right hand column of Table 6-9 – in this figure, all bar heights are equal to one.

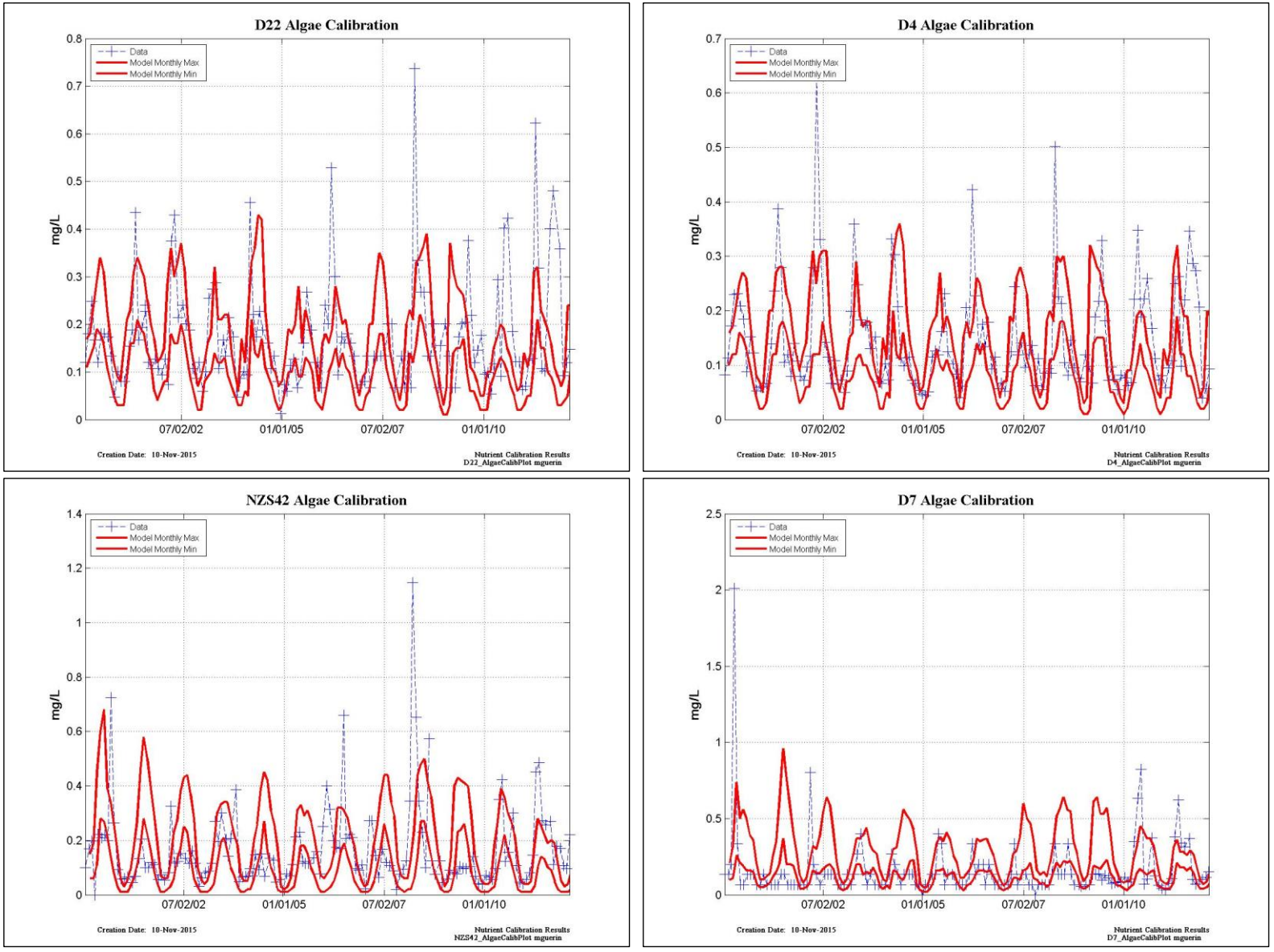

Figure 6-33 Time series plots of Algae data (from Chl-a) vs. model monthly Max and Min at selected locations.

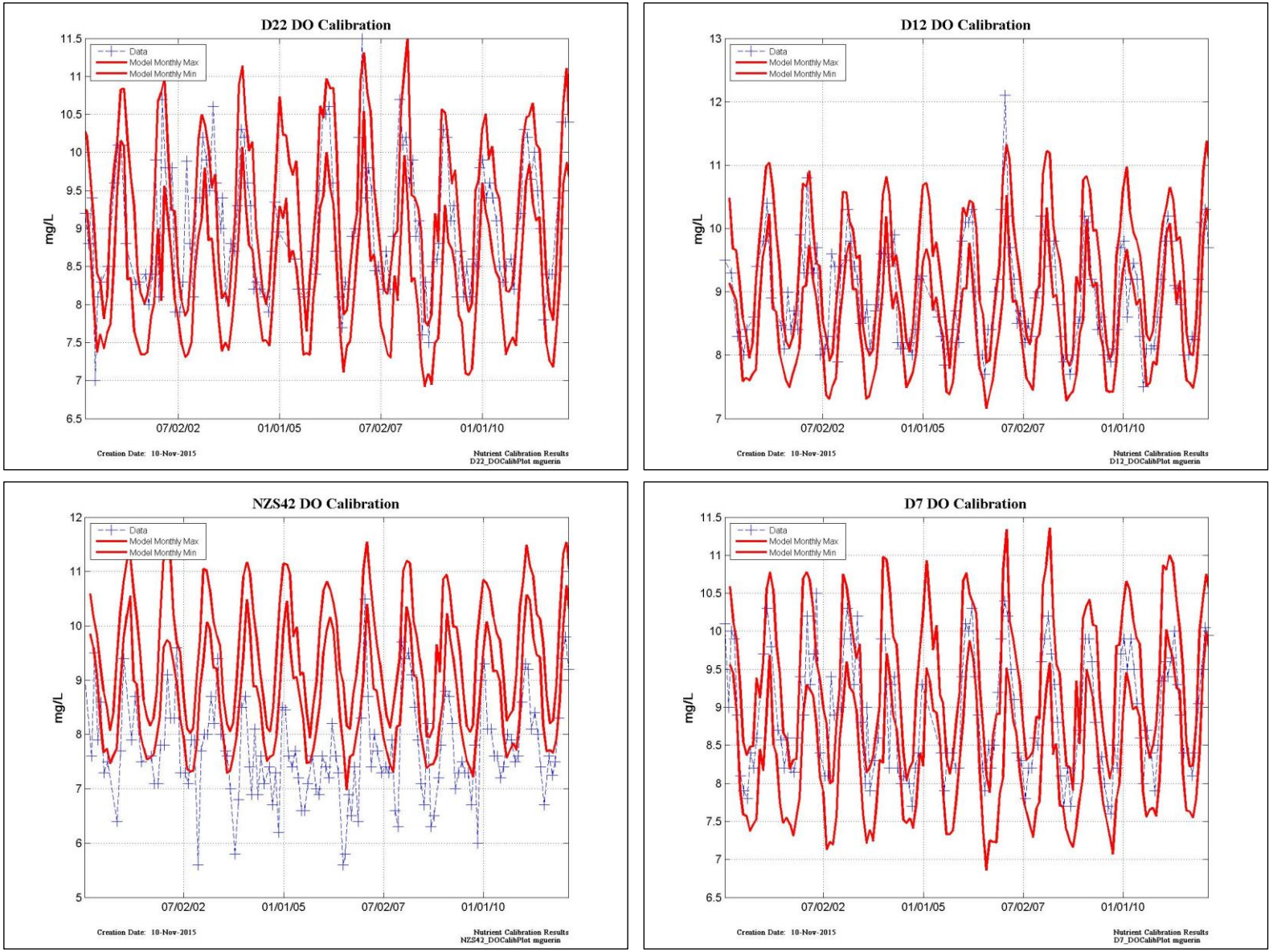

Figure 6-34 Time series plots of DO data vs. model monthly Max and Min at selected locations.

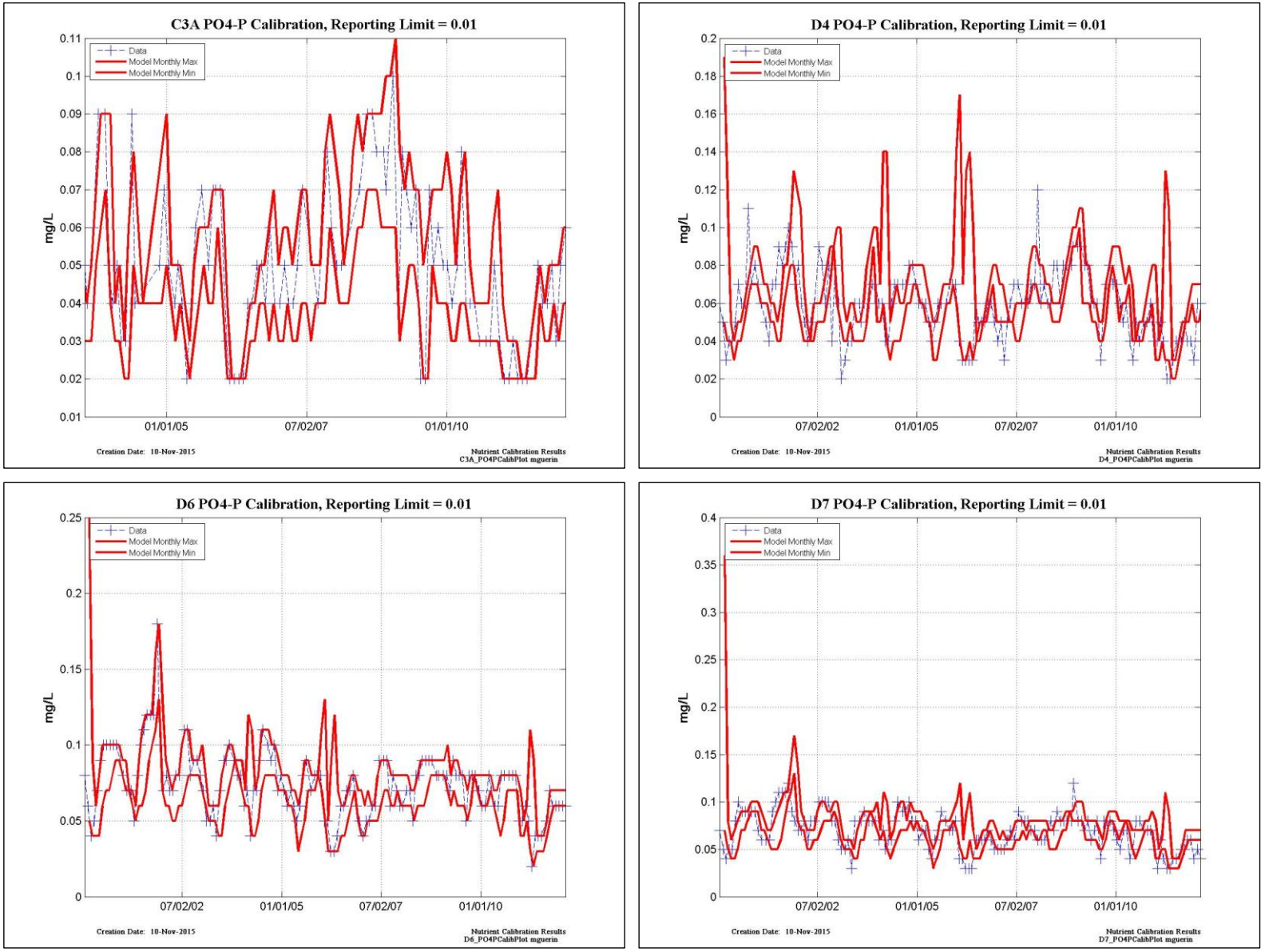

Figure 6-35 Time series plots of PO_4-P data vs. model monthly Max and Min at selected locations.

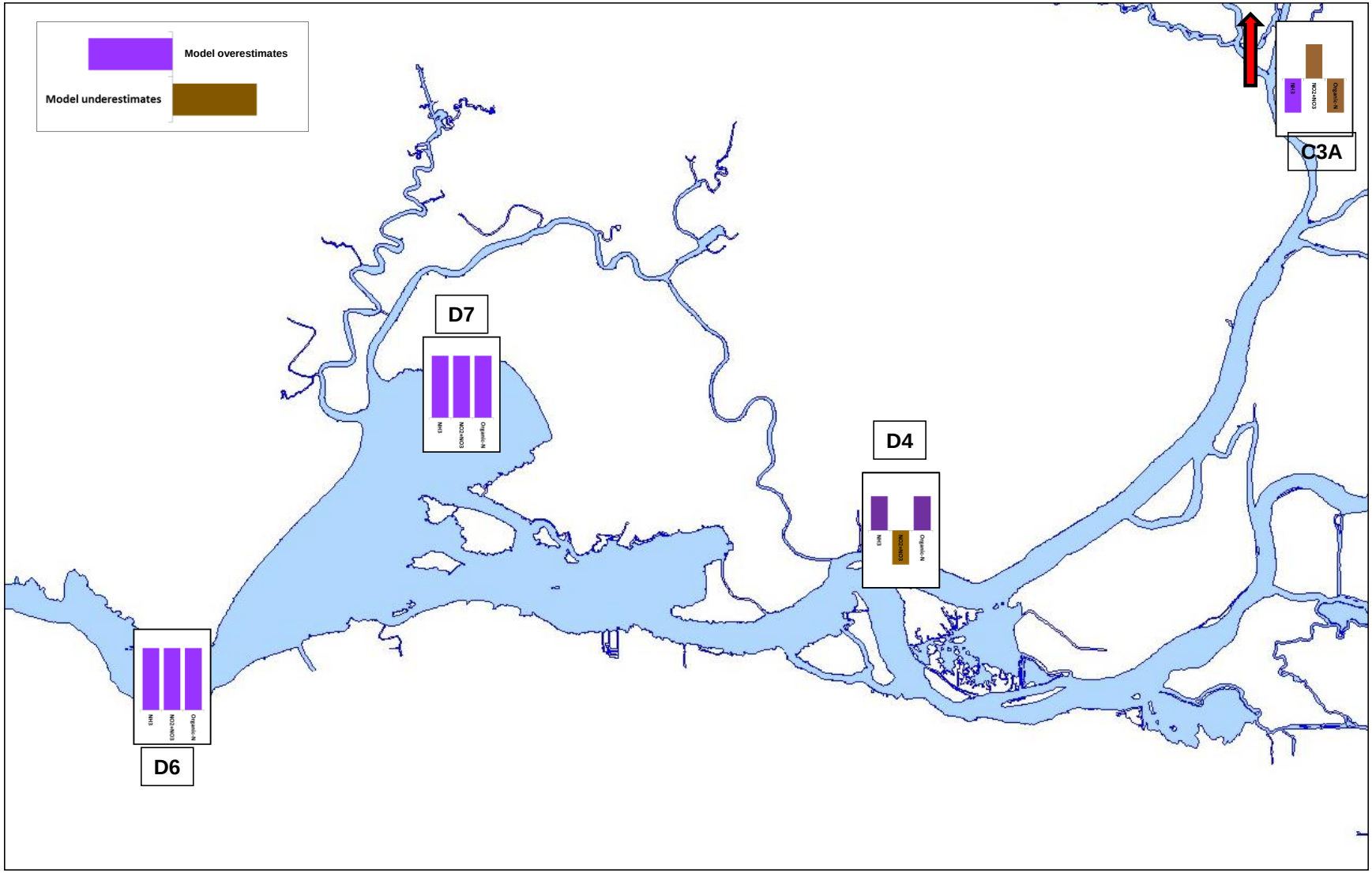

Figure 6-36 This graphical representation of model results shows the over or under-estimation Bias of three constituents – NH3, NO3+NO2, and Organic-N. The bar height represents the values shown in the right hand column of Table 6-9 – in this figure, all bar heights are equal to one.

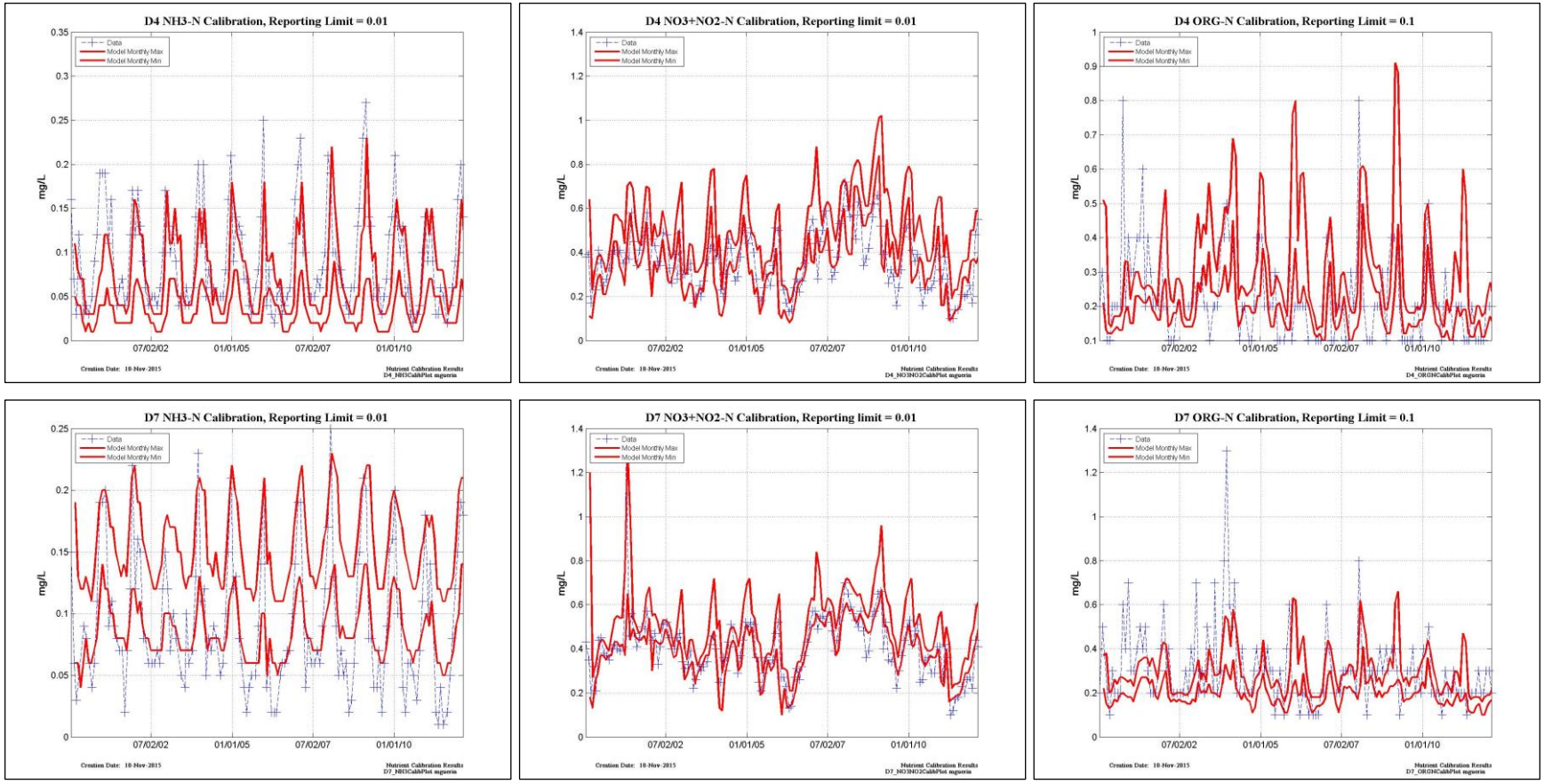

Figure 6-37 Time series plots of NH_3-N, NO_3+NO_2-N and Organic-N data vs. model monthly Max and Min at the EMP D4 and D7 data locations.

D10 - ALGAE	NSE	PBIAS	Bias	RSR
ALL	S	VG	Underestimate	S
Dry WY Calibration	G	VG	Underestimate	G
Wet WY Calibration	S	VG	Underestimate	S
Dry WY Validation	S	VG	Underestimate	U
Wet WY Validation	S	VG	Underestimate	S

D10 - DO	NSE	PBIAS	Bias	RSR
ALL	S	VG	Underestimate	U
Dry WY Calibration	U	VG	Underestimate	U
Wet WY Calibration	U	VG	Underestimate	U
Dry WY Validation	U	VG	Underestimate	U
Wet WY Validation	G	VG	Overestimate	S

D12 - ALGAE	NSE	PBIAS	Bias	RSR
ALL	G	VG	Underestimate	G
Dry WY Calibration	VG	VG	Underestimate	VG
Wet WY Calibration	S	VG	Underestimate	U
Dry WY Validation	S	VG	Underestimate	S
Wet WY Validation	VG	VG	Underestimate	VG

D12 - DO	NSE	PBIAS	Bias	RSR
ALL	VG	VG	Underestimate	VG
Dry WY Calibration	VG	VG	Underestimate	VG
Wet WY Calibration	VG	VG	Underestimate	VG
Dry WY Validation	VG	VG	Underestimate	VG
Wet WY Validation	VG	VG	Underestimate	VG

D16 - ALGAE	NSE	PBIAS	Bias	RSR
ALL	S	VG	Underestimate	U
Dry WY Calibration	S	VG	Underestimate	S
Wet WY Calibration	S	G	Underestimate	U
Dry WY Validation	S	VG	Underestimate	U
Wet WY Validation	VG	VG	Underestimate	VG

D16 - DO	NSE	PBIAS	Bias	RSR
ALL	VG	VG	Underestimate	VG
Dry WY Calibration	VG	VG	Underestimate	VG
Wet WY Calibration	VG	VG	Underestimate	G
Dry WY Validation	VG	VG	Underestimate	VG
Wet WY Validation	VG	VG	Underestimate	VG

D22 - ALGAE	NSE	PBIAS	Bias	RSR
ALL	S	VG	Underestimate	U
Dry WY Calibration	S	VG	Underestimate	S
Wet WY Calibration	S	VG	Underestimate	U
Dry WY Validation	S	VG	Underestimate	U
Wet WY Validation	S	VG	Underestimate	U

D22 - DO	NSE	PBIAS	Bias	RSR
ALL	VG	VG	Underestimate	VG
Dry WY Calibration	VG	VG	Underestimate	VG
Wet WY Calibration	G	VG	Underestimate	G
Dry WY Validation	VG	VG	Underestimate	VG
Wet WY Validation	VG	VG	Underestimate	VG

Figure 6-38 Categorical statistics for Algae and DO at selected locations.

D4 - ALGAE	NSE	PBIAS	Bias	RSR
ALL	G	VG	Underestimate	S
Dry WY Calibration	G	VG	Underestimate	G
Wet WY Calibration	S	VG	Underestimate	U
Dry WY Validation	G	VG	Underestimate	G
Wet WY Validation	S	VG	Underestimate	S

D4 - NH3	NSE	PBIAS	Bias	RSR
ALL	VG	VG	Underestimate	G
Dry WY Calibration	VG	VG	Underestimate	G
Wet WY Calibration	G	VG	Underestimate	G
Dry WY Validation	VG	G	Underestimate	S
Wet WY Validation	G	VG	Underestimate	S

D4 - NO3	NSE	PBIAS	Bias	RSR
ALL	VG	VG	Overestimate	G
Dry WY Calibration	S	VG	Overestimate	U
Wet WY Calibration	VG	VG	Overestimate	G
Dry WY Validation	S	VG	Overestimate	U
Wet WY Validation	VG	VG	Overestimate	VG

D4 - ORGN	NSE	PBIAS	Bias	RSR
ALL	S	VG	Underestimate	S
Dry WY Calibration	S	VG	Underestimate	U
Wet WY Calibration	S	VG	Underestimate	U
Dry WY Validation	G	VG	Underestimate	G
Wet WY Validation	S	VG	Overestimate	U

D4 - PO4	NSE	PBIAS	Bias	RSR
ALL	G	VG	Underestimate	G
Dry WY Calibration	S	VG	Underestimate	U
Wet WY Calibration	G	VG	Overestimate	G
Dry WY Validation	S	VG	Underestimate	S
Wet WY Validation	VG	VG	Overestimate	VG

Figure 6-39 Categorical statistics for nutrients at location D4.

D7 - ALGAE	NSE	PBIAS	Bias	RSR
ALL	S	VG	Overestimate	S
Dry WY Calibration	S	G	Overestimate	U
Wet WY Calibration	S	VG	Underestimate	S
Dry WY Validation	VG	VG	Overestimate	G
Wet WY Validation	VG	VG	Overestimate	VG

D7 - DO	NSE	PBIAS	Bias	RSR
ALL	VG	VG	Underestimate	VG
Dry WY Calibration	VG	VG	Underestimate	VG
Wet WY Calibration	VG	VG	Underestimate	VG
Dry WY Validation	VG	VG	Underestimate	VG
Wet WY Validation	VG	VG	Underestimate	VG

D7 - NH3	NSE	PBIAS	Bias	RSR
ALL	VG	VG	Overestimate	VG
Dry WY Calibration	VG	VG	Overestimate	VG
Wet WY Calibration	VG	VG	Overestimate	VG
Dry WY Validation	VG	VG	Overestimate	VG
Wet WY Validation	VG	VG	Overestimate	VG

D7 - NO3	NSE	PBIAS	Bias	RSR
ALL	VG	VG	Overestimate	VG
Dry WY Calibration	VG	VG	Overestimate	VG
Wet WY Calibration	VG	VG	Overestimate	VG
Dry WY Validation	VG	VG	Overestimate	VG
Wet WY Validation	VG	VG	Overestimate	VG

D7 - ORGN	NSE	PBIAS	Bias	RSR
ALL	S	VG	Underestimate	U
Dry WY Calibration	S	VG	Underestimate	U
Wet WY Calibration	S	G	Underestimate	U
Dry WY Validation	VG	VG	Underestimate	VG
Wet WY Validation	S	VG	Underestimate	U

D7 - PO4	NSE	PBIAS	Bias	RSR
ALL	VG	VG	Overestimate	VG
Dry WY Calibration	VG	VG	Underestimate	VG
Wet WY Calibration	VG	VG	Overestimate	VG
Dry WY Validation	VG	VG	Underestimate	VG
Wet WY Validation	VG	VG	Overestimate	VG

Figure 6-40 Categorical statistics for nutrients at location D7.

NZ032 - ALGAE	NSE	PBIAS	Bias	RSR
ALL	S	VG	Underestimate	U
Dry WY Calibration	S	VG	Overestimate	U
Wet WY Calibration	S	VG	Underestimate	U
Dry WY Validation	S	VG	Underestimate	U
Wet WY Validation	G	VG	Underestimate	G

NZS42 - ALGAE	NSE	PBIAS	Bias	RSR
ALL	S	VG	Underestimate	U
Dry WY Calibration	U	G	Overestimate	U
Wet WY Calibration	S	VG	Underestimate	U
Dry WY Validation	S	G	Underestimate	U
Wet WY Validation	S	G	Underestimate	U

NZ032 - DO	NSE	PBIAS	Bias	RSR
ALL	G	VG	Overestimate	G
Dry WY Calibration	G	VG	Overestimate	S
Wet WY Calibration	VG	VG	Overestimate	VG
Dry WY Validation	G	VG	Underestimate	G
Wet WY Validation	G	VG	Overestimate	U

NZS42 - DO	NSE	PBIAS	Bias	RSR
ALL	S	VG	Overestimate	U
Dry WY Calibration	S	VG	Overestimate	U
Wet WY Calibration	S	VG	Overestimate	U
Dry WY Validation	G	VG	Overestimate	U
Wet WY Validation	S	VG	Overestimate	U

Figure 6-41 Categorical statistics for Suisun Marsh locations - Algae and DO.

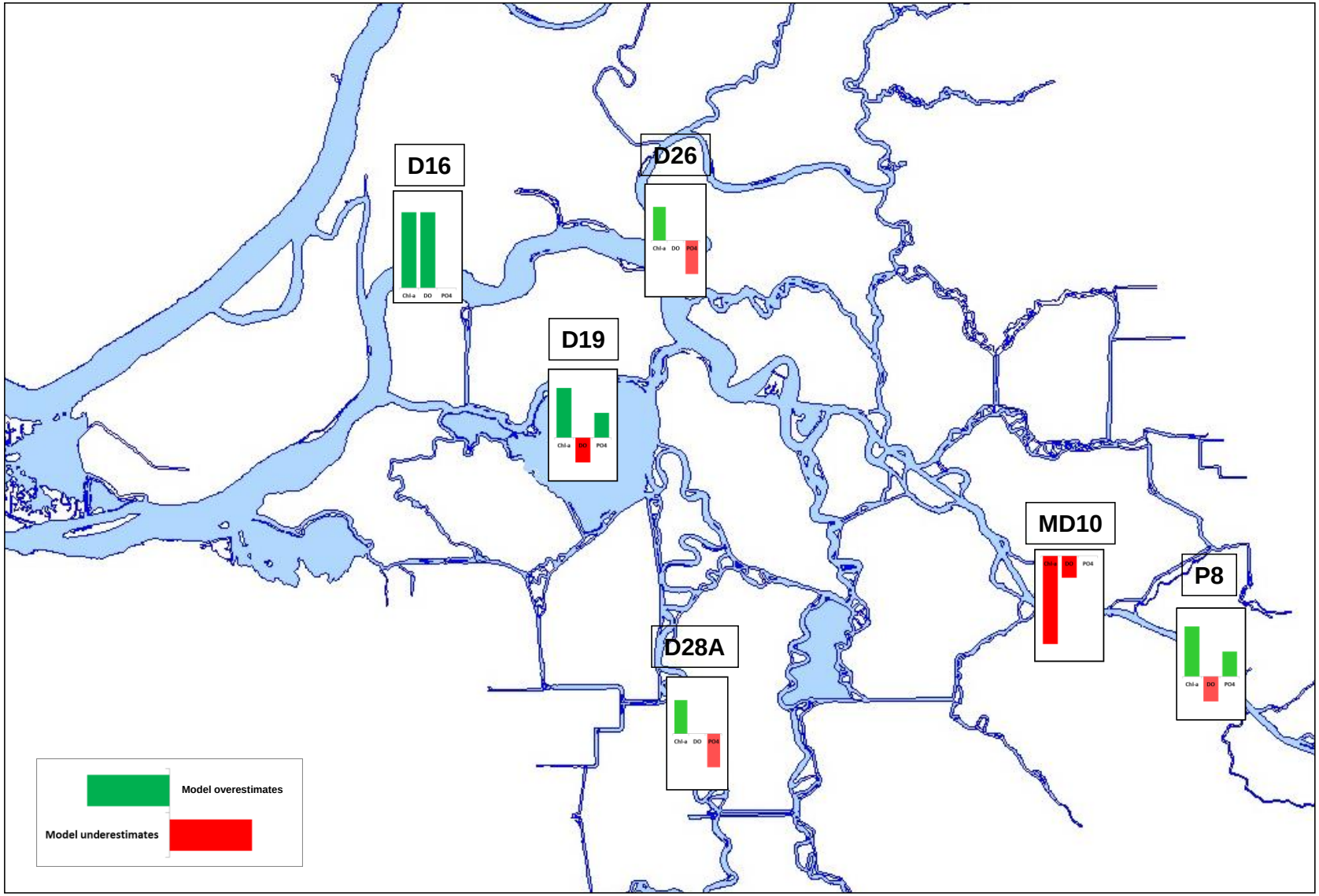

Figure 6-42 This graphical representation of model results shows the over- or under-estimation Bias of three constituents – Algae (measurement is Chlorophyll-a, Chl-a), DO and PO_4-P. The bar height represents the values shown in the right hand column of Table 6-9.

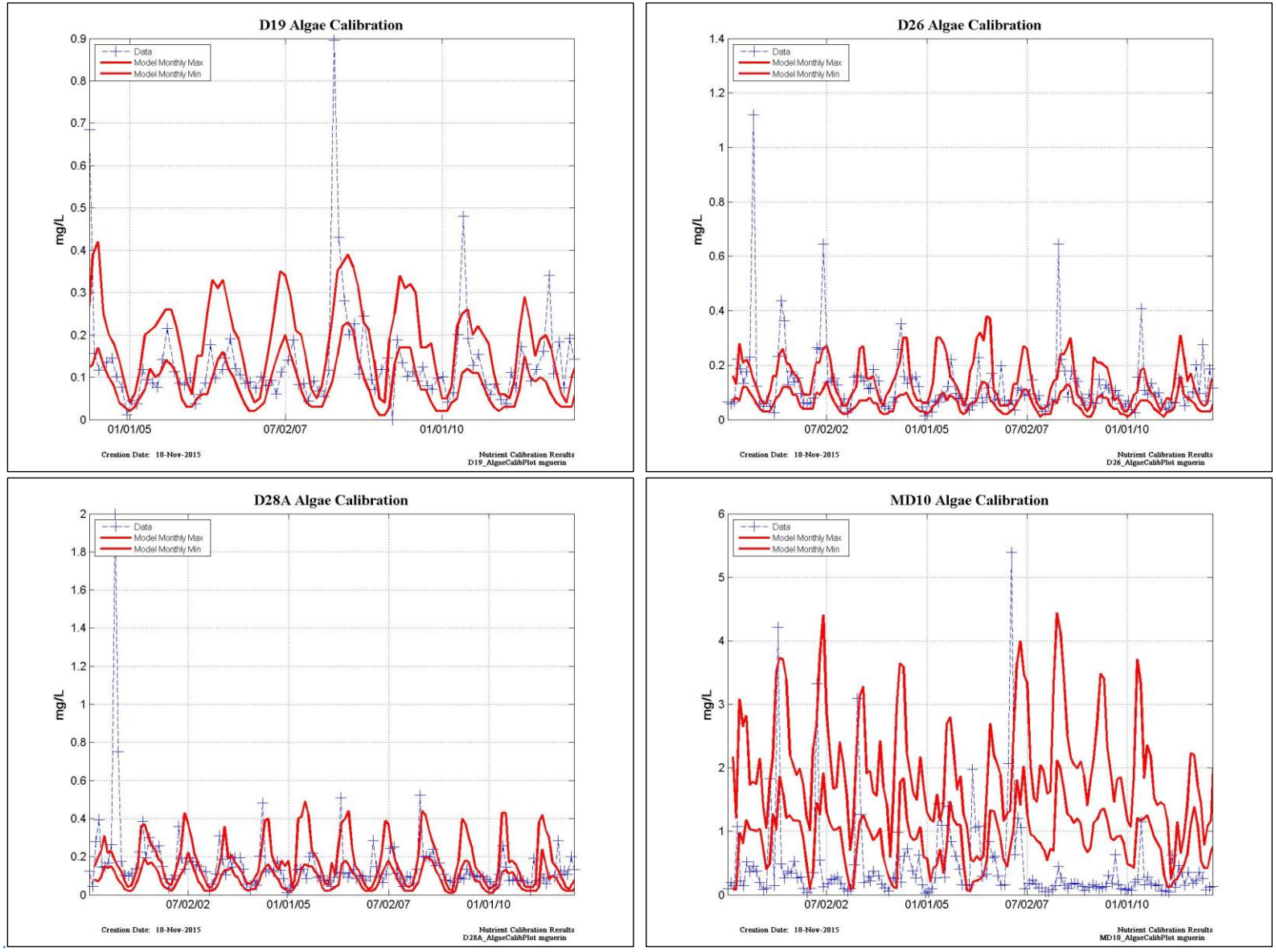

Figure 6-43 Time series plots of Algae data (from Chl-a) vs. model monthly Max and Min at selected locations.

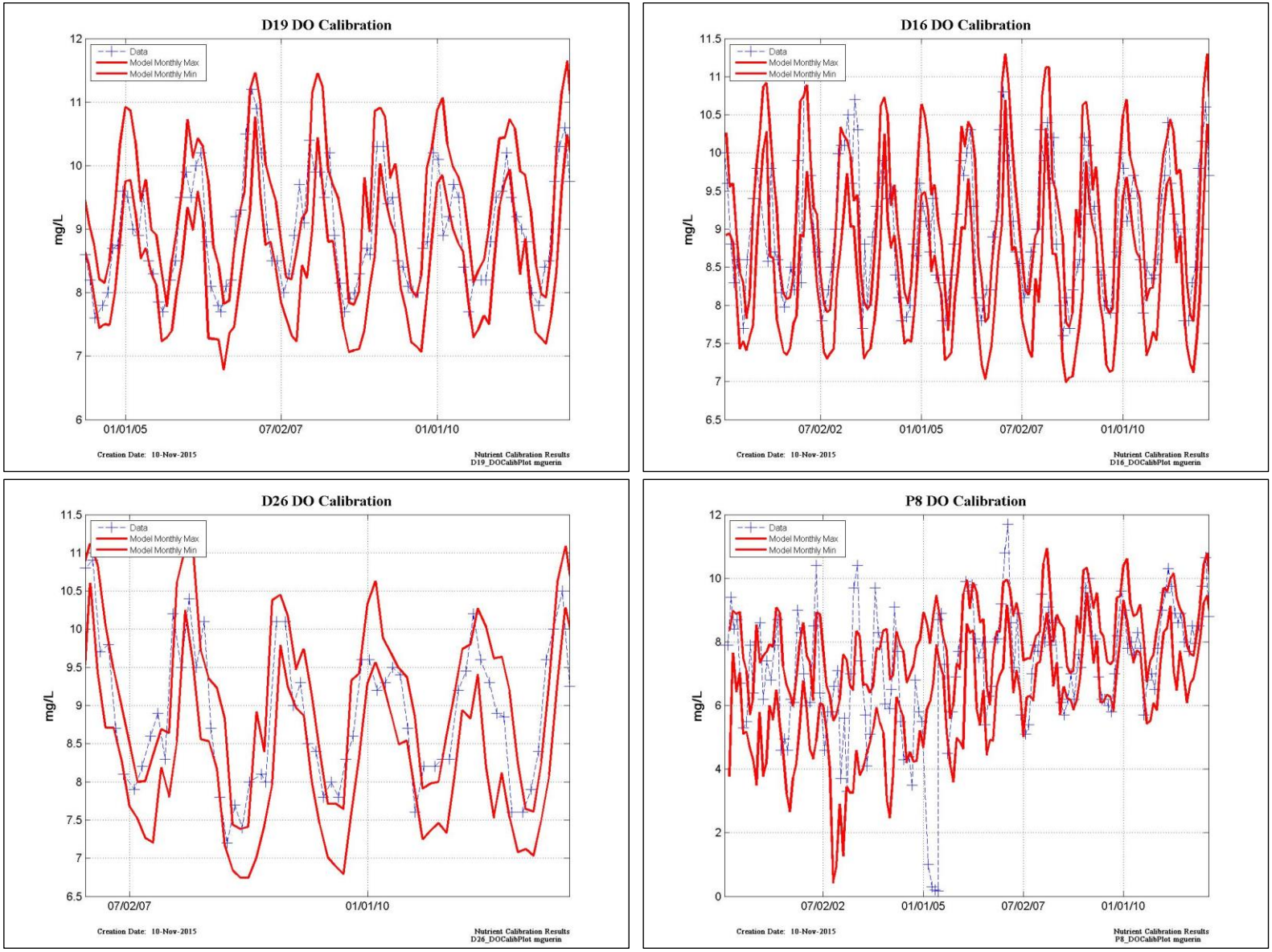

Figure 6-44 Time series plots of DO data vs. model monthly Max and Min at selected locations.

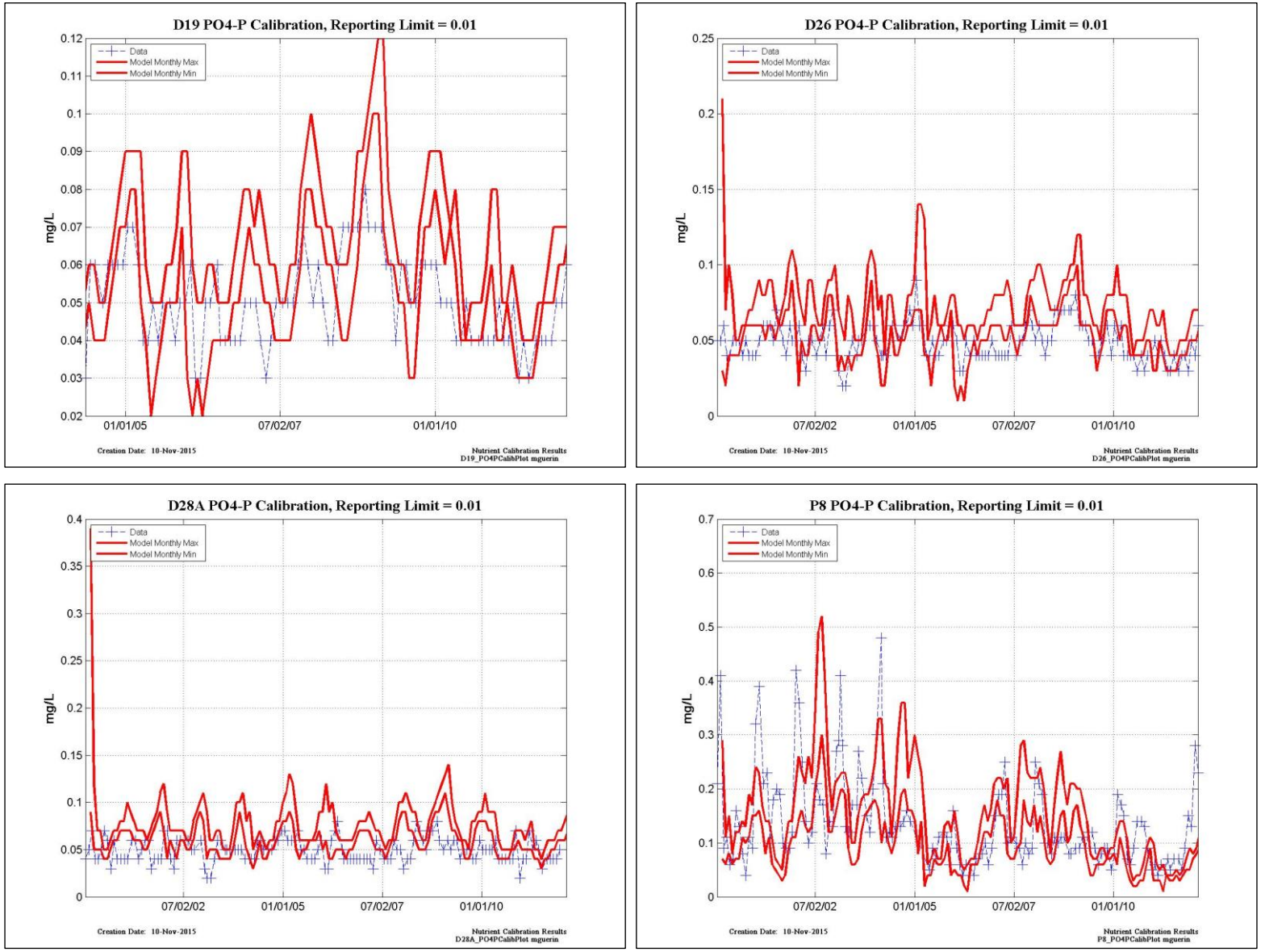

Figure 6-45 Time series plots of PO_4-P data vs. model monthly Max and Min at selected locations.

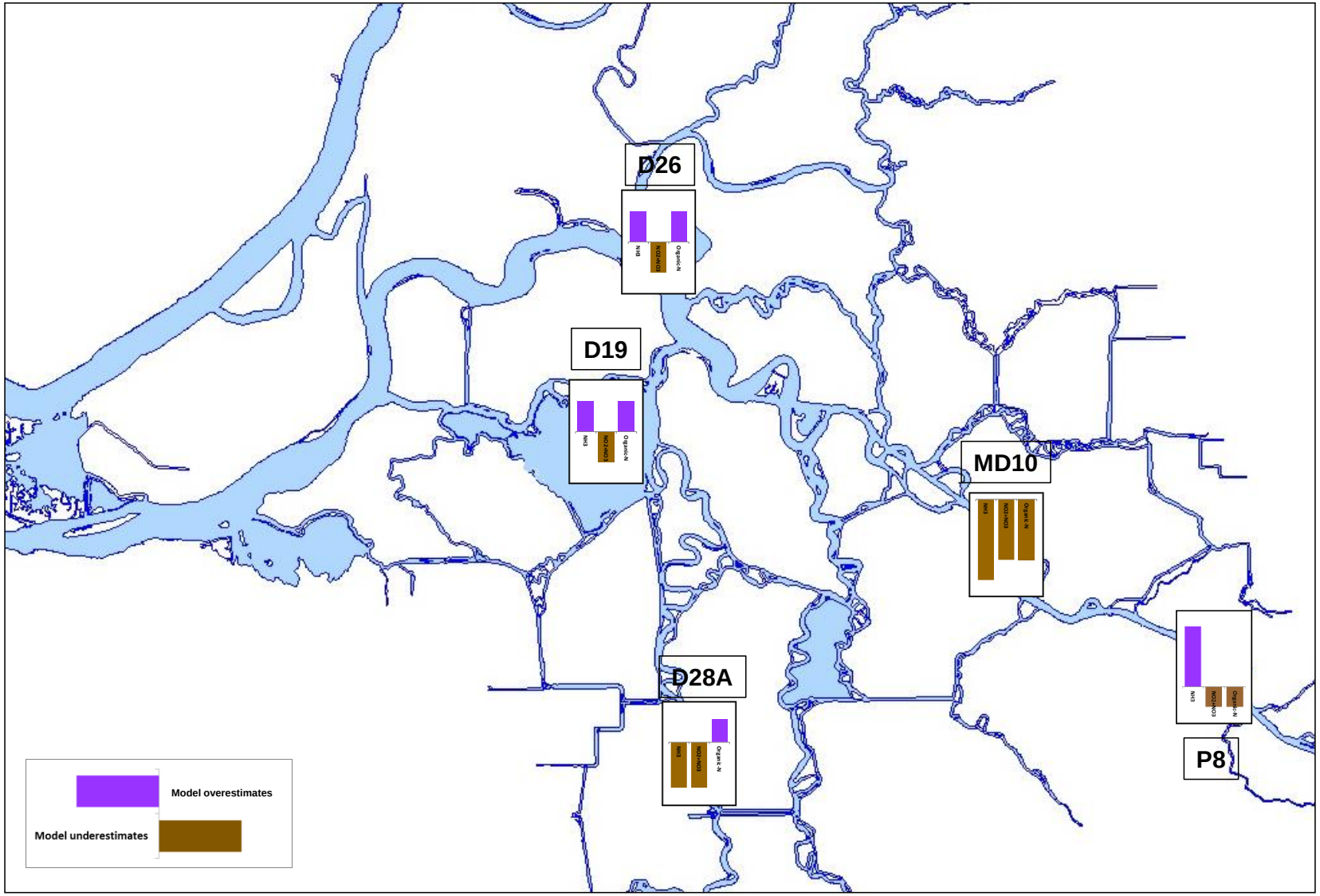

Figure 6-46 This graphical representation of model results shows the over or under-estimation Bias of three constituents – NH_3, NO_3+NO_2, and Organic-N. The bar height represents the values shown in the right hand column of Table 6-9.

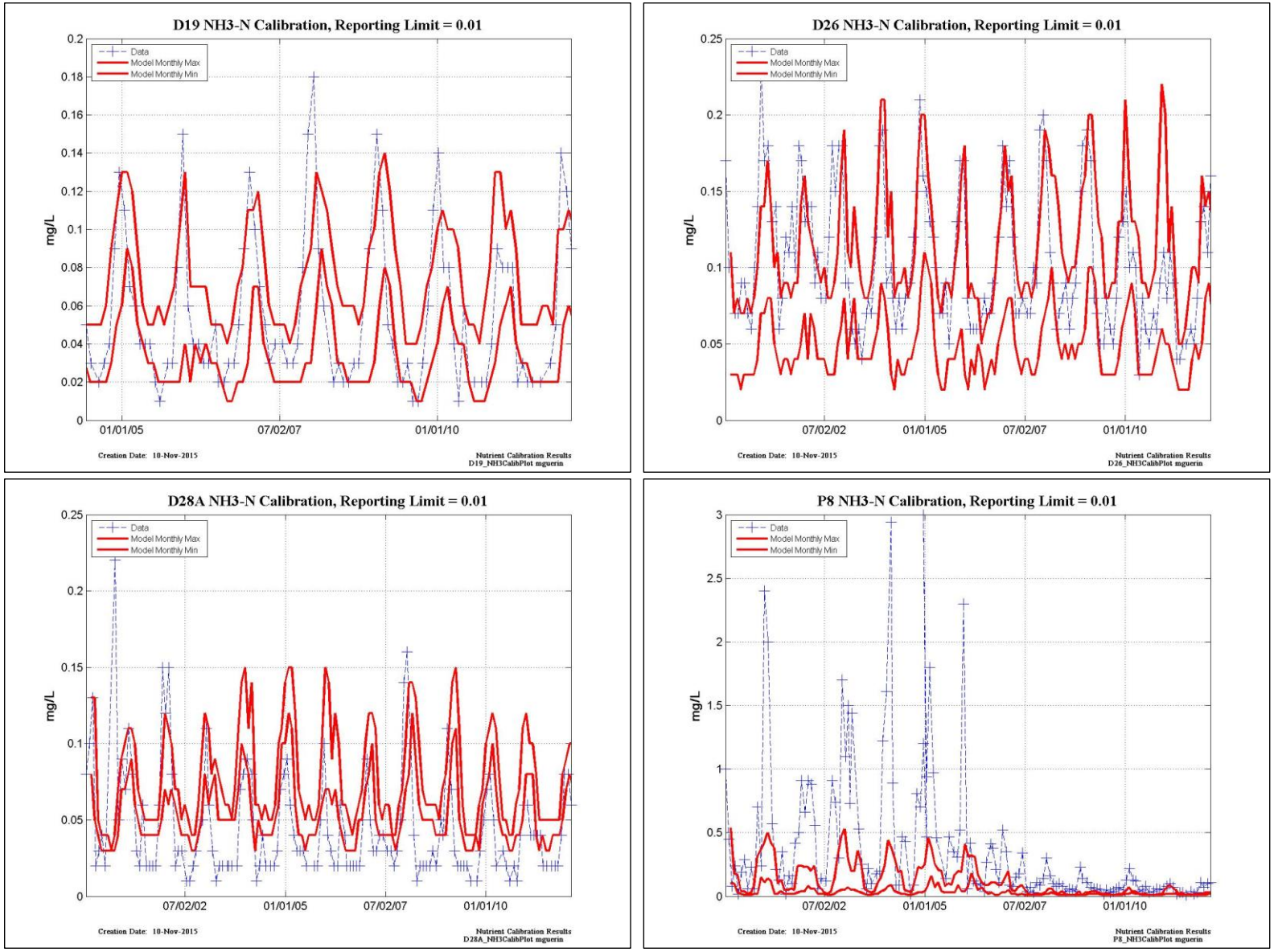

Figure 6-47 Time series plots of NH_3-N data vs. model monthly Max and Min at selected locations.

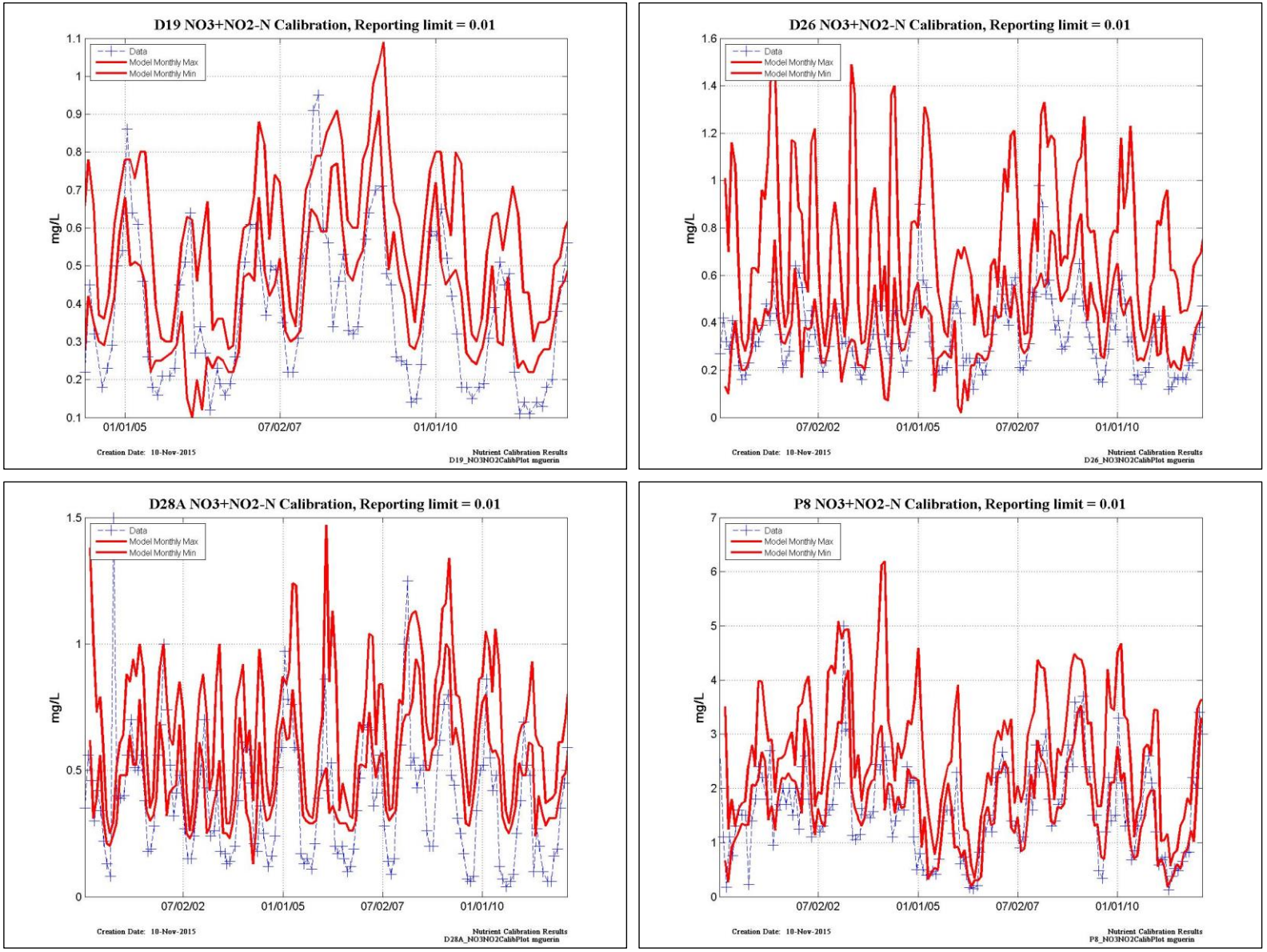

Figure 6-48 Time series plots of NO_3+NO_2-N data vs. model monthly Max and Min at selected locations.

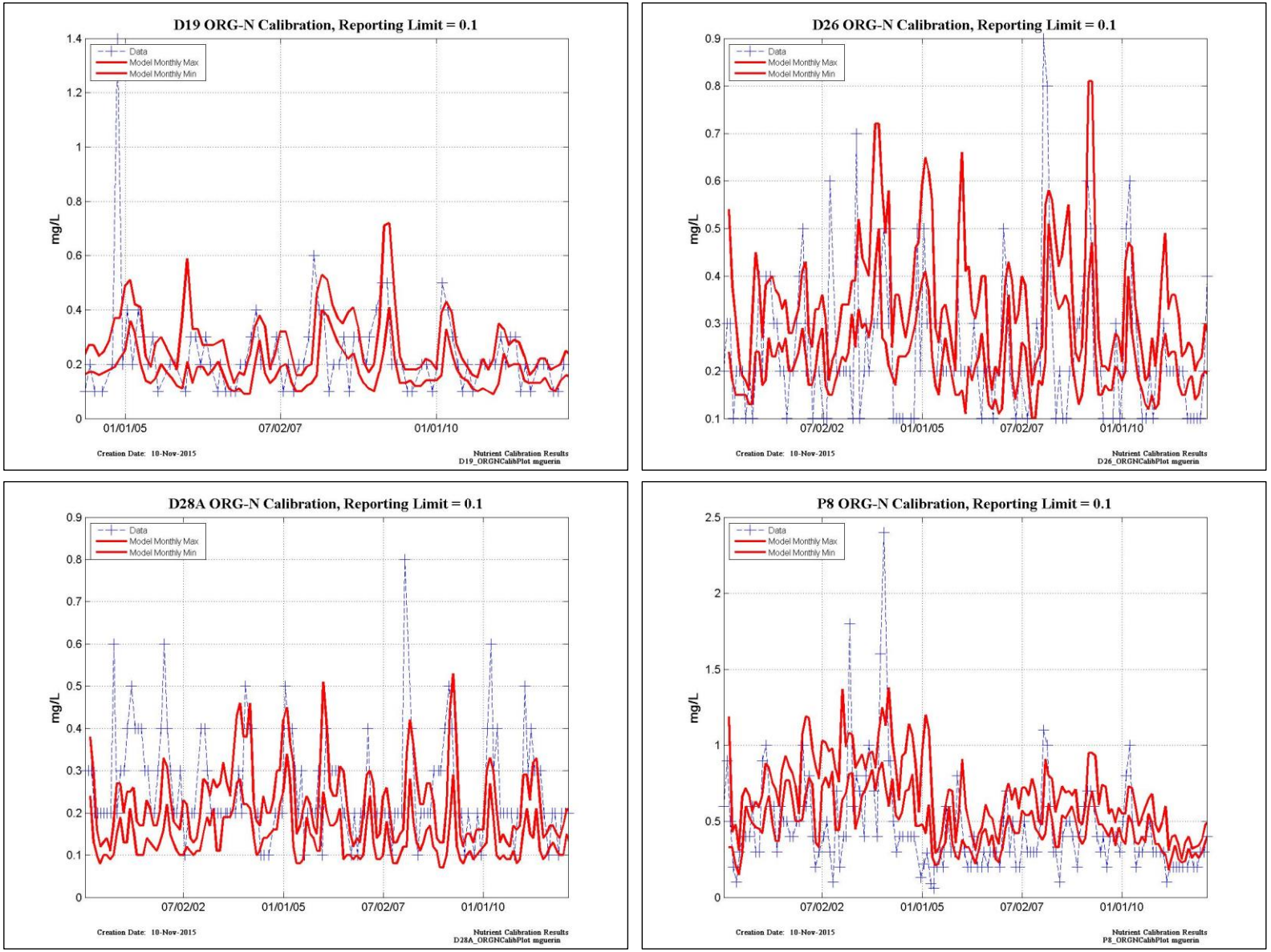

Figure 6-49 Time series plots of Organic-N data vs. model monthly Max and Min at selected locations.

D19 - ALGAE	NSE	PBIAS	Bias	RSR
ALL	S	VG	Underestimate	S
Dry WY Calibration	U	VG	Overestimate	U
Wet WY Calibration	S	G	Underestimate	U
Dry WY Validation	S	VG	Underestimate	S
Wet WY Validation	VG	VG	Overestimate	VG

D19 - DO	NSE	PBIAS	Bias	RSR
ALL	VG	VG	Underestimate	VG
Dry WY Calibration	VG	VG	Underestimate	VG
Wet WY Calibration	VG	VG	Underestimate	VG
Dry WY Validation	VG	VG	Underestimate	VG
Wet WY Validation	VG	VG	Overestimate	VG

D19 - NH3	NSE	PBIAS	Bias	RSR
ALL	VG	VG	Underestimate	VG
Dry WY Calibration	VG	VG	Underestimate	VG
Wet WY Calibration	VG	VG	Underestimate	VG
Dry WY Validation	VG	VG	Underestimate	VG
Wet WY Validation	VG	VG	Underestimate	VG

D19 - NO3	NSE	PBIAS	Bias	RSR
ALL	VG	VG	Overestimate	G
Dry WY Calibration	VG	G	Overestimate	U
Wet WY Calibration	VG	G	Overestimate	S
Dry WY Validation	S	VG	Overestimate	U
Wet WY Validation	VG	VG	Overestimate	VG

D19 - ORGN	NSE	PBIAS	Bias	RSR
ALL	S	VG	Underestimate	U
Dry WY Calibration	VG	VG	Underestimate	VG
Wet WY Calibration	VG	VG	Underestimate	VG
Dry WY Validation	VG	VG	Underestimate	G
Wet WY Validation	G	VG	Underestimate	G

D19 - PO4	NSE	PBIAS	Bias	RSR
ALL	S	VG	Overestimate	U
Dry WY Calibration	U	VG	Overestimate	U
Wet WY Calibration	S	VG	Overestimate	U
Dry WY Validation	S	VG	Overestimate	U
Wet WY Validation	S	VG	Overestimate	U

Figure 6-50 Categorical statistics for nutrients at location D19.

D26 - ALGAE	NSE	PBIAS	Bias	RSR
ALL	S	VG	Underestimate	U
Dry WY Calibration	G	VG	Underestimate	S
Wet WY Calibration	S	G	Underestimate	U
Dry WY Validation	S	VG	Underestimate	U
Wet WY Validation	S	VG	Underestimate	U

D26 - NH3	NSE	PBIAS	Bias	RSR
ALL	VG	VG	Underestimate	VG
Dry WY Calibration	VG	VG	Underestimate	G
Wet WY Calibration	VG	VG	Underestimate	VG
Dry WY Validation	VG	VG	Underestimate	VG
Wet WY Validation	VG	VG	Underestimate	VG

D26 - NO3	NSE	PBIAS	Bias	RSR
ALL	VG	VG	Overestimate	S
Dry WY Calibration	S	VG	Overestimate	U
Wet WY Calibration	VG	VG	Overestimate	S
Dry WY Validation	G	VG	Overestimate	U
Wet WY Validation	VG	VG	Overestimate	VG

D26 - ORGN	NSE	PBIAS	Bias	RSR
ALL	G	VG	Underestimate	G
Dry WY Calibration	S	VG	Underestimate	S
Wet WY Calibration	G	VG	Overestimate	G
Dry WY Validation	G	VG	Underestimate	G
Wet WY Validation	VG	VG	Overestimate	VG

D26 - PO4	NSE	PBIAS	Bias	RSR
ALL	S	VG	Overestimate	U
Dry WY Calibration	U	VG	Overestimate	U
Wet WY Calibration	S	VG	Overestimate	U
Dry WY Validation	S	VG	Overestimate	U
Wet WY Validation	S	VG	Overestimate	U

Figure 6-51 Categorical statistics for nutrients at location D26.

D28A - ALGAE	NSE	PBIAS	Bias	RSR
ALL	S	VG	Underestimate	U
Dry WY Calibration	VG	VG	Underestimate	VG
Wet WY Calibration	S	S	Underestimate	U
Dry WY Validation	G	VG	Underestimate	G
Wet WY Validation	VG	VG	Underestimate	VG

D28A - NH3	NSE	PBIAS	Bias	RSR
ALL	S	G	Overestimate	U
Dry WY Calibration	G	VG	Overestimate	S
Wet WY Calibration	S	VG	Overestimate	U
Dry WY Validation	G	G	Overestimate	G
Wet WY Validation	S	S	Overestimate	U

D28A - NO3	NSE	PBIAS	Bias	RSR
ALL	G	G	Overestimate	U
Dry WY Calibration	S	G	Overestimate	U
Wet WY Calibration	S	G	Overestimate	U
Dry WY Validation	G	G	Overestimate	U
Wet WY Validation	VG	VG	Overestimate	VG

D28A - ORGN	NSE	PBIAS	Bias	RSR
ALL	S	VG	Underestimate	U
Dry WY Calibration	S	G	Underestimate	U
Wet WY Calibration	S	VG	Underestimate	U
Dry WY Validation	S	G	Underestimate	U
Wet WY Validation	G	VG	Underestimate	U

D28A - PO4	NSE	PBIAS	Bias	RSR
ALL	U	VG	Overestimate	U
Dry WY Calibration	U	G	Overestimate	U
Wet WY Calibration	U	VG	Overestimate	U
Dry WY Validation	U	G	Overestimate	U
Wet WY Validation	U	VG	Overestimate	U

Figure 6-52 Categorical statistics for nutrients at location D28A.

MD10 - ALGAE	NSE	PBIAS	Bias	RSR
ALL	S	U	Overestimate	U
Dry WY Calibration	VG	U	Overestimate	U
Wet WY Calibration	S	U	Overestimate	U
Dry WY Validation	S	U	Overestimate	U
Wet WY Validation	S	VG	Overestimate	U

MD10 - DO	NSE	PBIAS	Bias	RSR
ALL	G	VG	Overestimate	G
Dry WY Calibration	VG	VG	Overestimate	G
Wet WY Calibration	VG	VG	Overestimate	VG
Dry WY Validation	S	VG	Overestimate	S
Wet WY Validation	VG	VG	Overestimate	VG

MD10 - NH3	NSE	PBIAS	Bias	RSR
ALL	S	U	Overestimate	U
Dry WY Calibration	U	U	Overestimate	U
Wet WY Calibration	U	U	Overestimate	U
Dry WY Validation	S	U	Overestimate	U
Wet WY Validation	S	U	Overestimate	U

MD10 - NO3	NSE	PBIAS	Bias	RSR
ALL	S	S	Overestimate	U
Dry WY Calibration	S	S	Overestimate	U
Wet WY Calibration	S	U	Overestimate	U
Dry WY Validation	S	S	Overestimate	U
Wet WY Validation	VG	G	Overestimate	G

MD10 - ORGN	NSE	PBIAS	Bias	RSR
ALL	S	S	Overestimate	U
Dry WY Calibration	S	S	Overestimate	U
Wet WY Calibration	U	S	Overestimate	U
Dry WY Validation	S	U	Overestimate	U
Wet WY Validation	U	G	Overestimate	U

Figure 6-53 Categorical statistics for nutrients at location MD10.

P8 - ALGAE	NSE	PBIAS	Bias	RSR
ALL	S	G	Underestimate	U
Dry WY Calibration	S	S	Underestimate	U
Wet WY Calibration	S	S	Underestimate	U
Dry WY Validation	G	VG	Underestimate	G
Wet WY Validation	S	G	Underestimate	U

P8 - DO	NSE	PBIAS	Bias	RSR
ALL	S	VG	Overestimate	S
Dry WY Calibration	VG	VG	Underestimate	VG
Wet WY Calibration	VG	VG	Underestimate	VG
Dry WY Validation	VG	VG	Overestimate	VG
Wet WY Validation	S	VG	Overestimate	U

P8 - NH3	NSE	PBIAS	Bias	RSR
ALL	S	S	Underestimate	U
Dry WY Calibration	S	S	Underestimate	U
Wet WY Calibration	S	U	Underestimate	U
Dry WY Validation	S	U	Underestimate	U
Wet WY Validation	S	U	Underestimate	U

P8 - NO3	NSE	PBIAS	Bias	RSR
ALL	VG	VG	Overestimate	VG
Dry WY Calibration	G	VG	Overestimate	U
Wet WY Calibration	VG	VG	Overestimate	VG
Dry WY Validation	VG	VG	Overestimate	VG
Wet WY Validation	VG	VG	Overestimate	VG

P8 - ORGN	NSE	PBIAS	Bias	RSR
ALL	S	VG	Overestimate	S
Dry WY Calibration	S	VG	Overestimate	U
Wet WY Calibration	S	VG	Overestimate	G
Dry WY Validation	G	VG	Overestimate	S
Wet WY Validation	S	VG	Overestimate	U

P8 - PO4	NSE	PBIAS	Bias	RSR
ALL	S	VG	Underestimate	S
Dry WY Calibration	S	VG	Underestimate	U
Wet WY Calibration	G	VG	Underestimate	S
Dry WY Validation	S	VG	Overestimate	U
Wet WY Validation	S	VG	Overestimate	U

Figure 6-54 Categorical statistics for nutrients at location P8.

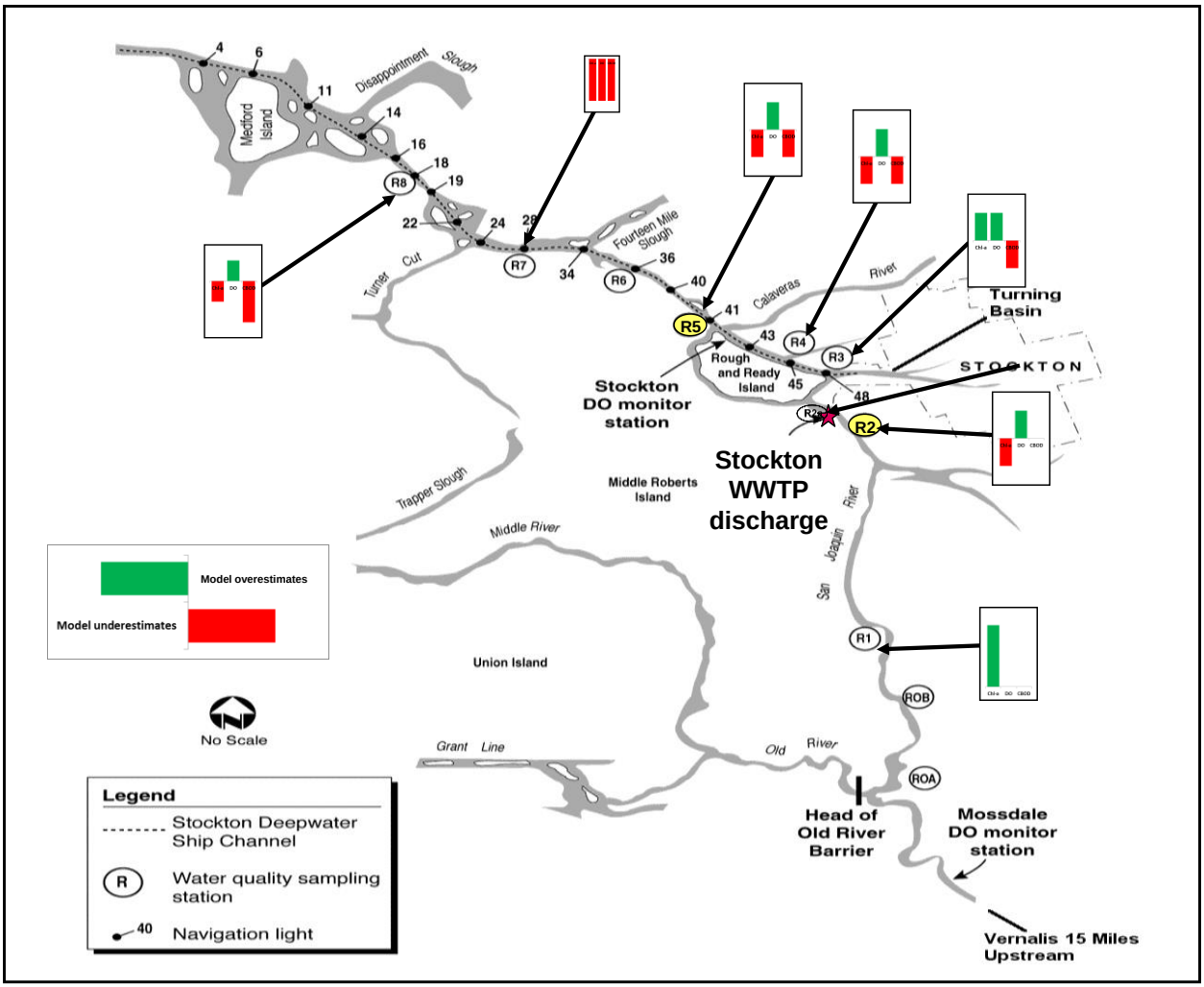

Figure 6-55 This graphical representation of model results shows the over or under-estimation Bias of three constituents – Algae (measurement is Chlorophyll-a, Chl-a), DO and PO_4-P. The bar height represents the values shown in the right hand column of Table 6-9.

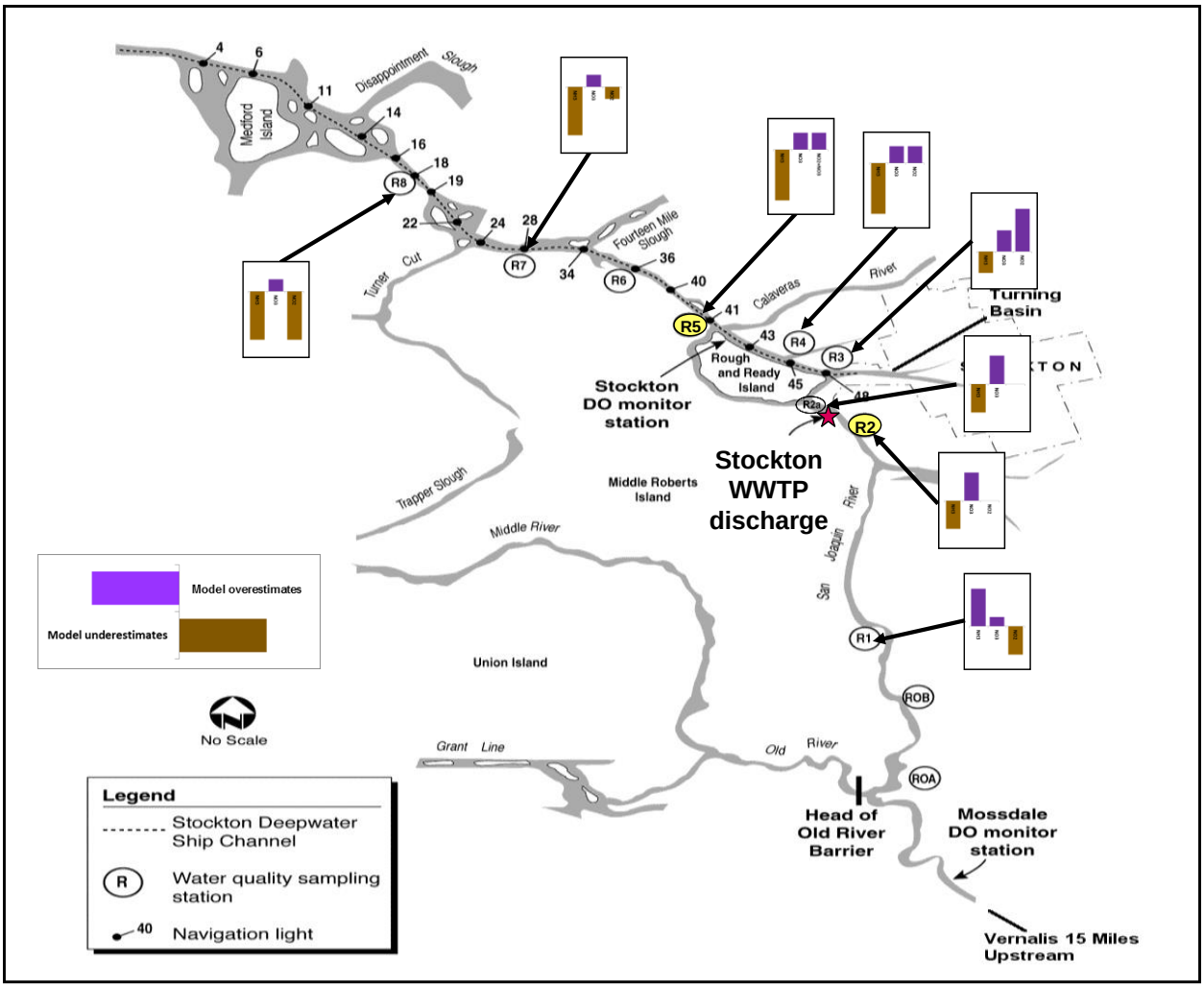

Figure 6-56 This graphical representation of model results shows the over or under-estimation Bias of three constituents – NH_3, NO_3+NO_2, and Organic-N. The bar height represents the values shown in the right hand column of Table 6-9.

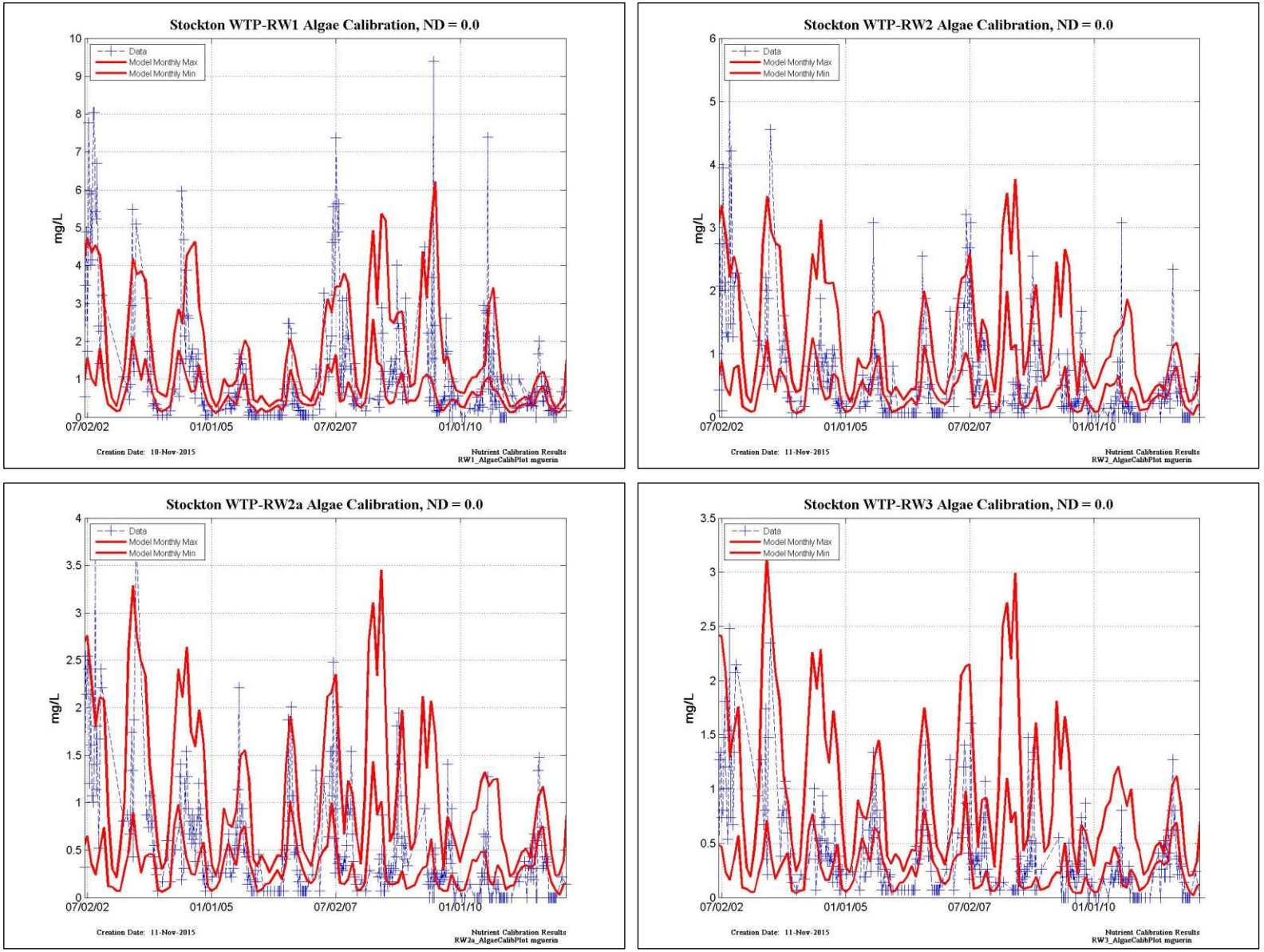

Figure 6-57 Algae at Stockton WWTP upstream RW locations.

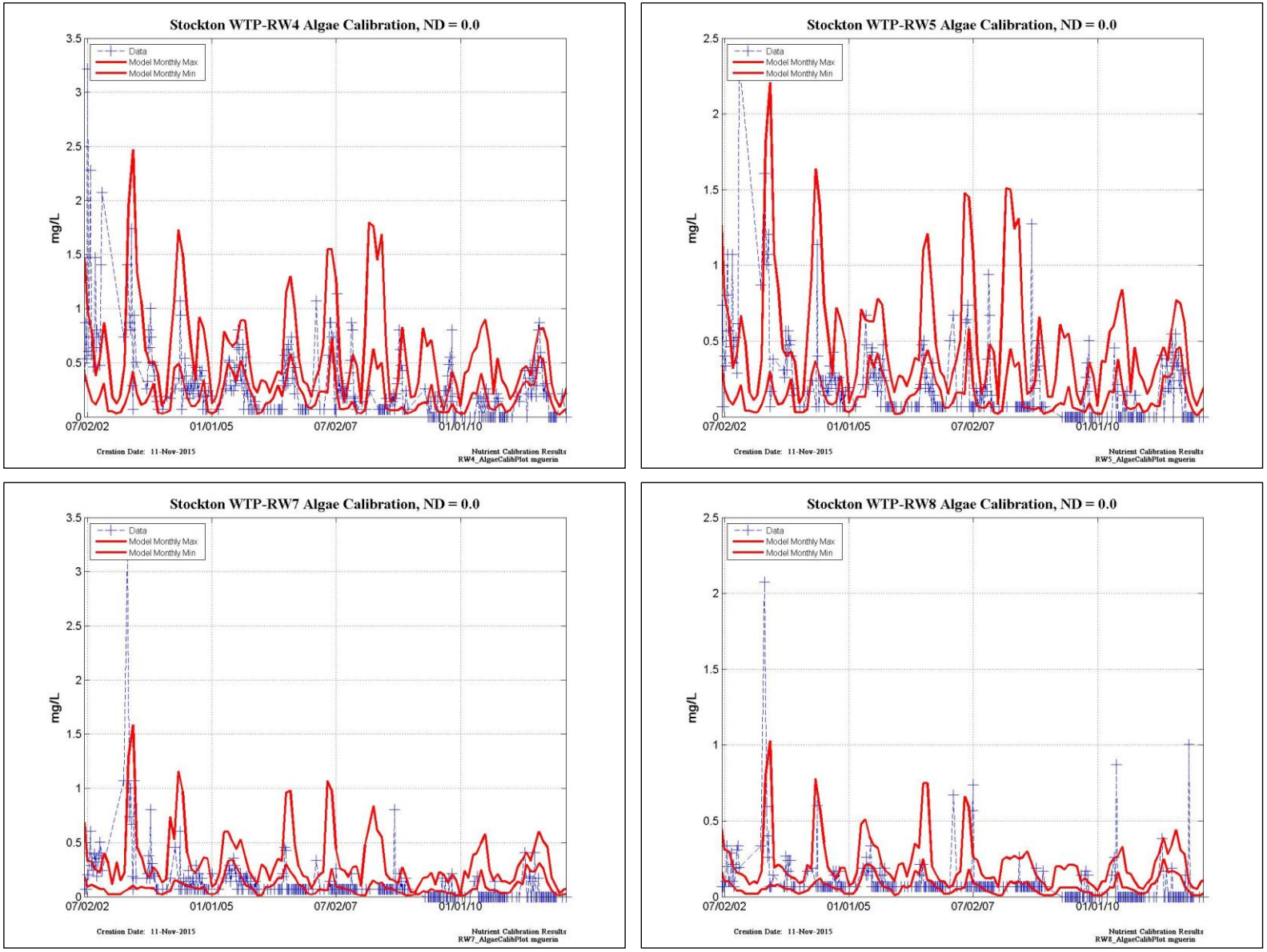

Figure 6-58 Algae at Stockton WWTP downstream RW locations.

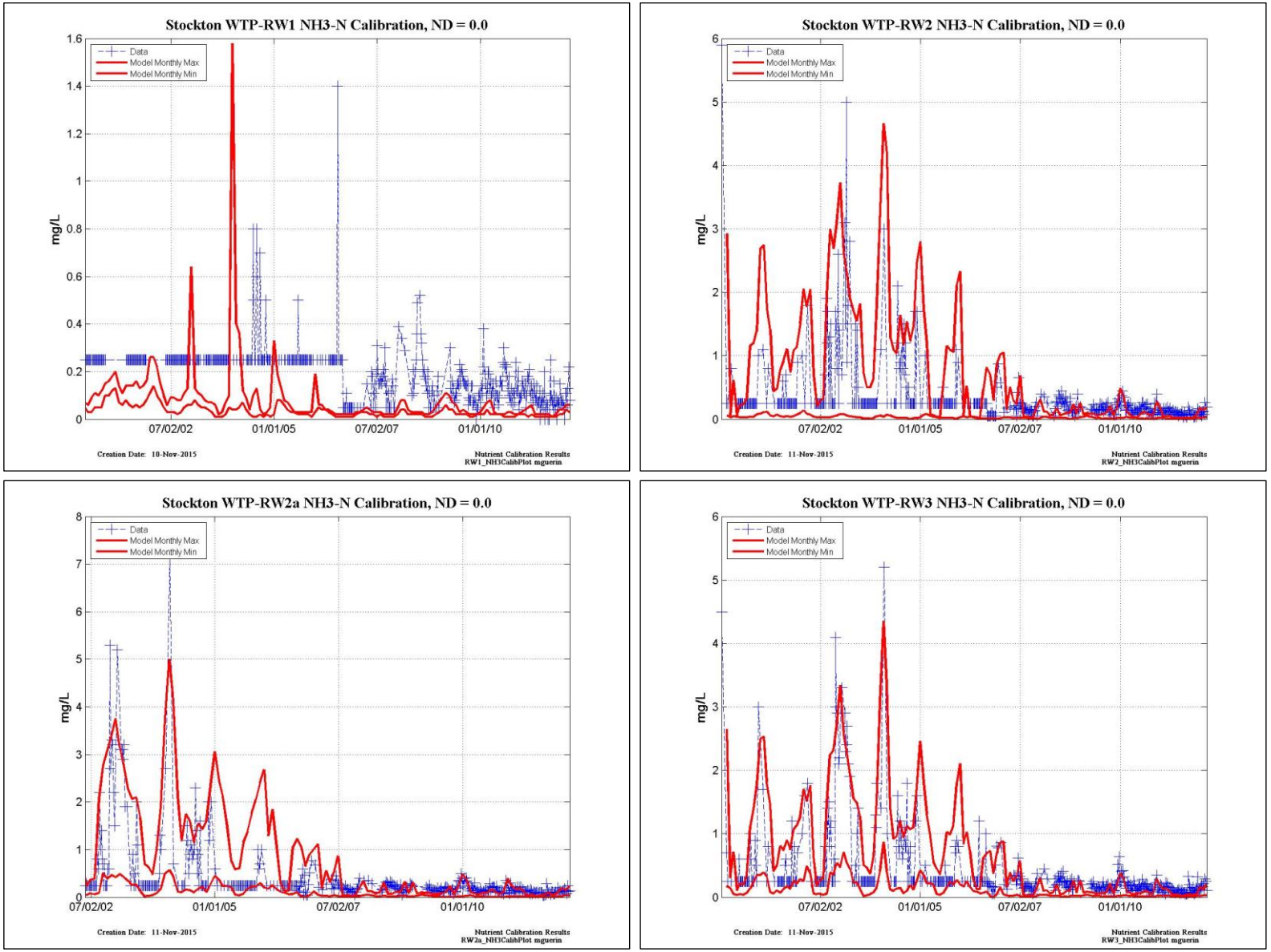

Figure 6-59 NH_3-N at Stockton WWTP upstream RW locations.

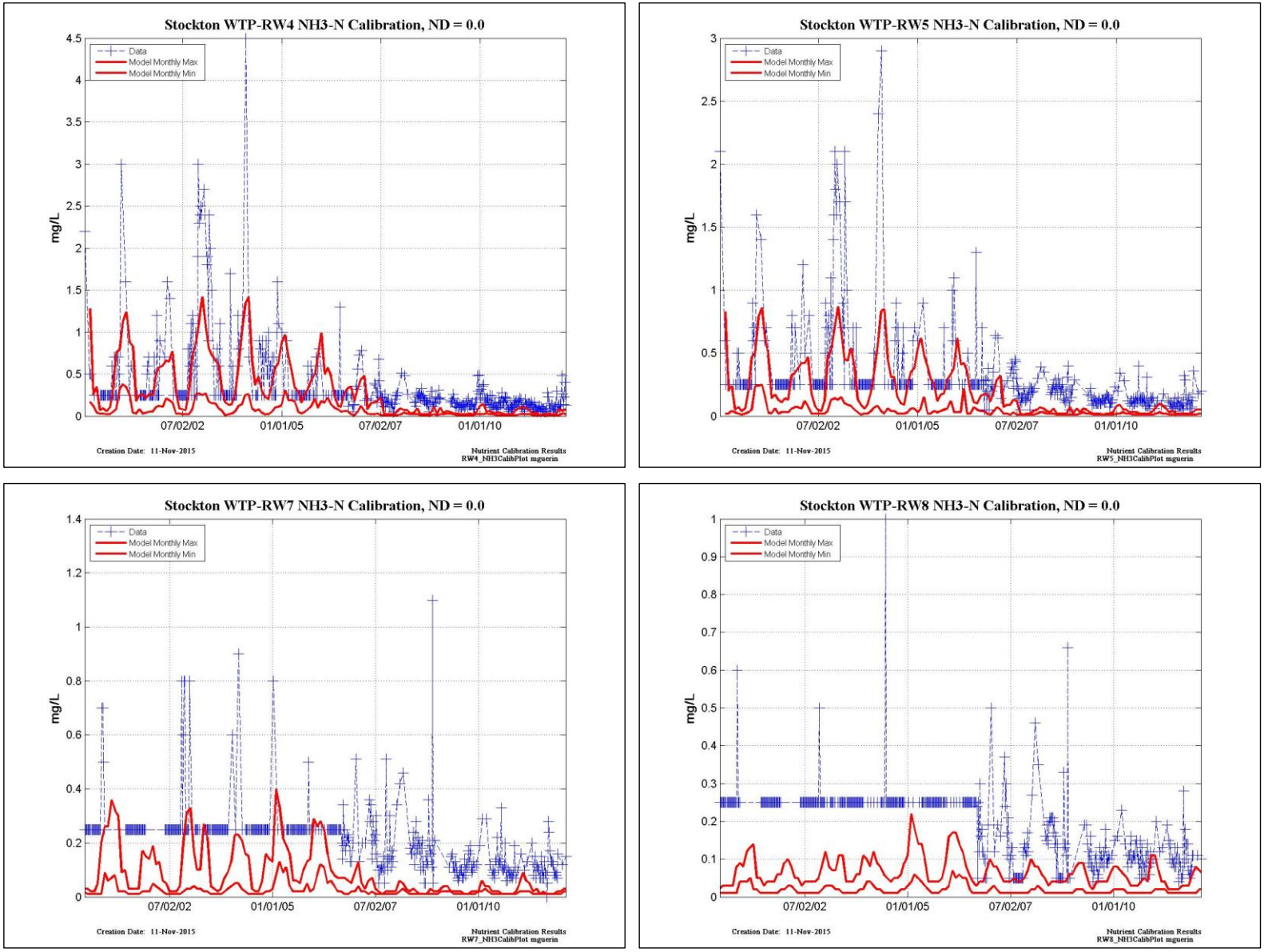

Figure 6-60 NH_3-N at Stockton WWTP downstream RW locations.

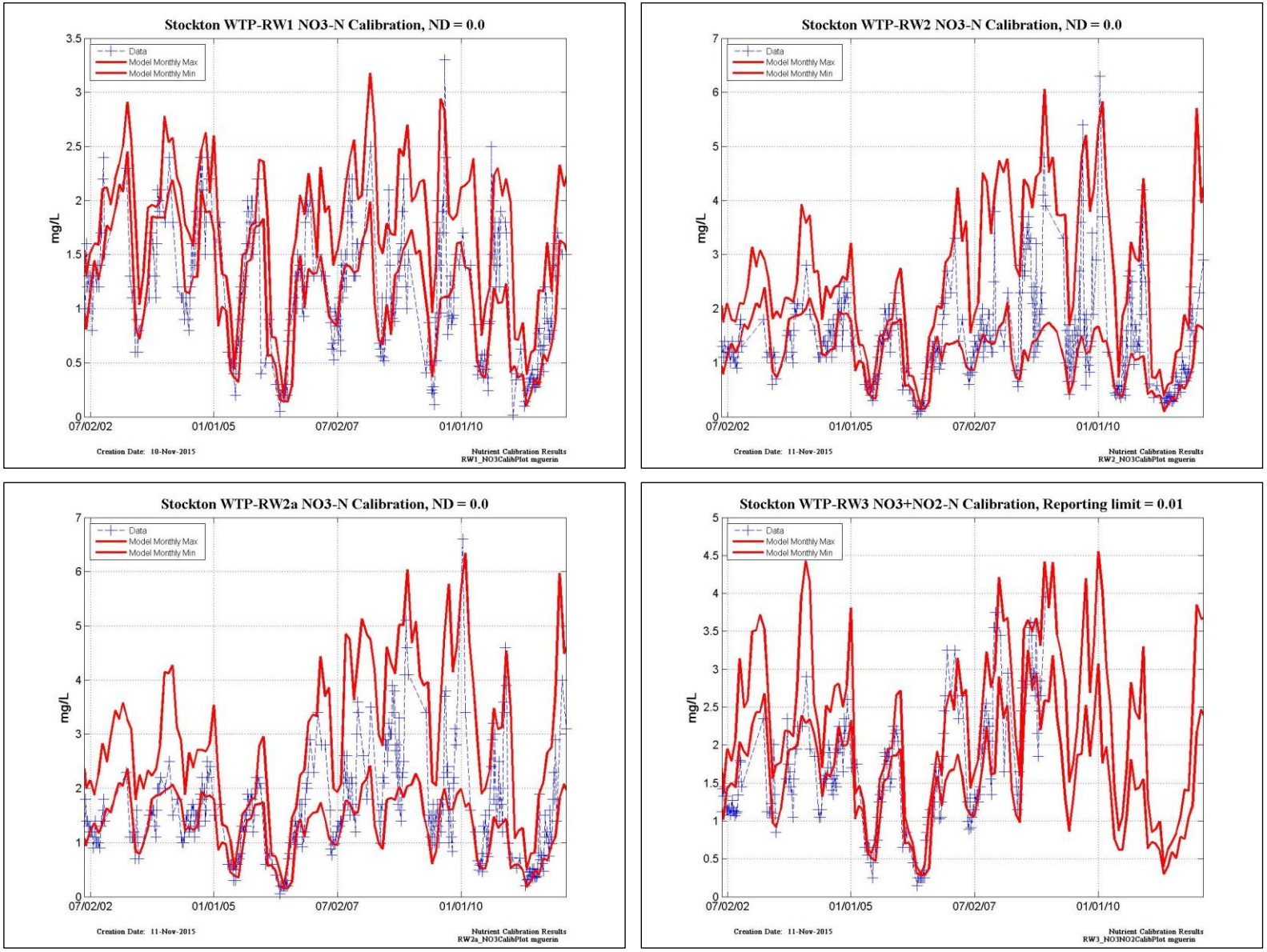

Figure 6-61 NO_3-N or NO_2+ NO_3-N at Stockton WWTP upstream RW locations.

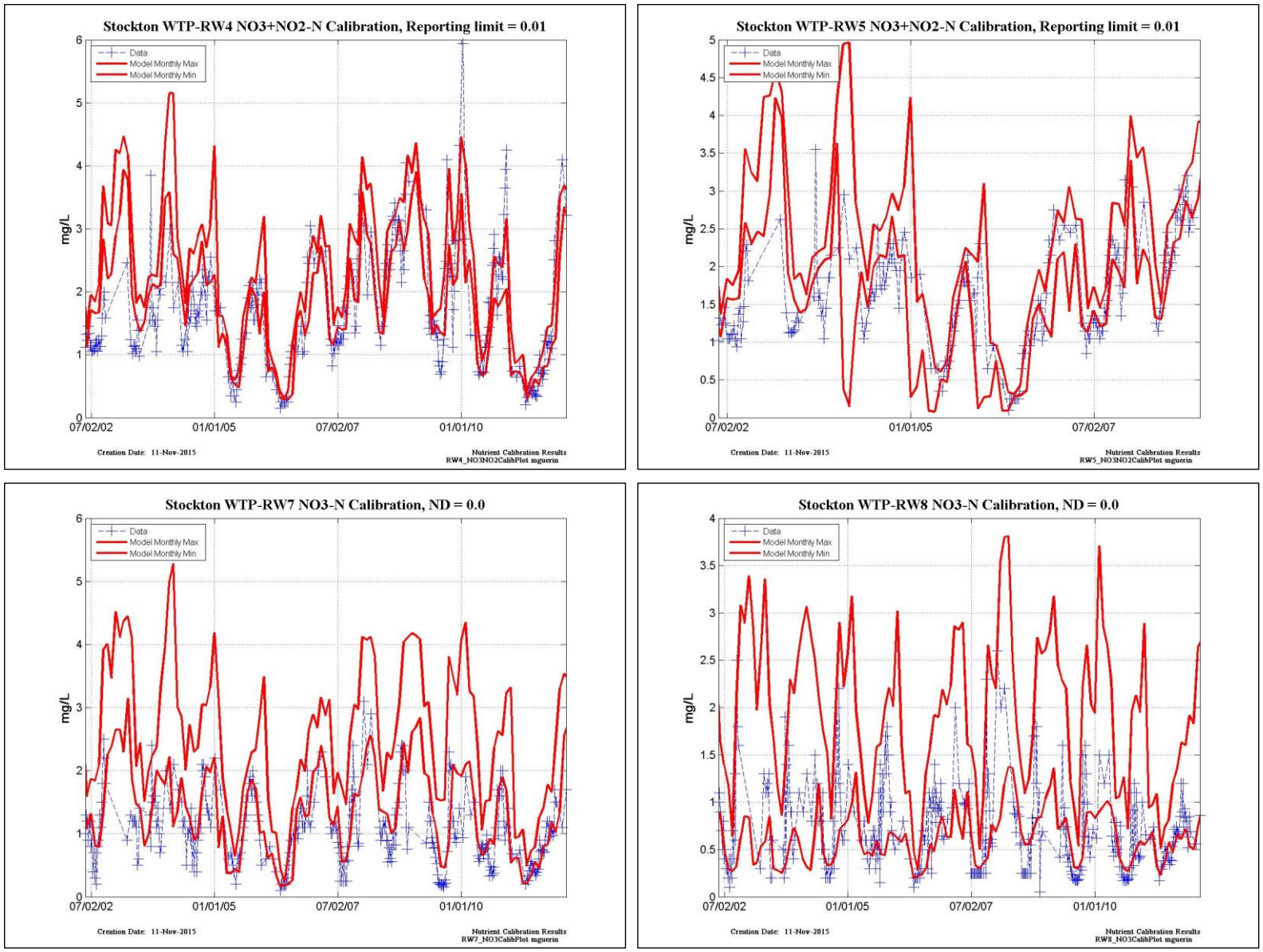

Figure 6-62 NO_3-N or NO_2+ NO_3-N at Stockton WWTP downstream RW locations.

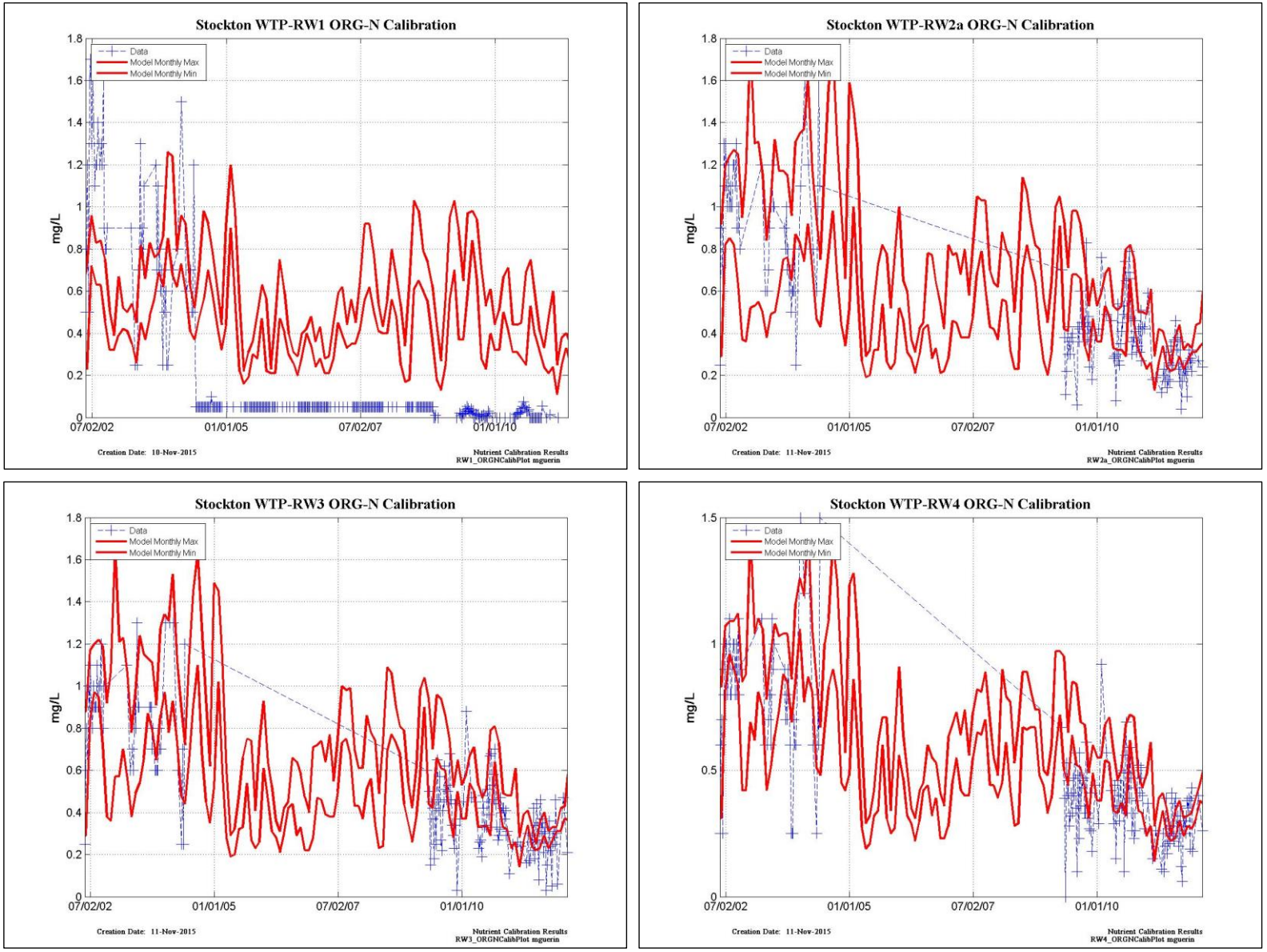

Figure 6-63 Organic-N at Stockton WWTP upstream RW locations.

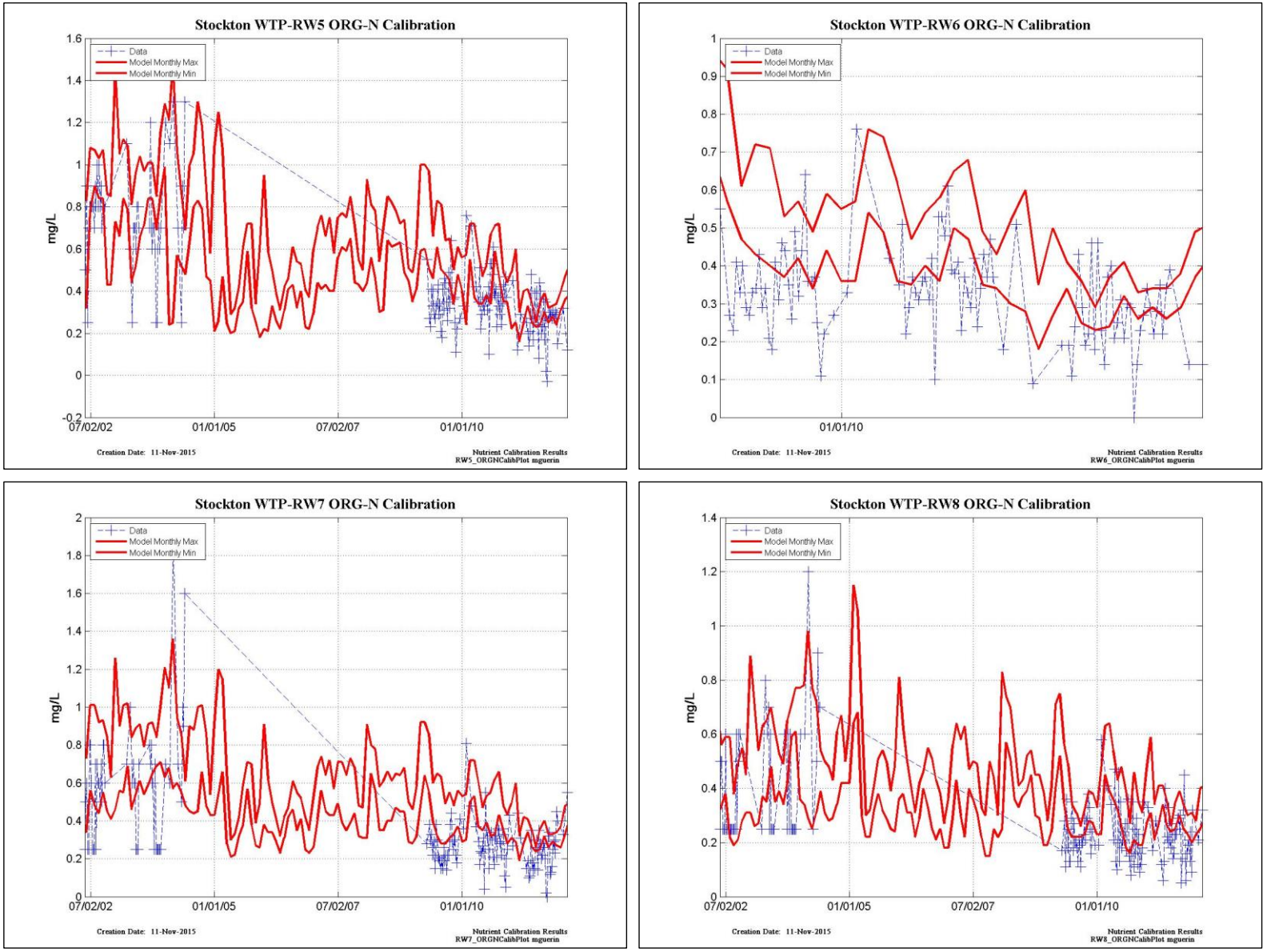

Figure 6-64 Organic-N at Stockton WWTP downstream RW locations.

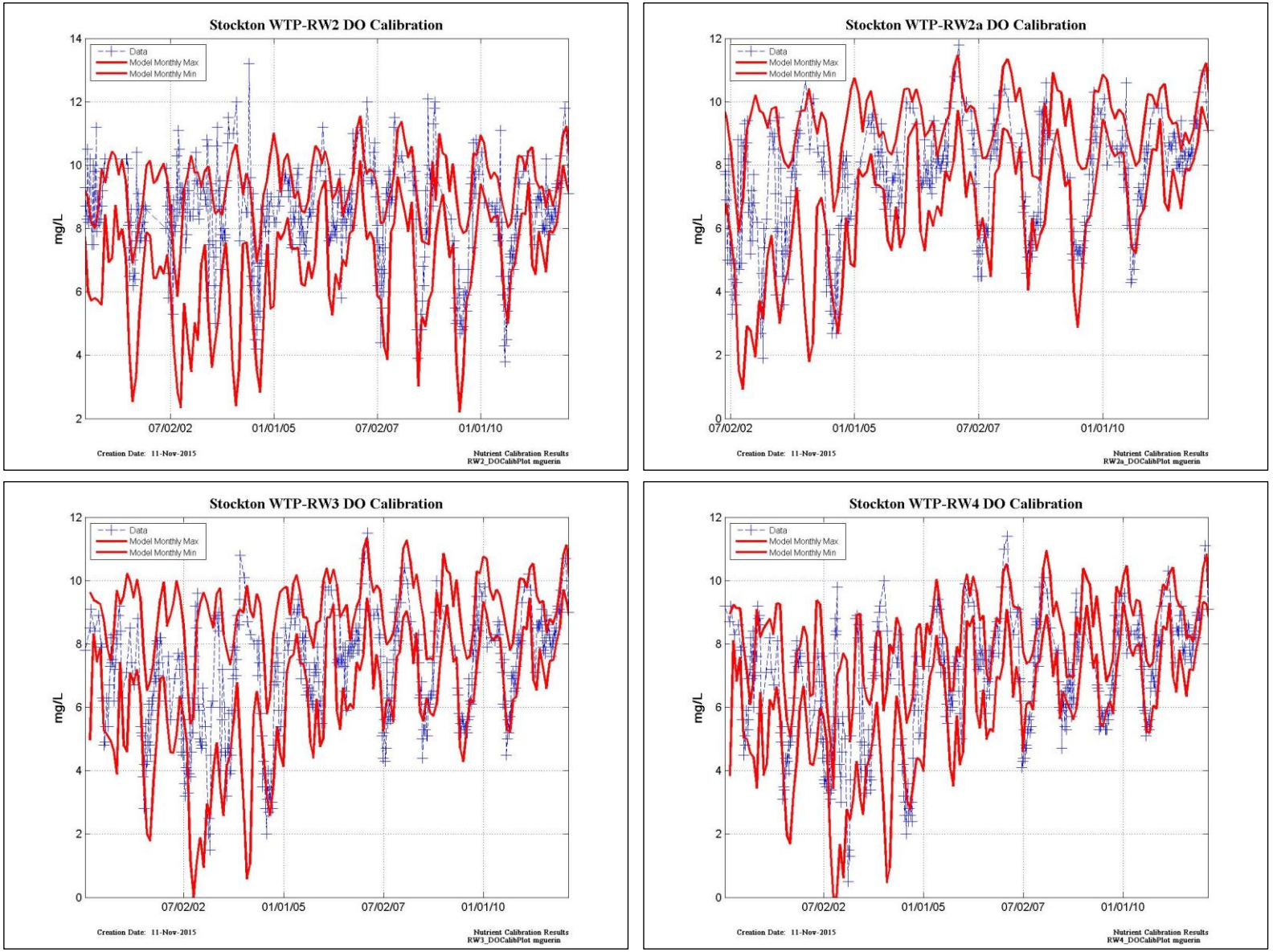

Figure 6-65 DO at Stockton WWTP upstream RW locations.

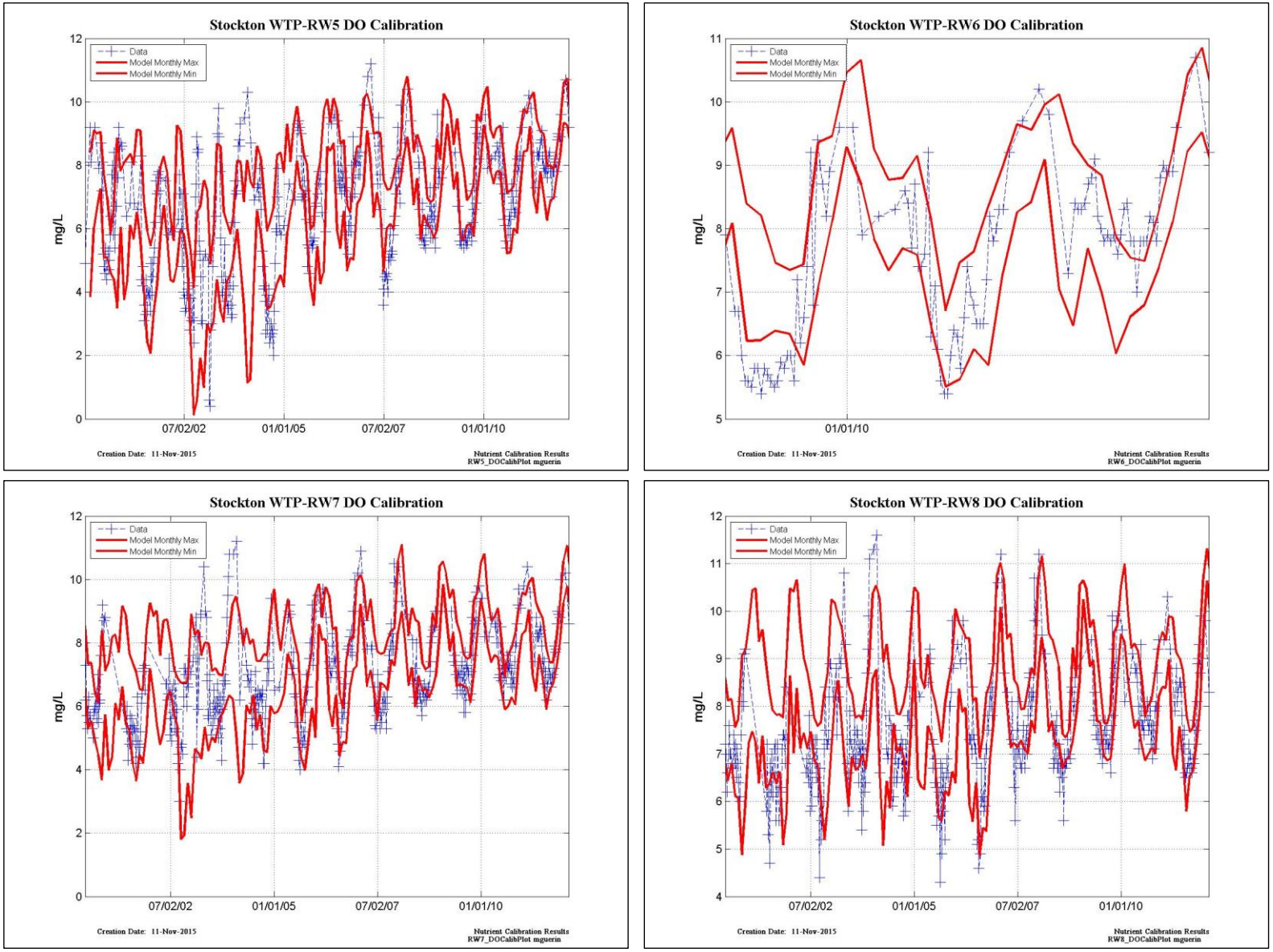

Figure 6-66 DO at Stockton WWTP downstream RW locations.

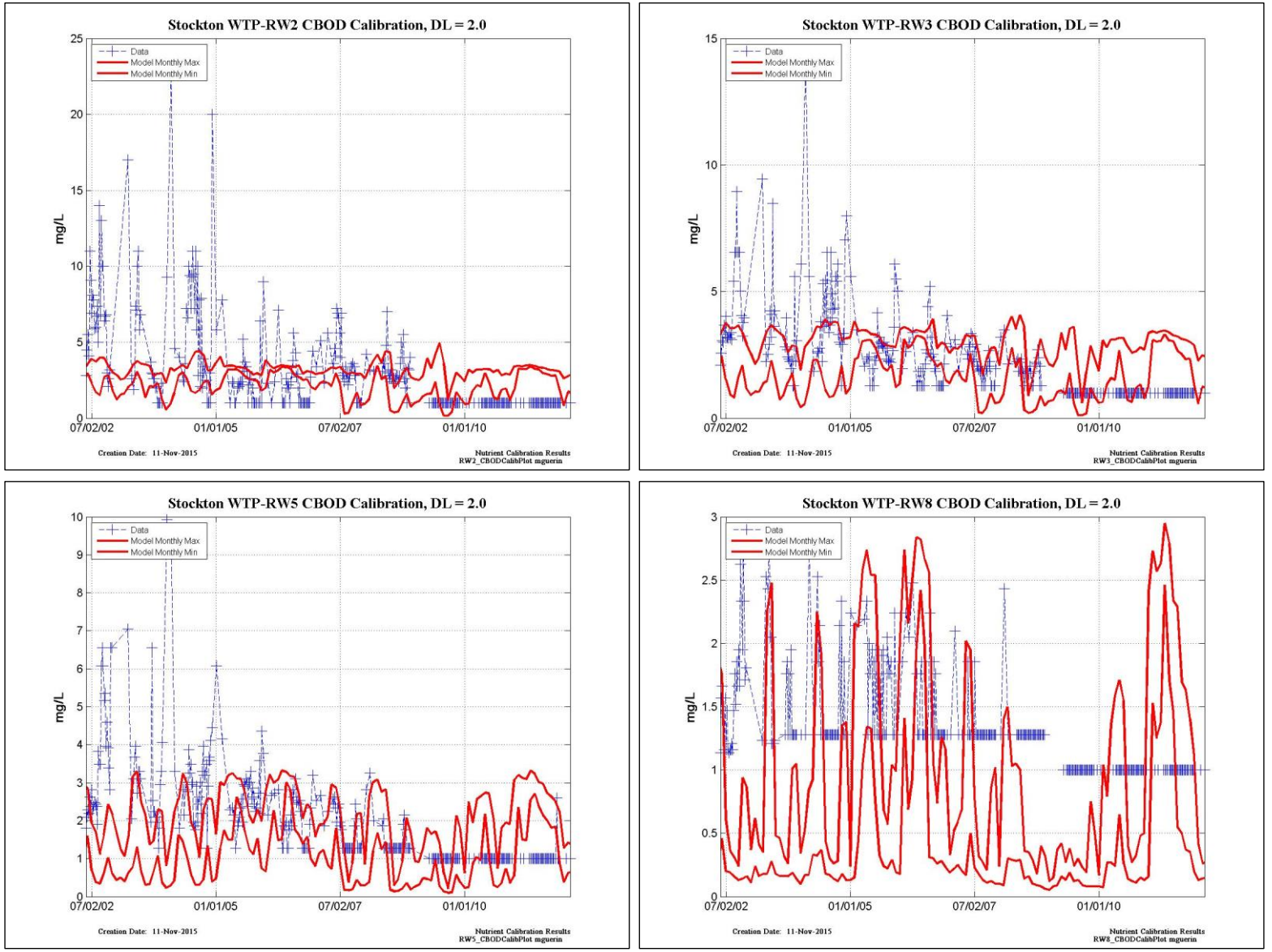

Figure 6-67 BOD data and modeled CBOD at selected Stockton WWTP RW locations.

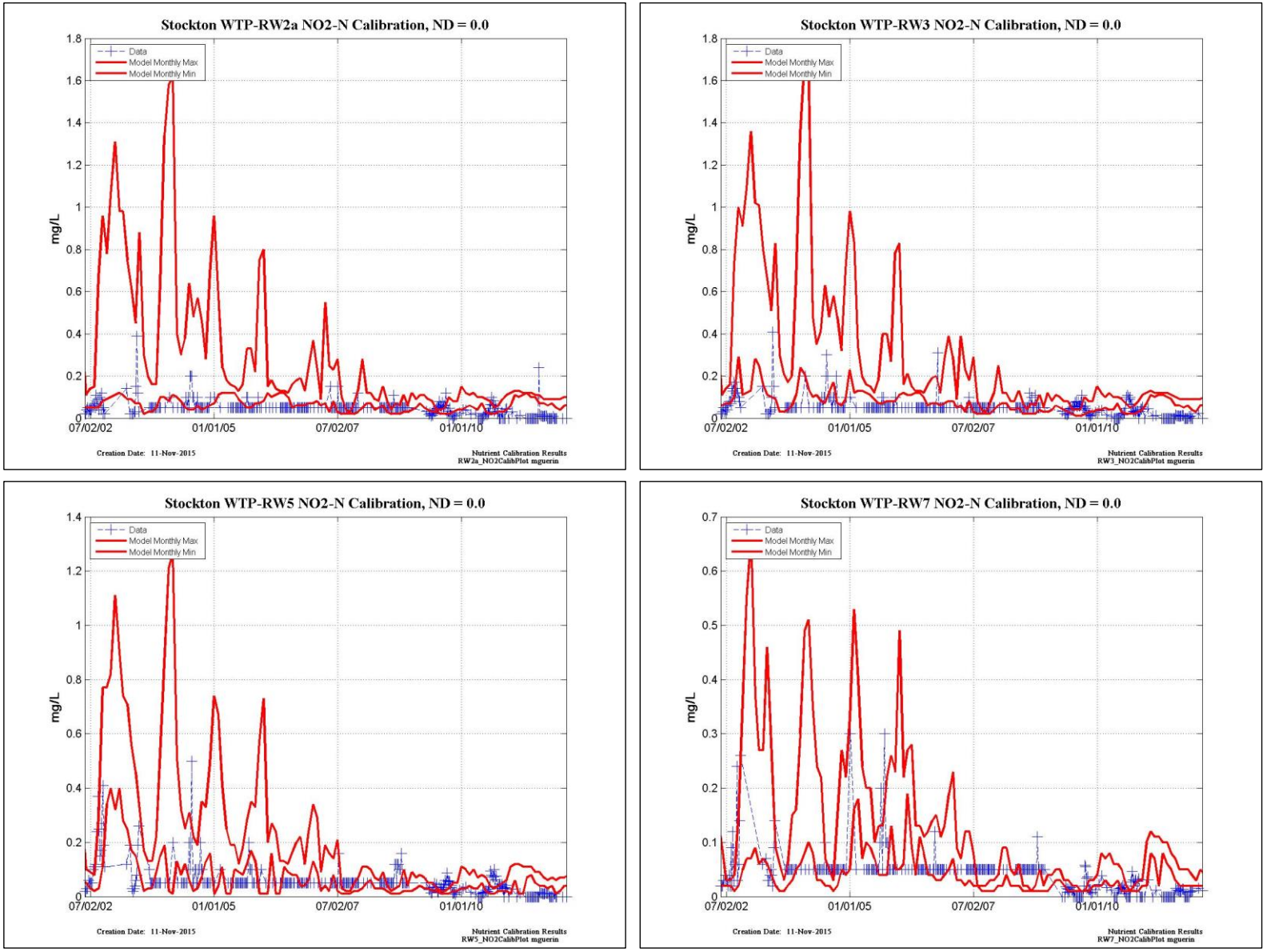

Figure 6-68 NO_2-N at selected Stockton WWTP RW locations.

RW1 - ALGAE	NSE	PBIAS	Bias	RSR
ALL	VG	VG	Underestimate	VG
Dry WY Calibration	VG	VG	Underestimate	VG
Wet WY Calibration	VG	VG	Underestimate	VG
Dry WY Validation	G	VG	Underestimate	G
Wet WY Validation	VG	VG	Overestimate	VG

RW1 - NH3	NSE	PBIAS	Bias	RSR
ALL	S	U	Underestimate	U
Dry WY Calibration	S	S	Underestimate	U
Wet WY Calibration	S	S	Underestimate	U
Dry WY Validation	S	U	Underestimate	U
Wet WY Validation	U	U	Underestimate	U

RW1 - NO2	NSE	PBIAS	Bias	RSR
ALL	U	S	Overestimate	U
Dry WY Calibration	U	S	Overestimate	U
Wet WY Calibration	U	U	Overestimate	U
Dry WY Validation	U	VG	Overestimate	U
Wet WY Validation	VG	U	Overestimate	U

RW1 - NO3	NSE	PBIAS	Bias	RSR
ALL	VG	VG	Overestimate	VG
Dry WY Calibration	VG	VG	Overestimate	G
Wet WY Calibration	VG	VG	Overestimate	VG
Dry WY Validation	VG	VG	Overestimate	VG
Wet WY Validation	VG	VG	Overestimate	VG

RW1 - ORGN	NSE	PBIAS	Bias	RSR
ALL	S	U	Overestimate	U
Dry WY Calibration	S	VG	Overestimate	U
Wet WY Calibration	S	VG	Overestimate	U
Dry WY Validation	U	U	Overestimate	U
Wet WY Validation	VG	U	Overestimate	U

Figure 6-69 Categorical statistics for nutrients at receiving water location RW1.

RW2 - ALGAE	NSE	PBIAS	Bias	RSR
ALL	VG	VG	Overestimate	VG
Dry WY Calibration	G	VG	Underestimate	G
Wet WY Calibration	VG	VG	Underestimate	VG
Dry WY Validation	VG	VG	Overestimate	VG
Wet WY Validation	VG	VG	Overestimate	VG

RW2 - DO	NSE	PBIAS	Bias	RSR
ALL	VG	VG	Underestimate	VG
Dry WY Calibration	G	VG	Underestimate	S
Wet WY Calibration	G	VG	Underestimate	G
Dry WY Validation	VG	VG	Underestimate	G
Wet WY Validation	VG	VG	Underestimate	VG

RW2 - NH3	NSE	PBIAS	Bias	RSR
ALL	VG	VG	Underestimate	VG
Dry WY Calibration	VG	VG	Underestimate	VG
Wet WY Calibration	VG	VG	Underestimate	VG
Dry WY Validation	S	S	Underestimate	U
Wet WY Validation	G	G	Underestimate	S

RW2 - NO3	NSE	PBIAS	Bias	RSR
ALL	VG	VG	Overestimate	VG
Dry WY Calibration	VG	VG	Overestimate	VG
Wet WY Calibration	VG	VG	Overestimate	VG
Dry WY Validation	VG	VG	Overestimate	VG
Wet WY Validation	VG	VG	Overestimate	VG

RW2A - ALGAE	NSE	PBIAS	Bias	RSR
ALL	VG	VG	Overestimate	VG
Dry WY Calibration	VG	VG	Underestimate	VG
Wet WY Calibration	VG	VG	Underestimate	VG
Dry WY Validation	G	VG	Overestimate	G
Wet WY Validation	VG	VG	Overestimate	VG

RW2A - NH3	NSE	PBIAS	Bias	RSR
ALL	VG	VG	Underestimate	VG
Dry WY Calibration	VG	VG	Underestimate	VG
Wet WY Calibration	VG	VG	Underestimate	VG
Dry WY Validation	U	S	Underestimate	U
Wet WY Validation	VG	VG	Underestimate	VG

RW2A - DO	NSE	PBIAS	Bias	RSR
ALL	VG	VG	Overestimate	VG
Dry WY Calibration	VG	VG	Overestimate	VG
Wet WY Calibration	VG	VG	Overestimate	VG
Dry WY Validation	VG	VG	Overestimate	VG
Wet WY Validation	VG	VG	Underestimate	VG

RW2A - NO3	NSE	PBIAS	Bias	RSR
ALL	VG	VG	Overestimate	VG
Dry WY Calibration	VG	VG	Overestimate	VG
Wet WY Calibration	VG	VG	Overestimate	VG
Dry WY Validation	VG	VG	Overestimate	VG
Wet WY Validation	VG	VG	Overestimate	VG

Figure 6-70 Categorical statistics for nutrients at receiving water locations RW2 and RW2a.

RW3 - ALGAE	NSE	PBIAS	Bias	RSR
ALL	VG	VG	Overestimate	VG
Dry WY Calibration	VG	VG	Underestimate	VG
Wet WY Calibration	VG	VG	Overestimate	VG
Dry WY Validation	S	VG	Overestimate	S
Wet WY Validation	VG	G	Overestimate	VG

RW3 - NH3	NSE	PBIAS	Bias	RSR
ALL	VG	VG	Underestimate	VG
Dry WY Calibration	VG	VG	Underestimate	VG
Wet WY Calibration	VG	VG	Underestimate	VG
Dry WY Validation	U	S	Underestimate	U
Wet WY Validation	S	VG	Underestimate	S

RW3 - CBOD	NSE	PBIAS	Bias	RSR
ALL	S	VG	Underestimate	U
Dry WY Calibration	S	VG	Underestimate	S
Wet WY Calibration	S	G	Overestimate	U
Dry WY Validation	VG	VG	Underestimate	VG
Wet WY Validation	S	VG	Overestimate	U

RW3 - NO2	NSE	PBIAS	Bias	RSR
ALL	S	G	Overestimate	U
Dry WY Calibration	U	G	Overestimate	U
Wet WY Calibration	S	U	Overestimate	U
Dry WY Validation	S	VG	Underestimate	U
Wet WY Validation	U	S	Overestimate	U

RW3 - DO	NSE	PBIAS	Bias	RSR
ALL	VG	VG	Overestimate	VG
Dry WY Calibration	VG	VG	Overestimate	VG
Wet WY Calibration	VG	VG	Overestimate	VG
Dry WY Validation	VG	VG	Overestimate	VG
Wet WY Validation	VG	VG	Overestimate	VG

RW3 - NO3	NSE	PBIAS	Bias	RSR
ALL	VG	VG	Overestimate	VG
Dry WY Calibration	VG	VG	Overestimate	VG
Wet WY Calibration	VG	VG	Overestimate	VG
Dry WY Validation	VG	VG	Overestimate	VG
Wet WY Validation	VG	VG	Overestimate	VG

Figure 6-71 Categorical statistics for nutrients at receiving water location RW3.

RW4 - ALGAE	NSE	PBIAS	Bias	RSR
ALL	S	VG	Underestimate	S
Dry WY Calibration	S	G	Underestimate	U
Wet WY Calibration	VG	VG	Overestimate	VG
Dry WY Validation	S	VG	Overestimate	S
Wet WY Validation	VG	G	Overestimate	VG

RW4 - NH3	NSE	PBIAS	Bias	RSR
ALL	S	S	Underestimate	U
Dry WY Calibration	G	S	Underestimate	S
Wet WY Calibration	S	S	Underestimate	U
Dry WY Validation	S	U	Underestimate	U
Wet WY Validation	S	VG	Underestimate	U

RW4 - CBOD	NSE	PBIAS	Bias	RSR
ALL	S	VG	Underestimate	U
Dry WY Calibration	S	S	Underestimate	U
Wet WY Calibration	U	VG	Overestimate	U
Dry WY Validation	S	VG	Underestimate	U
Wet WY Validation	U	VG	Overestimate	U

RW4 - NO3	NSE	PBIAS	Bias	RSR
ALL	VG	VG	Overestimate	VG
Dry WY Calibration	VG	VG	Overestimate	G
Wet WY Calibration	VG	VG	Overestimate	VG
Dry WY Validation	VG	VG	Overestimate	VG
Wet WY Validation	VG	VG	Overestimate	VG

RW4 - DO	NSE	PBIAS	Bias	RSR
ALL	VG	VG	Overestimate	VG
Dry WY Calibration	VG	VG	Overestimate	VG
Wet WY Calibration	VG	VG	Underestimate	VG
Dry WY Validation	VG	VG	Overestimate	VG
Wet WY Validation	VG	VG	Underestimate	VG

RW4 - NO3+NO2	NSE	PBIAS	Bias	RSR
ALL	VG	VG	Overestimate	VG
Dry WY Calibration	G	VG	Overestimate	S
Wet WY Calibration	G	VG	Overestimate	G
Dry WY Validation	VG	VG	Overestimate	VG
Wet WY Validation	VG	VG	Overestimate	VG

Figure 6-72 Categorical statistics for nutrients at receiving water location RW4.

RW5 - NH3	NSE	PBIAS	Bias	RSR
ALL	S	S	Underestimate	U
Dry WY Calibration	G	S	Underestimate	U
Wet WY Calibration	S	S	Underestimate	U
Dry WY Validation	S	U	Underestimate	U
Wet WY Validation	S	S	Underestimate	U

RW5 - NO2	NSE	PBIAS	Bias	RSR
ALL	S	VG	Overestimate	U
Dry WY Calibration	G	VG	Overestimate	G
Wet WY Calibration	S	U	Overestimate	U
Dry WY Validation	U	G	Underestimate	U
Wet WY Validation	U	S	Overestimate	U

RW5 - NO3	NSE	PBIAS	Bias	RSR
ALL	VG	VG	Overestimate	VG
Dry WY Calibration	VG	VG	Overestimate	S
Wet WY Calibration	VG	VG	Overestimate	VG
Dry WY Validation	VG	VG	Overestimate	VG
Wet WY Validation	VG	VG	Overestimate	VG

RW5 - NO3+NO2	NSE	PBIAS	Bias	RSR
ALL	VG	VG	Overestimate	G
Dry WY Calibration	S	S	Overestimate	U
Wet WY Calibration	S	VG	Overestimate	U
Dry WY Validation	VG	VG	Overestimate	VG
Wet WY Validation	VG	VG	Overestimate	VG

RW5 - ALGAE	NSE	PBIAS	Bias	RSR
ALL	VG	VG	Overestimate	VG
Dry WY Calibration	VG	VG	Overestimate	S
Wet WY Calibration	VG	VG	Overestimate	VG
Dry WY Validation	VG	VG	Overestimate	VG
Wet WY Validation	VG	VG	Overestimate	VG

RW5 - CBOD	NSE	PBIAS	Bias	RSR
ALL	S	VG	Underestimate	U
Dry WY Calibration	S	S	Underestimate	U
Wet WY Calibration	U	VG	Overestimate	U
Dry WY Validation	S	VG	Underestimate	U
Wet WY Validation	U	VG	Underestimate	U

RW5 - DO	NSE	PBIAS	Bias	RSR
ALL	VG	VG	Overestimate	VG
Dry WY Calibration	VG	VG	Overestimate	VG
Wet WY Calibration	VG	VG	Overestimate	VG
Dry WY Validation	VG	VG	Overestimate	VG
Wet WY Validation	VG	VG	Underestimate	VG

Figure 6-73 Categorical statistics for nutrients at receiving water location RW5.

RW7 - ALGAE	NSE	PBIAS	Bias	RSR
ALL	S	VG	Underestimate	S
Dry WY Calibration	S	G	Underestimate	U
Wet WY Calibration	S	G	Underestimate	S
Dry WY Validation	S	VG	Overestimate	U
Wet WY Validation	S	S	Overestimate	U

RW7 - NH3	NSE	PBIAS	Bias	RSR
ALL	S	U	Underestimate	U
Dry WY Calibration	S	S	Underestimate	U
Wet WY Calibration	S	U	Underestimate	U
Dry WY Validation	S	U	Underestimate	U
Wet WY Validation	U	S	Underestimate	U

RW7 - CBOD	NSE	PBIAS	Bias	RSR
ALL	U	VG	Underestimate	U
Dry WY Calibration	S	S	Underestimate	U
Wet WY Calibration	U	VG	Overestimate	U
Dry WY Validation	U	G	Underestimate	U
Wet WY Validation	U	VG	Underestimate	U

RW7 - NO3	NSE	PBIAS	Bias	RSR
ALL	G	VG	Overestimate	U
Dry WY Calibration	S	G	Overestimate	U
Wet WY Calibration	S	VG	Overestimate	U
Dry WY Validation	G	VG	Overestimate	S
Wet WY Validation	VG	VG	Overestimate	VG

RW7 - DO	NSE	PBIAS	Bias	RSR
ALL	VG	VG	Underestimate	VG
Dry WY Calibration	VG	VG	Overestimate	VG
Wet WY Calibration	VG	VG	Underestimate	VG
Dry WY Validation	VG	VG	Overestimate	VG
Wet WY Validation	VG	VG	Underestimate	VG

RW7 - NO2	NSE	PBIAS	Bias	RSR
ALL	S	VG	Underestimate	S
Dry WY Calibration	VG	VG	Underestimate	VG
Wet WY Calibration	VG	VG	Overestimate	VG
Dry WY Validation	U	G	Underestimate	U
Wet WY Validation	S	G	Overestimate	U

Figure 6-74 Categorical statistics for nutrients at receiving water location RW7.

RW8 - ALGAE	NSE	PBIAS	Bias	RSR
ALL	S	VG	Underestimate	U
Dry WY Calibration	S	VG	Underestimate	U
Wet WY Calibration	S	G	Underestimate	U
Dry WY Validation	S	VG	Underestimate	U
Wet WY Validation	S	G	Overestimate	U

RW8 - NH3	NSE	PBIAS	Bias	RSR
ALL	S	U	Underestimate	U
Dry WY Calibration	S	U	Underestimate	U
Wet WY Calibration	S	U	Underestimate	U
Dry WY Validation	S	S	Underestimate	U
Wet WY Validation	U	U	Underestimate	U

RW8 - CBOD	NSE	PBIAS	Bias	RSR
ALL	U	G	Underestimate	U
Dry WY Calibration	S	S	Underestimate	U
Wet WY Calibration	U	VG	Underestimate	U
Dry WY Validation	U	S	Underestimate	U
Wet WY Validation	U	VG	Underestimate	U

RW8 - NO3	NSE	PBIAS	Bias	RSR
ALL	VG	VG	Overestimate	VG
Dry WY Calibration	VG	VG	Overestimate	VG
Wet WY Calibration	VG	VG	Overestimate	VG
Dry WY Validation	VG	VG	Overestimate	VG
Wet WY Validation	VG	VG	Overestimate	VG

RW8 - DO	NSE	PBIAS	Bias	RSR
ALL	VG	VG	Overestimate	VG
Dry WY Calibration	VG	VG	Overestimate	VG
Wet WY Calibration	VG	VG	Overestimate	VG
Dry WY Validation	VG	VG	Overestimate	VG
Wet WY Validation	VG	VG	Overestimate	VG

RW8 - NO2	NSE	PBIAS	Bias	RSR
ALL	S	U	Underestimate	U
Dry WY Calibration	S	U	Underestimate	U
Wet WY Calibration	S	U	Underestimate	U
Dry WY Validation	S	U	Underestimate	U
Wet WY Validation	U	U	Underestimate	U

Figure 6-75 Categorical statistics for nutrients at receiving water location RW8.

6.8 Regions Used for Mass Balance Calculations

One of the primary uses for the recalibrated DSM2 nutrient model output for this project was to refine the spatial understanding of where and when nutrient mass was lost or gained in the Delta. For project purposes, only nitrogen-species were used in these analyses. In order to refine the spatial understanding of nutrient dynamics, seven subregions in the DSM2 model domain were defined, as shown in Figure 6-76. These regions were based in part on the subdivision of the model domain into three DICU regions, as shown in Figure 6-13, and in part on the desire to minimize the number of channels allowing flows between regions (to simplify calculations). Figure 6-77 shows the regional boundaries in the DSM2 grid. Details on the calculations to define mass transport are explained below.

6.8.1 Rationale for the Seven Mass Balance Regions

The North and East regions in Figure 6-76 were based on the former North region in Figure 6-13, cut at the channel where the Delta Cross Channel is located. The West and Southeast DICU regions were combined and then subdivided, The West region in Figure 6-76 has no DICU locations, simplifying calculations for the mass load calculations. The SJR region includes the main effluent and boundary inflow sources along the upper reaches of the San Joaquin River, split at a single downstream channel in DSM2. The Central Region includes the main open water areas in the model domain (the "reservoirs"), apart from Liberty Island. The Confluence region makes hydrodynamic sense, including the bi-directional flows through Threemile Slough and the confluence. The main CCWD export location at Old River, and the SWP and CVP export locations are in the South region.

6.8.2 Regional Calculations Defined

At each channel that crosses a regional boundary, the monthly average flow was calculated, and the direction of the flow (into or out of) a region was noted. Monthly average model concentrations at this channel location were converted to mass loads (such as kg-NO_3) using these monthly average flows. Load exchange in a Region was calculated from the load into region from boundary inflows, DICU inflow, and exchange into region from the boundary regions and the load out of the region due to exports, outflow and DICU diversions (both the latter loads leave the model domain), and to boundary regions (these loads remain in the model).

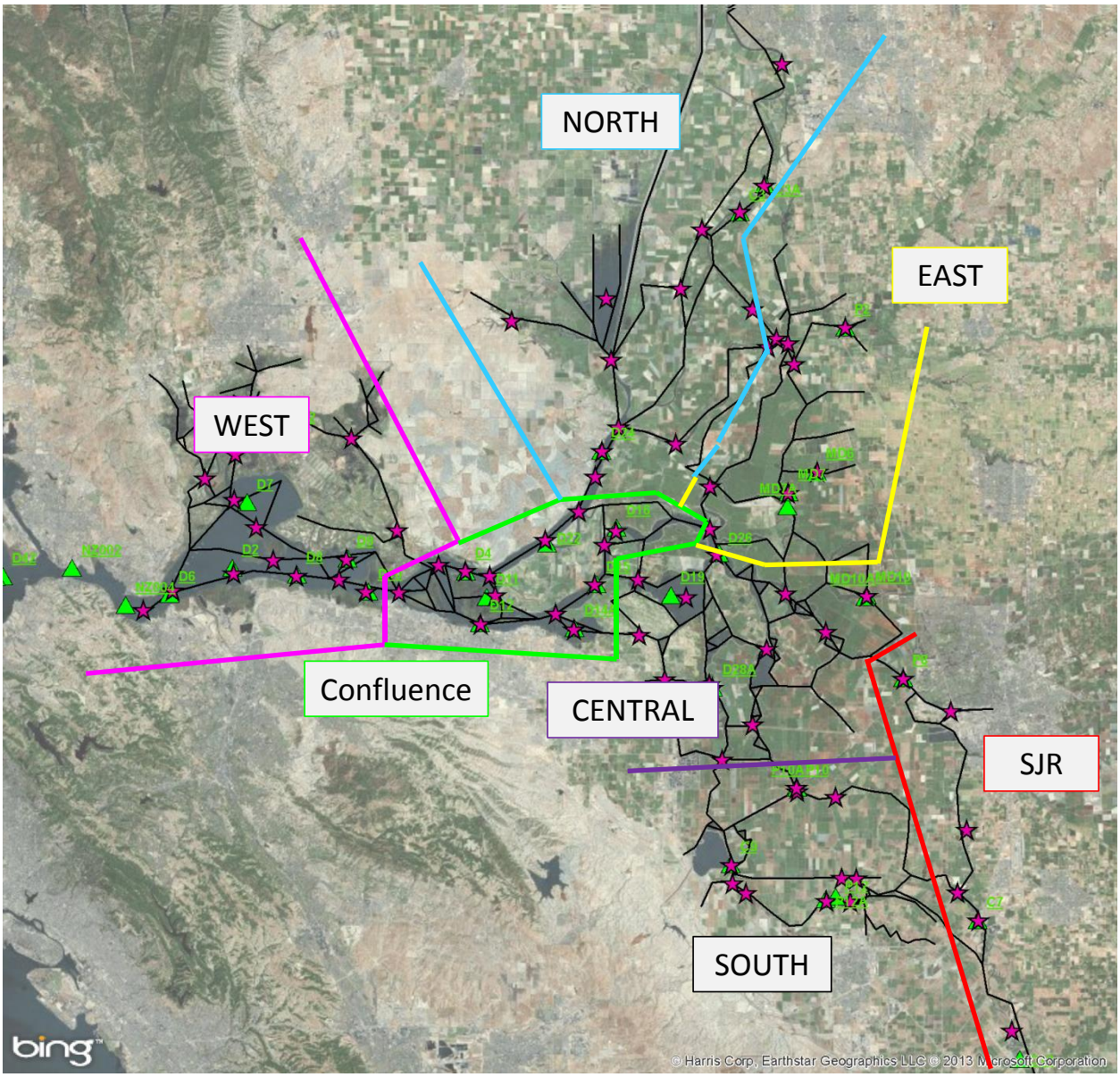

Figure 6-76 The seven regions defined to understand mass balances within the DSM2 model domain.

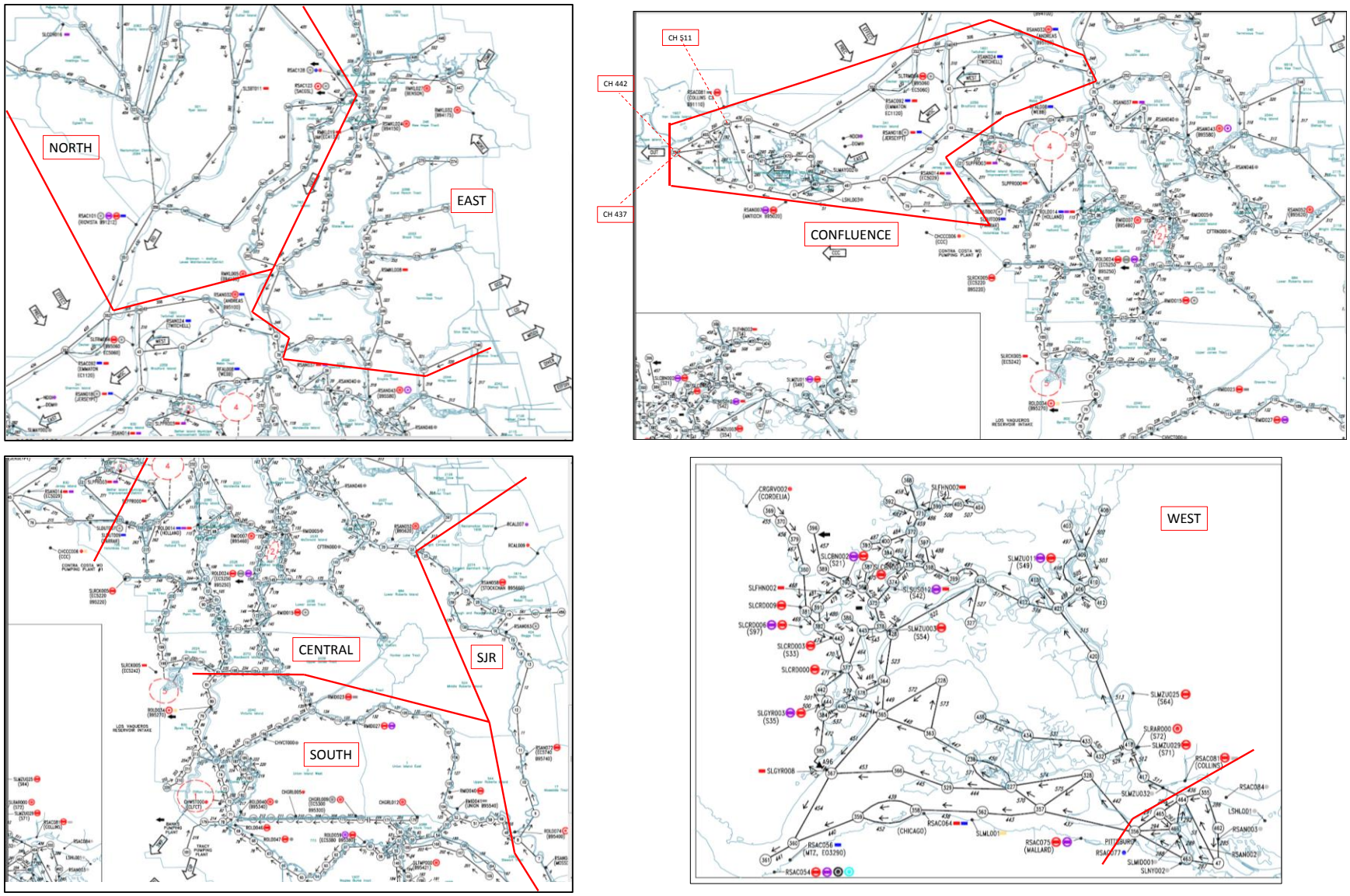

Figure 6-77 Definition of the seven regions are outlined in the DSM2 grid.

6.9 QUAL Volumetric Calculations

Figure 6-78 demonstrates the type of output plot that can be created from DSM2-QUAL volumetric model output. The daily average model output was monthly averaged, and several locations with low percentages were combined – the San Joaquin and Calaveras percentages were combined, as were the Sacramento River and Yolo Bypass, and the volumes from all WWTP sources reaching this location. The contributions from DICU sources are denoted “From-Ag”, while the combined source “From-East” is the combined volume from the Cosumnes and Mokelumne Rivers.

Although Sacramento River water (light blue percentage) dominates the volumetric percentage for mots time periods, on occasion, high flow periods on the San Joaquin River (purple percentage) can also dominate the und at Prisoner’s Point. During low Sacramento and San Joaquin River inflows, agricultural sources (green percentage) are calculated to provide up to ten percent of the volume, although this contribution is subject to greater uncertainty as agricultural source terms are calculated within the DICU model, and these sources are not gauged. The volume percentage of water from the model boundary at Martinez is shown in red, while the sum of all WWTP sources is shown in grey.

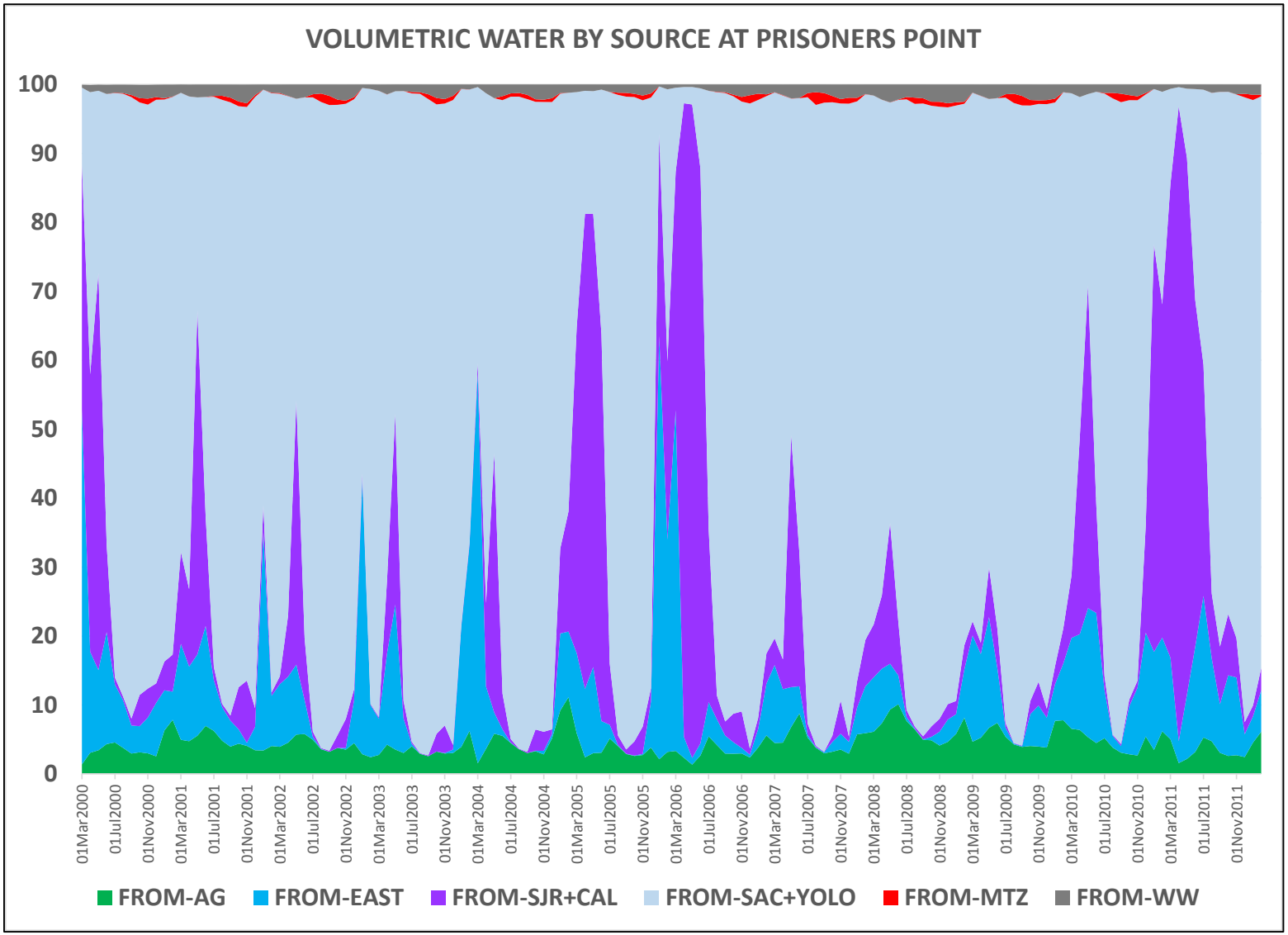

Figure 6-78 Example of monthly averaged volumetric output at Prisoner's Point on the San Joaquin River.

6.10 Discussion of Calibration Results and Model Skill

6.10.1.1 Ranking Model Skill by Constituent

This section discusses the DSM2-QUAL nutrient model calibration Model Skill by constituent. The results are separated by the source agency of the calibration data. Comparison between model output and EMP data is summarized categorically and for Model Skill in Figure 6-79 through Figure 6-84, while Stockton WWTP receiving water data along the San Joaquin River is summarized in Figure 6-85 through Figure 6-90.

In each figure, the categorical assessment of the model constituent is documented in the left hand table while the numerical values from Table 6-9 used to calculate Model Skill for the three main statistical measures (NSE, PBIAS and RSR) is documented in the right hand table. The model-wide Model Skill is the average of the numerical values at the available locations. Sections 6.7.4 and 6.7.5 discuss these statistics in detail. In general the PBIAS statistics is less strict than the NSE and RSR statistics as PBIAS ranges are specific to N- and P-constituents, while the other ranges are more generally applied to stream flow or sediment transport. As seen in many of the tables, the RSR rating is generally lower than the other two ratings, with PBIAS generally the most optimistic.

For the EMP data calibration results, several locations were not modeled well for any of the constituents, notably MD10 (Disappointment Slough), D28A (Old River at Rancho Del Rio) and, for some constituents, P8 (Buckley Cove). For the Stockton WWTP receiving water data, the results tended to be worse for certain constituents, rather than by location – notably for NO_2-N, CBOD and for locations downstream of the WWTP, NH_3-N. Note that the receiving water data was actually BOD-5 or BOD-10, not the model constituent CBOD – and the model CBOD underestimated BOD which is not surprising as BOD includes NBOD (see Section 6.3.2.3 for further detail). The quality of the model calibration on the San Joaquin River for N-constituents tended to change at the time the Stockton WWTP went to tertiary treatment.

Figure 6-79 and Figure 6-85 give the calibration results for the modeled Algae constituent for EMP and Stockton WWTP data, respectively. The Model Skill for Algae ranges from Very Good to Satisfactory, with the lower 'Satisfactory' RSR value for EMP data explained by two factors – some locations missed peak values and some locations were not modeled well for any constituent.

Only the EMP dataset had PO_4-P measurements – the results are shown in Figure 6-80. The Model Skill for the PO_4-P constituent ranges from Very Good to Satisfactory. The lower RSR values occurred in locations in the Eastern and Central Delta where generally there were fewer data locations to use in calibrating the model.

Figure 6-81 and Figure 6-86 give the calibration results for the modeled DO constituent for the EMP and Stockton WWTP data, respectively. The Model Skill for DO ranges from Very Good to Good, with San Joaquin River Model Skill somewhat better than that for EMP locations.

Figure 6-82 and Figure 6-87 give the calibration results for the modeled NH_3-N constituent for the EMP and Stockton WWTP data, respectively. The Model Skill for NH_3-N ranges from Good to Satisfactory. The San Joaquin River Model Skill is somewhat worse than that for EMP locations, in part due to the difficulty with representing this constituent before and after the WWTP switch to tertiary treatment.

Figure 6-83 and Figure 6-88 give the calibration results for the modeled NO_3+NO_2-N or the NO_3-N constituents for the EMP and Stockton WWTP data, respectively. . The Model Skill ranges from Very Good to Good – if considering these results without few poorly modeled EMP locations, the results for these constituents are generally Very Good. Note that there was somewhat of a trade-off between getting the calibration of these constituents correct, and getting the NH_3-N constituent calibration correct.

Only the EMP dataset had enough Organic-N measurements to consider for statistics – the results are shown in Figure 6-84. The Model Skill for this constituent ranges from Very Good to Satisfactory.

6.10.1.2 Discussion of Model Skill

When viewed over the DSM2 model domain, the QUAL nutrient Model Skill ranges from Very Good to Satisfactory, with the RSR skill value generally lower than the NSE or PBIAS values. There were a few locations that were modeled poorly for all constituents, and these locations tended to be in areas with less calibration data in their vicinity, for example D28A on Old River at Rancho Del Rio. D28A is well downstream of the model boundaries and there is little nutrient data nearby the help set rate coefficients in the surrounding Delta and much of the water passing this location originated at the Sacramento River boundary. Another EMP data location that is poorly modeled is Disappointment Slough, MD10 – this is an area with many agricultural influences which is well off the main stem of the San Joaquin River.

Those model constituents with the most data, Algae and DO, generally had the best Model Skill ratings. The Sacramento and San Joaquin River model boundaries had hourly DO boundary condition data which clearly influenced the Very Good Model Skill results. Algae data (from chl-a) had the additional benefit of having many temperature-dependent calibration parameters with which to calibrate the model results. In some areas, algae concentrations decreased at times when other locations and physical conditions indicated they should be increasing, raising the possibility that benthic activity from one or more species of clam were drawing down algal species growth.

For the N-bearing constituents, NH_3-N and NO_3-N, it was somewhat surprising that the NO_3-N Model Skill was notably better given that there are no rate parameters in the model for calibrating NO_3-N while there are several for NH_3-N. The model seemed to have difficulty handling the high NH_3-N loads from both the Sacramento Regional and Stockton WWTPs. In addition, there was no upstream data for setting the NH_3-N boundary condition on the Sacramento River.

In summary, Model Skill for constituents that had calibration data ranged from Very Good to Satisfactory over the three statistics used in the assessment of skill. Those constituents with the most data had the best results.

All WYs - ALGAE	NSE	PBIAS	Bias	RSR
C10	VG	VG	Underestimate	VG
C3A	VG	VG	Underestimate	VG
C7	G	VG	Underestimate	G
D10	S	VG	Underestimate	S
D12	G	VG	Underestimate	G
D16	S	VG	Underestimate	U
D19	S	VG	Underestimate	S
D22	S	VG	Underestimate	U
D24A	VG	VG	Underestimate	VG
D26	S	VG	Underestimate	U
D28A	S	VG	Underestimate	U
D4	G	VG	Underestimate	S
D6	VG	VG	Underestimate	VG
D7	S	VG	Overestimate	S
MD10	S	U	Overestimate	U
NZ032	S	VG	Underestimate	U
NZS42	S	VG	Underestimate	U
P8	S	G	Underestimate	U

ALGAE	NSE	PBIAS	RSR
C10	1	1	1
C3A	1	1	1
C7	2	1	2
D10	3	1	3
D12	2	1	2
D16	3	1	4
D19	3	1	3
D22	3	1	4
D24A	1	1	1
D26	3	1	4
D28A	3	1	4
D4	2	1	3
D6	1	1	1
D7	3	1	3
MD10	3	4	4
NZ032	3	1	4
NZS42	3	1	4
P8	3	2	4
MODEL	Good	Very Good	Satisfactory
SKILL	2	1	3

Figure 6-79 Summary of Residual Analysis and Model Skill for Algae (from Chl-a) at available EMP data locations. Model Skill is the average of the categorical values for all water years at each location (see Table 6-9).

All WYs PO4	NSE	PBIAS	Bias	RSR
C10	VG	VG	Underestimate	VG
D19	S	VG	Overestimate	U
D26	S	VG	Overestimate	U
D28A	U	VG	Overestimate	U
D4	G	VG	Underestimate	G
D6	VG	VG	Underestimate	VG
D7	VG	VG	Overestimate	VG
P8	S	VG	Underestimate	S

PO4	NSE	PBIAS	RSR
C10	1	1	1
D19	3	1	4
D26	3	1	4
D28A	4	1	4
D4	2	1	2
D6	1	1	1
D7	1	1	1
P8	3	1	3
MODEL	Good	Very Good	Saisfactory
SKILL	2	1	3

Figure 6-80 Summary of Residual Analysis and Model Skill for PO_4-P at available EMP data locations. Model Skill is the average of the categorical values for all water years at each location (see Table 6-9).

All WYs DO	NSE	PBIAS	Bias	RSR
C10	VG	VG	Overestimate	VG
C3A	VG	VG	Overestimate	VG
D10	S	VG	Underestimate	U
D12	VG	VG	Underestimate	VG
D16	VG	VG	Underestimate	VG
D19	VG	VG	Underestimate	VG
D22	VG	VG	Underestimate	VG
D6	VG	VG	Underestimate	VG
D7	VG	VG	Underestimate	VG
MD10	G	VG	Overestimate	G
NZ032	G	VG	Overestimate	G
NZS42	S	VG	Overestimate	U
P8	S	VG	Overestimate	S

DO	NSE	PBIAS	RSR
C10	1	1	1
C3A	1	1	1
D10	3	1	4
D12	1	1	1
D16	1	1	1
D19	1	1	1
D22	1	1	1
D6	1	1	1
D7	1	1	1
MD10	2	1	2
NZ032	2	1	2
NZS42	3	1	4
P8	3	1	3
MODEL	Good	Very Good	Good
SKILL	2	1	2

Figure 6-81 Summary of Residual Analysis and Model Skill for DO at available EMP data locations. Model Skill is the average of the categorical values for all water years at each location (see Table 6-9).

All WYs - NH3	NSE	PBIAS	Bias	RSR
C10	VG	VG	Underestimate	VG
C3A	VG	VG	Overestimate	VG
D19	VG	VG	Underestimate	VG
D26	VG	VG	Underestimate	VG
D28A	S	G	Overestimate	U
D4	VG	VG	Underestimate	G
D6	VG	VG	Underestimate	VG
D7	VG	VG	Overestimate	VG
MD10	S	U	Overestimate	U
P8	S	S	Underestimate	U

NH3	NSE	PBIAS	RSR
C10	1	1	1
C3A	1	1	1
D19	1	1	1
D26	1	1	1
D28A	3	2	4
D4	1	1	2
D6	1	1	1
D7	1	1	1
MD10	3	4	4
P8	3	3	4
MODEL	Good	Good	Good
SKILL	2	2	2

Figure 6-82 Summary of Residual Analysis and Model Skill for NH_3-N at available EMP data locations. Model Skill is the average of the categorical values for all water years at each location (see Table 6-9).

All WYs - NO3+NO2	NSE	PBIAS	Bias	RSR
C10	VG	VG	Overestimate	VG
C3A	VG	VG	Underestimate	VG
D19	VG	VG	Overestimate	G
D26	VG	VG	Overestimate	S
D28A	G	G	Overestimate	U
D4	VG	VG	Overestimate	G
D6	VG	VG	Overestimate	VG
D7	VG	VG	Overestimate	VG
MD10	S	S	Overestimate	U
P8	VG	VG	Overestimate	VG

NO3+NO2	NSE	PBIAS	RSR
C10	1	1	1
C3A	1	1	1
D19	1	1	2
D26	1	1	3
D28A	2	2	4
D4	1	1	2
D6	1	1	1
D7	1	1	1
MD10	3	3	4
P8	1	1	1
MODEL	Very Good	Very Good	Good
SKILL	1	1	2

Figure 6-83 Summary of Residual Analysis and Model Skill for NO_3+NO_2-N at available EMP data locations. Model Skill is the average of the categorical values for all water years at each location (see Table 6-9).

All WYs - ORGN	NSE	PBIAS	Bias	RSR
C10	VG	VG	Overestimate	VG
C3A	VG	VG	Overestimate	VG
D19	S	VG	Underestimate	U
D26	G	VG	Underestimate	G
D28A	S	VG	Underestimate	U
D4	S	VG	Underestimate	S
D6	VG	VG	Underestimate	VG
D7	S	VG	Underestimate	U
MD10	S	S	Overestimate	U
P8	S	VG	Overestimate	S

ORG-N	NSE	PBIAS	RSR
C10	1	1	1
C3A	1	1	1
D19	3	1	4
D26	2	1	2
D28A	3	1	4
D4	3	1	3
D6	1	1	1
D7	3	1	4
MD10	3	3	4
P8	3	1	3
MODEL	Good	Very Good	Satisfactory
SKILL	2	1	3

Figure 6-84 Summary of Residual Analysis and Model Skill for Organic-N at available EMP data locations. Model Skill is the average of the categorical values for all water years at each location (see Table 6-9).

All WYs - ALGAE	NSE	PBIAS	Bias	RSR
RW1	VG	VG	Underestimate	VG
RW2	VG	VG	Overestimate	VG
RW2A	VG	VG	Overestimate	VG
RW3	VG	VG	Overestimate	VG
RW4	S	VG	Underestimate	S
RW5	VG	VG	Overestimate	VG
RW7	S	VG	Underestimate	S
RW8	S	VG	Underestimate	U

ALGAE	NSE	PBIAS	RSR
RW1	1	1	1
RW2	1	1	1
RW2A	1	1	1
RW3	1	1	1
RW4	3	1	3
RW5	1	1	1
RW7	3	1	3
RW8	3	1	4
MODEL	Good	Very Good	Good
SKILL	2	1	2

Figure 6-85 Summary of Residual Analysis and Model Skill for Algae (from Chl-a) at available Stockton WWTP data locations. Model Skill is the average of the categorical values for all water years at each location (see Table 6-9).

All WYs - DO	NSE	PBIAS	Bias	RSR
RW2	VG	VG	Underestimate	VG
RW2A	VG	VG	Overestimate	VG
RW3	VG	VG	Overestimate	VG
RW4	VG	VG	Overestimate	VG
RW5	VG	VG	Overestimate	VG
RW7	VG	VG	Underestimate	VG
RW8	VG	VG	Overestimate	VG

DO	NSE	PBIAS	RSR
RW2	1	1	1
RW2A	1	1	1
RW3	1	1	1
RW4	1	1	1
RW5	1	1	1
RW7	1	1	1
RW8	1	1	1
MODEL	Very Good	Very Good	Very Good
SKILL	1	1	1

Figure 6-86 Summary of Residual Analysis and Model Skill for DO at available Stockton WWTP data locations. Model Skill is the average of the categorical values for all water years at each location (see Table 6-9).

All WYs - NH3	NSE	PBIAS	Bias	RSR
RW1	S	U	Underestimate	U
RW2	VG	VG	Underestimate	VG
RW2A	VG	VG	Underestimate	VG
RW3	VG	VG	Underestimate	VG
RW4	S	S	Underestimate	U
RW5	S	S	Underestimate	U
RW7	S	U	Underestimate	U
RW8	S	U	Underestimate	U

NH3	NSE	PBIAS	RSR
RW1	3	4	4
RW2	1	1	1
RW2A	1	1	1
RW3	1	1	1
RW4	3	3	4
RW5	3	3	4
RW7	3	4	4
RW8	3	4	4
MODEL	Good	Satisfactory	Satisfactory
SKILL	2	3	3

Figure 6-87 Summary of Residual Analysis and Model Skill for NH_3-N at available Stockton WWTP data locations. Model Skill is the average of the categorical values for all water years at each location (see Table 6-9).

All WYs - NO3	NSE	PBIAS	Bias	RSR
RW1	VG	VG	Overestimate	VG
RW2	VG	VG	Overestimate	VG
RW3	VG	VG	Overestimate	VG
RW4	VG	VG	Overestimate	VG
RW5	VG	VG	Overestimate	VG
RW7	G	VG	Overestimate	U
RW8	VG	VG	Overestimate	VG

NO3	NSE	PBIAS	RSR
RW1	1	1	1
RW2	1	1	1
RW3	1	1	1
RW4	1	1	1
RW5	1	1	1
RW7	2	1	4
RW8	1	1	1
MODEL	Very Good	Very Good	Very Good
SKILL	1	1	1

Figure 6-88 Summary of Residual Analysis and Model Skill for NO_3-N at available Stockton WWTP data locations. Model Skill is the average of the categorical values for all water years at each location (see Table 6-9).

All WYs - NO2	NSE	PBIAS	Bias	RSR
RW1	U	S	Overestimate	U
RW3	S	G	Overestimate	U
RW5	S	VG	Overestimate	U
RW7	S	VG	Underestimate	S
RW8	S	U	Underestimate	U

NO2	NSE	PBIAS	RSR
RW1	4	3	4
RW3	3	2	4
RW5	3	1	4
RW7	3	1	3
RW8	3	4	4
MODEL	Satisfactory	Good	Unsatisfactory
SKILL	3	2	4

Figure 6-89 Summary of Residual Analysis and Model Skill for NO_2-N at available Stockton WWTP data locations. Model Skill is the average of the categorical values for all water years at each location (see Table 6-9).

All WYs - CBOD	NSE	PBIAS	Bias	RSR
RW3	S	VG	Underestimate	U
RW4	S	VG	Underestimate	U
RW5	S	VG	Underestimate	U
RW7	U	VG	Underestimate	U
RW8	U	G	Underestimate	U

CBOD	NSE	PBIAS	RSR
RW3	3	1	4
RW4	3	1	4
RW5	3	1	4
RW7	4	1	4
RW8	4	2	4
MODEL	Satisfactory	Very Good	Unsatisfactory
SKILL	3	1	4

Figure 6-90 Summary of Residual Analysis and Model Skill for CBOD/BOD at available Stockton WWTP data locations. Model Skill is the average of the categorical values for all water years at each location (see Table 6-9).

6.11References

Anderson, J. 2002. California Department of Water Resources: 2002 Annual Progress Report. Chap 14: DSM2 Fingerprinting Methodology.

Brake, B. E. Biochemical Oxygen Demand and Carbonaceous BOD in Water and Wastewater. 1998. Washington State Department of Ecology.

Brown, L. C., and T. O. Barnwell, Jr. 1987.The Enhanced Stream Water Quality Models QUAL2E and QUAL2E-UNCAS: Documentation and User Manual.EPA-600/3-87/007. U.S. Environmental Protection Agency.

Chapra, S., G. Pelletier and H. Tao. 2008. QUAL2K Model Documentation: A modeling framework for simulating river and stream water quality.

Chilmakuri, C. 2010. Overview of Recent DSM2 Recalibration for BDCP. http://baydeltaoffice.water.ca.gov/modeling/deltamodeling/DSM2UsersGroup/DSM2_Recalibration_102709.pdf

Clesceri, L.S., A.E. Greenberg and A.D. Eaton (eds). 1999. Standard Methods for Examination of Water and Wastewater 20th edition. American Public Health. Association. Washington DC

Cole, T.M. and S. A. Wells. 2008. CE-Qual-W2: User's Manual. U.S. Army Corps of Engineers.

Cole, T.M. 1994. CE-QUAL-W2. Version 2.0," Vol. E-94-1. U.S. Army Corps of Engineers.

DWR, 1995a. "Estimation of Delta Island Diversions and Return Flows". California Department of Water Resources, Division of Planning.

DWR, 1995b. "Representative Delta Island Return Flow Quality for Use in DSM2". California Department of Water Resources, Division of Planning. February.

Guerin, M., Modeling the Fate and Transport of Nutrients Using DSM2: Calibration/Validation Report, Prepared for SFWCA and SWC, November 2011.

Jobson, H.E. 1997. Enhancements to the Branched Lagrangian Transport Modeling System. USGS Water resources Investigation Report 97-4050.

Lanbein, W.B. and W.H. Durum, The Aeration Capacity of Streams, Geological Survey Circular 542, 1967.

Lehman, P. W. S. Mayr, L. Mecum. C. Enright. (2010) The freshwater tidal wetland Liberty Island, CA was both a source and a sink of inorganic and organic material to the San Francisco estuary. Aquatic Ecology. 0(0) pp. 1-14.

Modeling Support Branch, Representative Delta Island Return Flow Quality for Use in DSM2: Memorandum Report May 1995, Division of Planning, Department of Water Resources.

Moriasi, D.N., J.G. Arnold, M.W. Van Liew, R.L. Bingner, R.D. Harmel, and T.L. Vieth. 2007 Model evaluation guidelines for systematic quantification of accuracy in watershed simulations. Transactions of the ASABE. Vol. 50(3).

Rajbhandari, H. 2005. California Department of Water Resources: 2005 Annual Progress Report, Chap 4: Sensitivity of DSM2 Temperature Simulations to Time Step Size.

Rajbhandari, H. DWR 2004. Annual Progress Report, Chap 4: Modeling Dissolved Oxygen and Temperature in DSM2 Planning Studies. 2004.

Rajbhandari, H. 2003. California Department of Water Resources: 2003 Annual Progress Report, Chap 3: Extending DSM2-QUAL Calibration of Dissolved Oxygen.

Rajbhandari, H. 2001. California Department of Water Resources: 2001 Annual Progress Report, Chap 6: Dissolved Oxygen and Temperature Modeling Using DSM2.

Rajbhandari, H. 2000. California Department of Water Resources: 2000 Annual Progress Report, Chap 9: Dissolved Oxygen Modeling Using DSM2-QUAL.

Rajbhandari, H. 1995a. Dynamic simulation of water quality in surface water systems utilizing a Lagrangian reference frame. Ph.D. Dissertation. University of California, Davis.

Rajbhandari, H. 1995b. California Department of Water Resources: 1995 Annual Progress Report, Chap 3: Water Quality.

Stull, R. Wet bulb temperature from relative humidity and air temperature, American Meteorological Society, Nov, 2011.

Swift, T., R. DuVall, S. Balachandra. 2009. Jones Tract Flood Water Quality Investigations. Division of Environmental Services, California Department of Water Resources.

USGS, 2008. The Computer Program FourPt (Version 95.01). Water Resources Investigation Report 97-4016.

6.12 Chapter 6 Appendix

6.12.1 Selected Nutrient Boundary Conditions

This section documents the modeled output in comparison with the available boundary condition data from EMP and in Liberty Island (Lehman, 2010). The Freeport boundary constituent concentrations were estimated and then compared with the EMP data at Greenes Landing and Hood (C3A). At Martinez and Vernalis, the data was available for the main constituents (excepting CBOD and Organic-P). The data in Liberty Island was averaged over the February 2004 to July 2005 data from 4 locations within Liberty Island to compare with model output of the zero-dimensional reservoir Liberty.

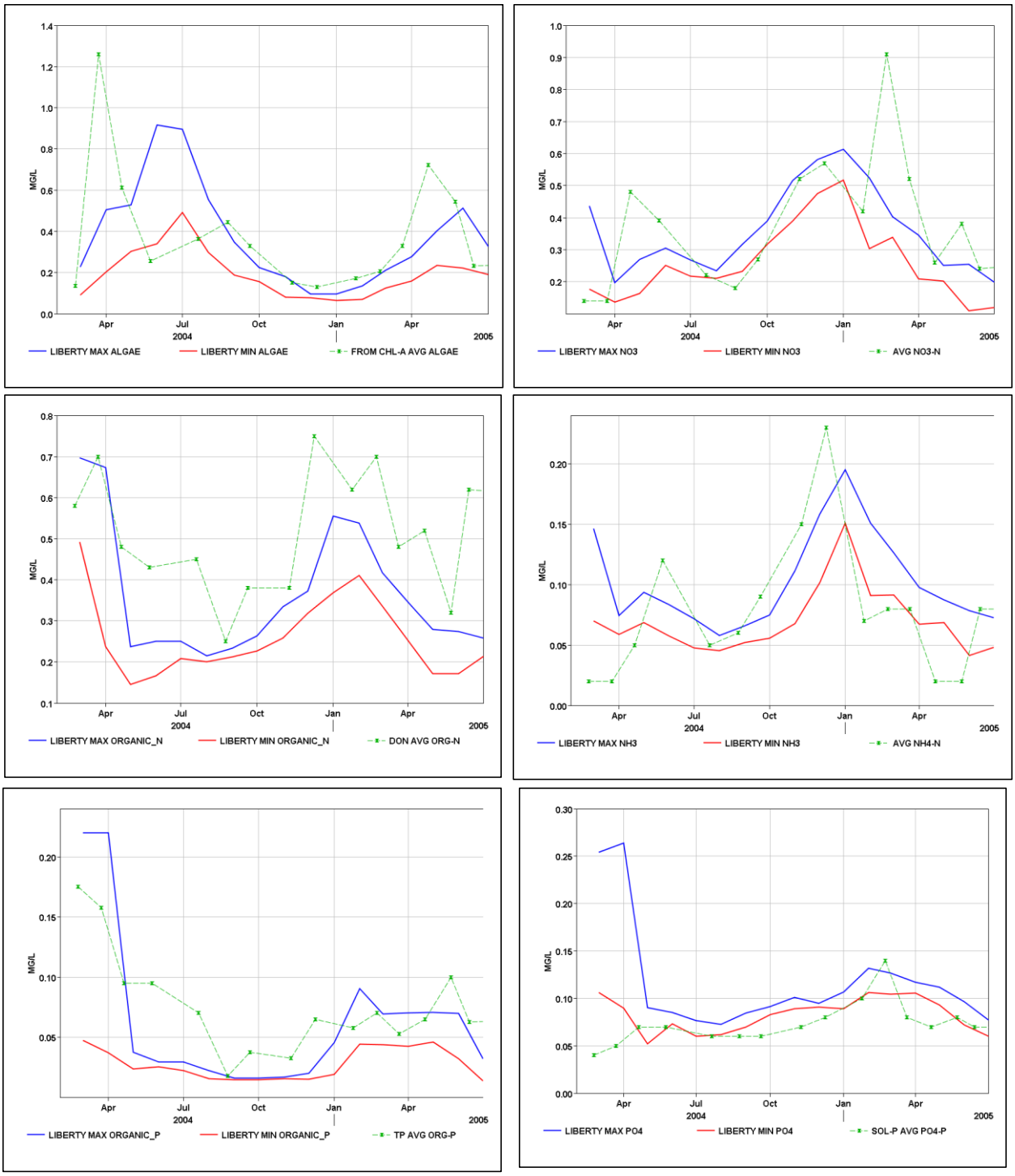

Figure 6-91 Data averaged from four locations in Liberty Island was used to set the constant concentration boundary conditions at the Yolo/Toe Drain data boundary in DSM2.

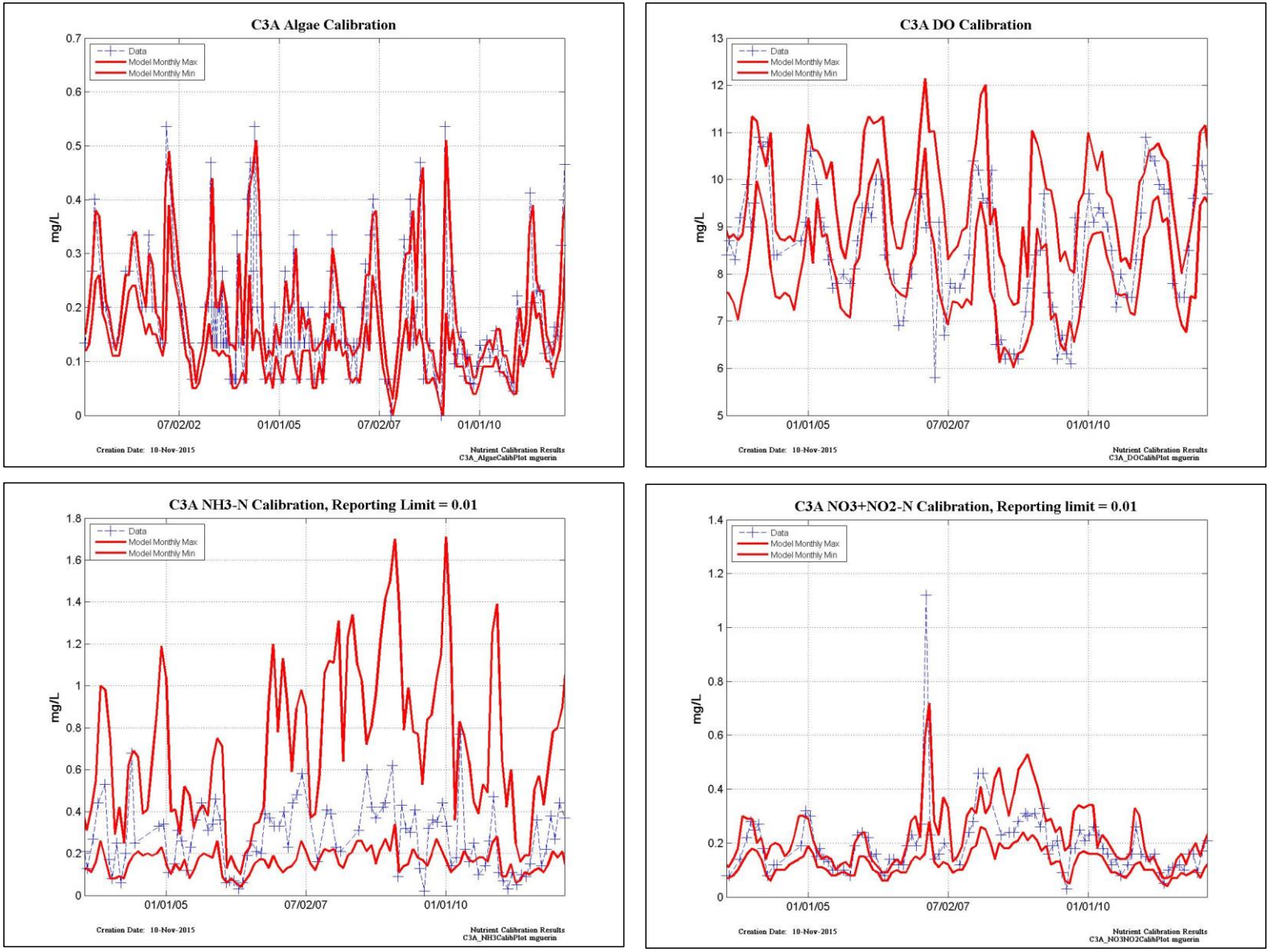

Figure 6-92 Modeled Algae, DO, NH_3-N and NO_3+NO_2-N at Hood (C3A).

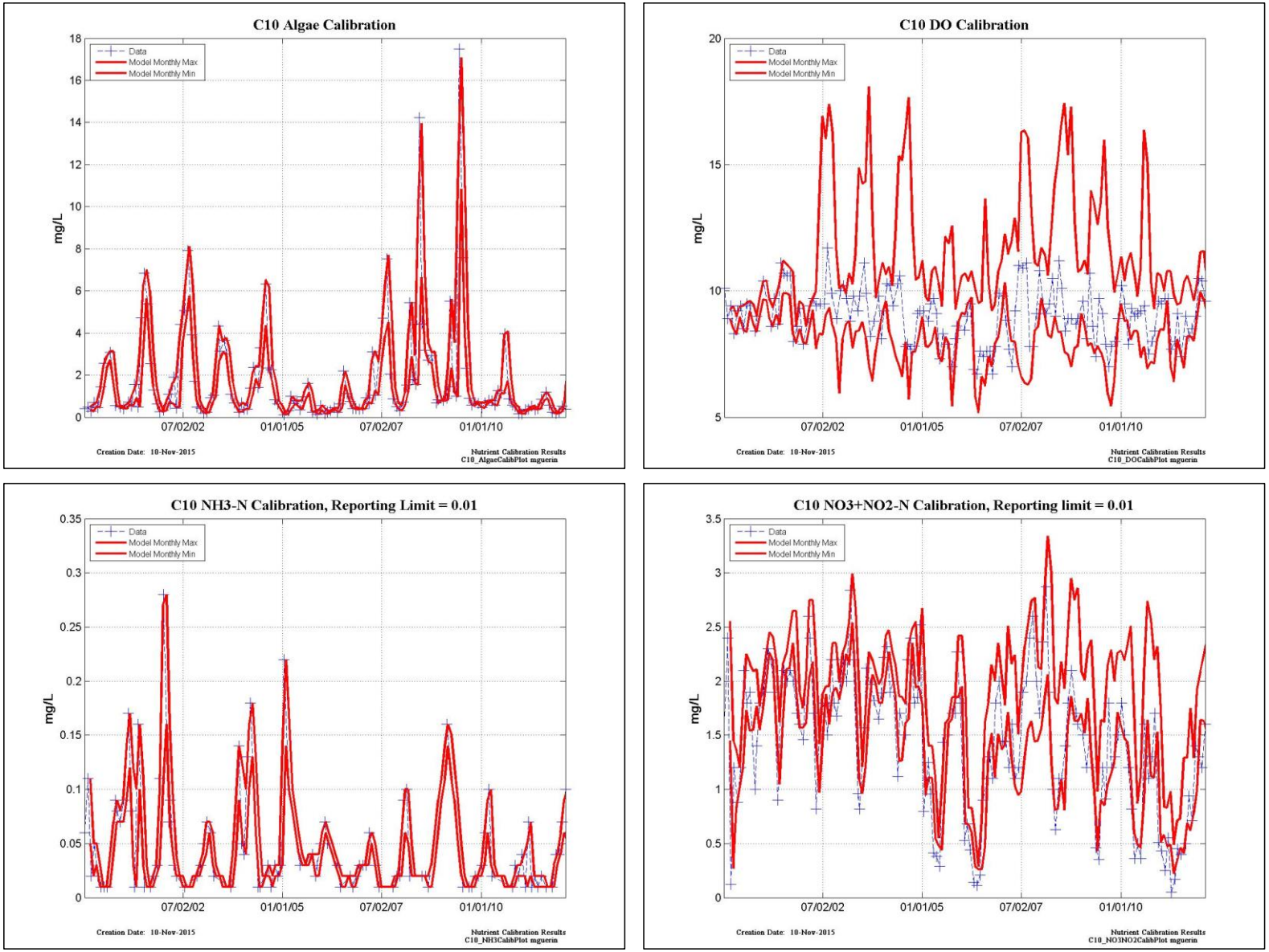

Figure 6-93 Modeled Algae, DO, NH_3-N and NO_3+NO_2-N at Vernalis (C10).

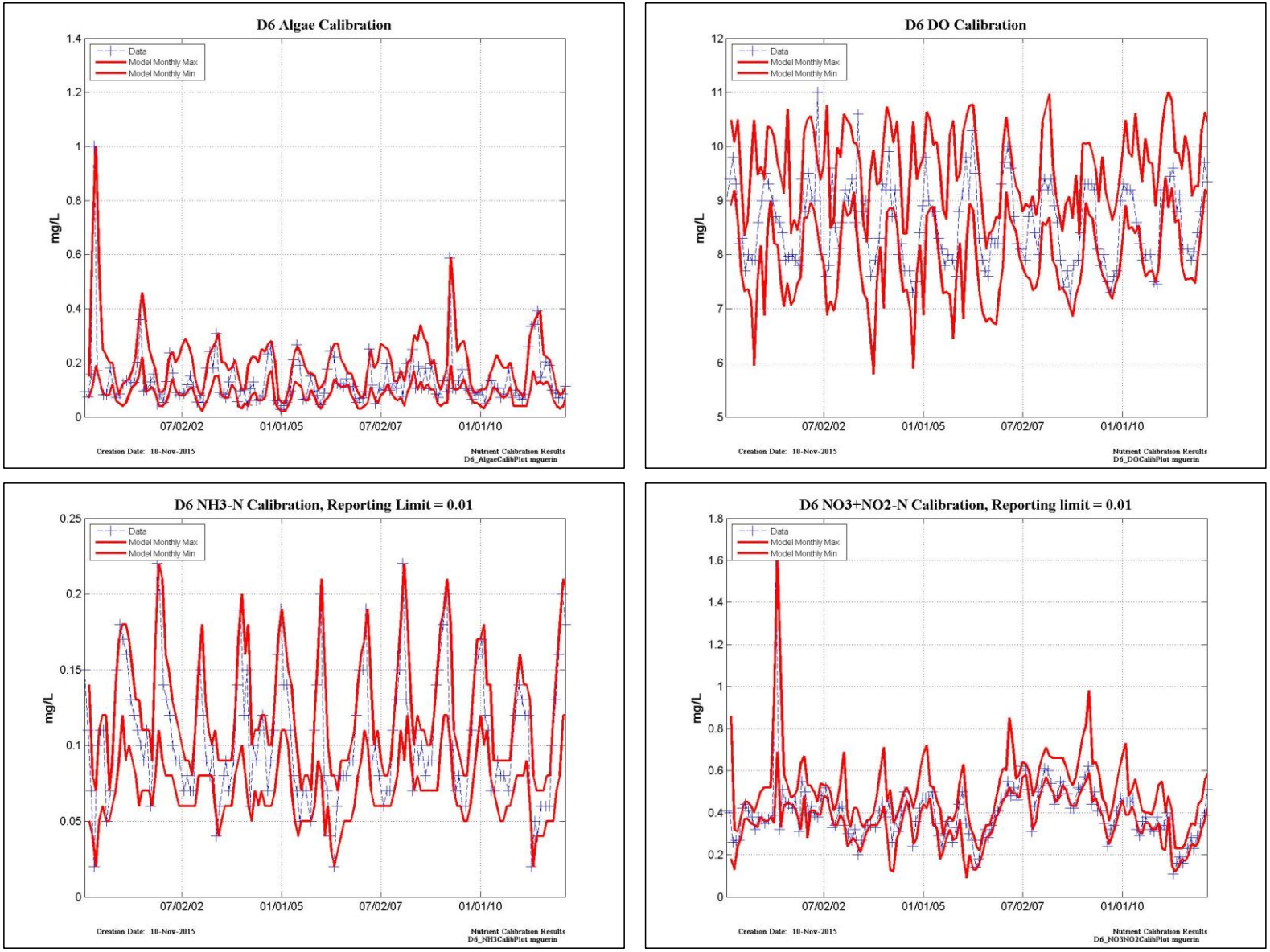

Figure 6-94 Modeled Algae, DO, NH_3-N and NO_3+NO_2-N at Martinez (D6).

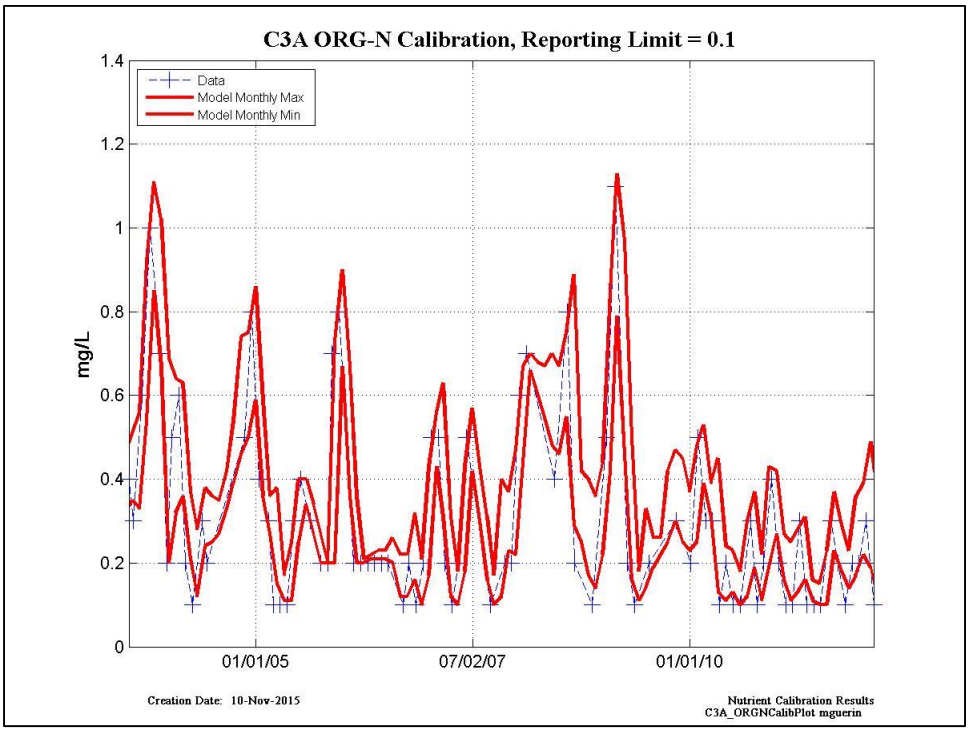

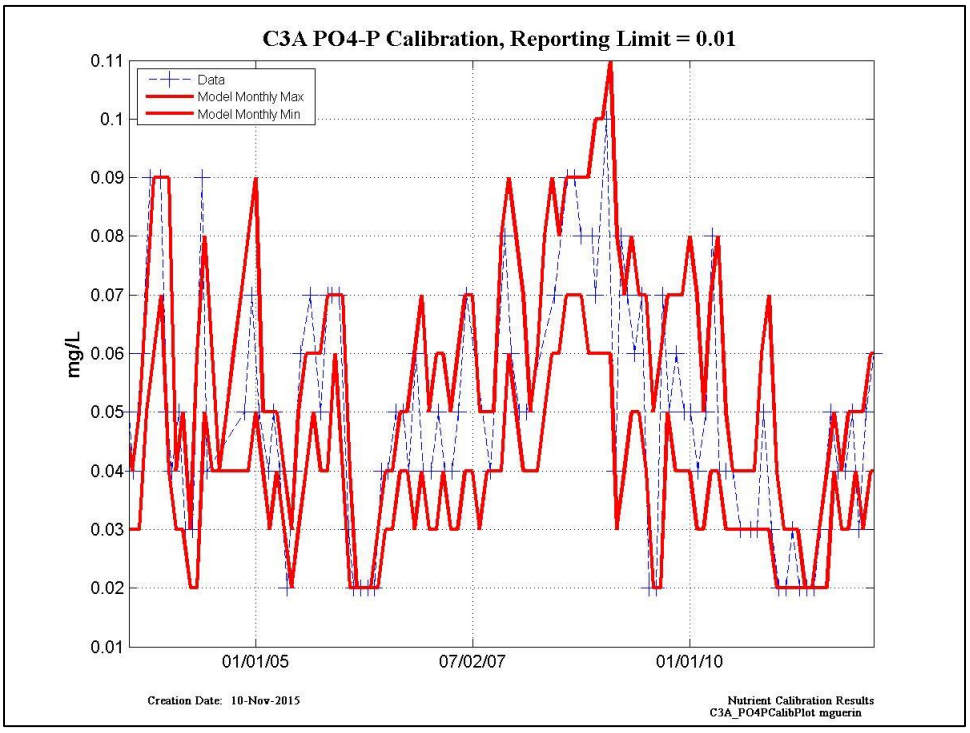

Figure 6-95 Modeled Organic-N and PO_4-P at Hood (C3A)

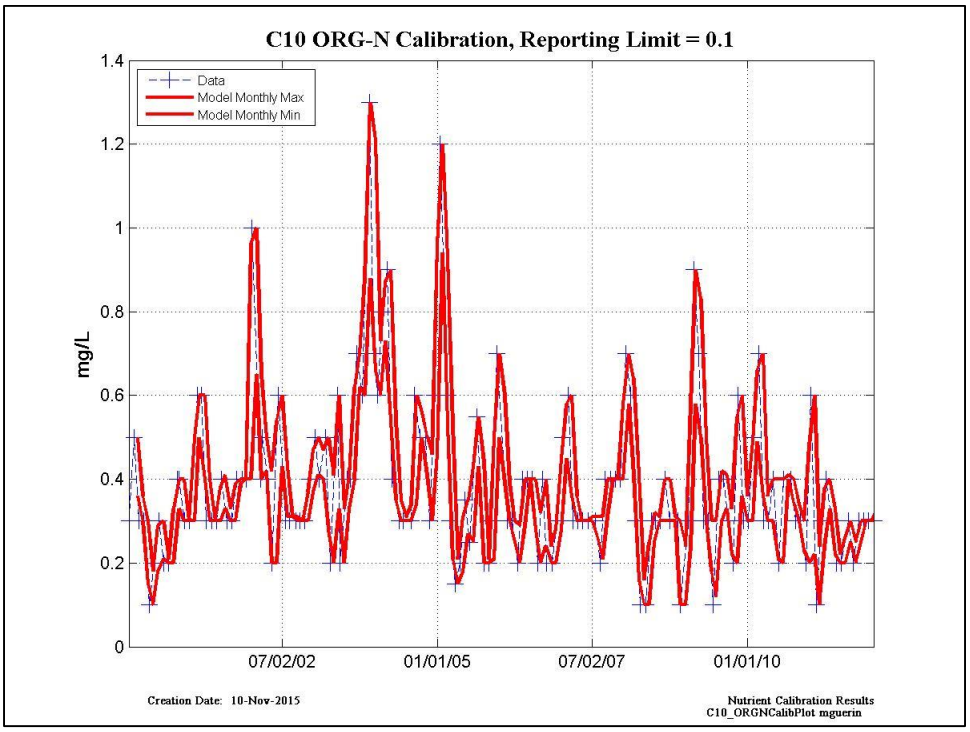

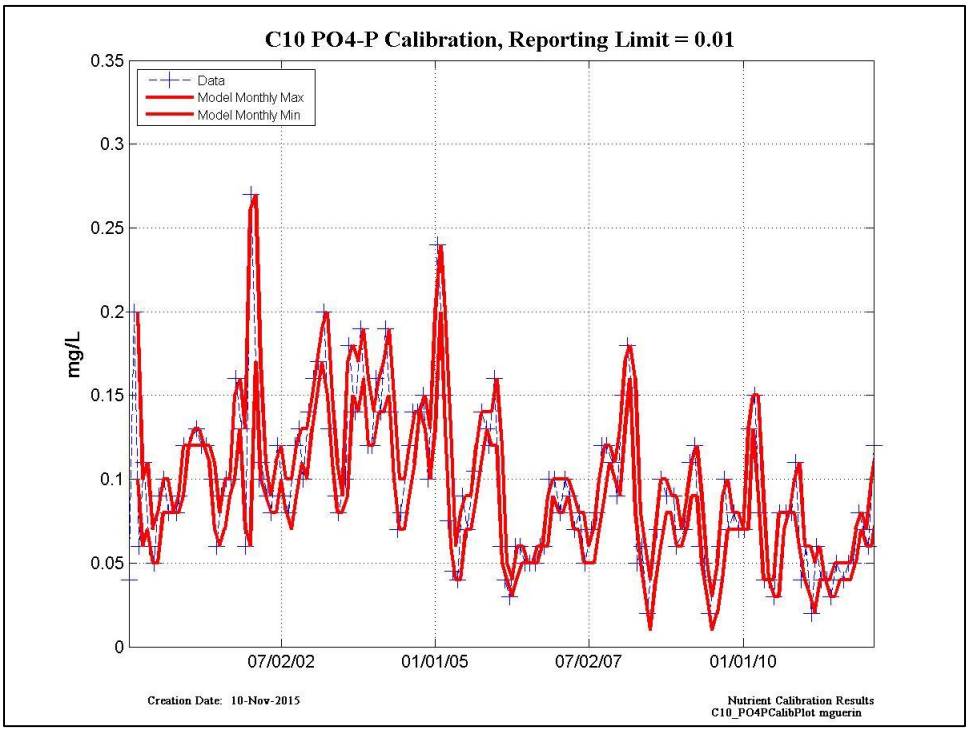

Figure 6-96 Modeled Organic-N and PO_4-P at Vernalis (C10).

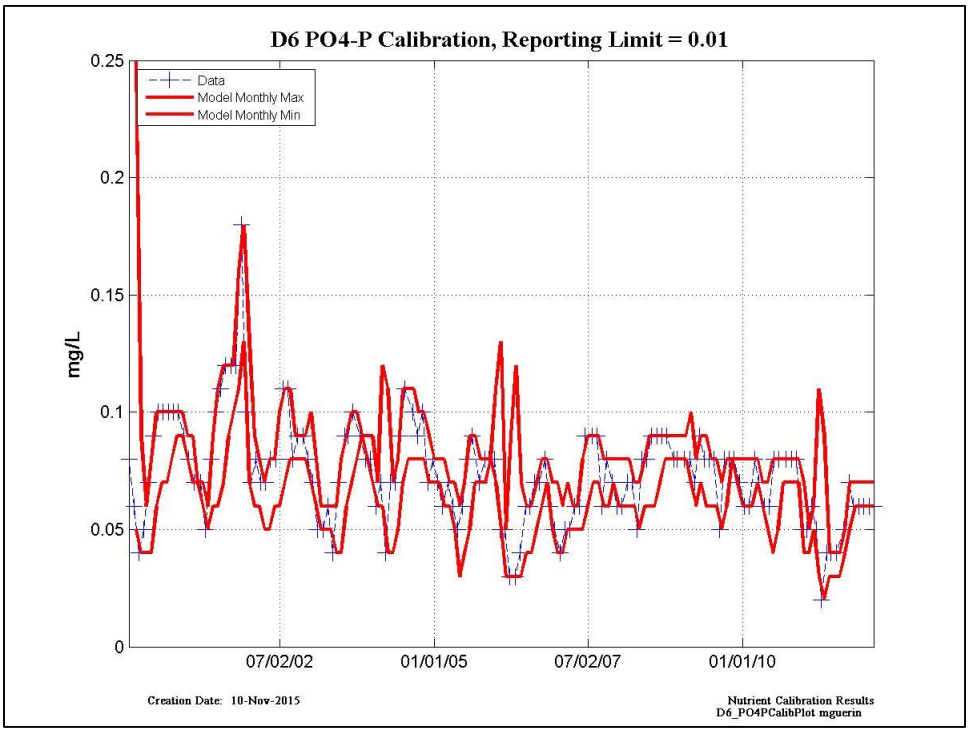

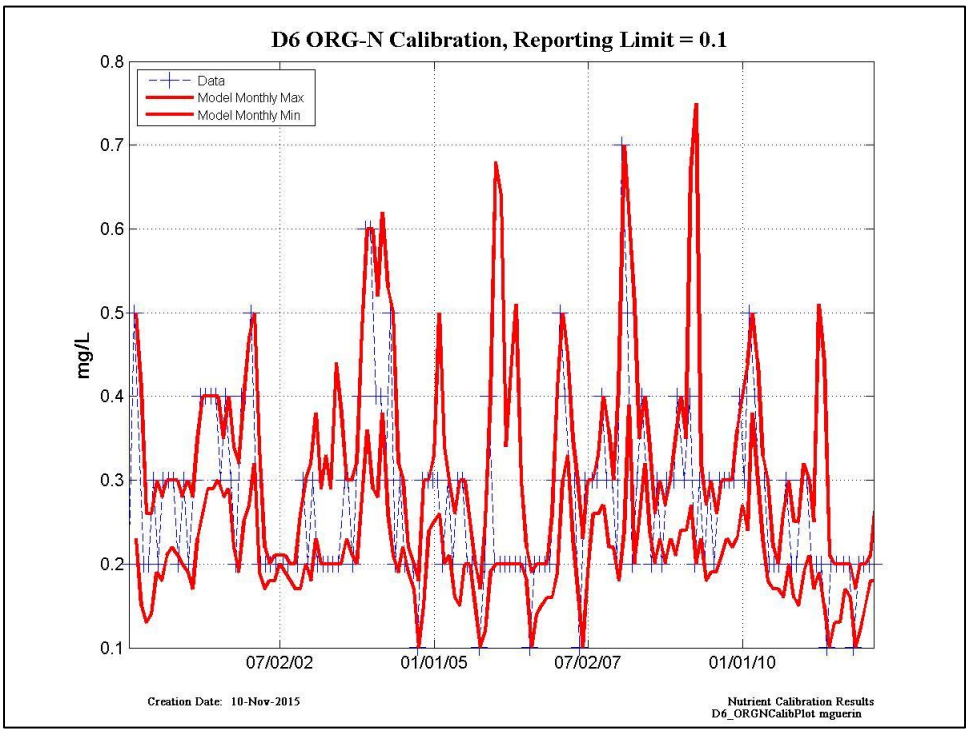

Figure 6-97 Modeled Organic-N and PO_4-P at Martinez (D6).

6.12.2 WWTP Receiving Water Nutrient Plots

This section has selected plots of WWTP receiving water data for constituents that were above detection limits.

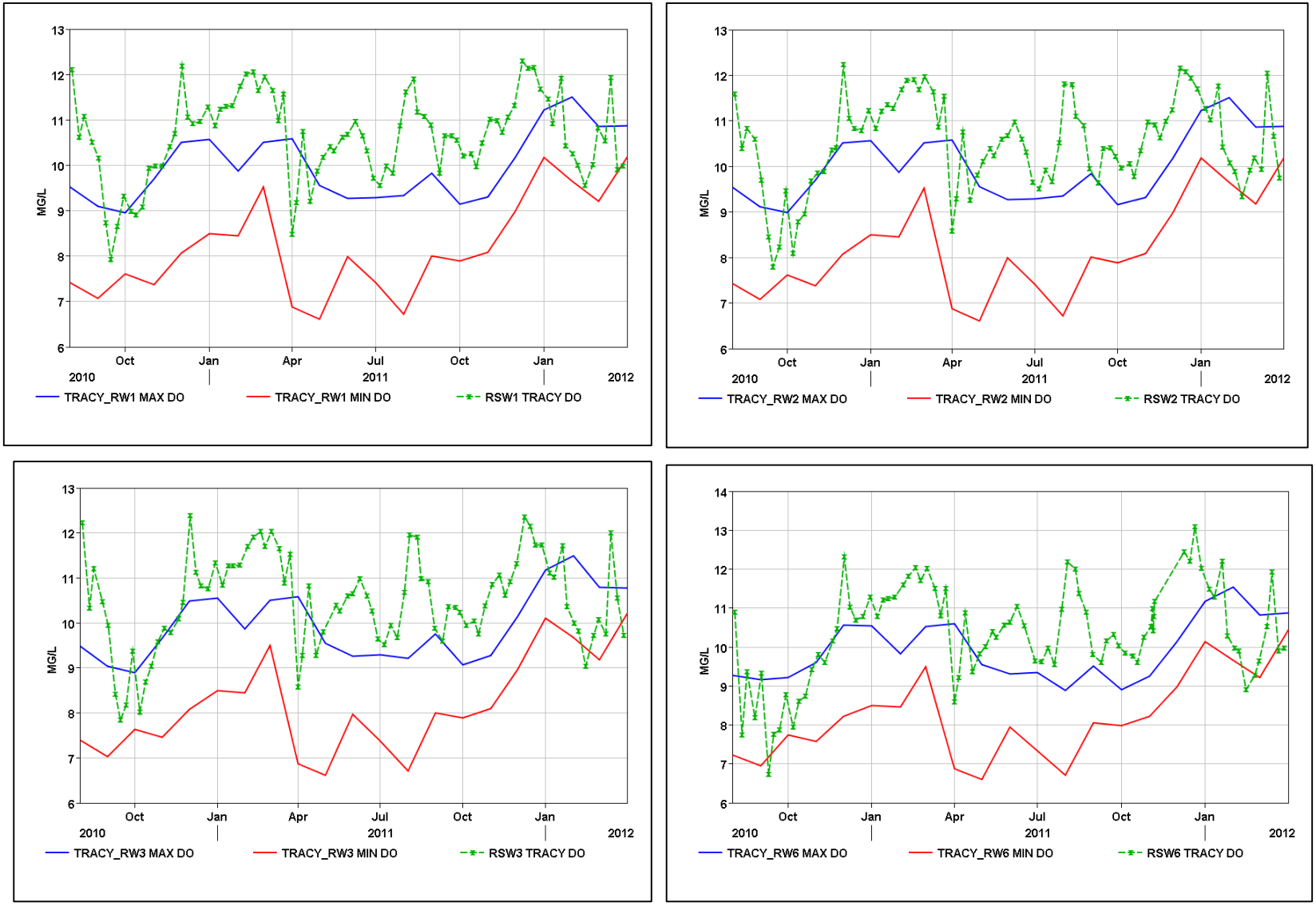

Figure 6-98 Tracy WWTP receiving water locations for DO.

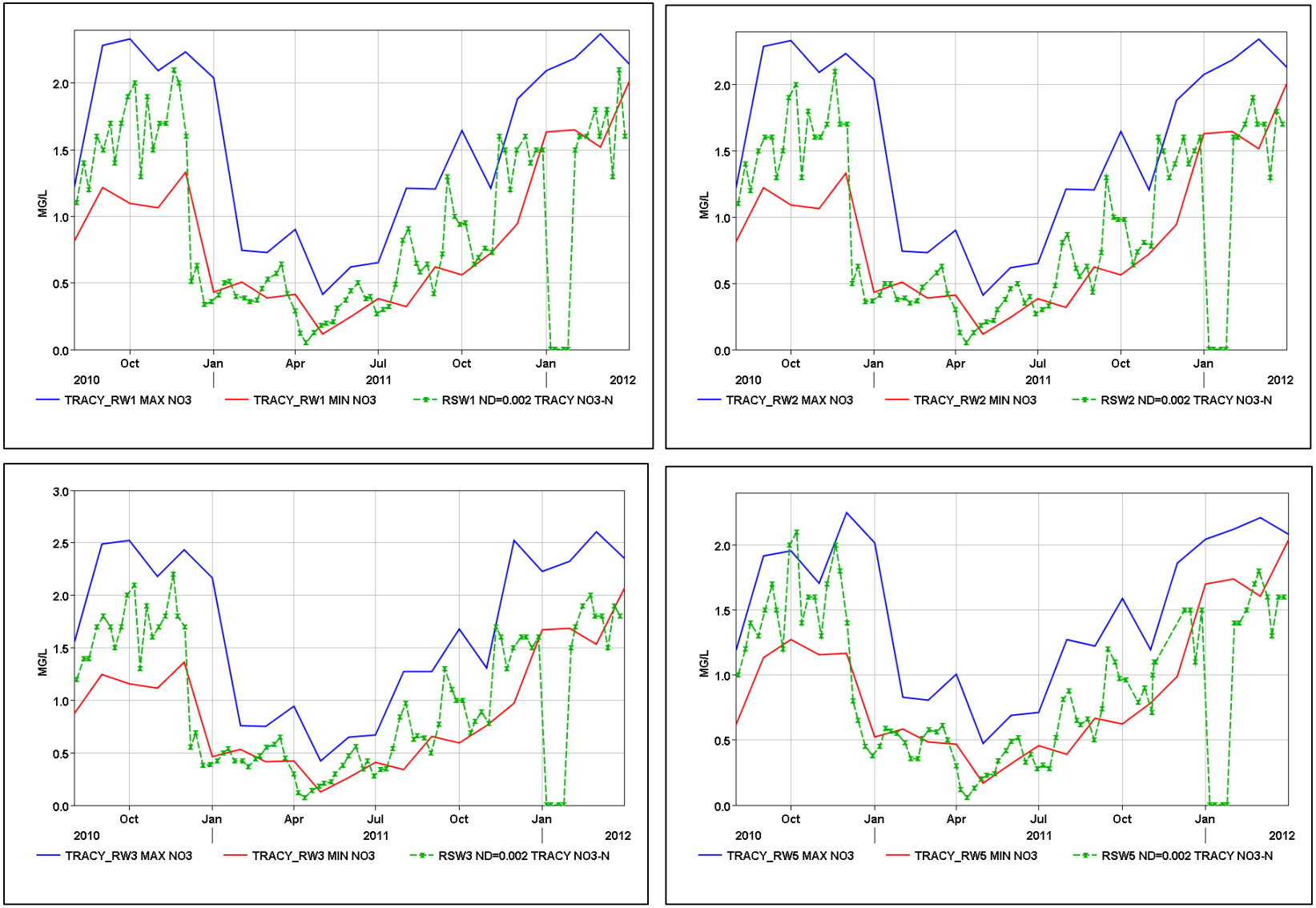

Figure 6-99 Tracy WWTP receiving water locations for NO_3.

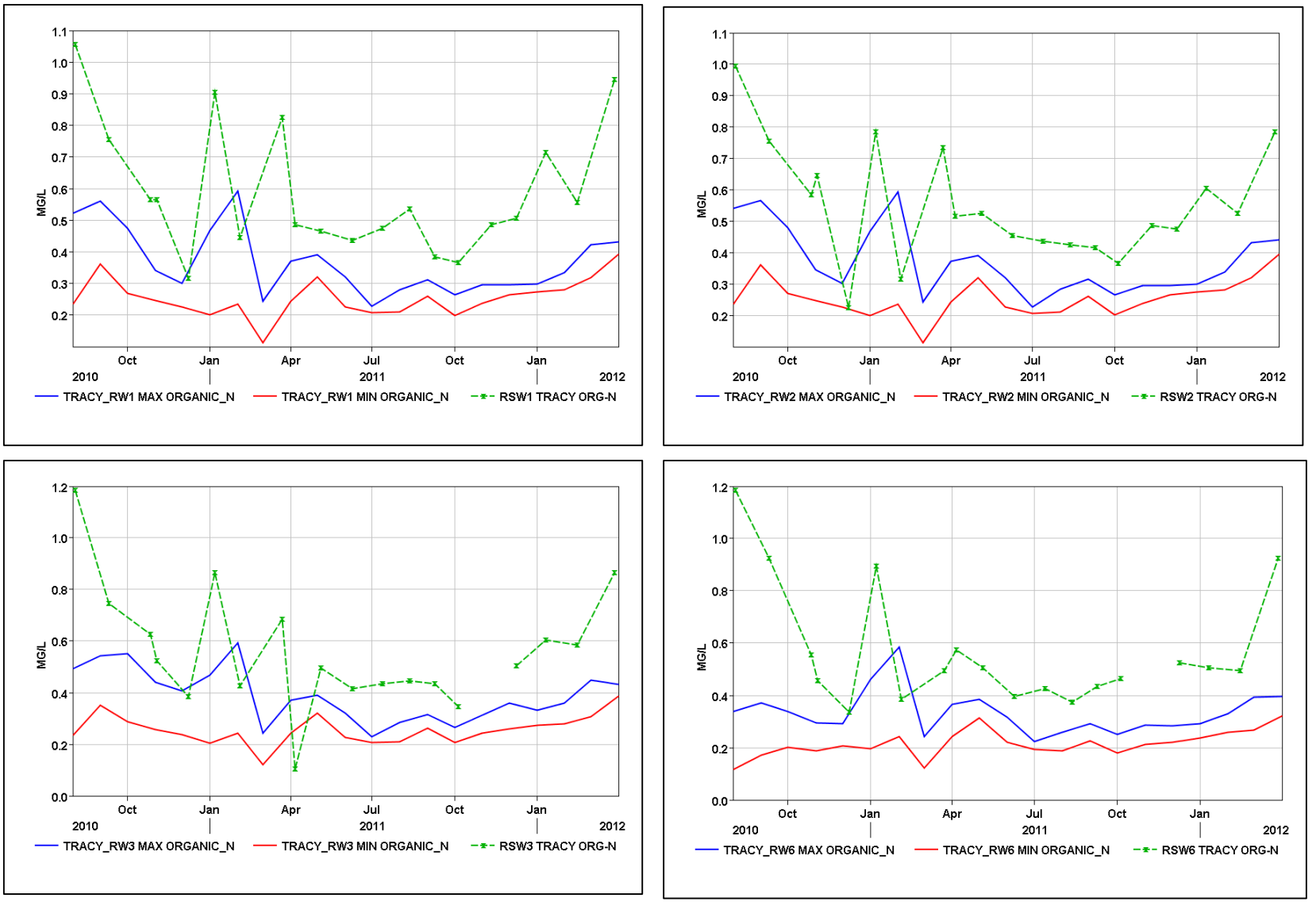

Figure 6-100 Tracy WWTP receiving water locations for Organic-N.

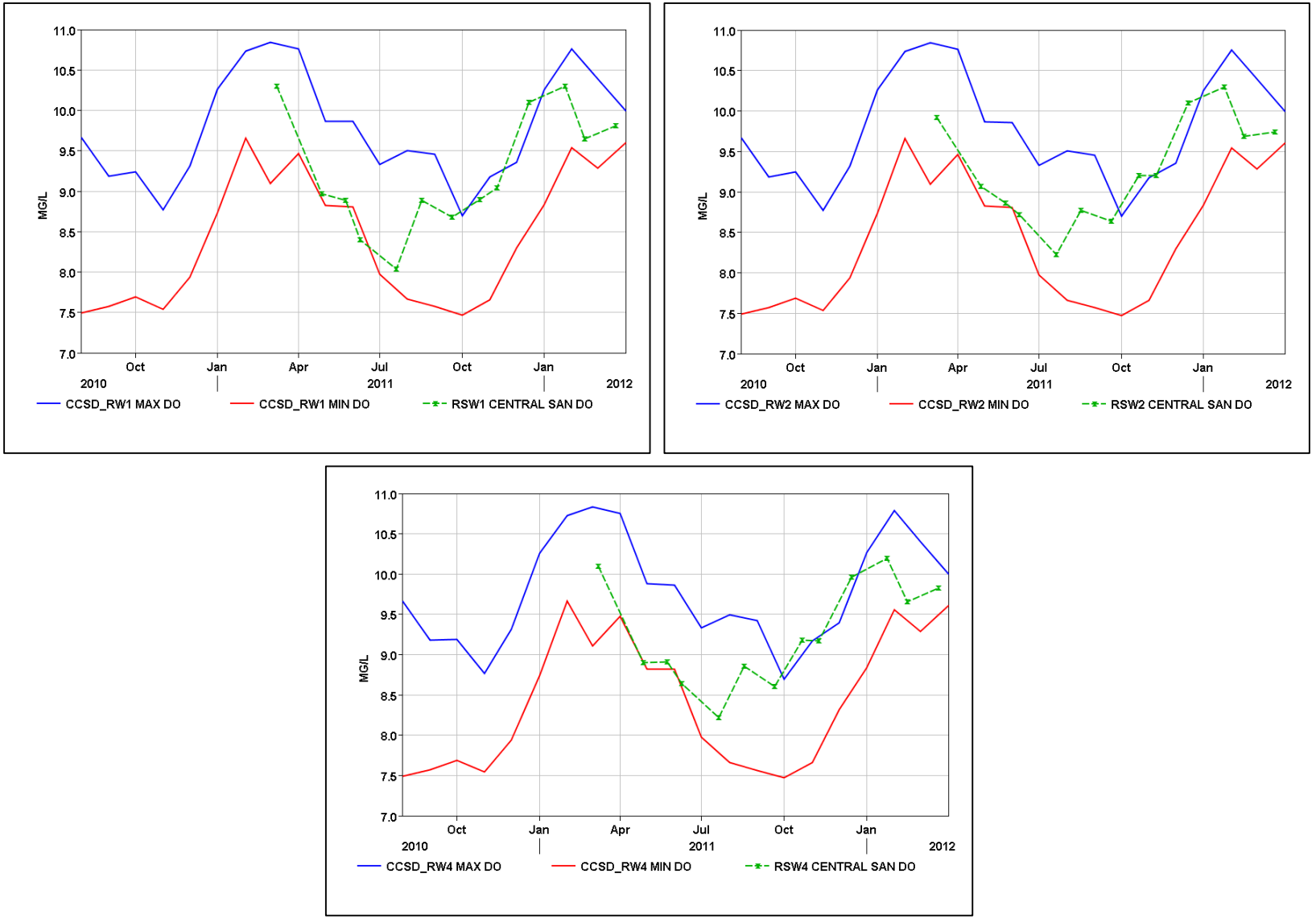

Figure 6-101 Central Contra Costa Sanitary District WWTP receiving water locations for DO.

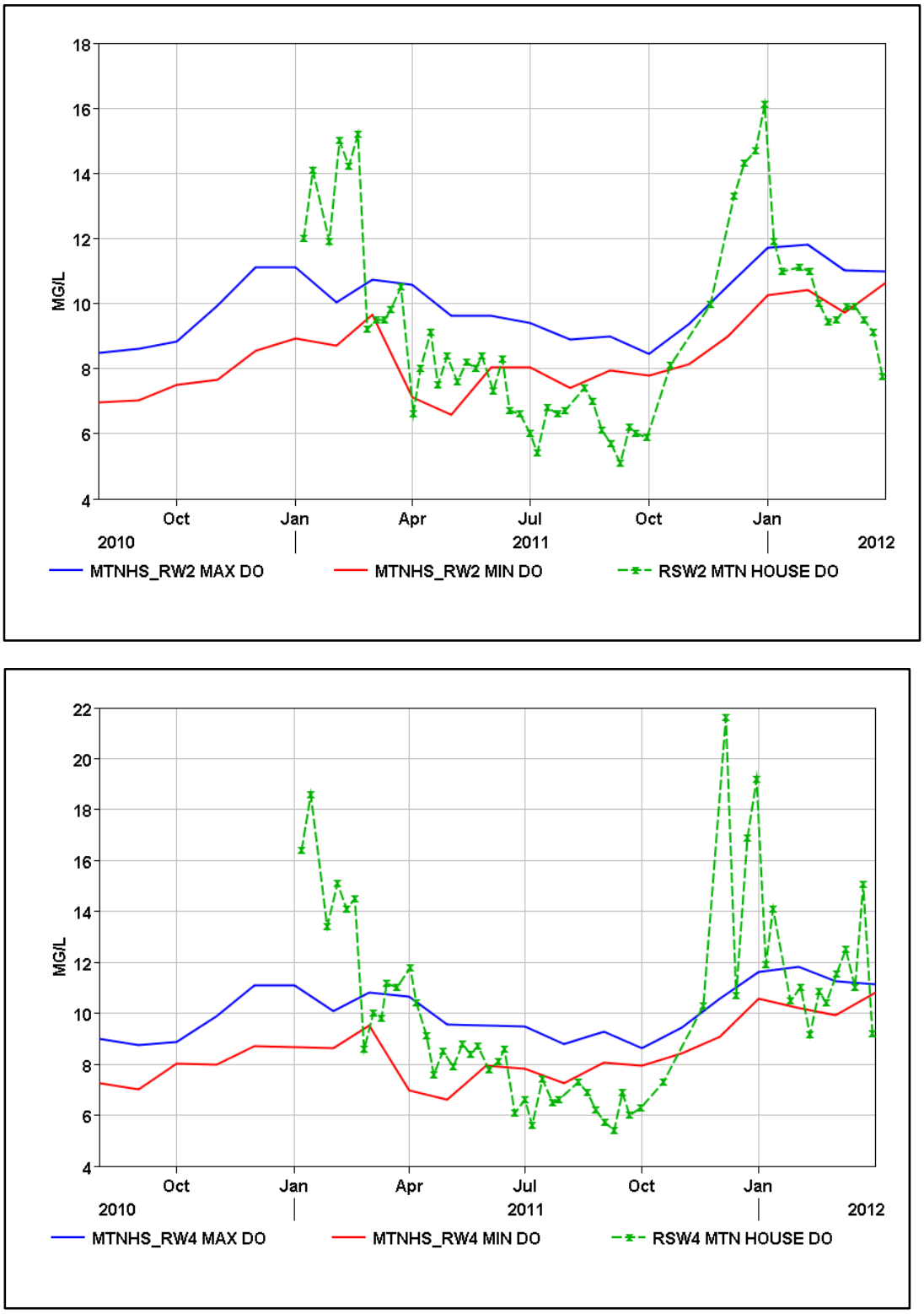

Figure 6-102 Mountain House WWTP receiving water locations for DO.

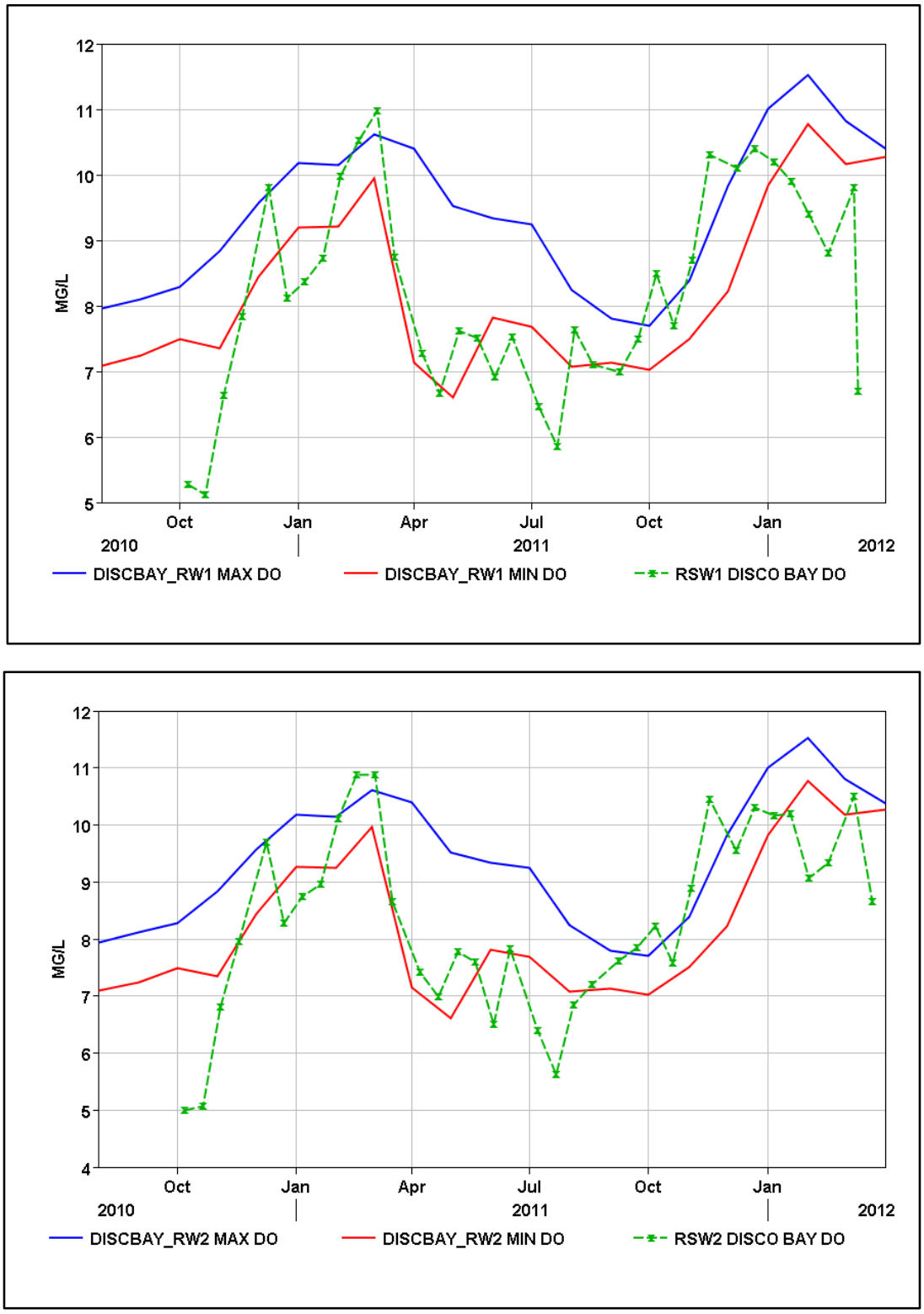

Figure 6-103 Discovery Bay WWTP receiving water locations for DO.

6.12.3 Flow boundary condition plots

The following set of plots document the inflow and outflow boundary conditions for the DSM2 HYDRO historical simulation period.

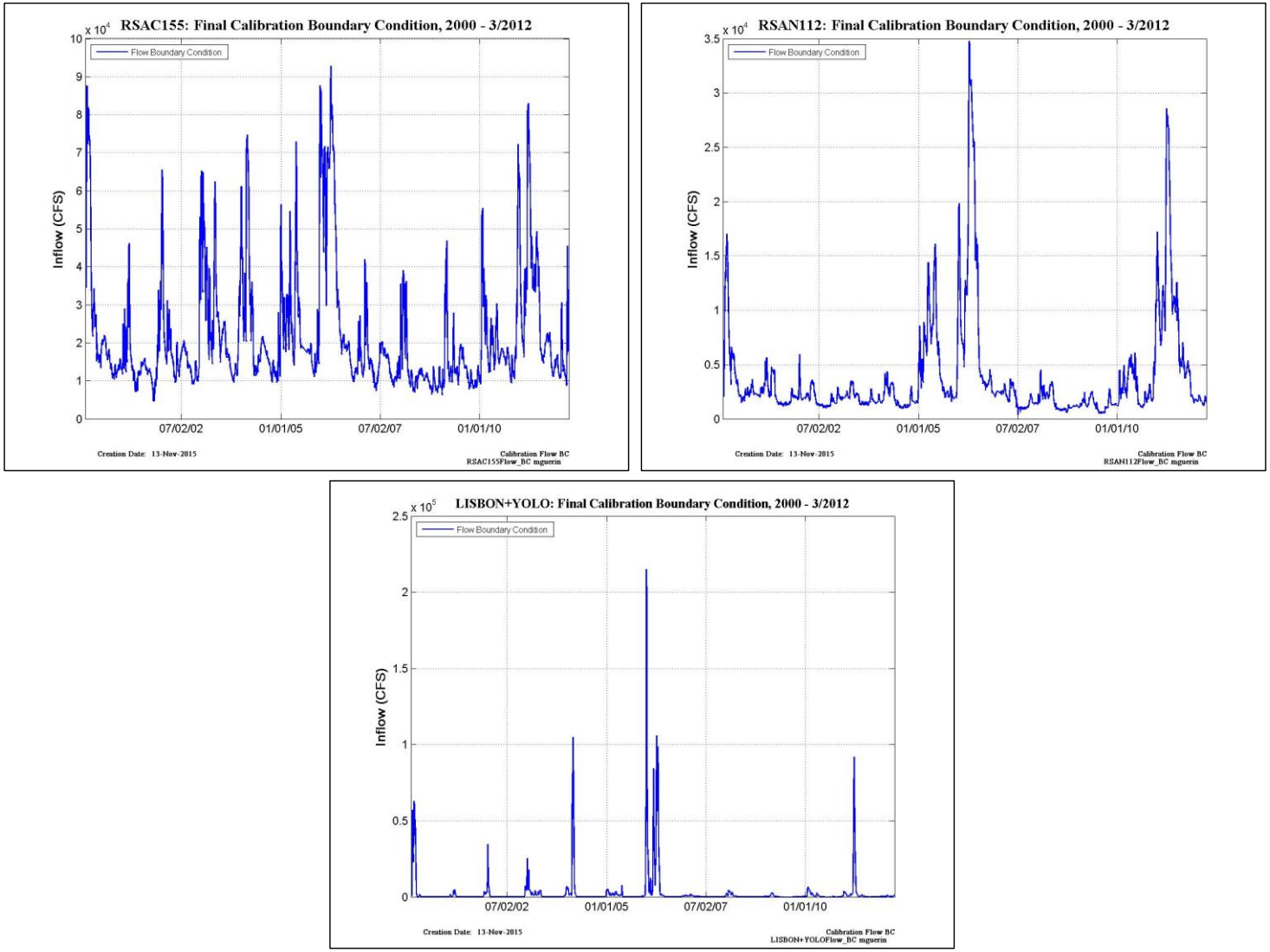

Figure 6-104 Model Inflow at Sacramento River (upper left), San Joaquin River (upper right), and the combined flow through the Yolo Bypass and the Lisbon Toe Drain (lower).

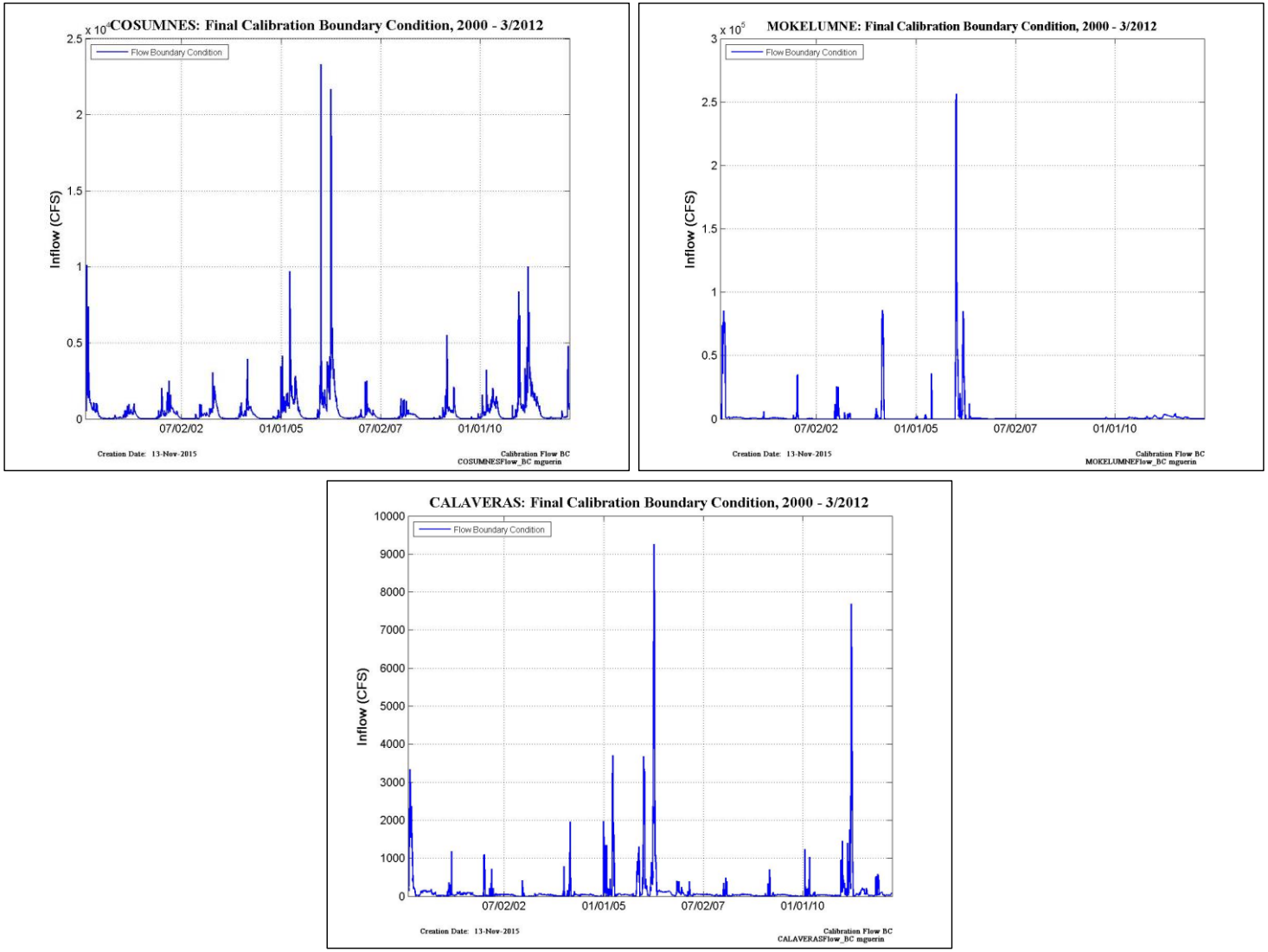

Figure 6-105 Model Inflow at Cosumnes River (upper left), Mokelumne River (upper right), and Calaveras River (lower).

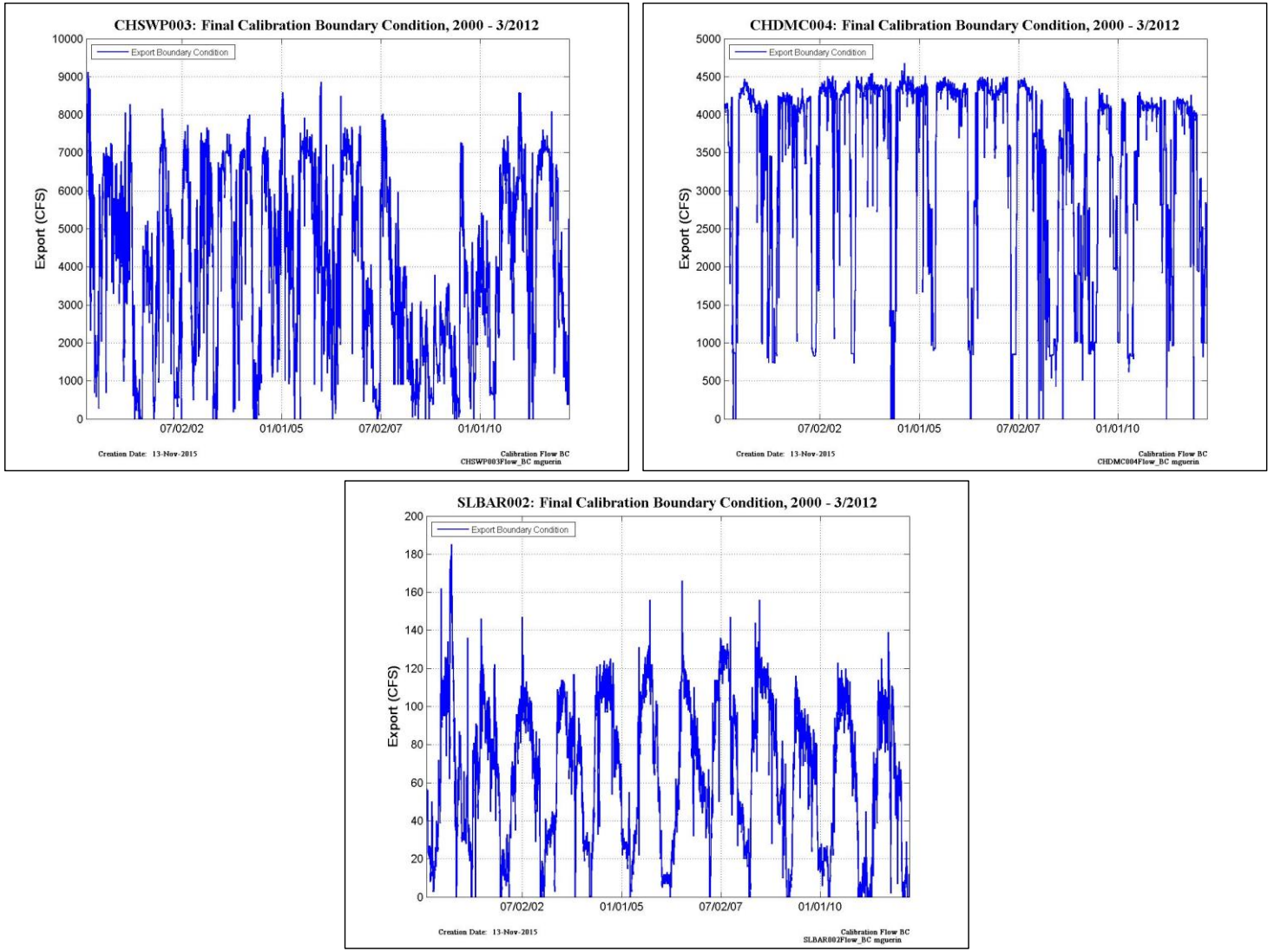

Figure 6-106 Model export at the SWP (upper left), the CVP (upper right), and at the North Bay Aqueduct (lower).

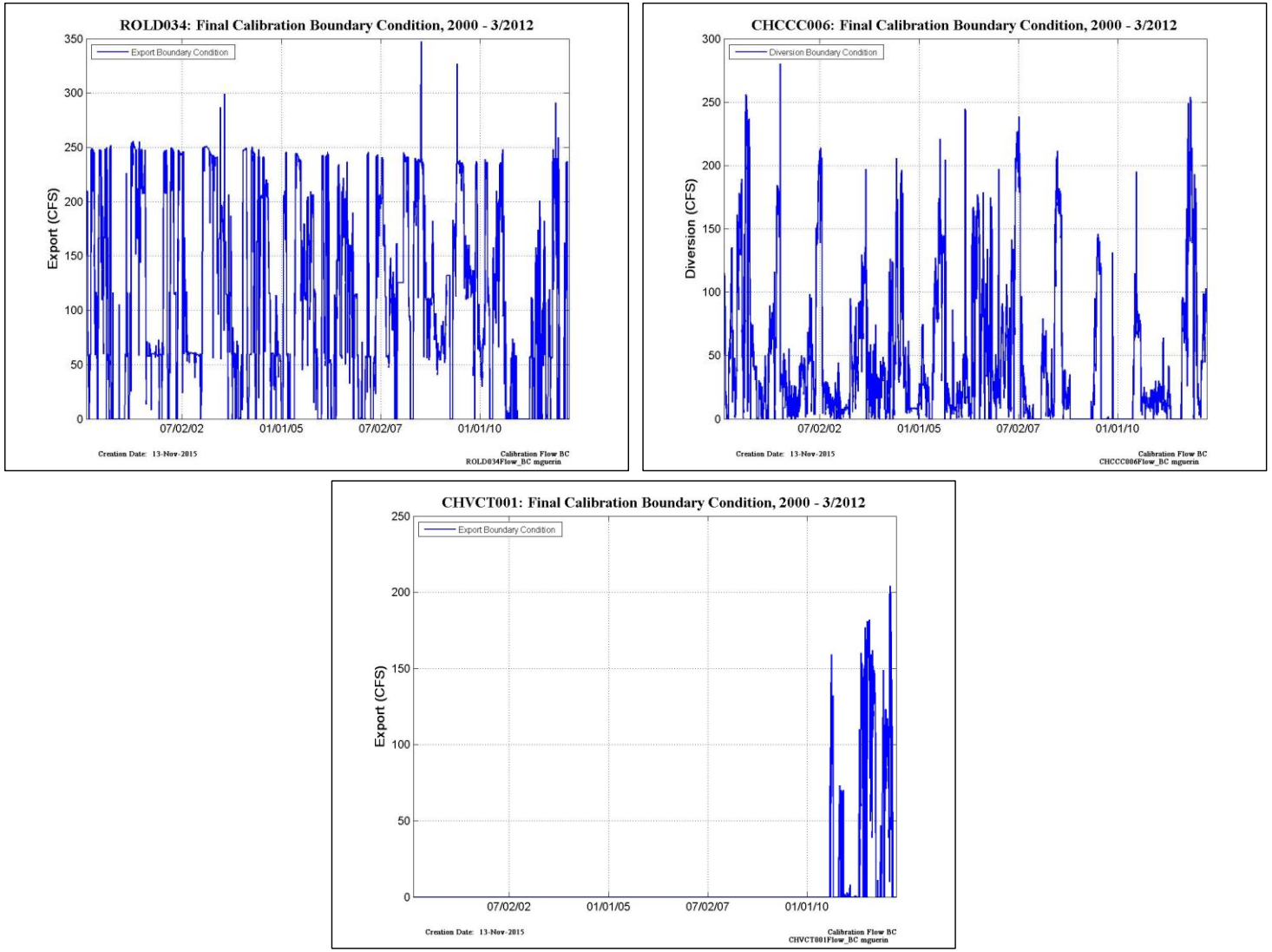

Figure 6-107 Model export at CCWD's Old River location (upper left), Contra Costa Canal location (upper right), and Victoria Canal location (lower).

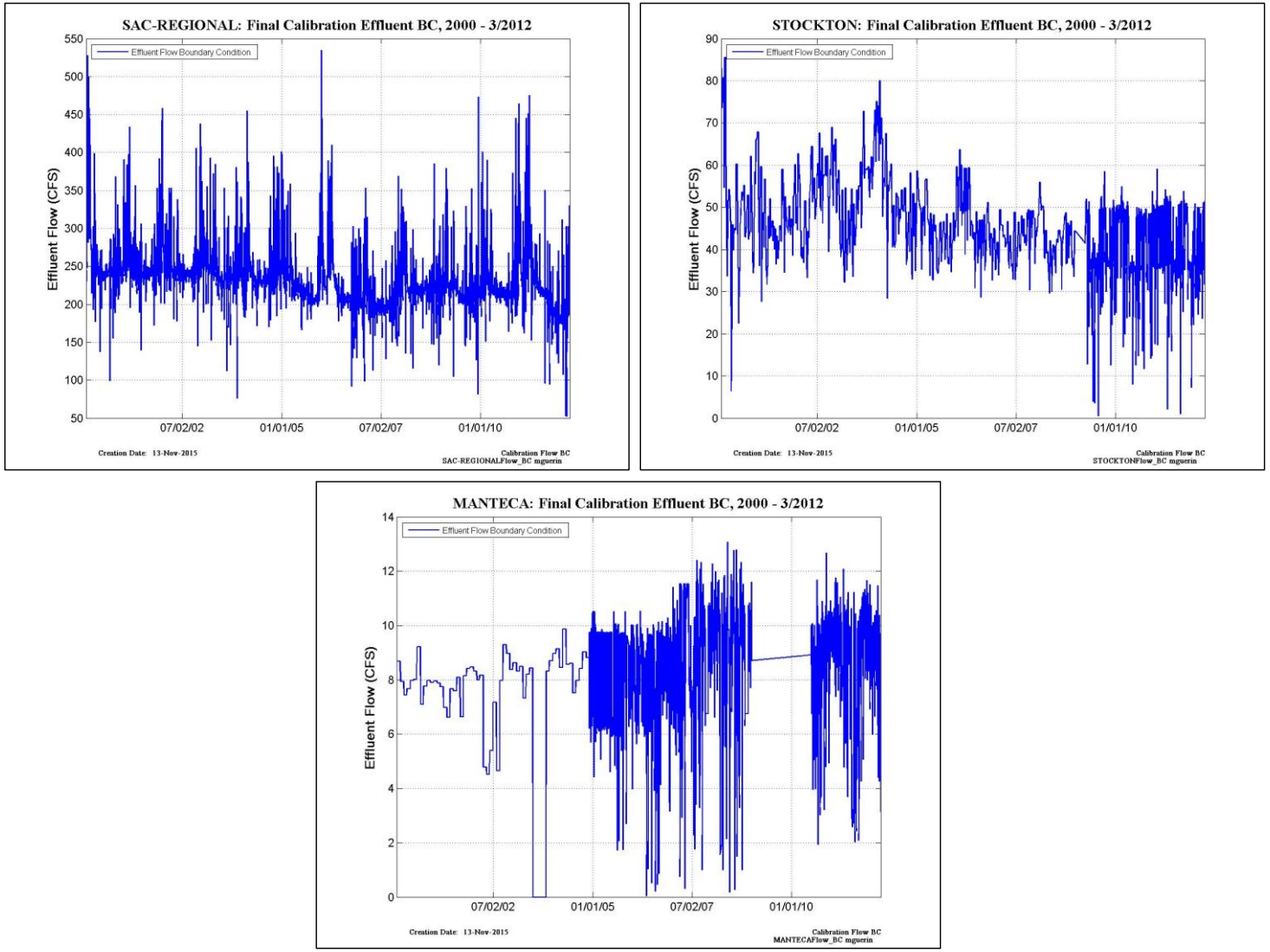

Figure 6-108 Effluent inflow from wastewater treatment plants at Sacramento (upper left), Stockton (upper right) and Manteca (lower).

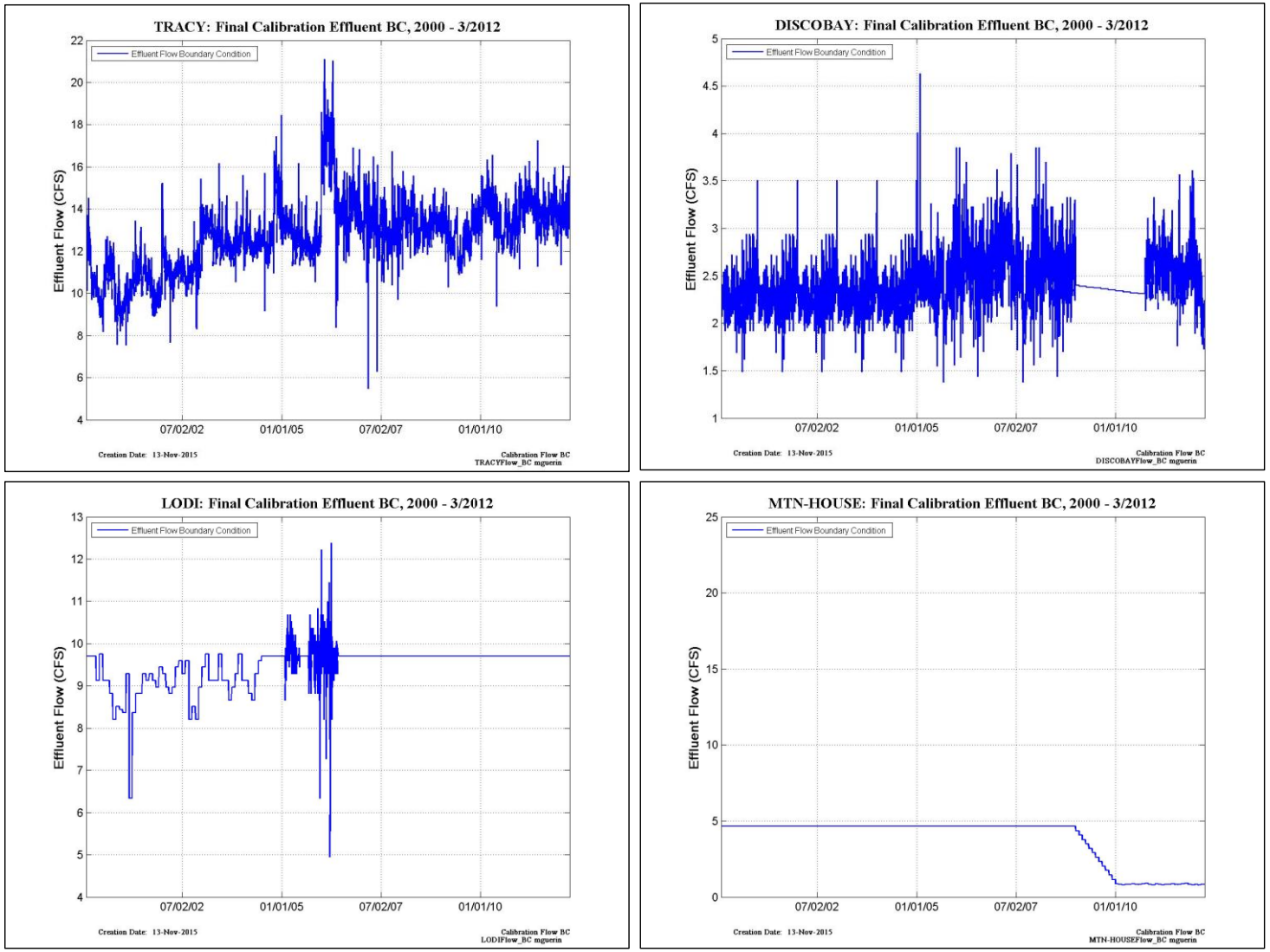

Figure 6-109 Effluent inflow from wastewater treatment plants at Tracy (upper left), Discovery Bay (upper right), Lodi (lower left), and Mountain House (lower left).

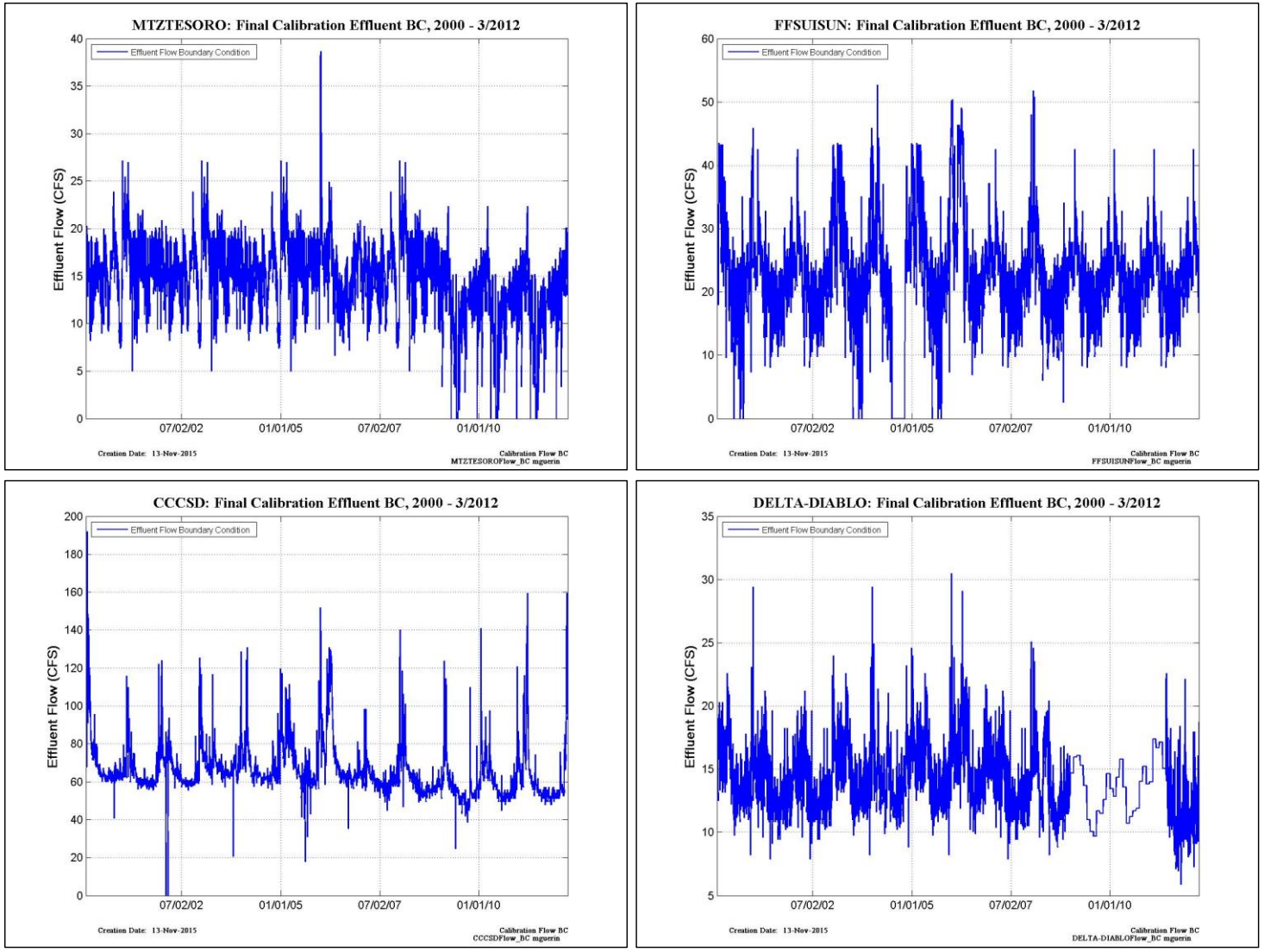

Figure 6-110 Effluent inflow from wastewater treatment plants at Martinez-Tesoro plant (upper left), Fairfield-Suisun (upper right), Central Contra Costa Sanitary District (lower left), and Delta-Diablo (lower left).

6.12.4 Detailed Calibration Statistics

The next several sections document the residual histograms for all available EMP data for all of the modeled years (top histogram in each plot, 01/2000 – 03/2012), and for the Wet calibration (2000, 2003, and 2011) and validation water years (2005 and 2006) (lower two plots in the upper figure) and for the Dry calibration (2001, 2002, and 2009) and validation water years (2007 and 2008) (lower two plots in the lower figure).

The subsections have plots sorted by constituent.

6.12.4.1 Statistics for Modeled Algae– EMP Data

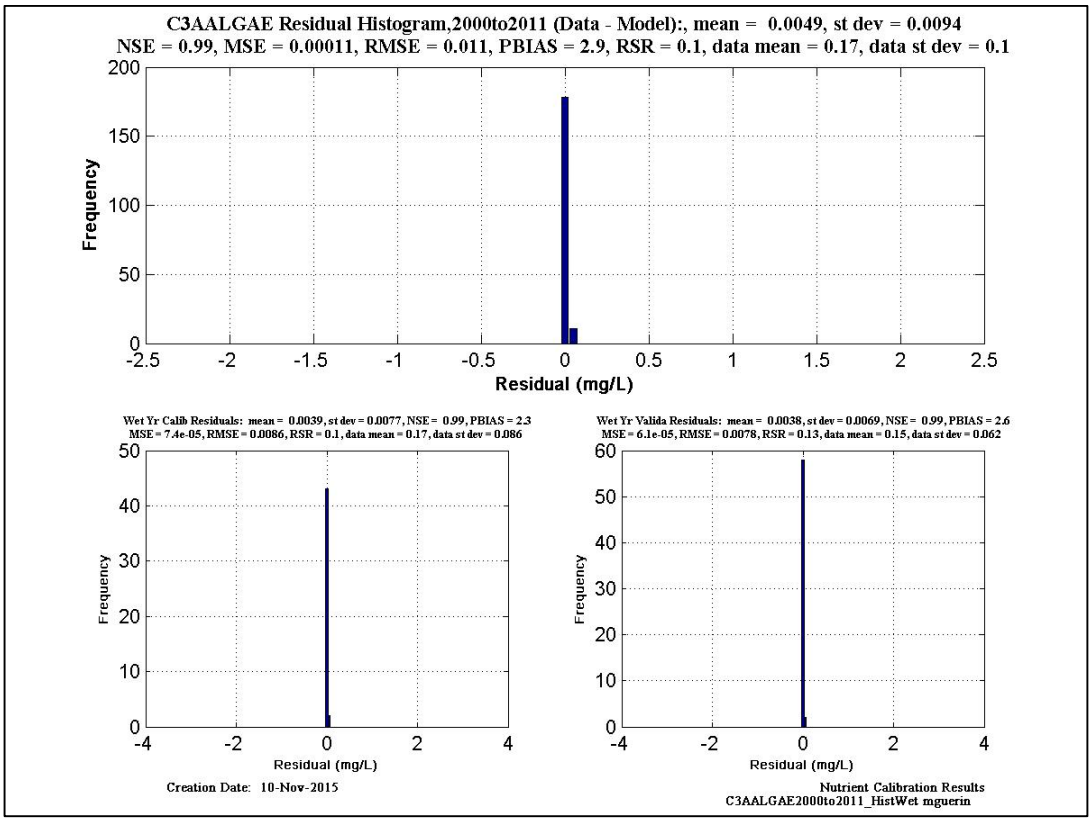

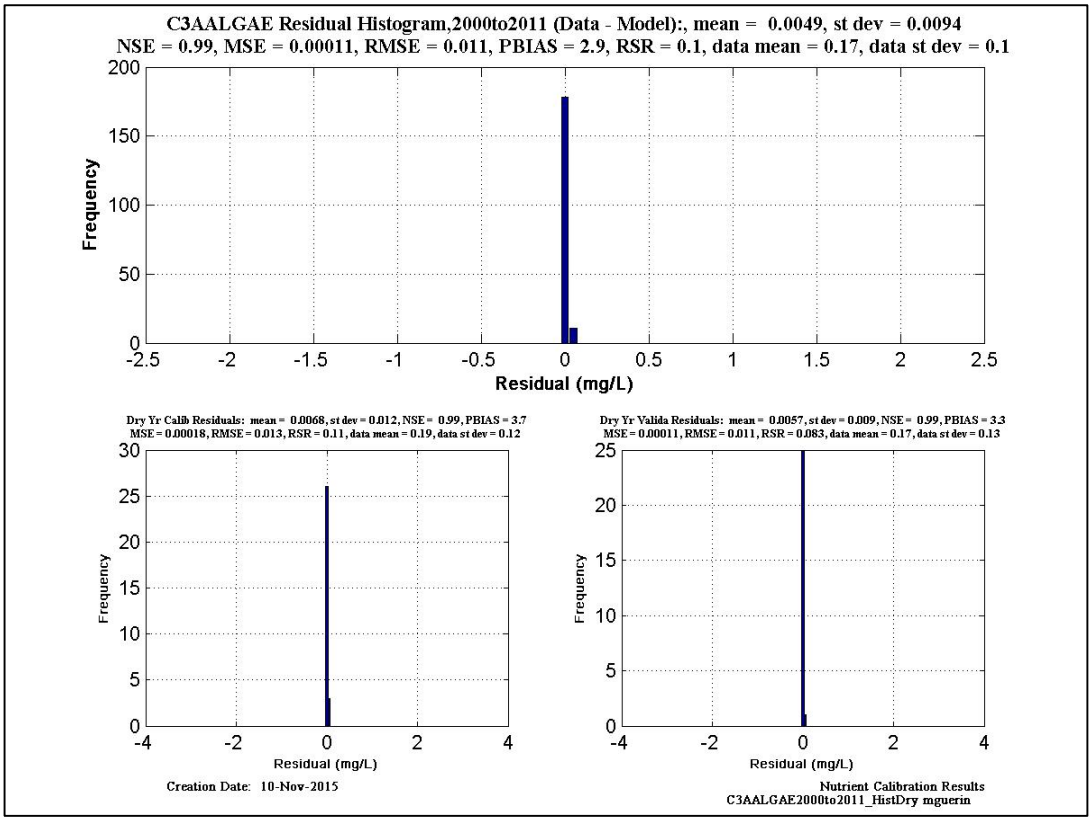

Figure 6-111 Algae histogram and statistics at EMP location C3A.

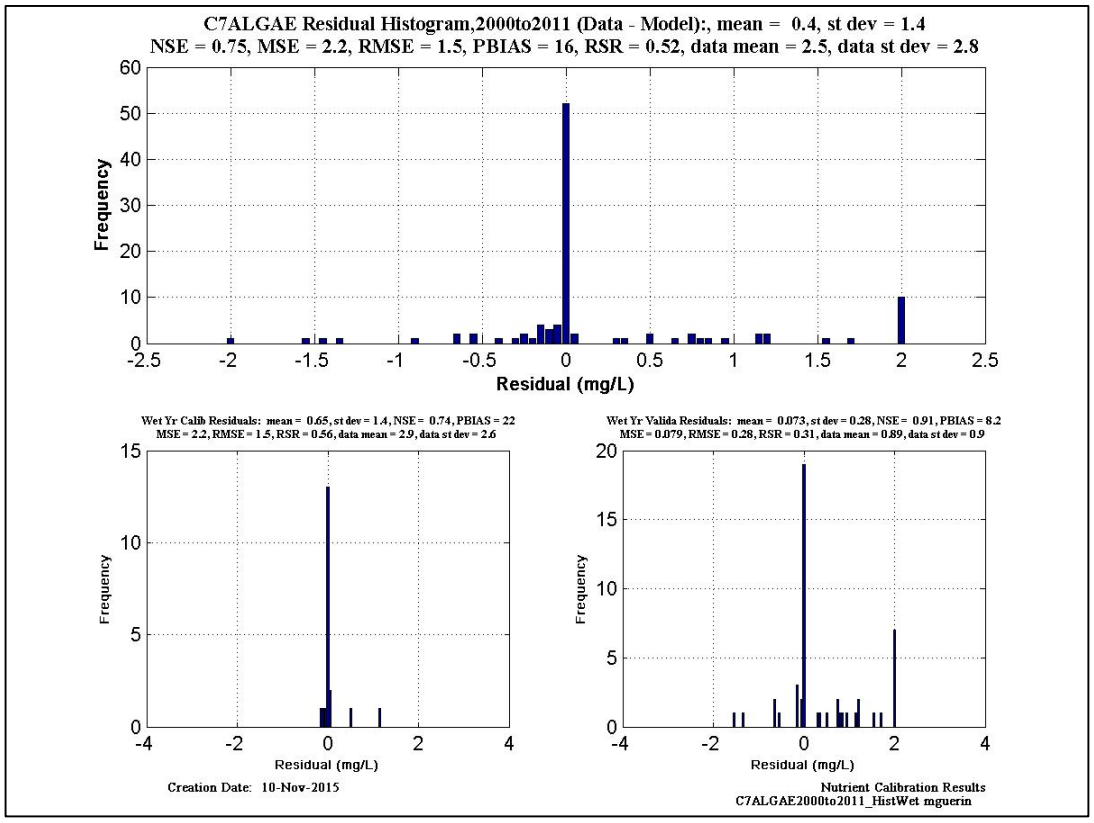

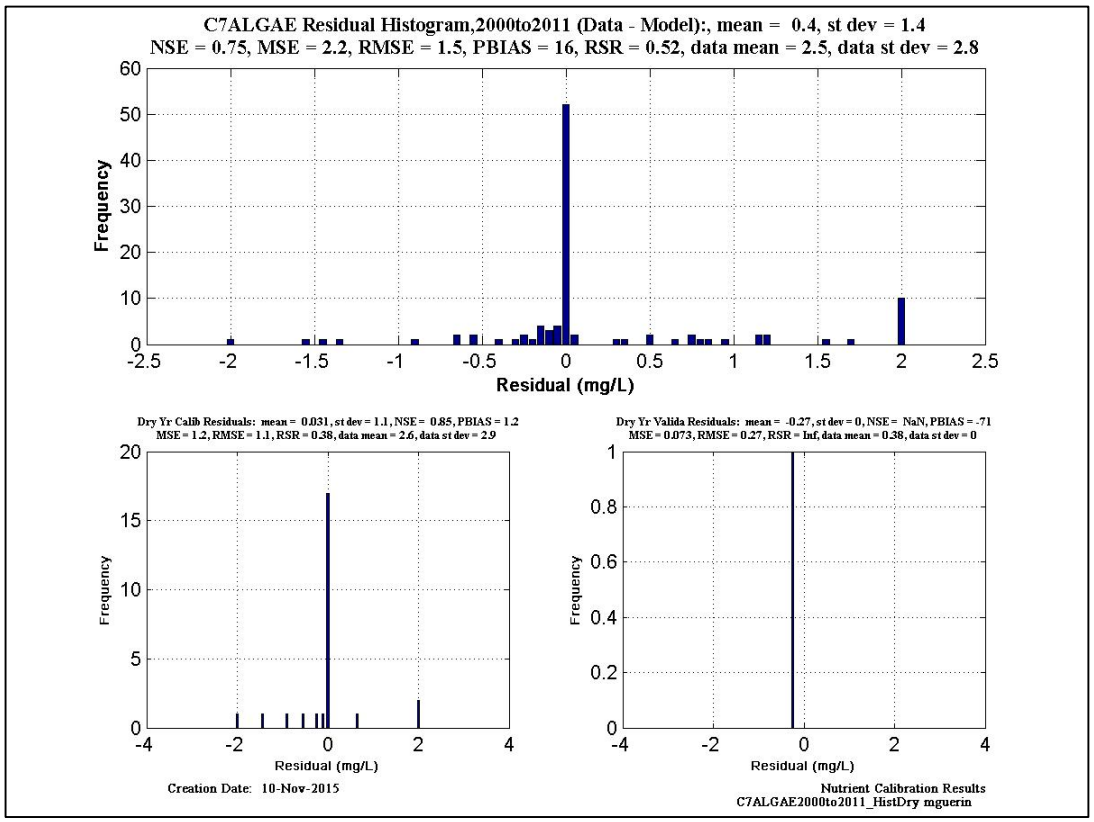

Figure 6-112 Algae histogram and statistics at EMP location C7.

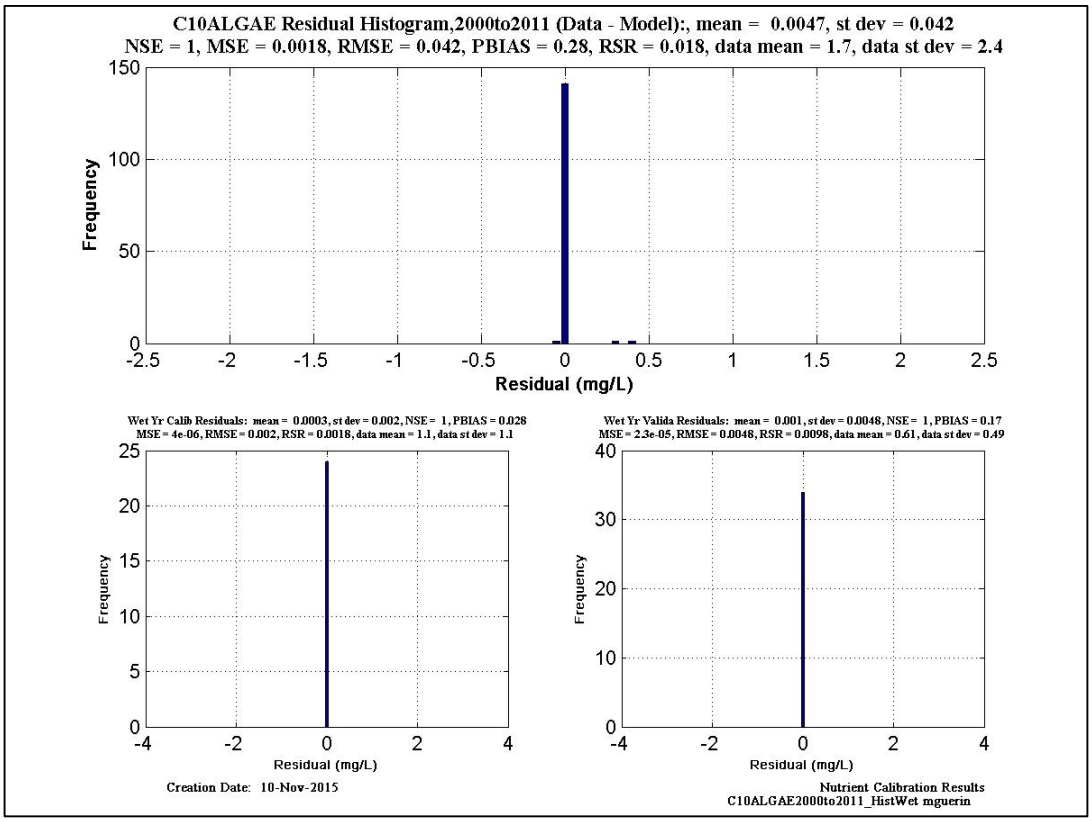

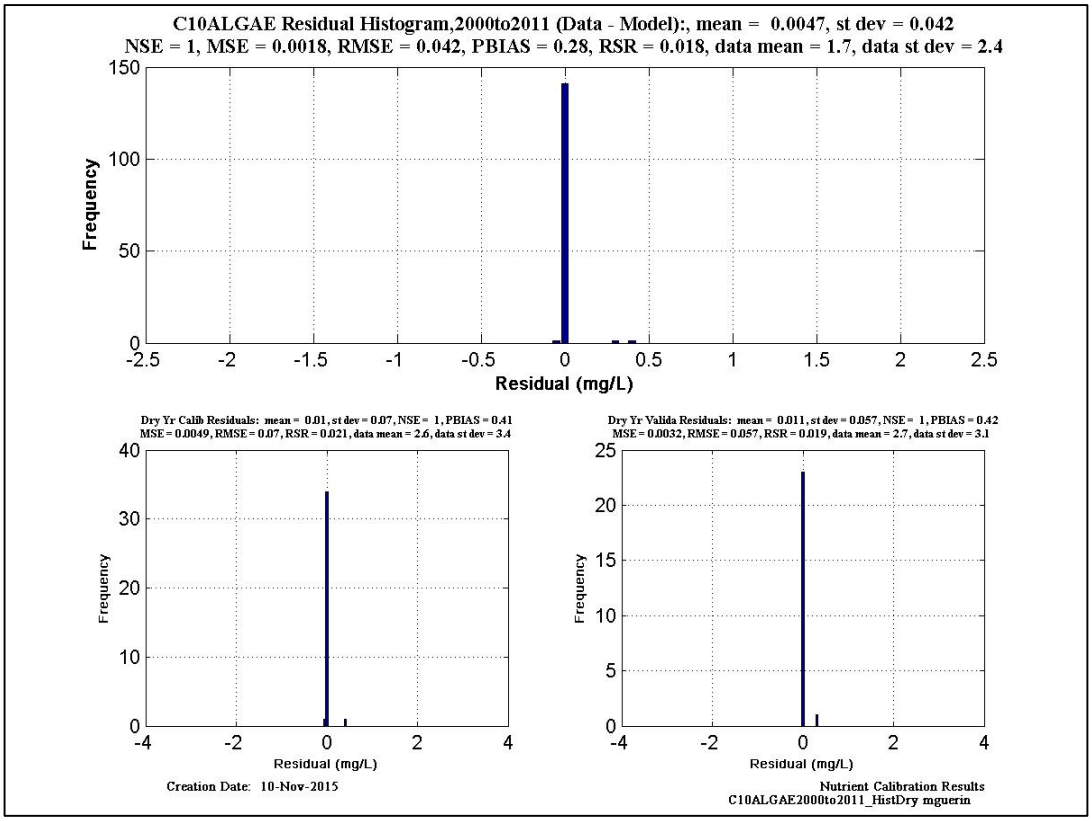

Figure 6-113 Algae histogram and statistics at EMP location C10.

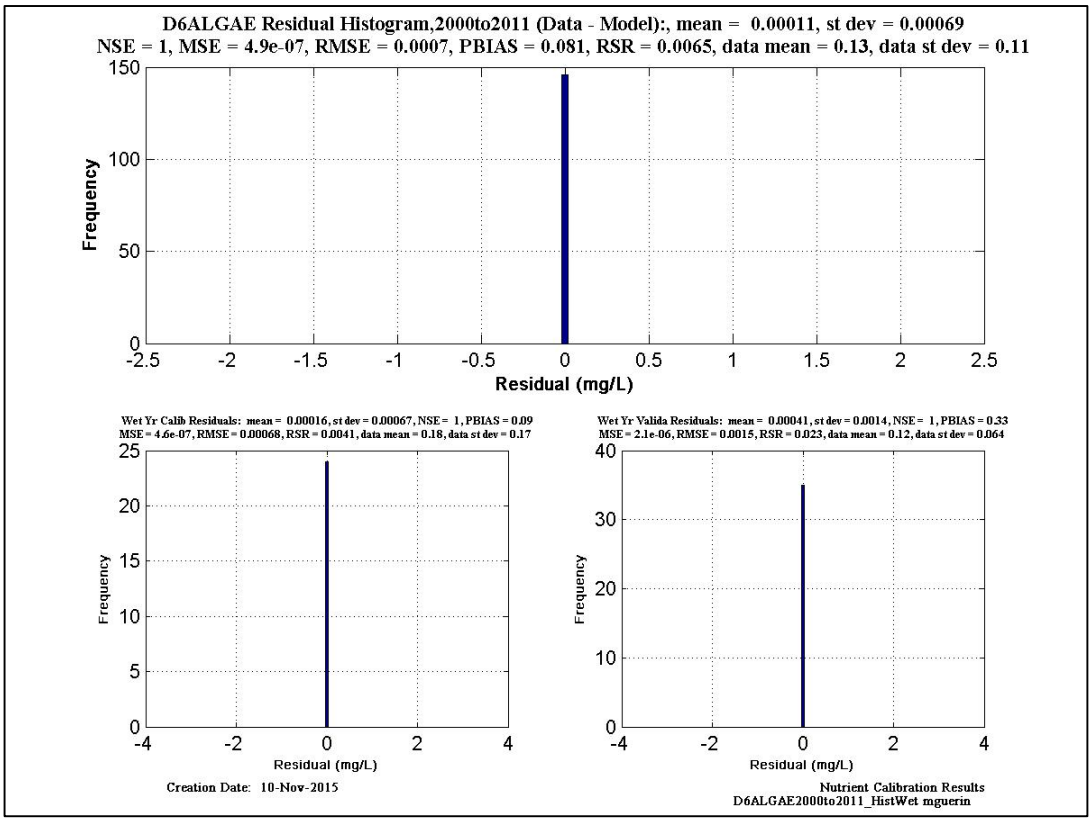

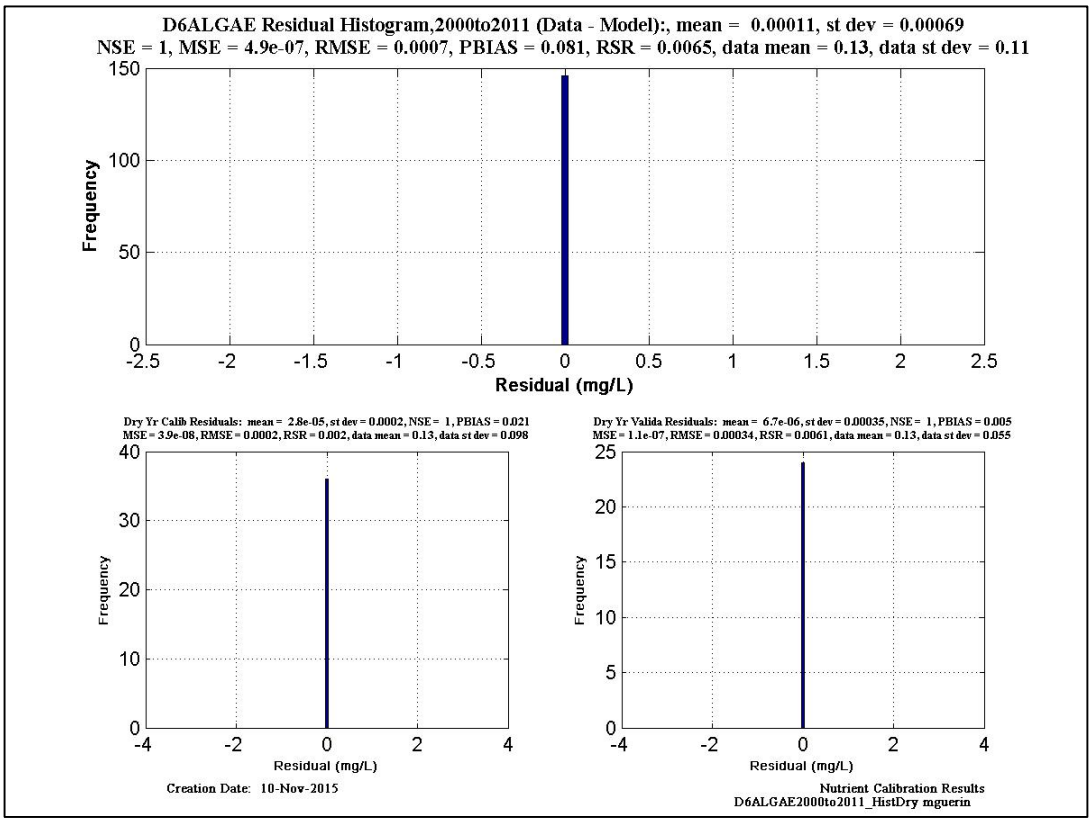

Figure 6-114 Algae histogram and statistics at EMP location C11.

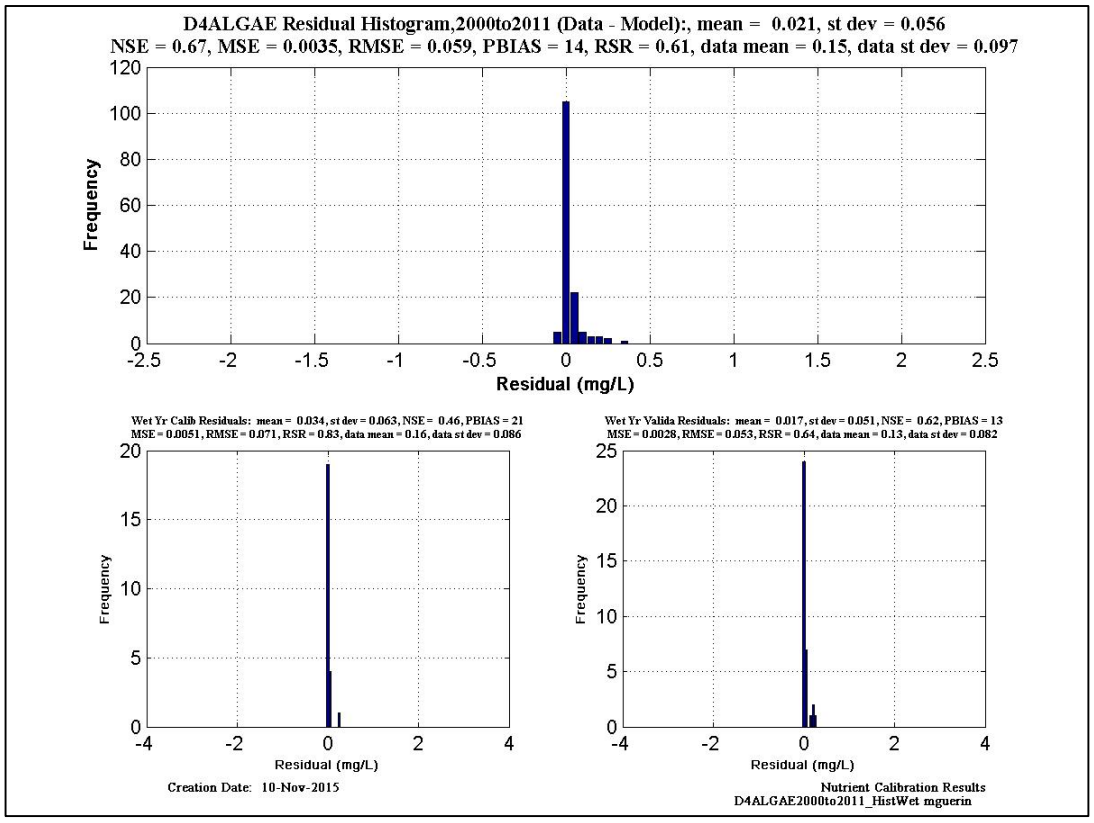

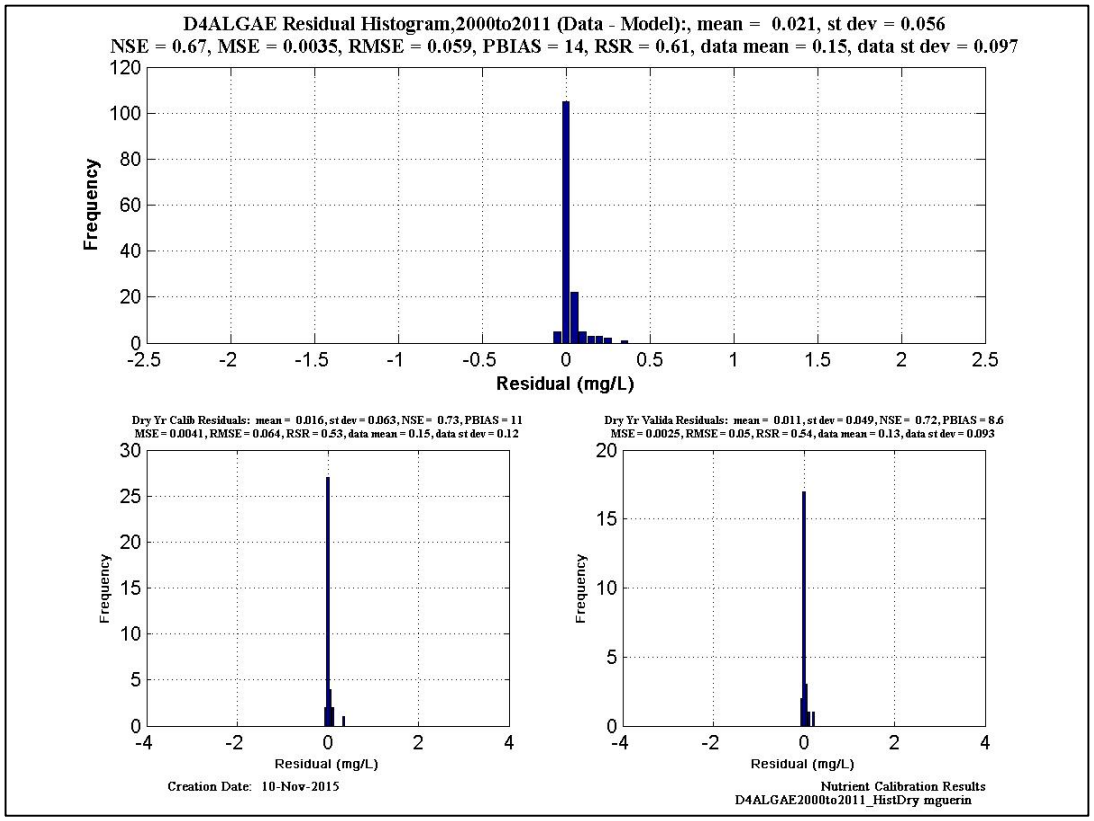

Figure 6-115 Algae histogram and statistics at EMP location D4.

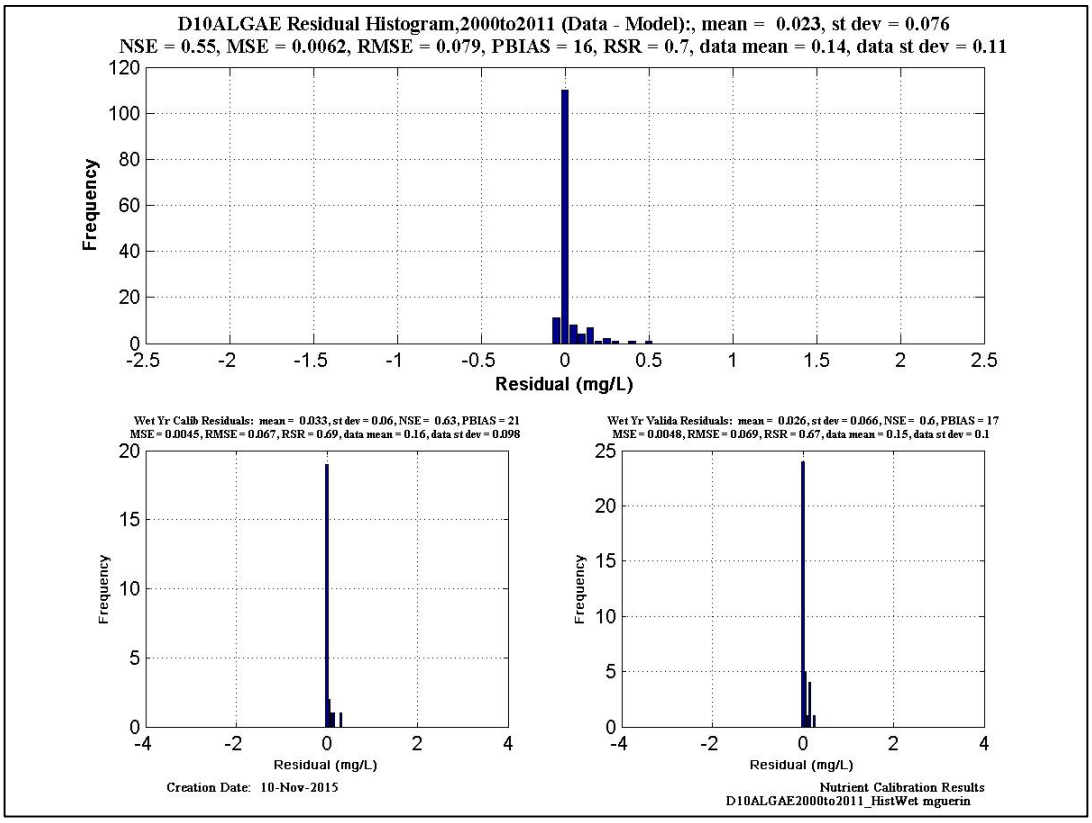

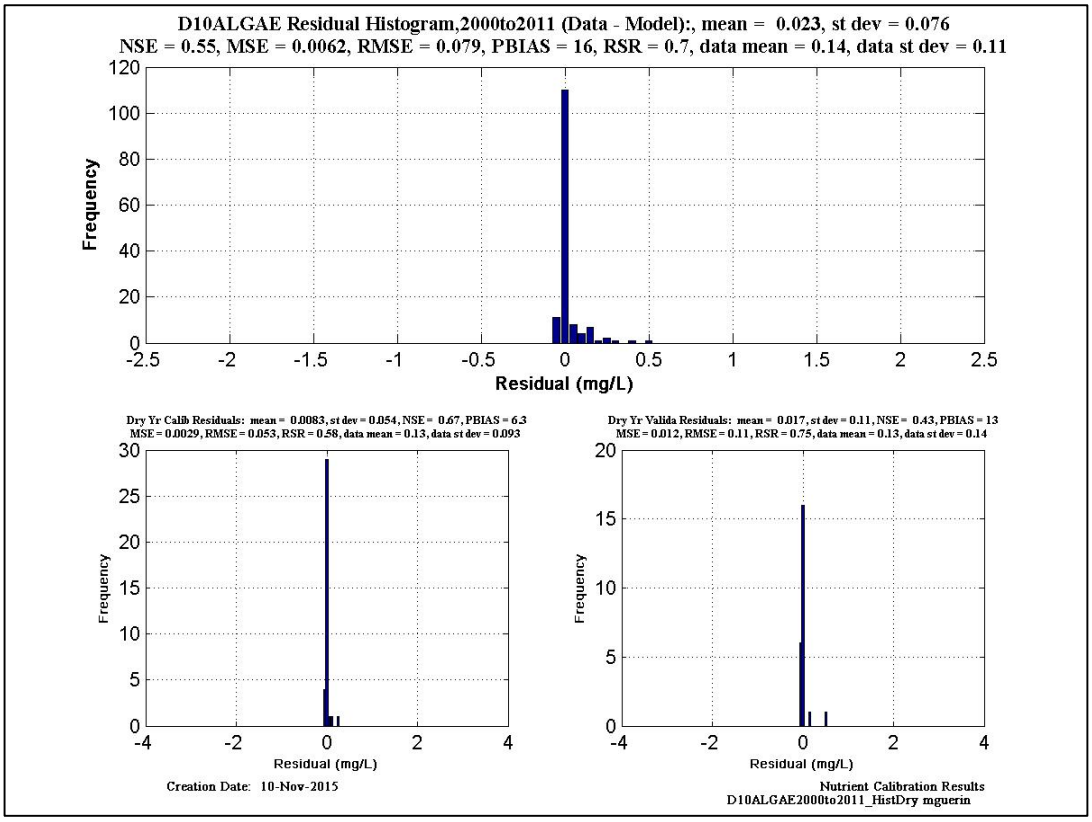

Figure 6-116 Algae histogram and statistics at EMP location D10.

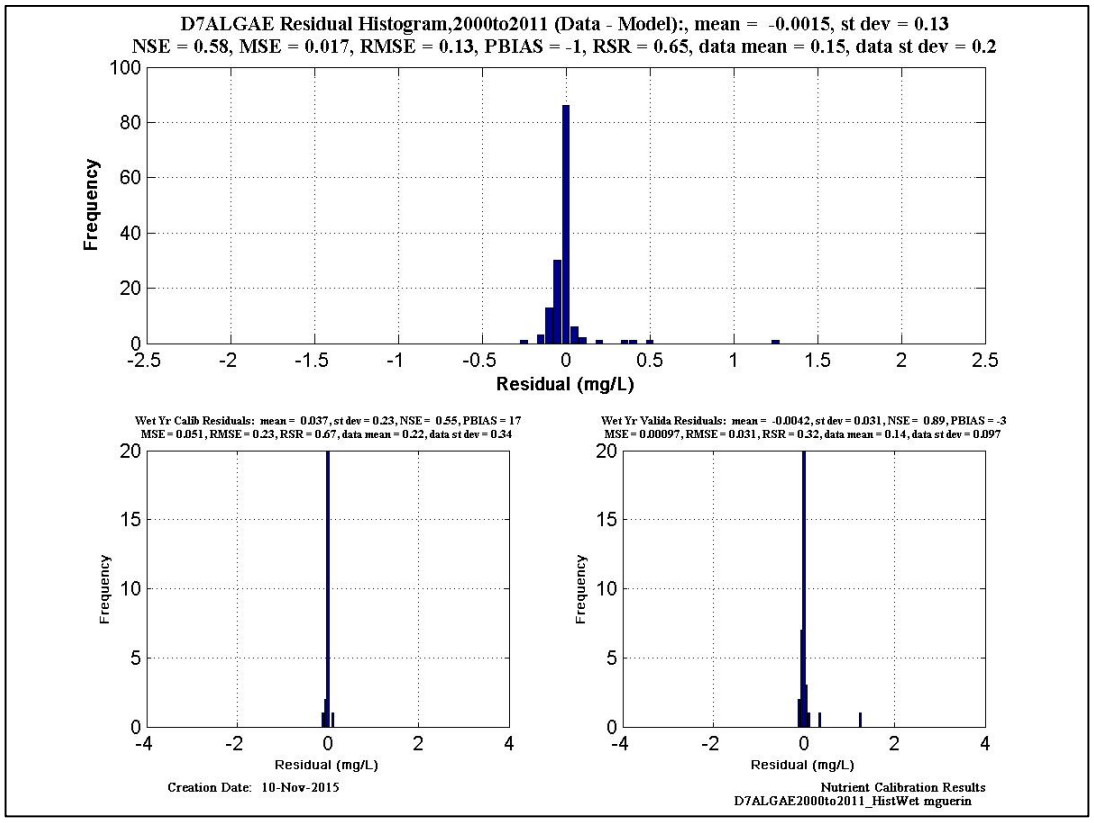

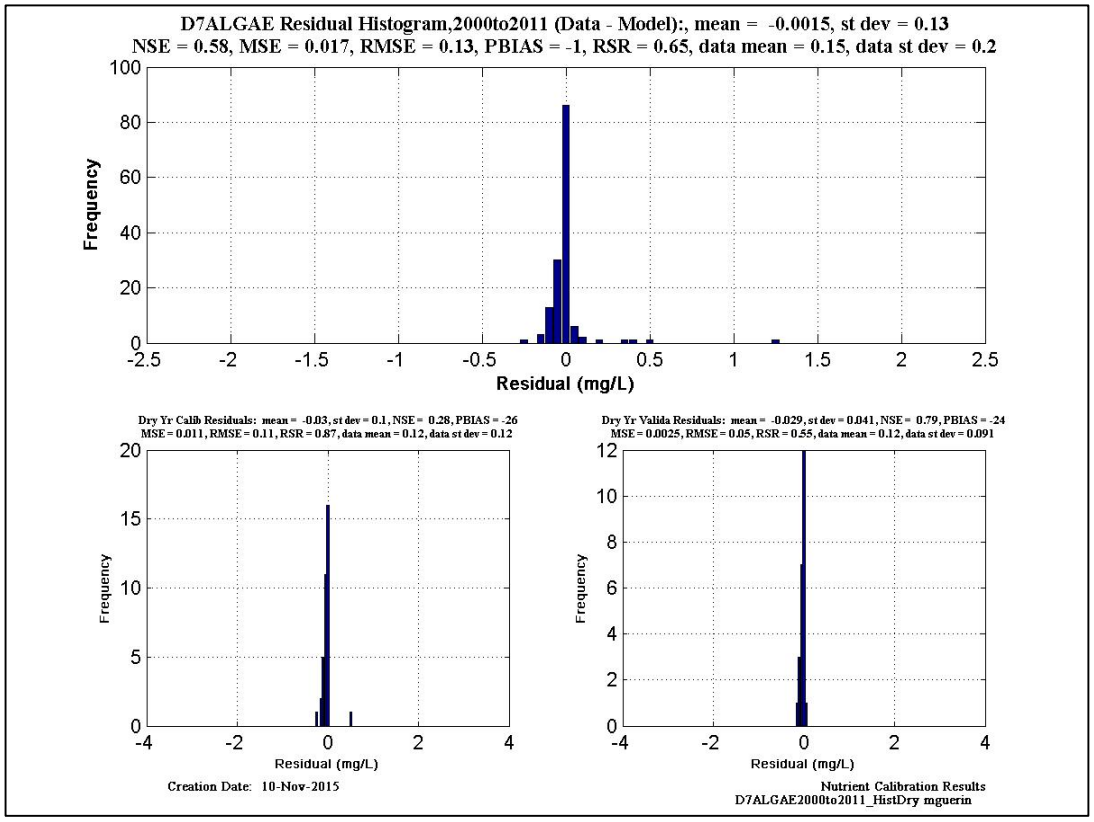

Figure 6-117 Algae histogram and statistics at EMP location D7.

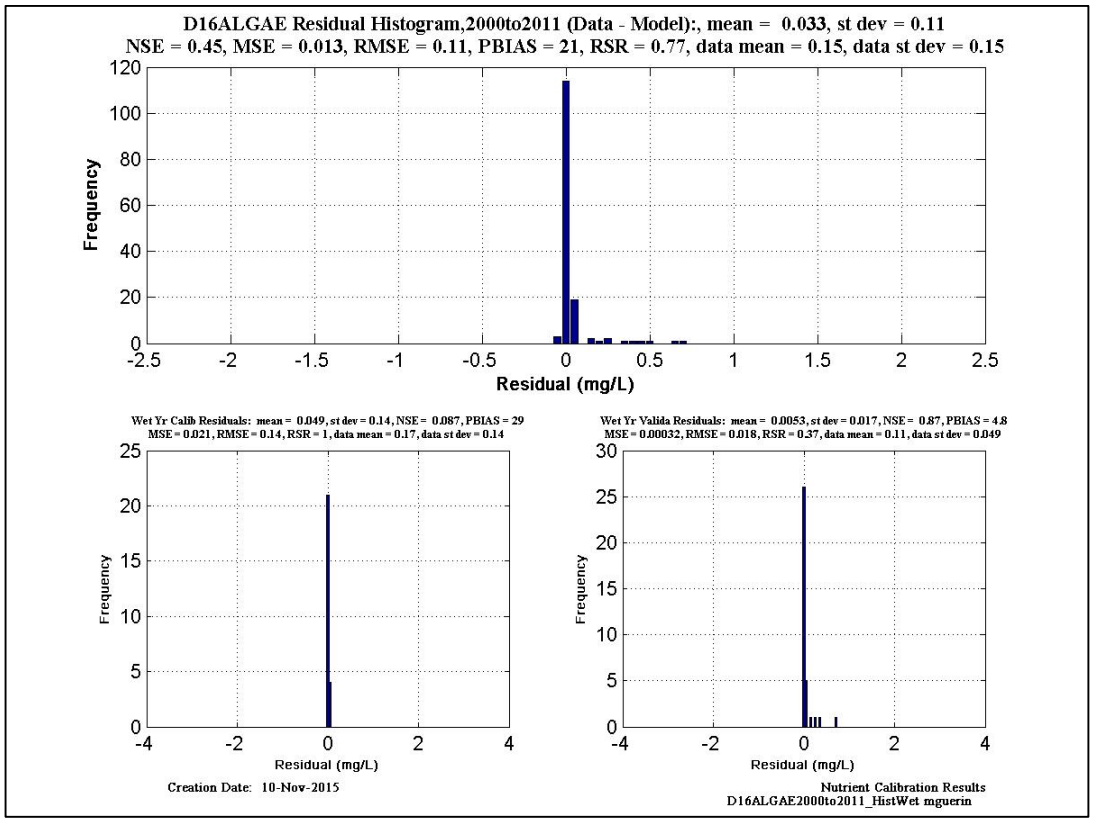

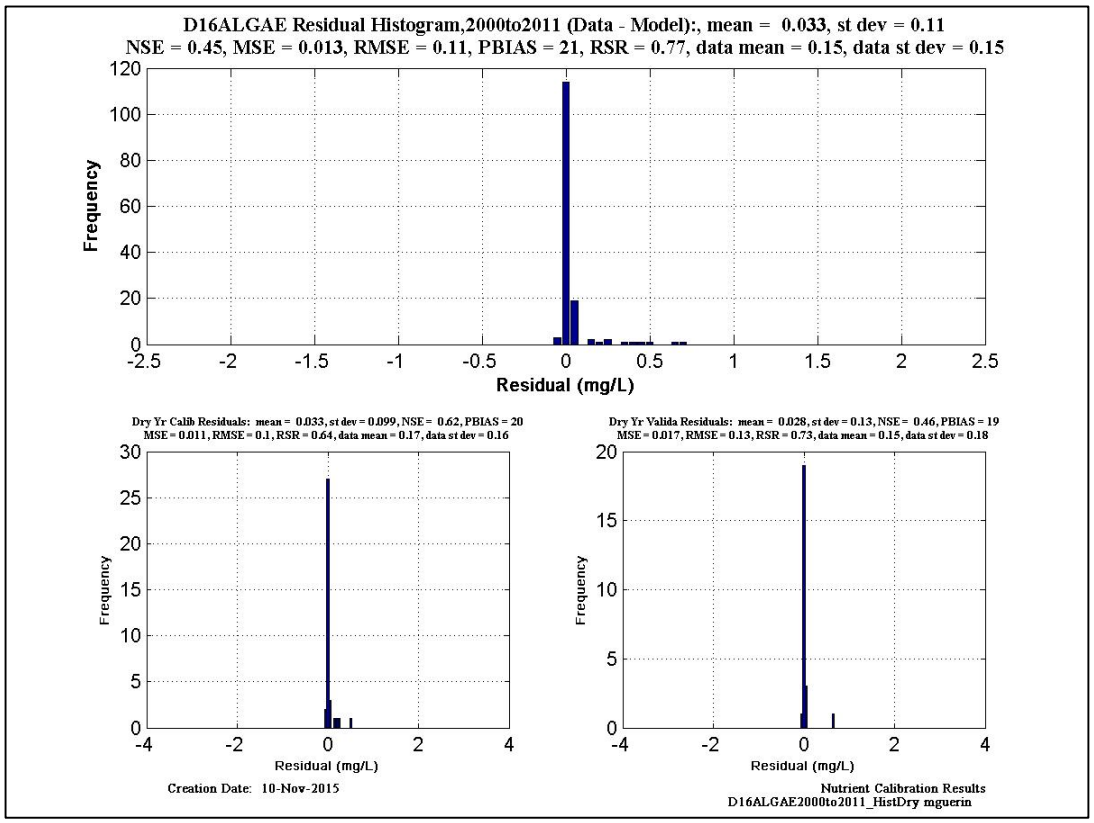

Figure 6-118 Algae histogram and statistics at EMP location D16.

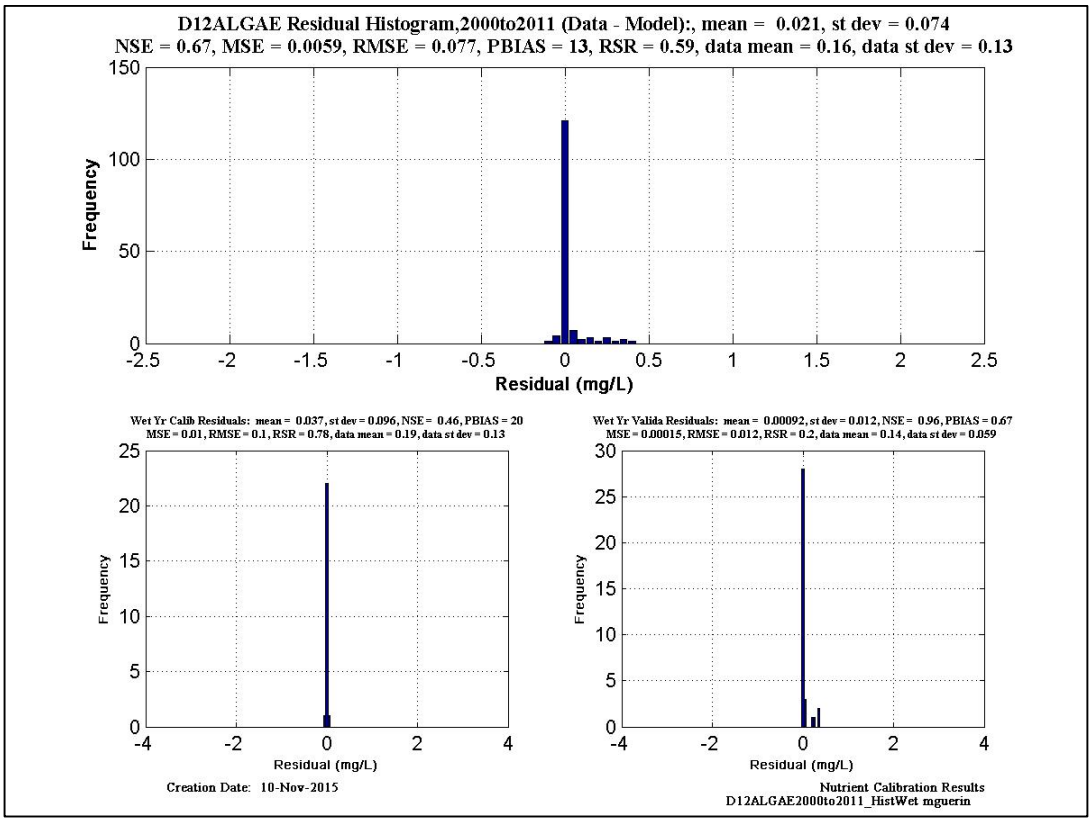

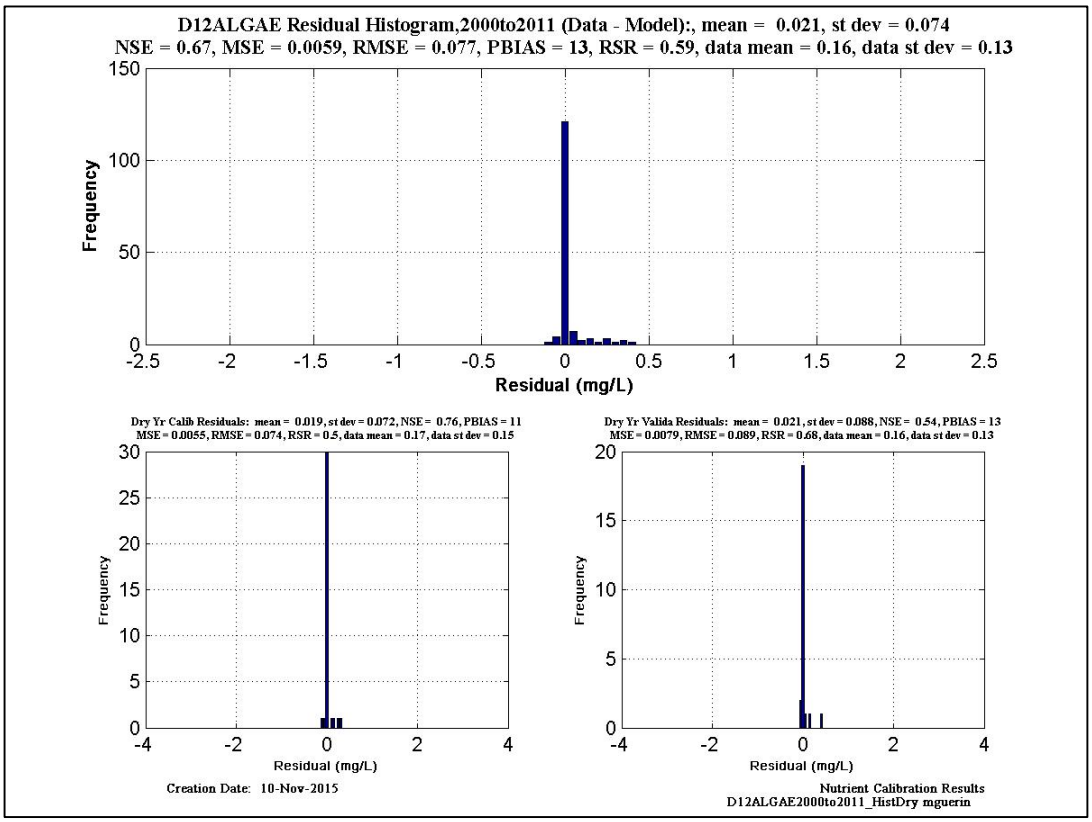

Figure 6-119 Algae histogram and statistics at EMP location D12.

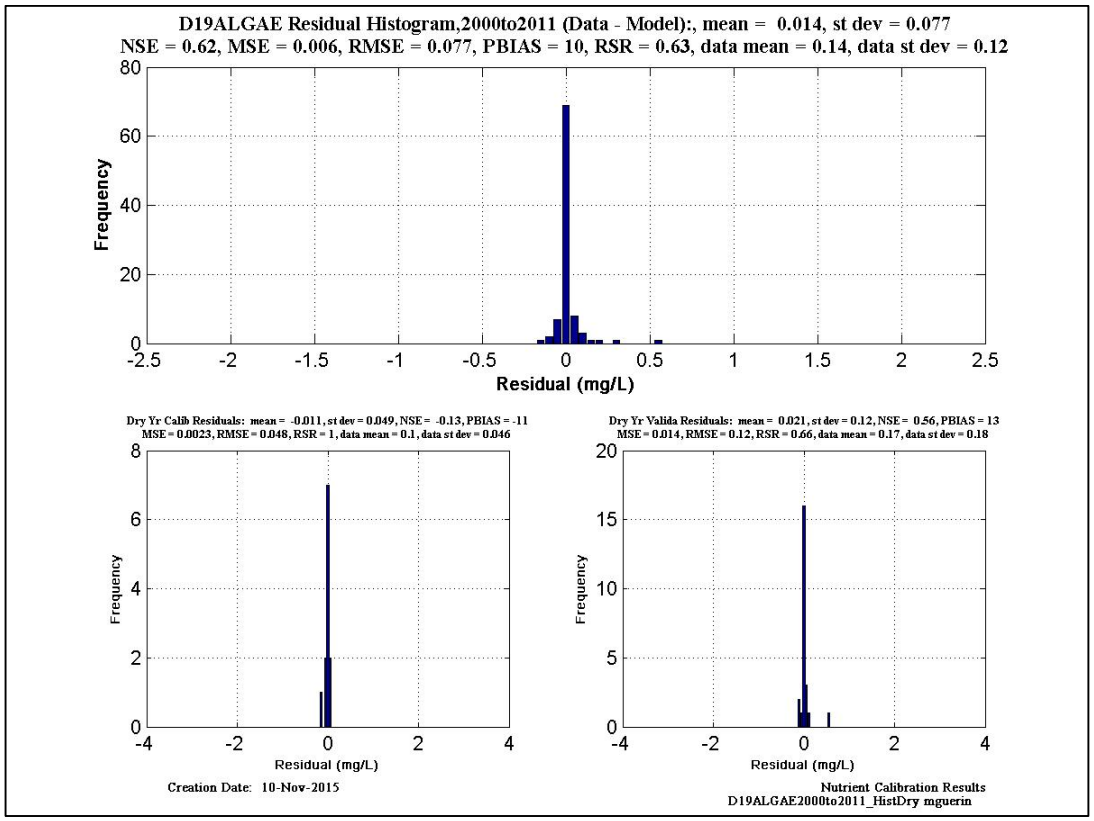

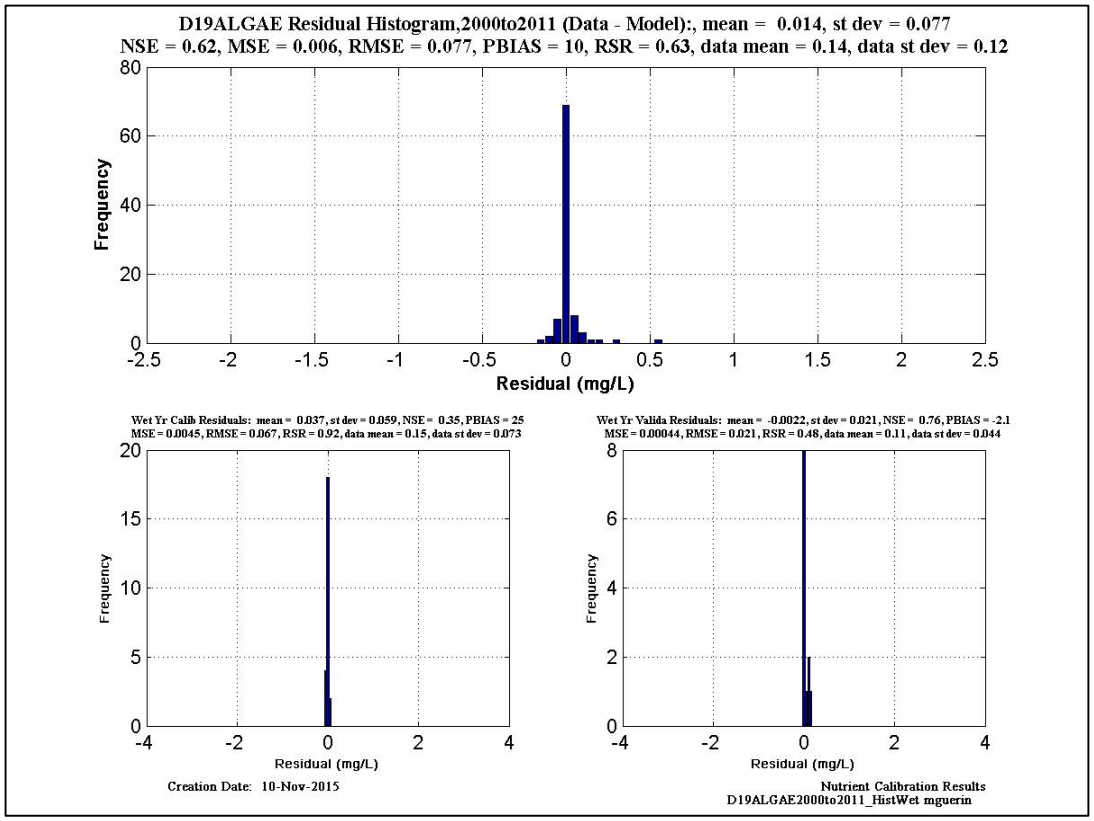

Figure 6-120 Algae histogram and statistics at EMP location D19.

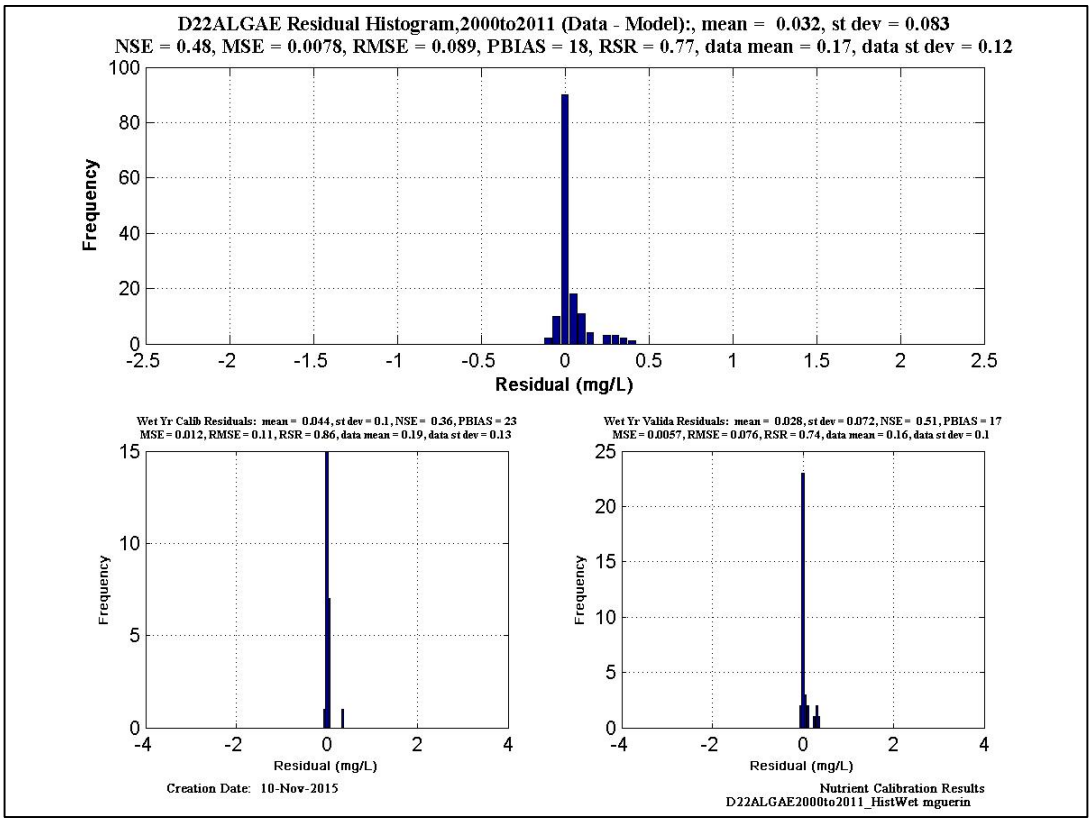

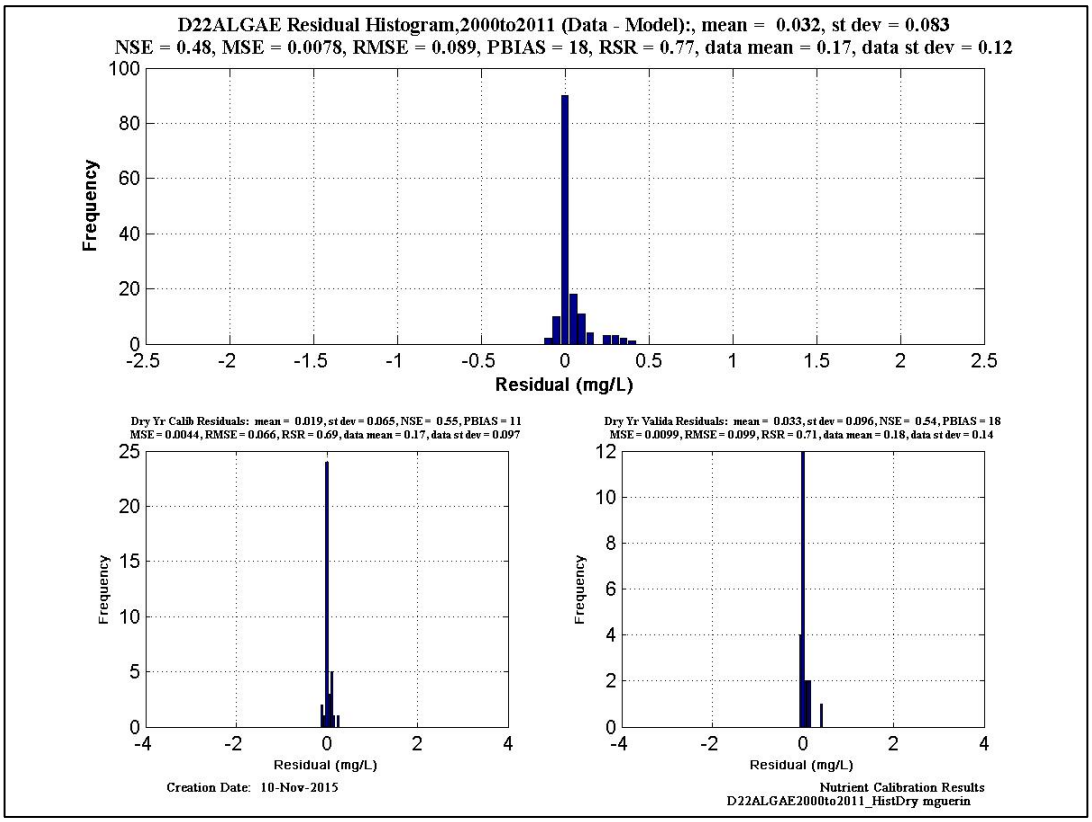

Figure 6-121 Algae histogram and statistics at EMP location D22.

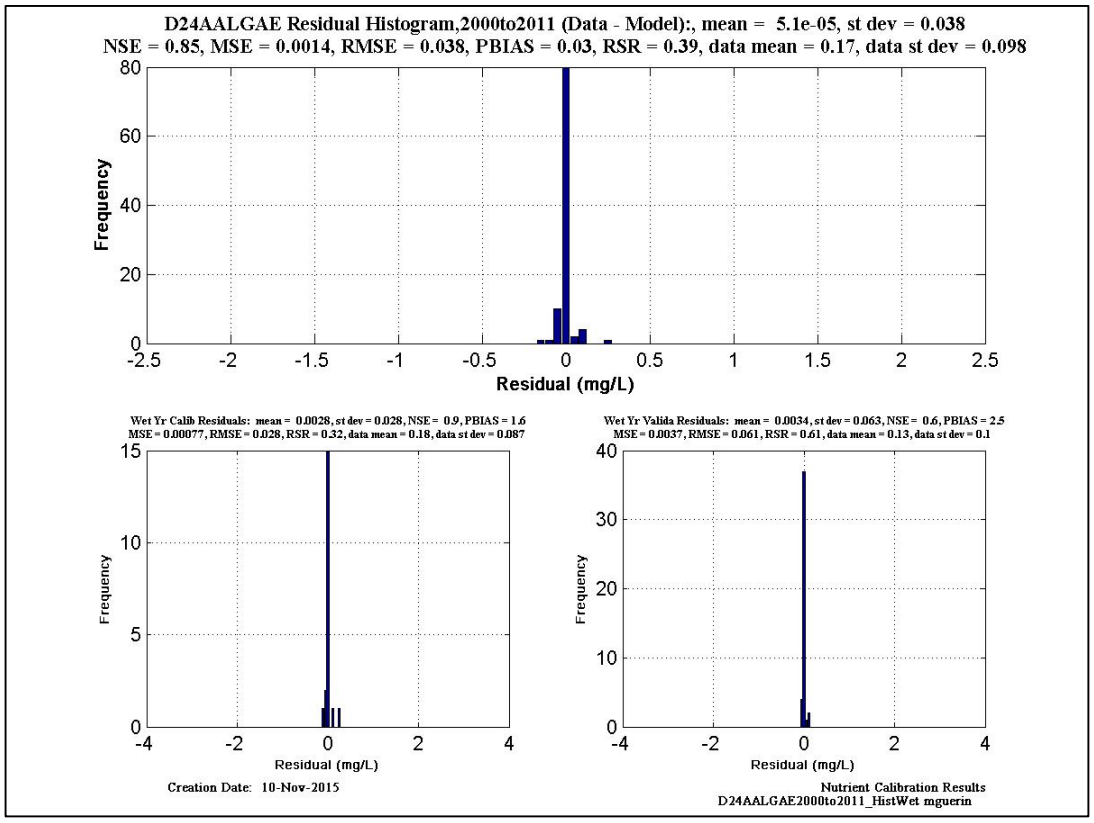

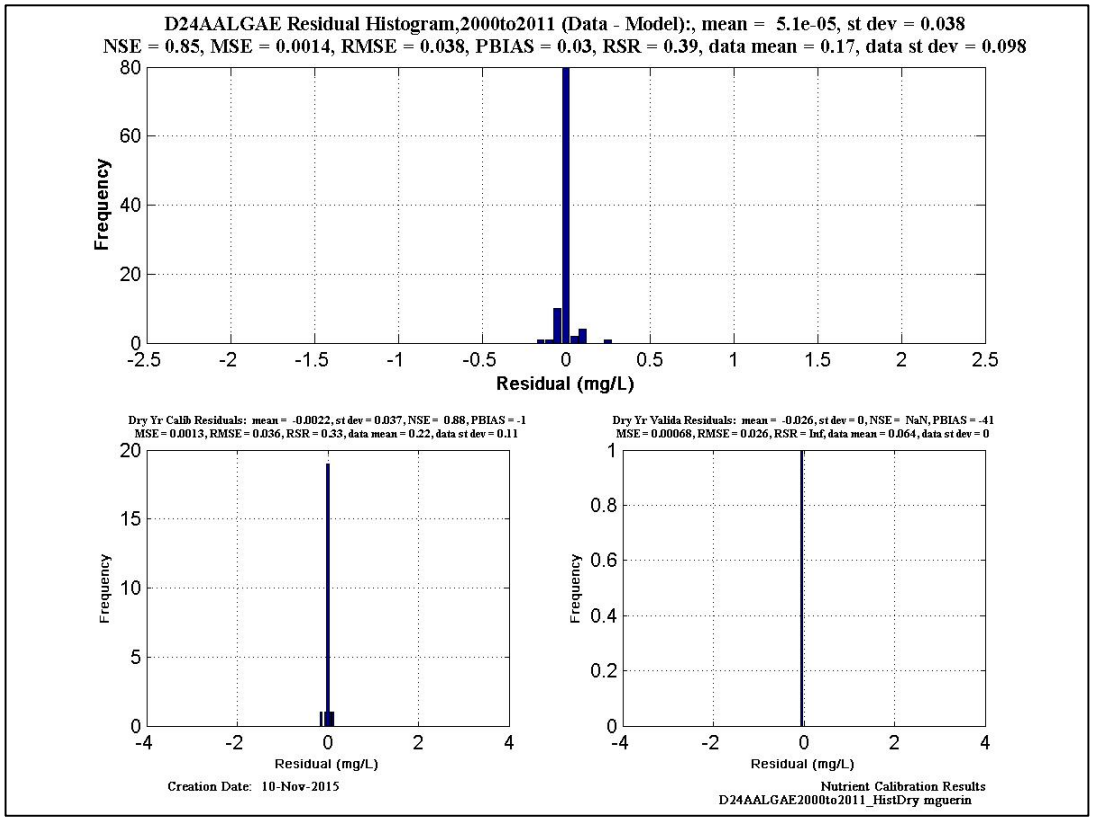

Figure 6-122 Algae histogram and statistics at EMP location D24A.

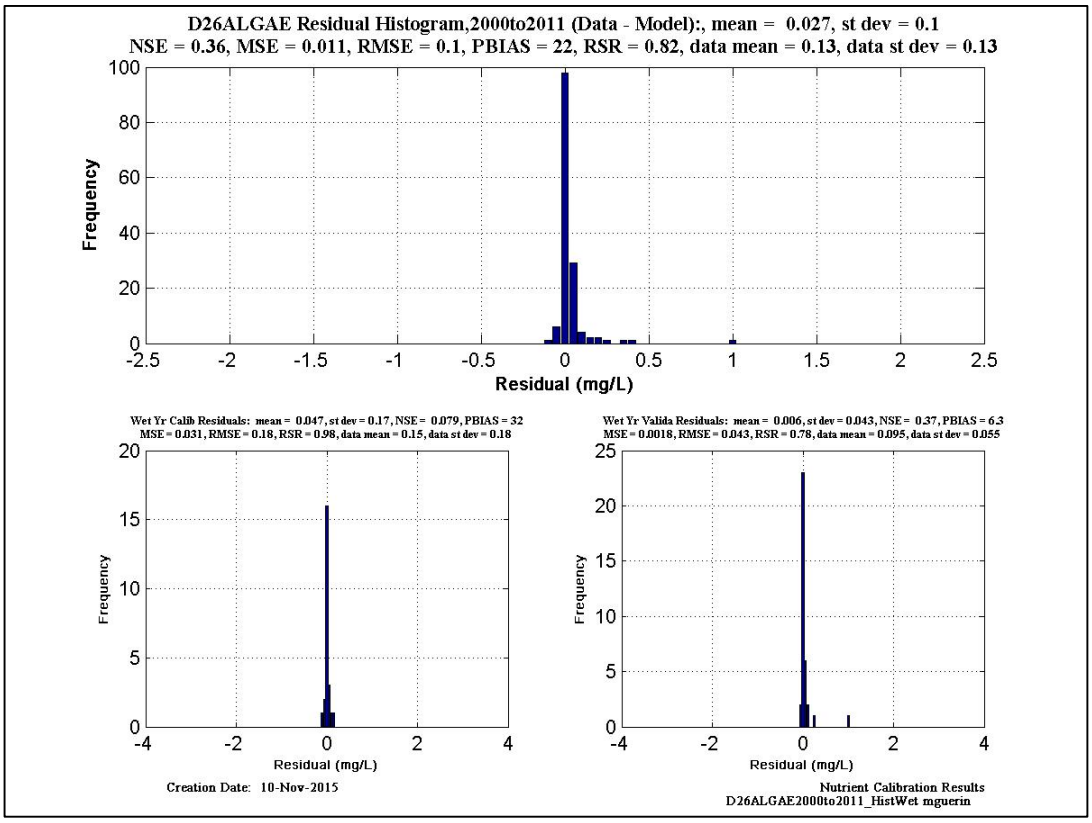

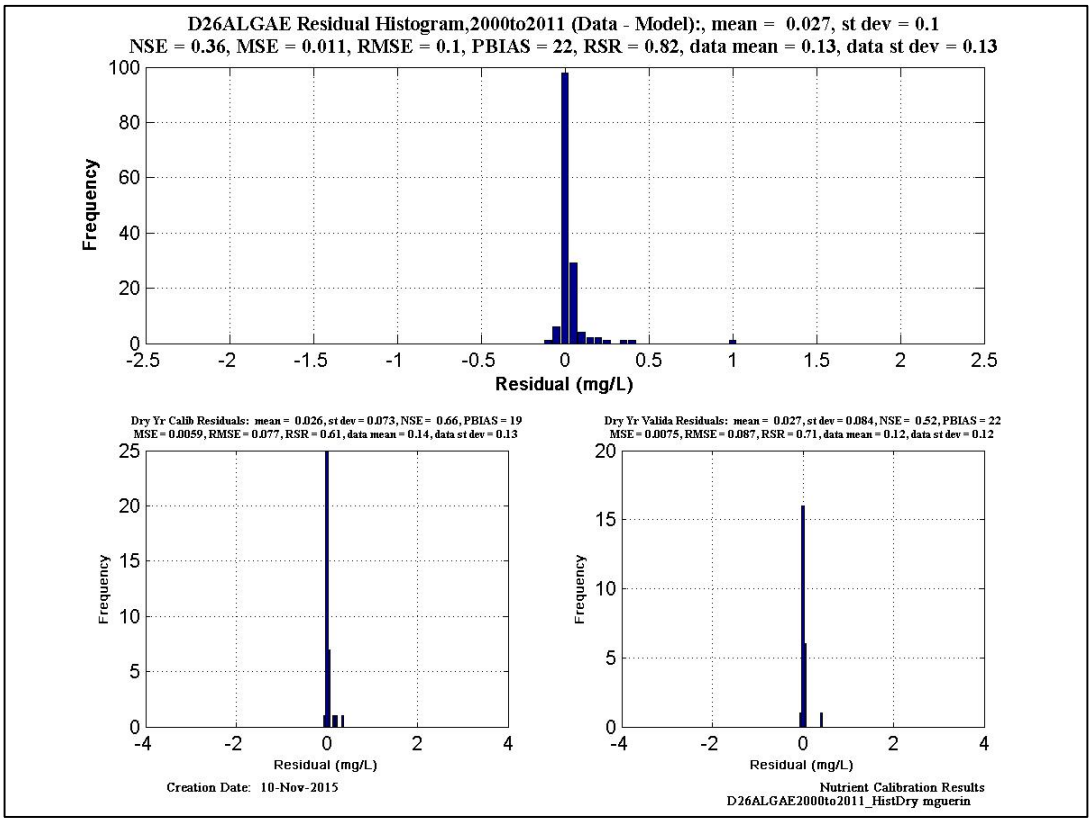

Figure 6-123 Algae histogram and statistics at EMP location D26.

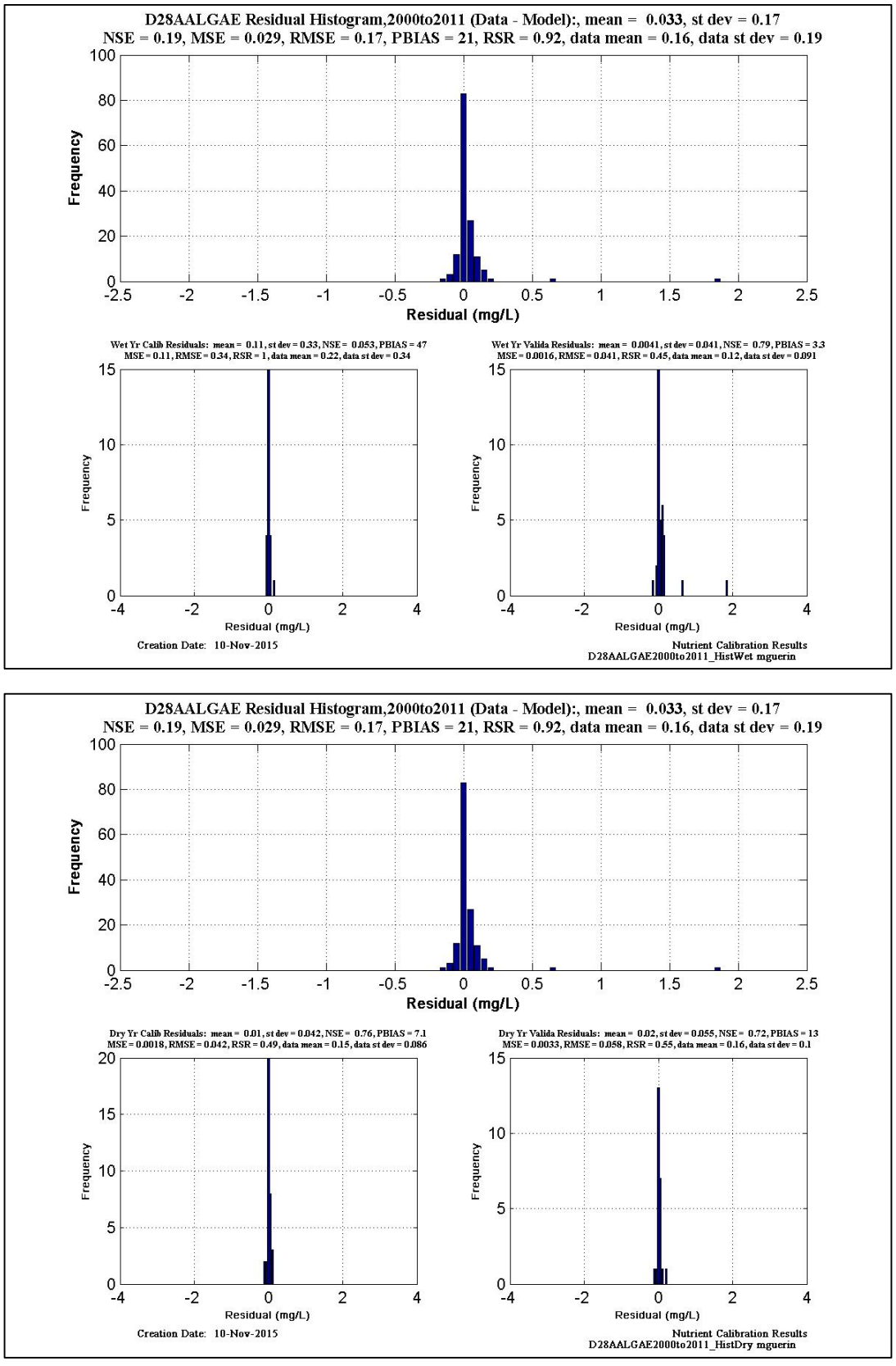

Figure 6-124 Algae histogram and statistics at EMP location D28A.

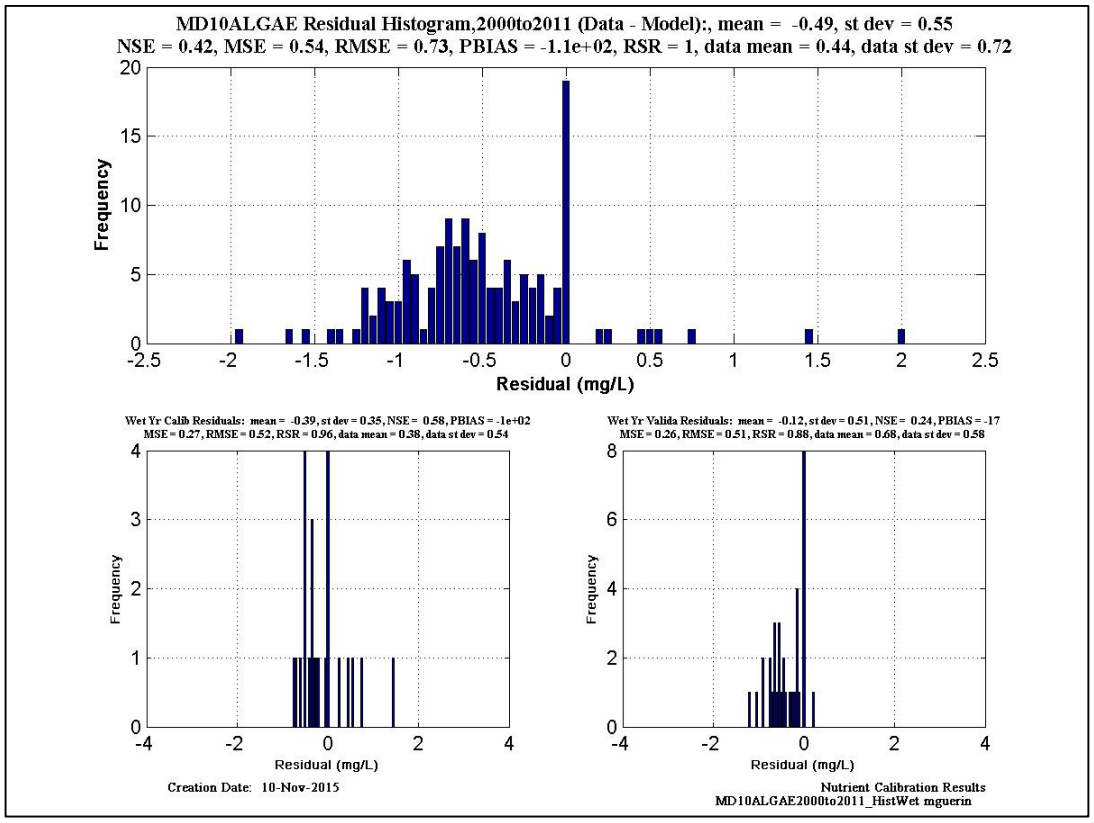

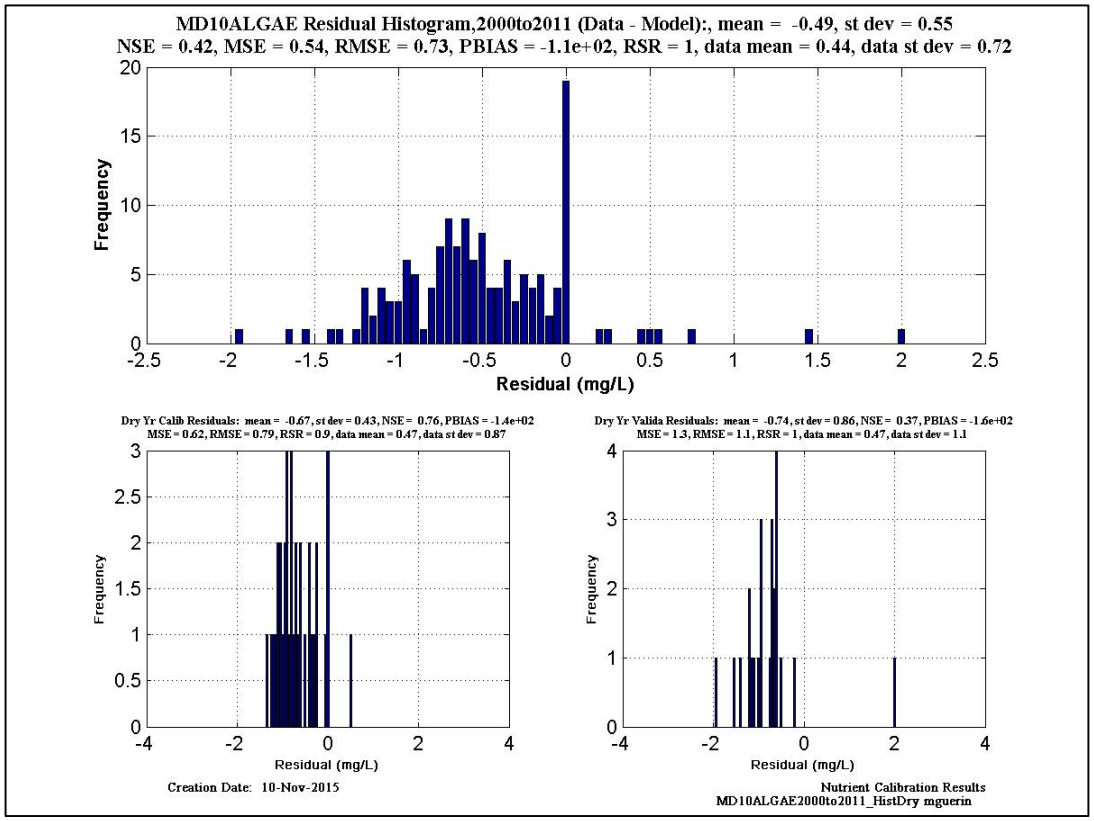

Figure 6-125 Algae histogram and statistics at EMP location MD10.

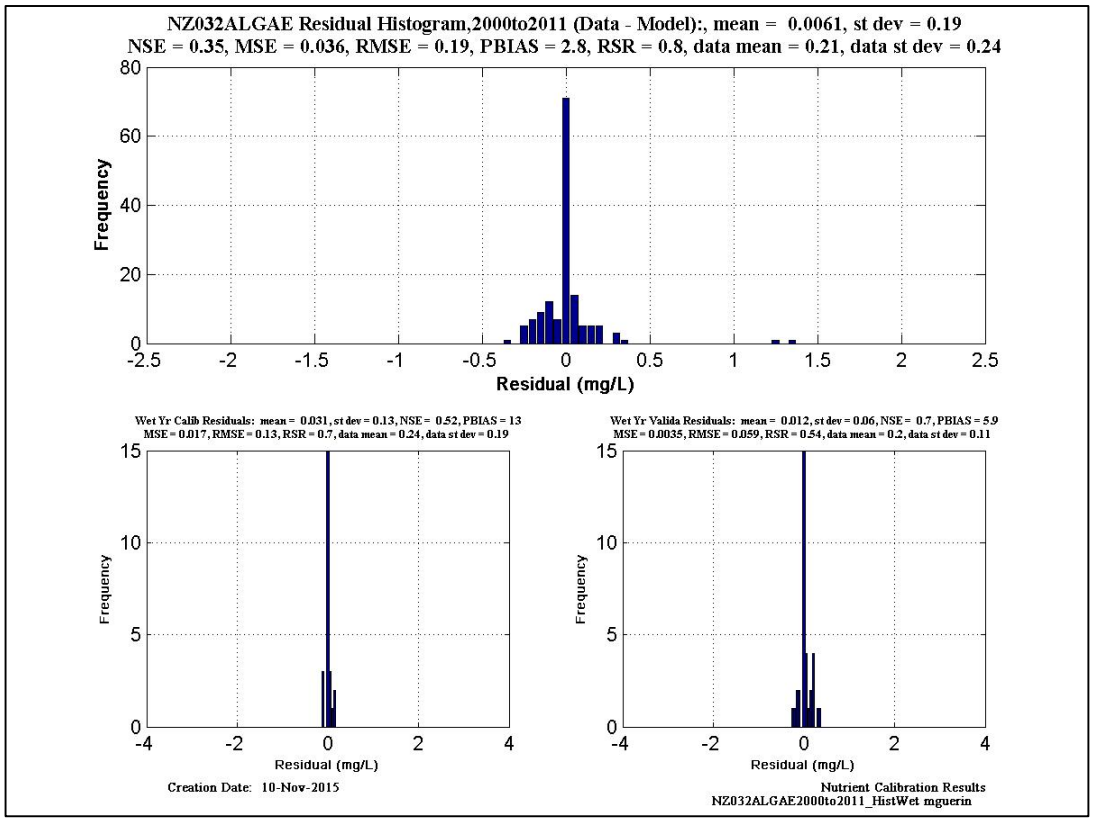

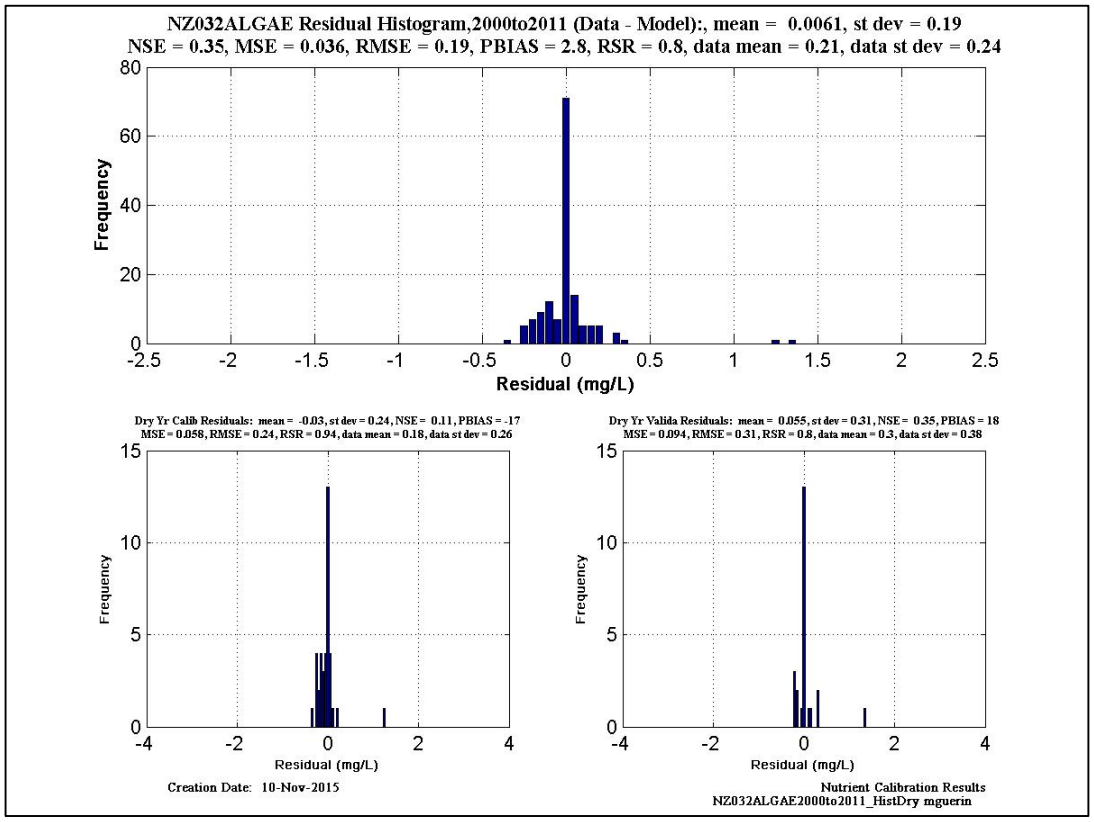

Figure 6-126 Algae histogram and statistics at EMP location NZ032.

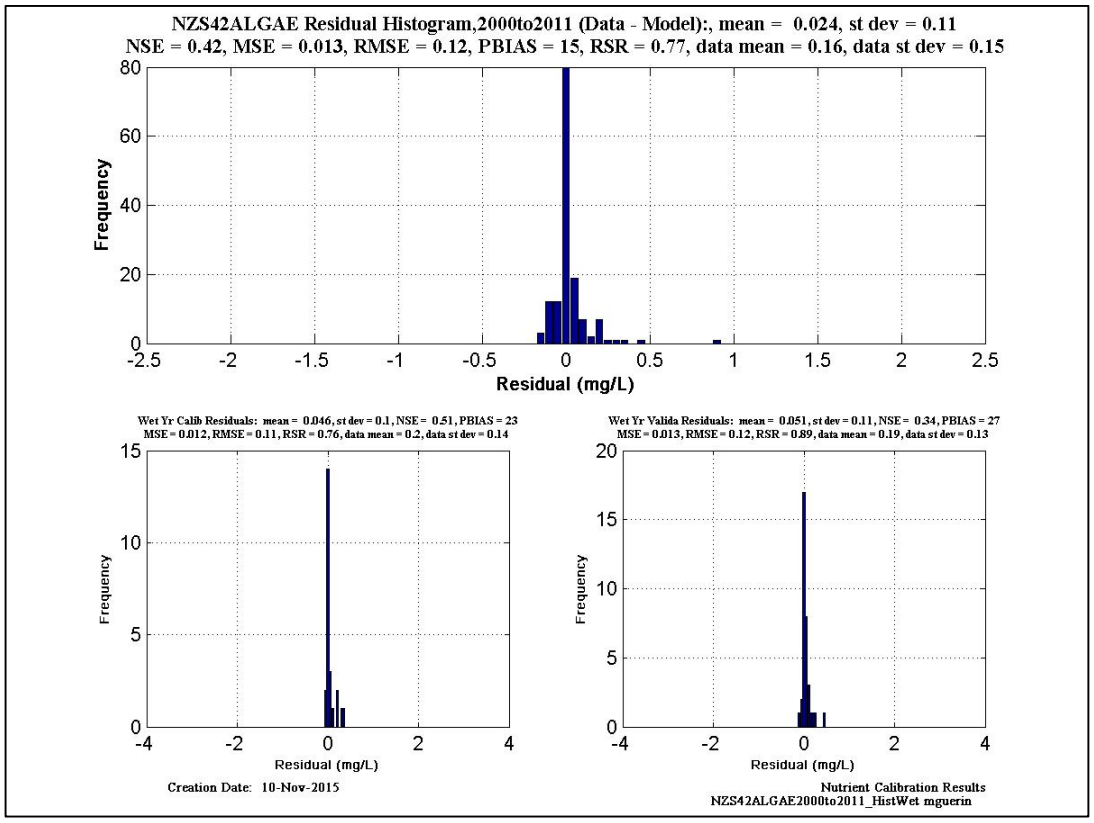

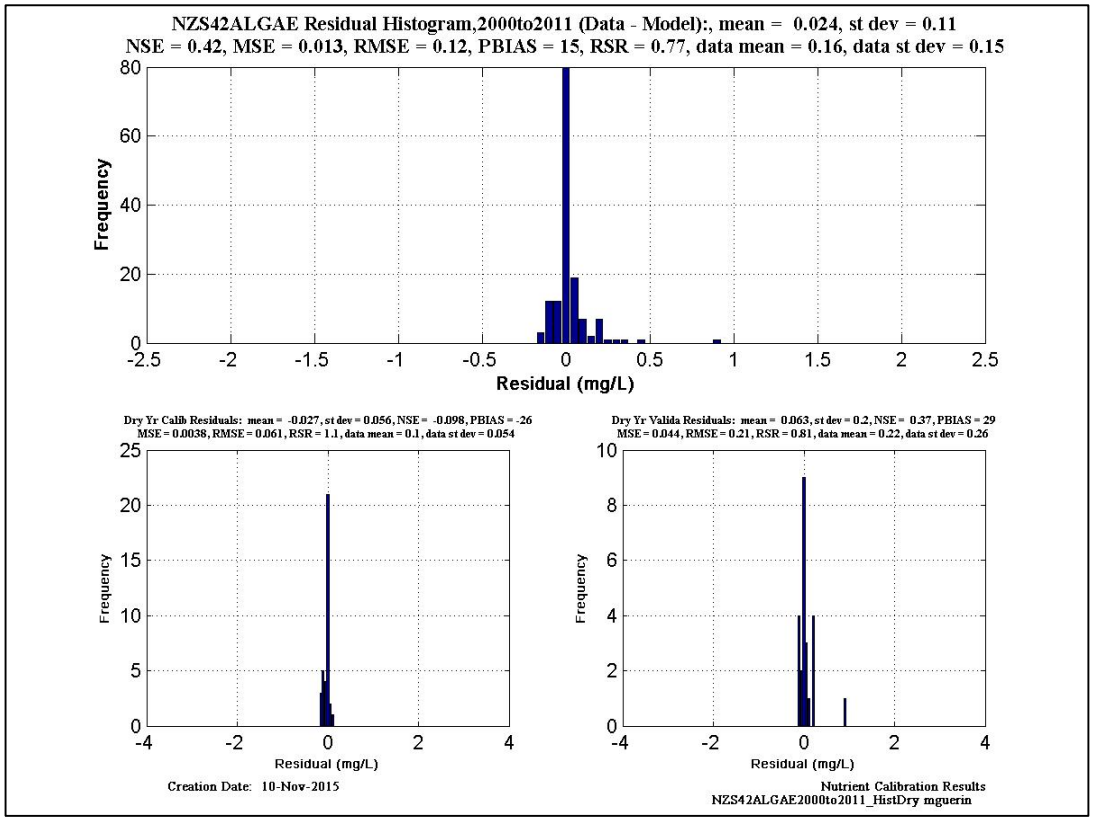

Figure 6-127 Algae histogram and statistics at EMP location NZS42.

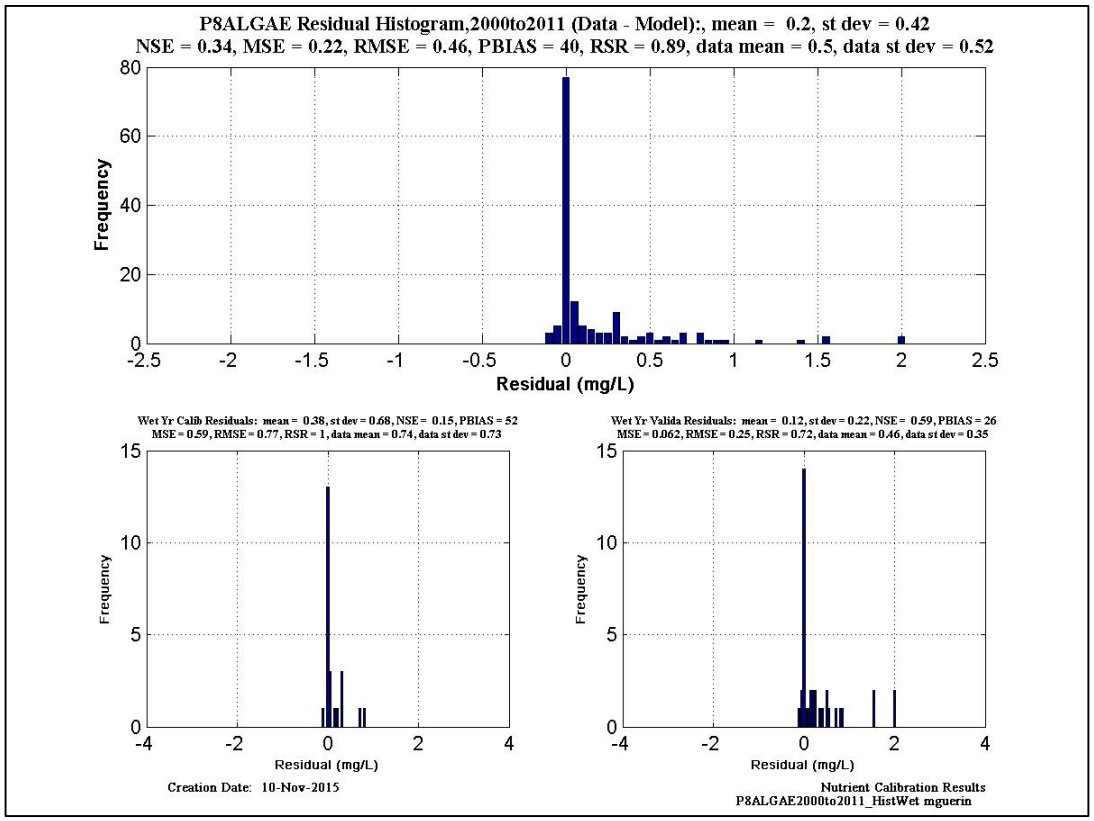

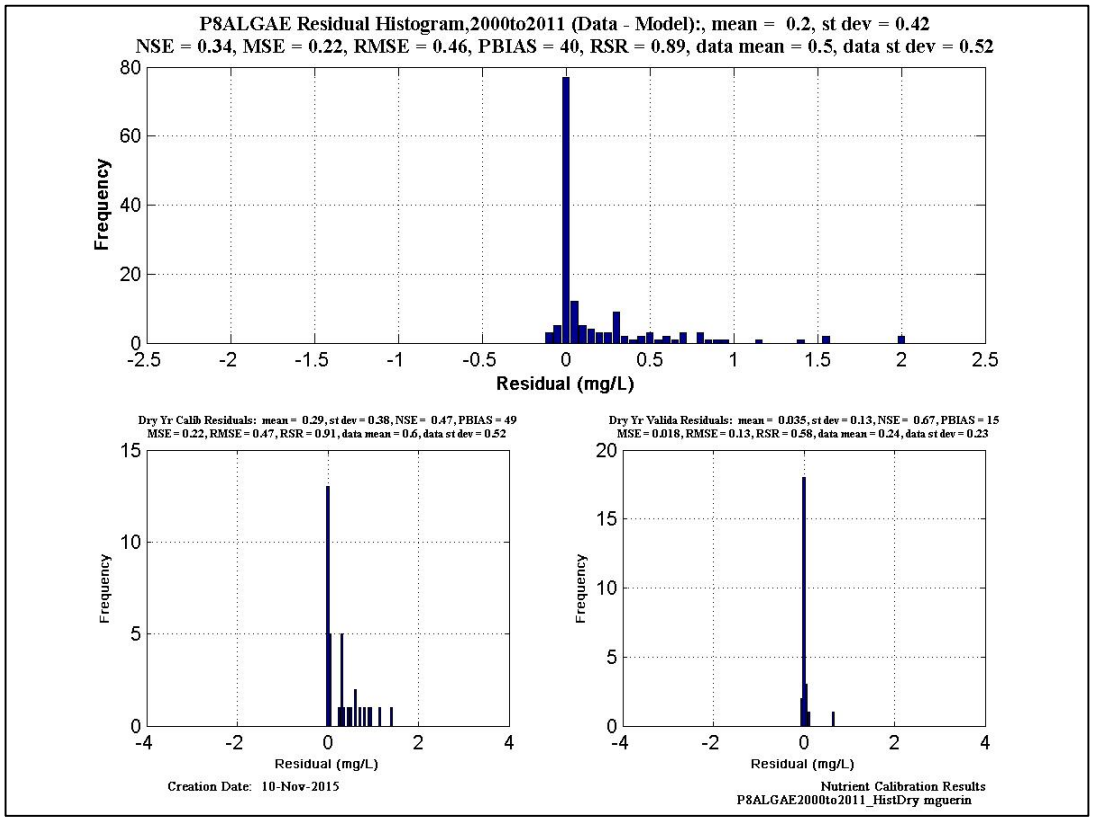

Figure 6-128 Algae histogram and statistics at EMP location P8.

6.12.4.2 Statistics for Modeled DO – EMP Data

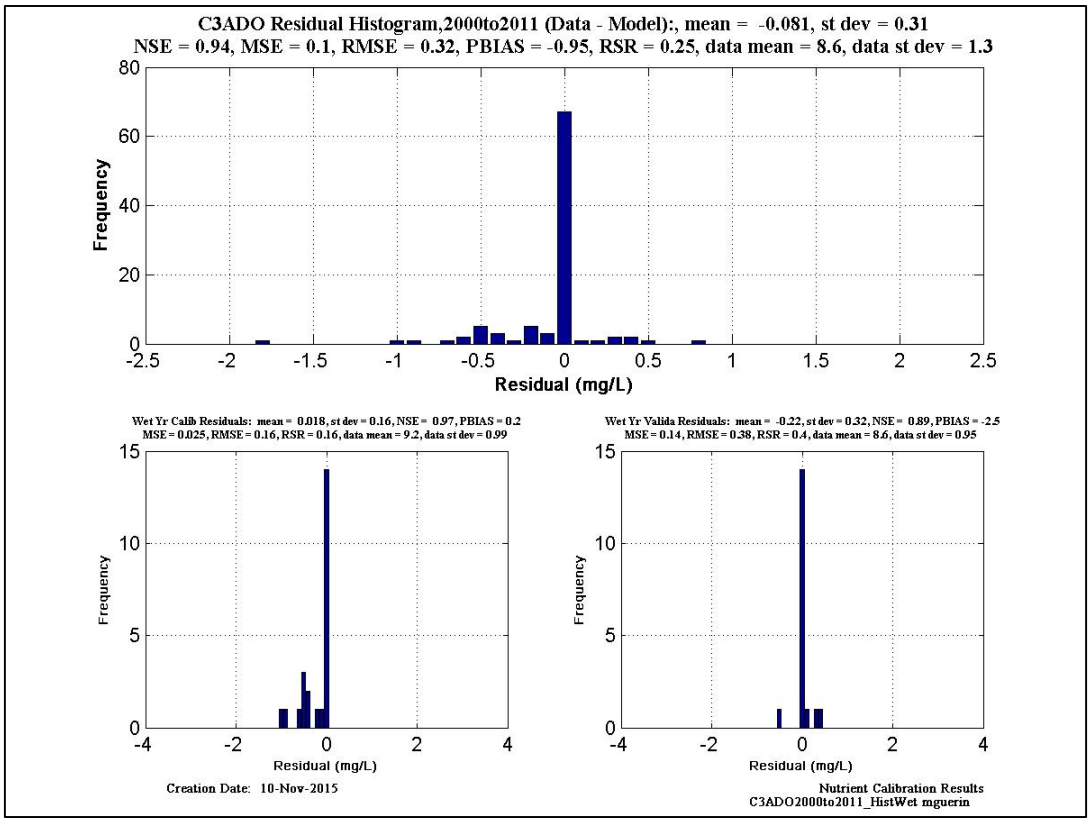

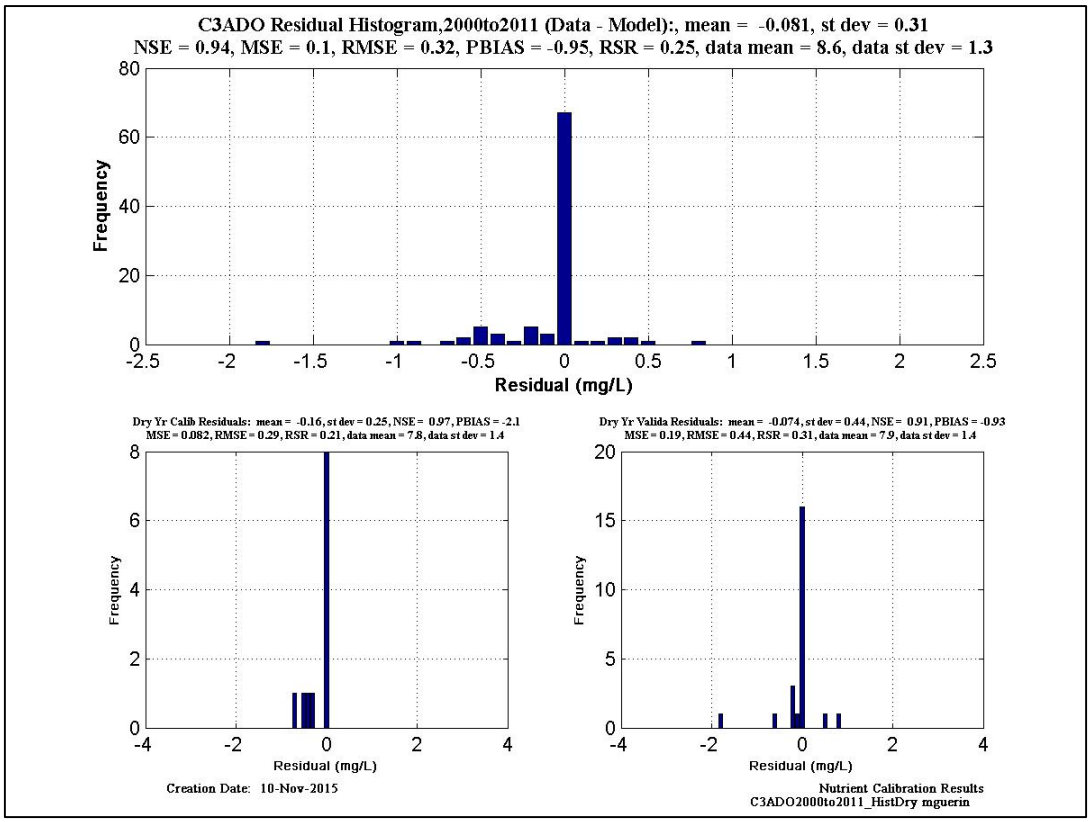

Figure 6-129 DO histogram and statistics at EMP location C3A.

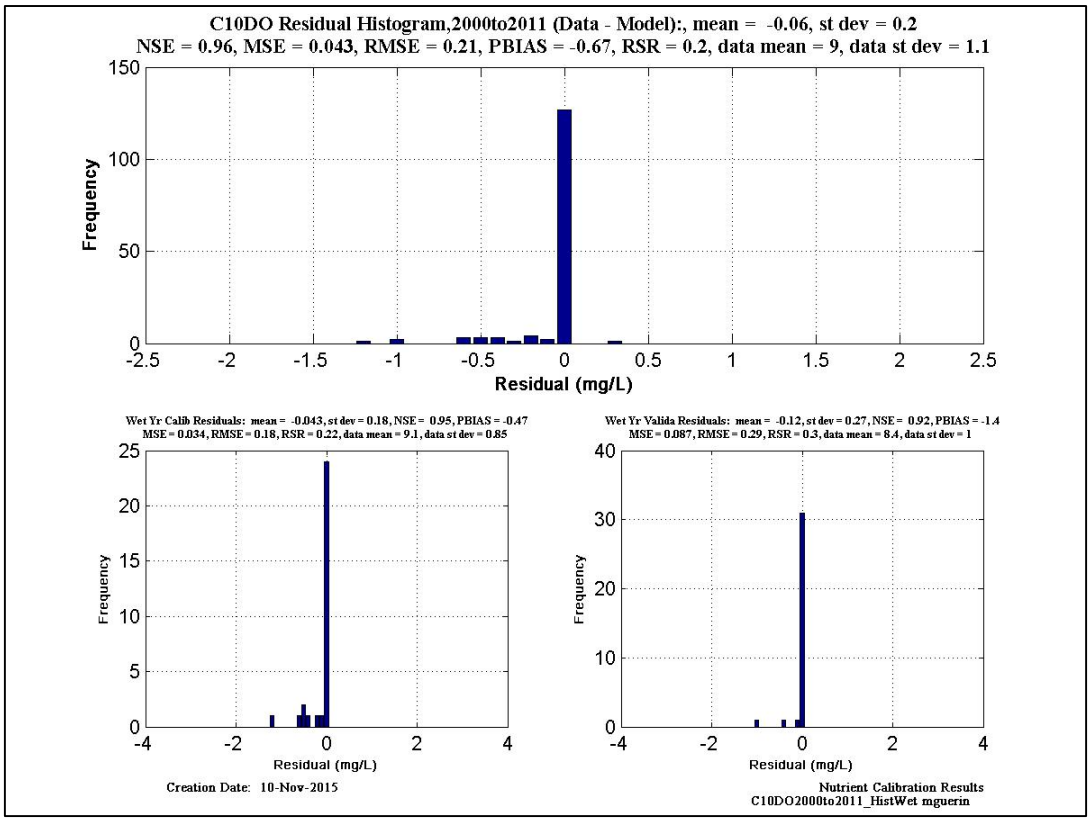

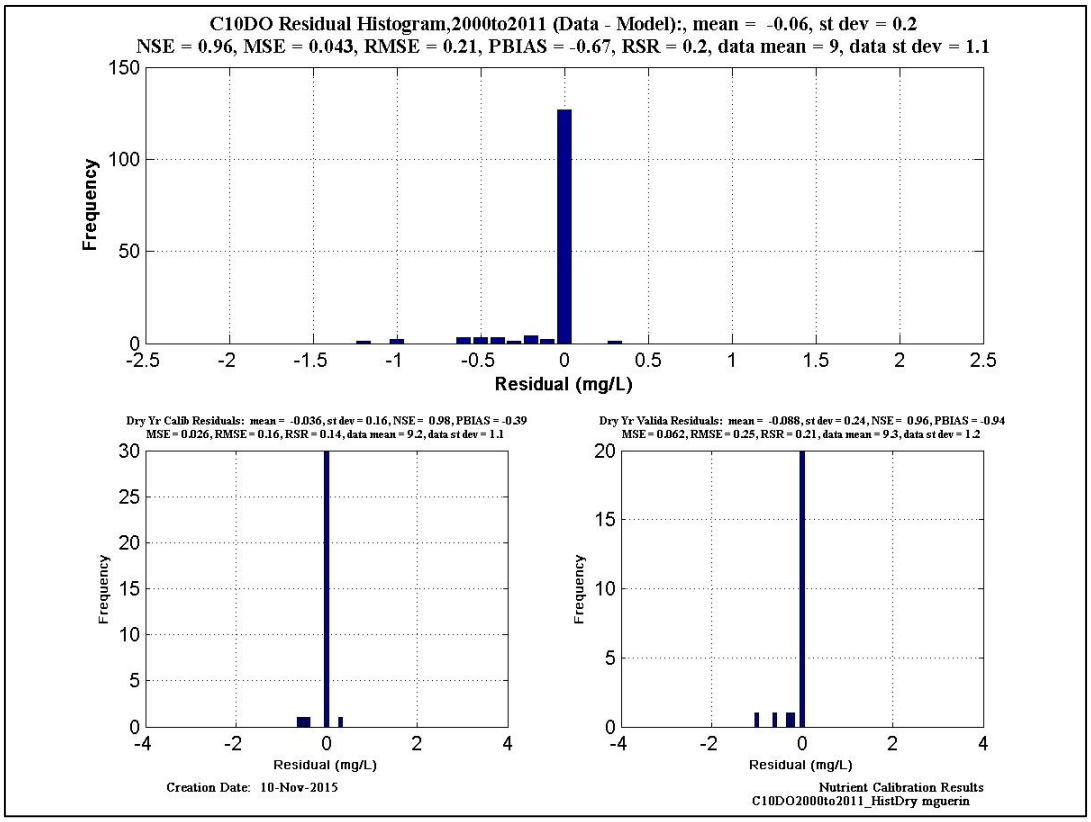

Figure 6-130 DO histogram and statistics at EMP location C3A. C10.

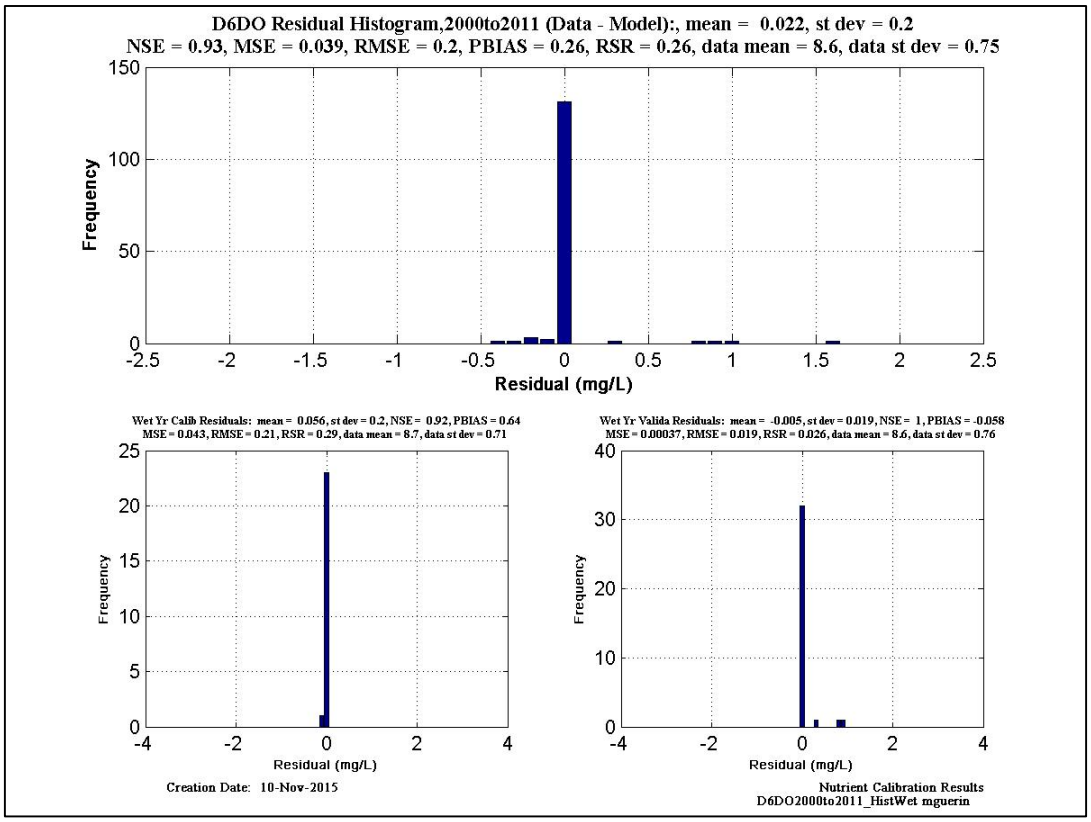

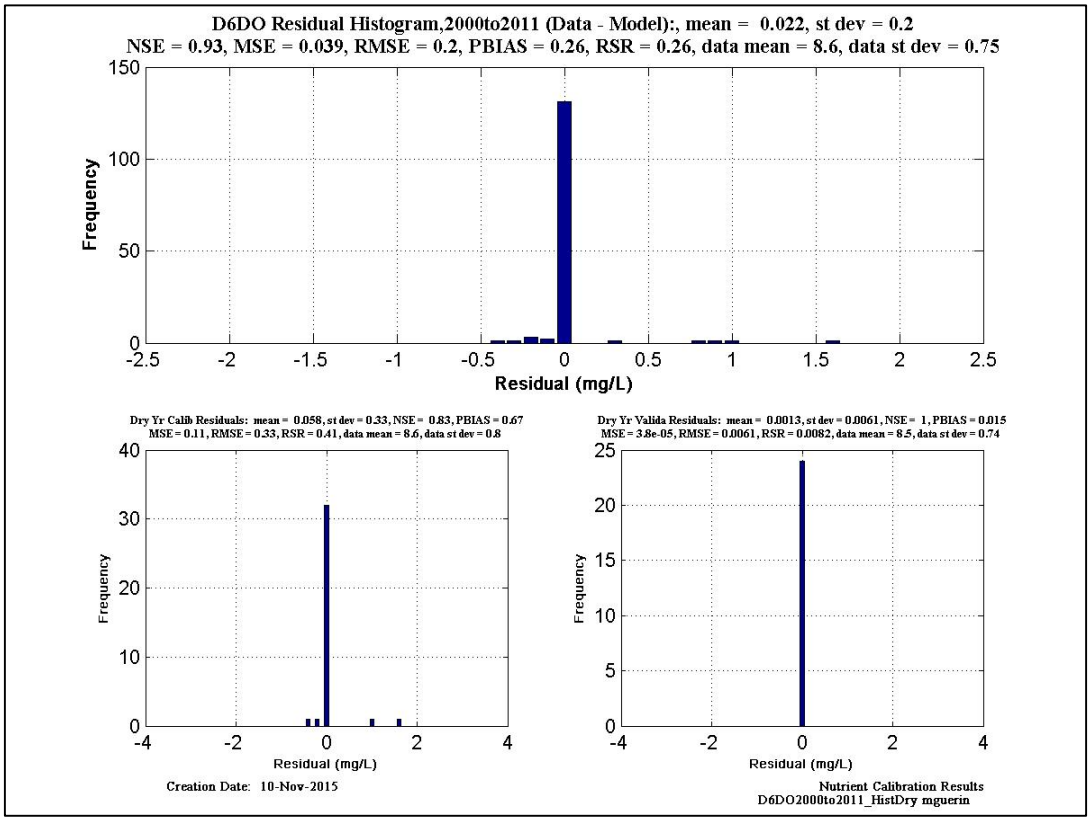

Figure 6-131 DO histogram and statistics at EMP location D6.

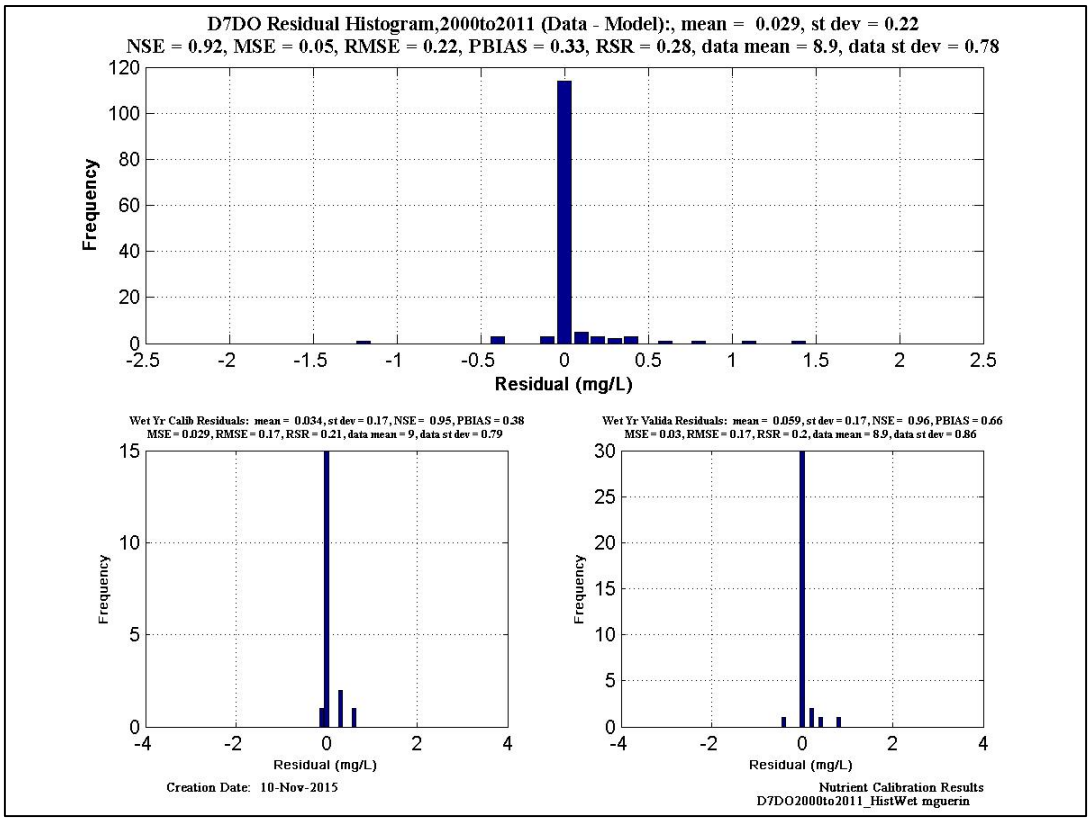

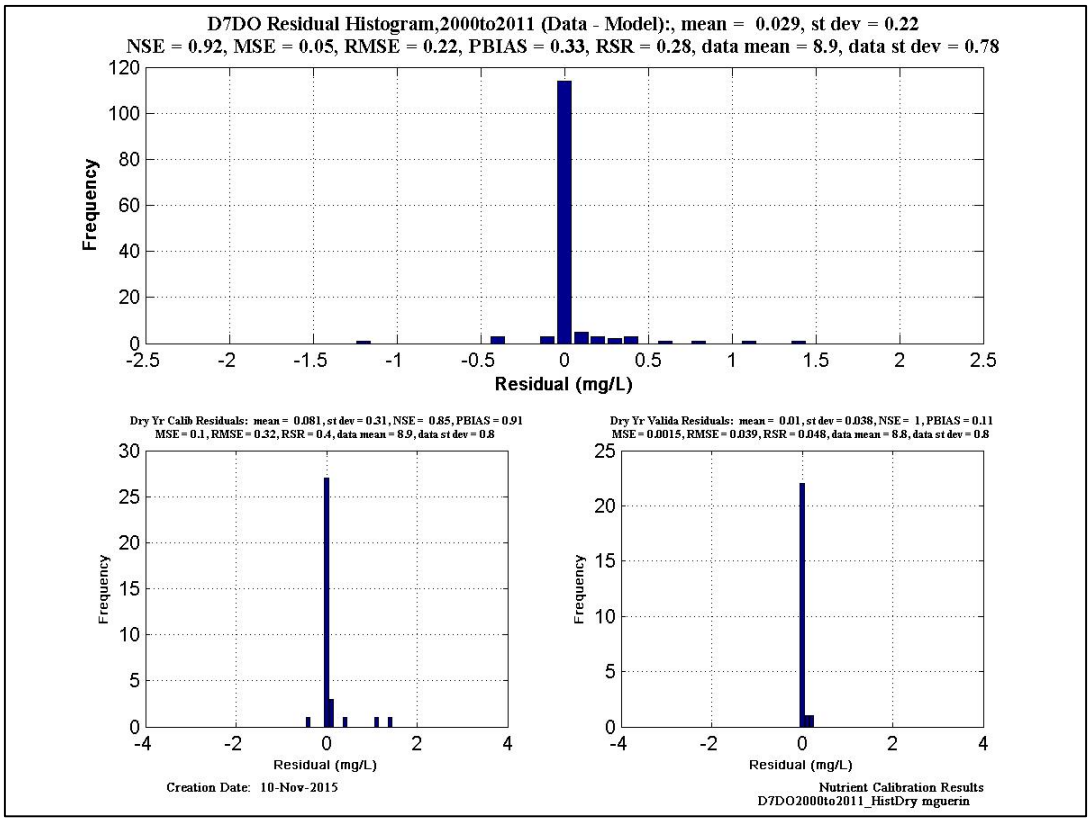

Figure 6-132 DO histogram and statistics at EMP location D7.

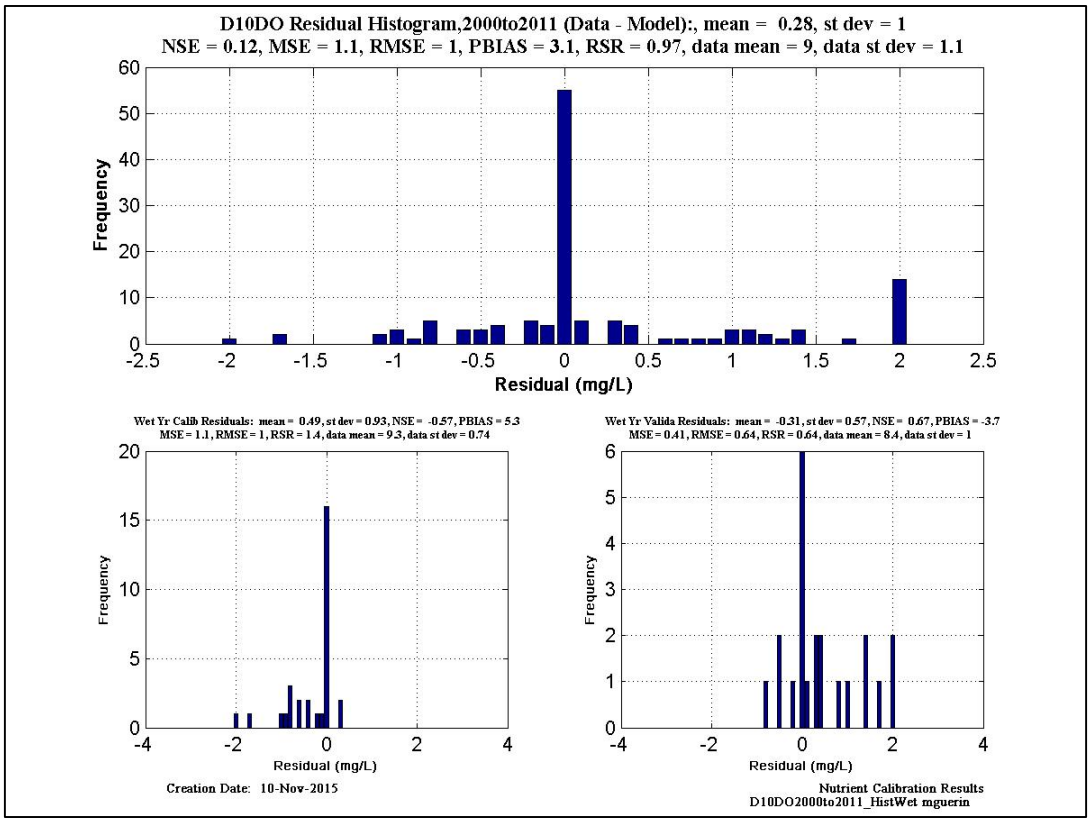

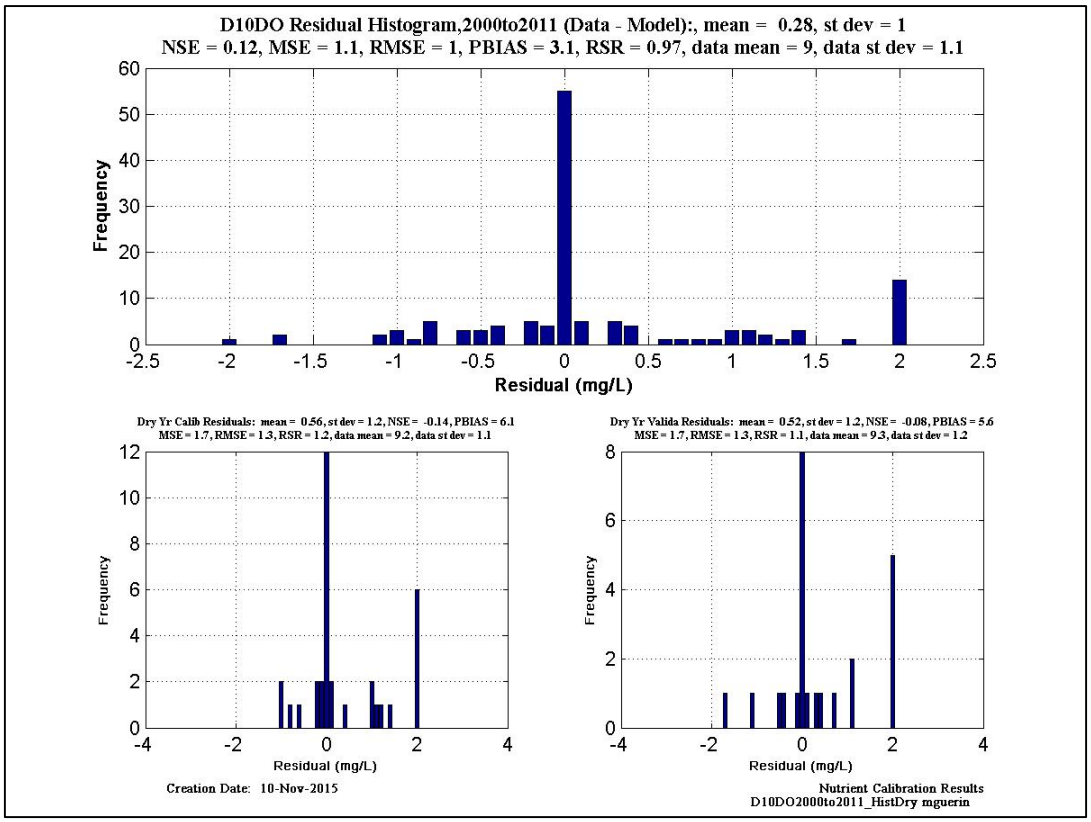

Figure 6-133 DO histogram and statistics at EMP location D10.

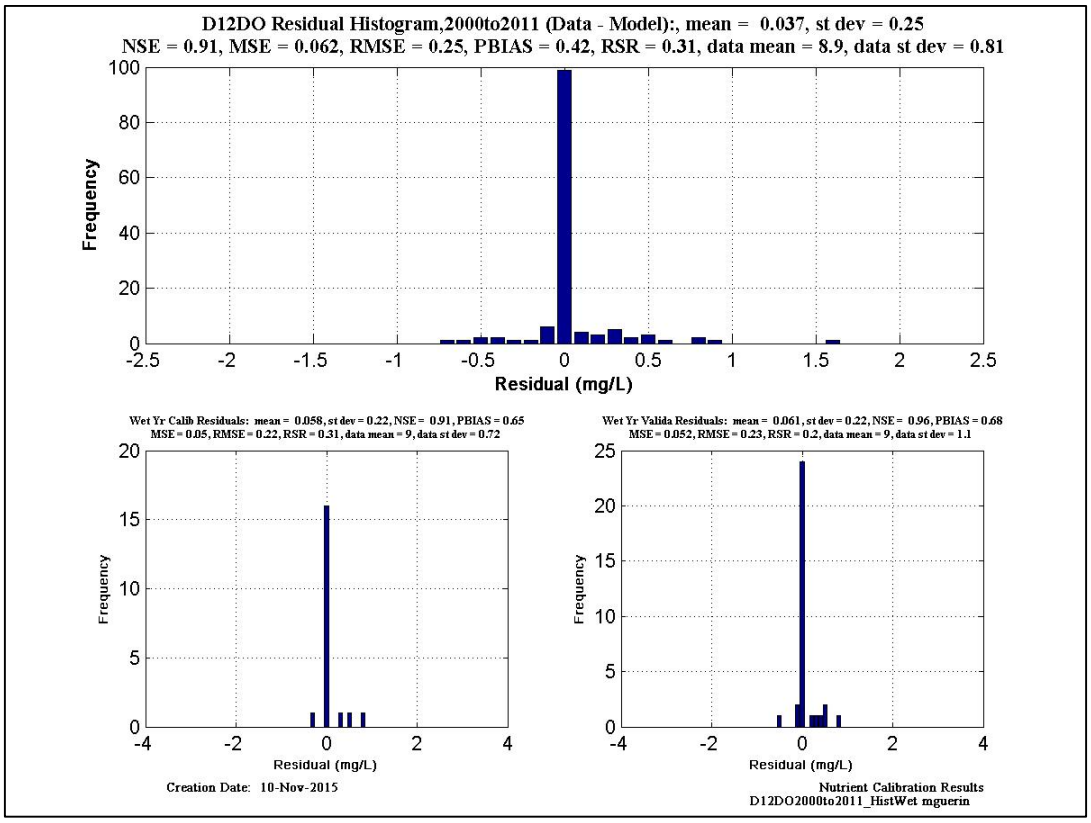

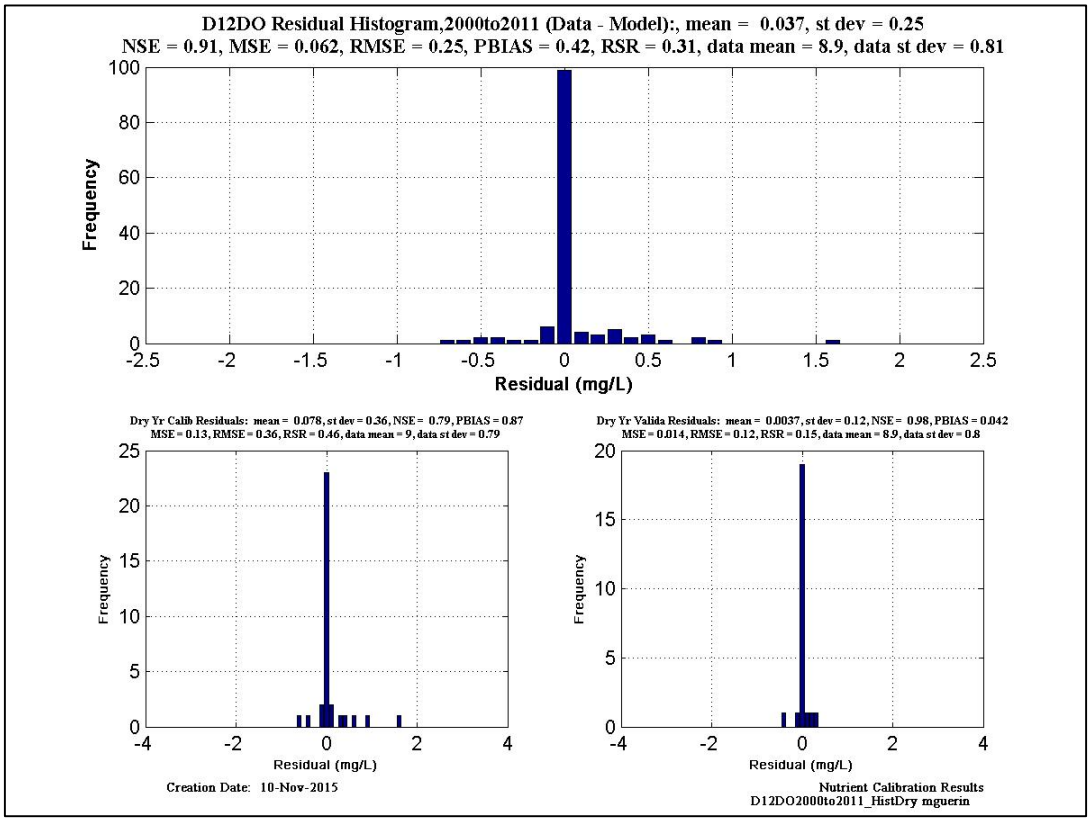

Figure 6-134 DO histogram and statistics at EMP location D12.

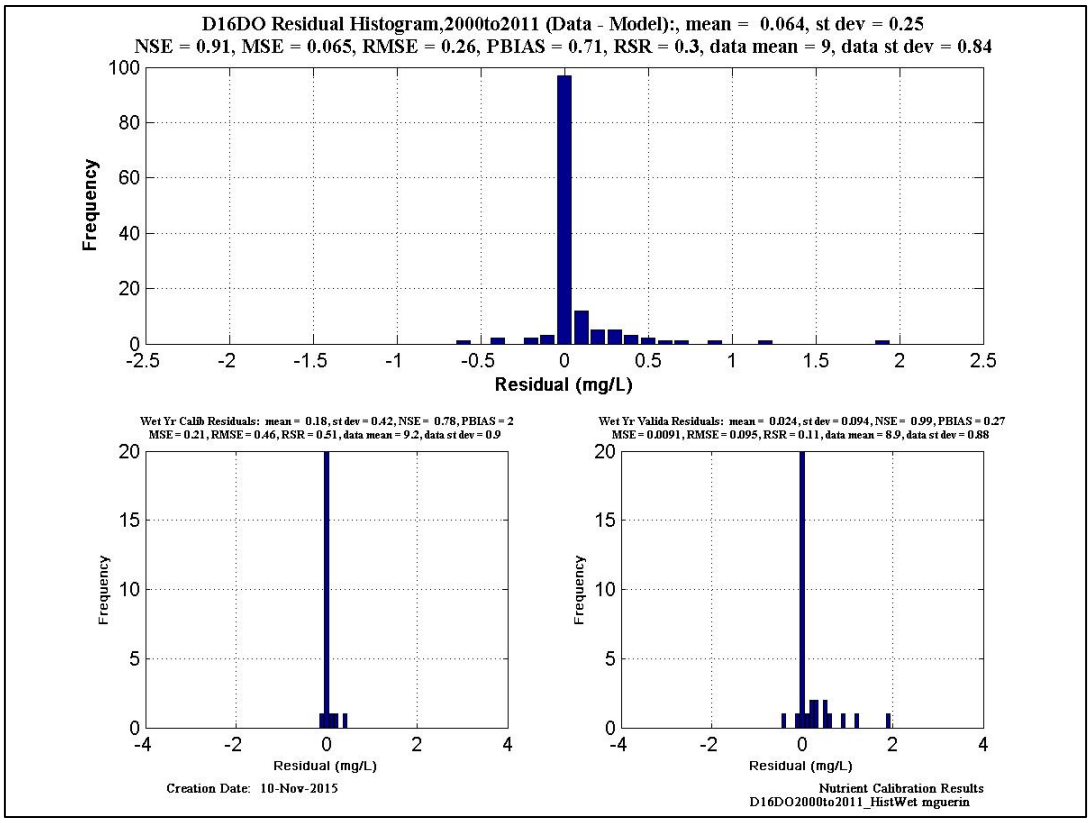

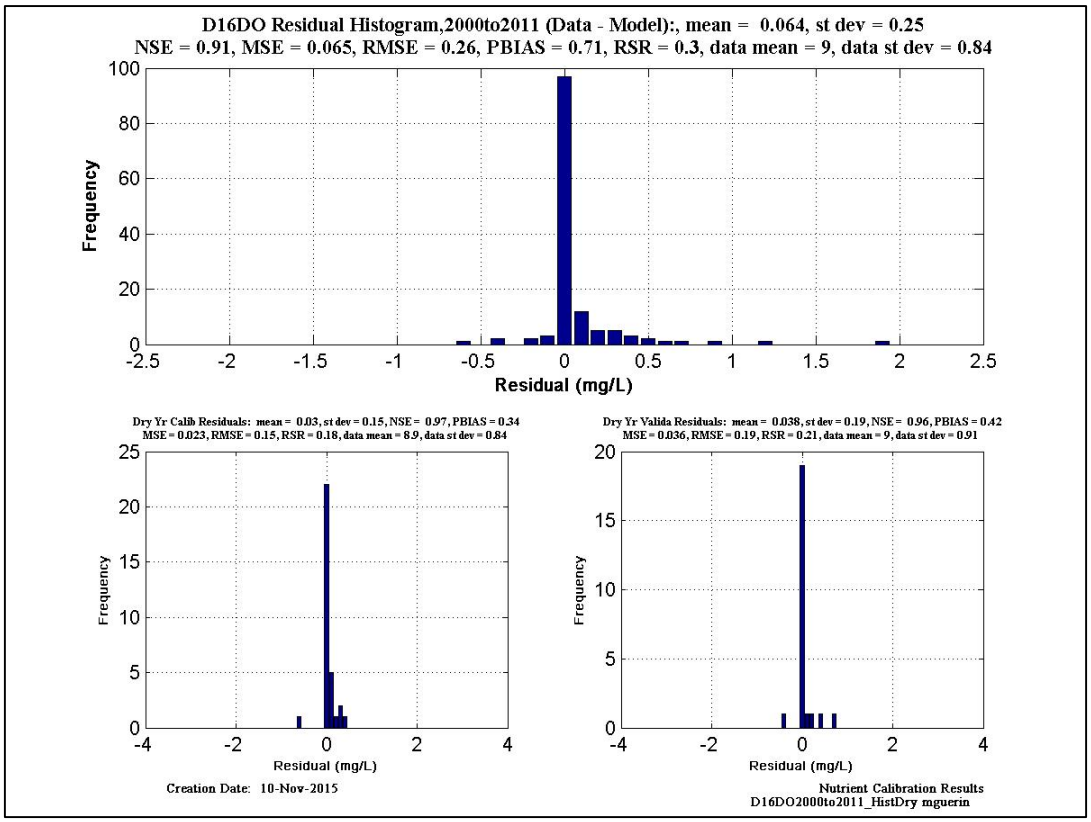

Figure 6-135 DO histogram and statistics at EMP location D16.

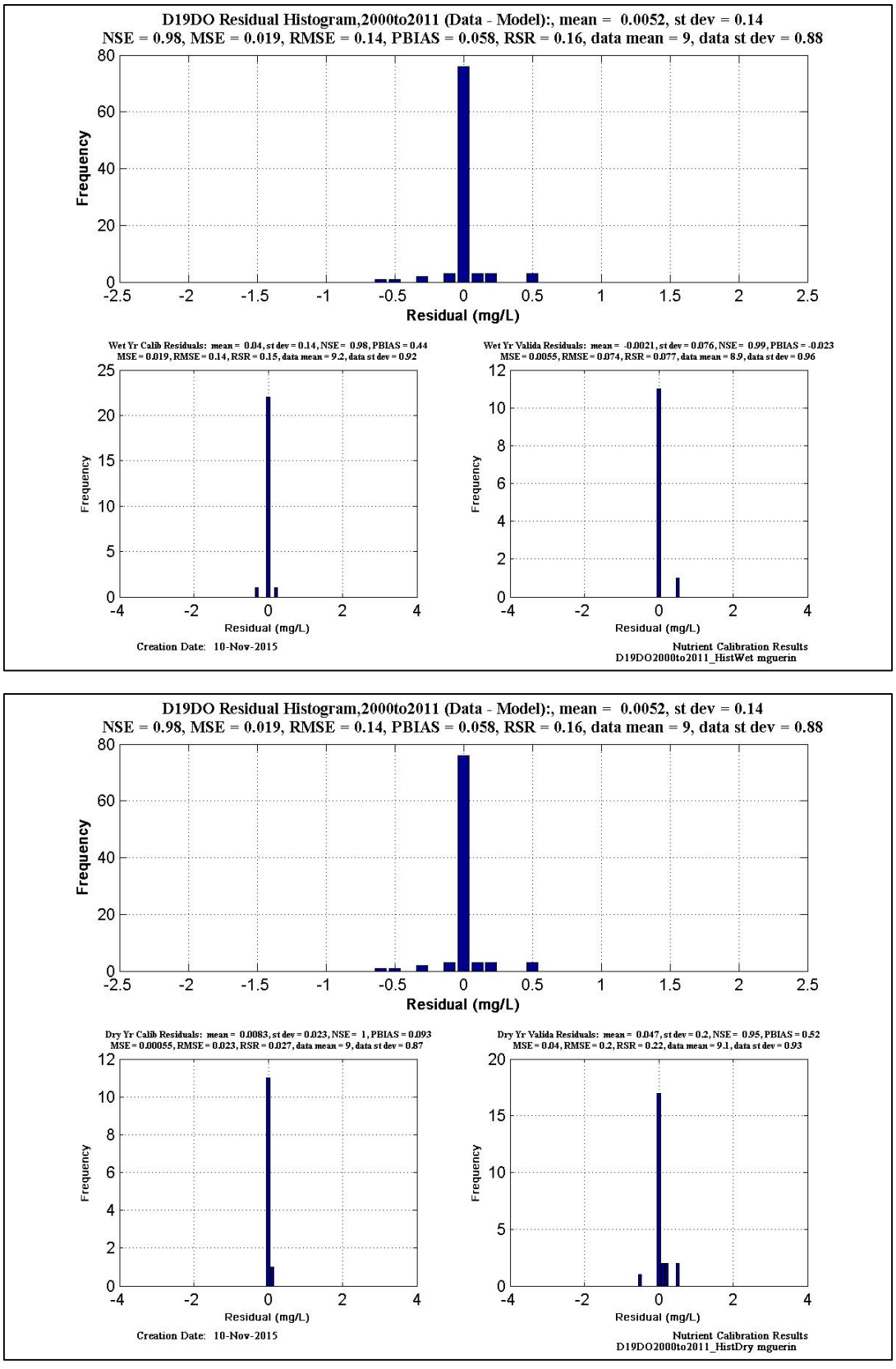

Figure 6-136 DO histogram and statistics at EMP location D19.

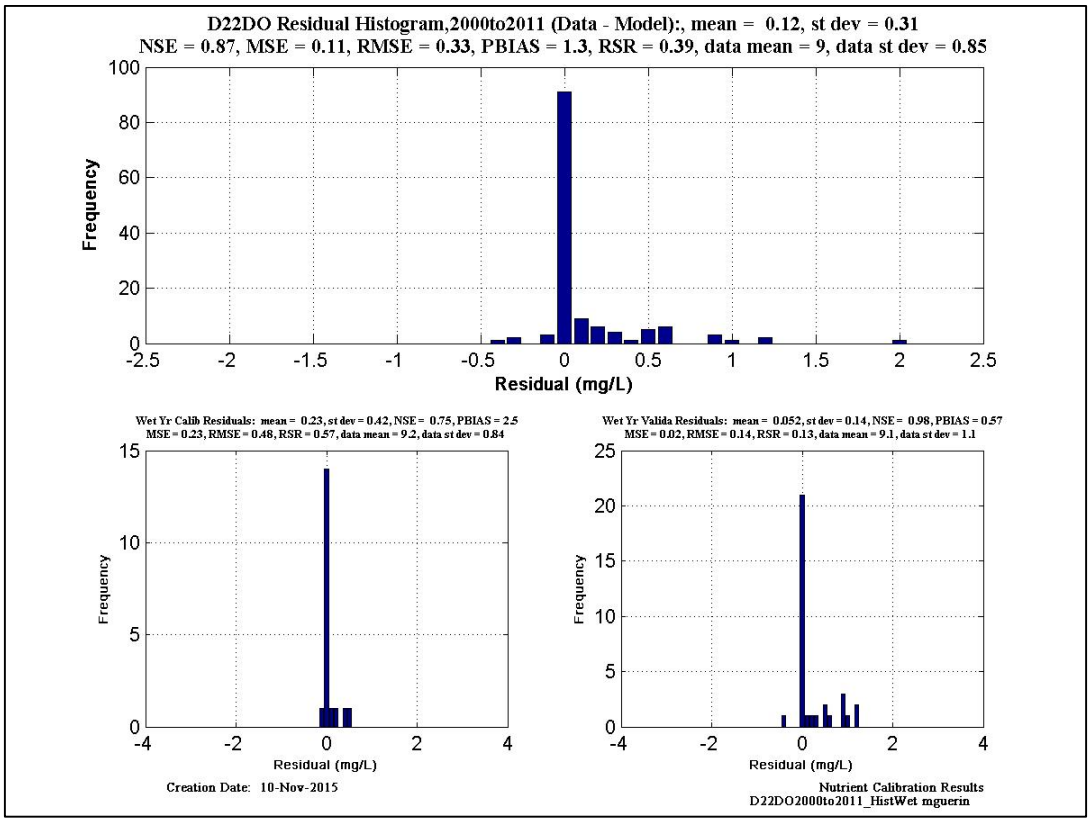

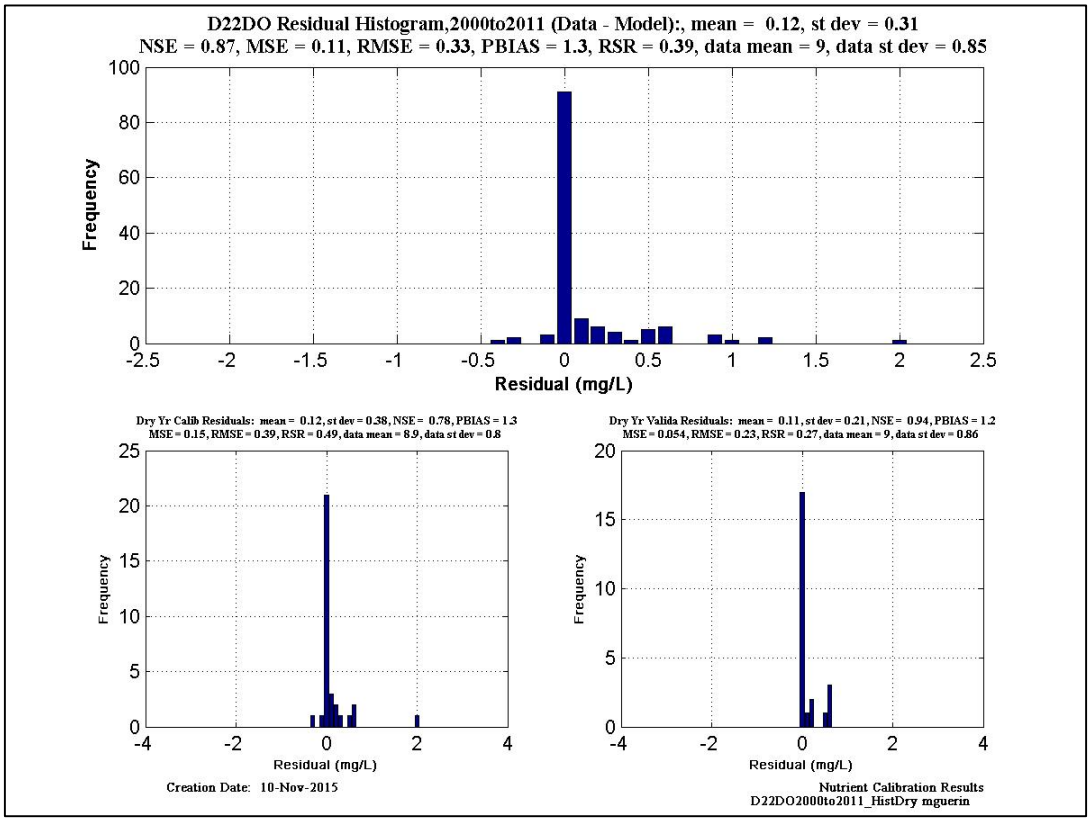

Figure 6-137 DO histogram and statistics at EMP location D22.

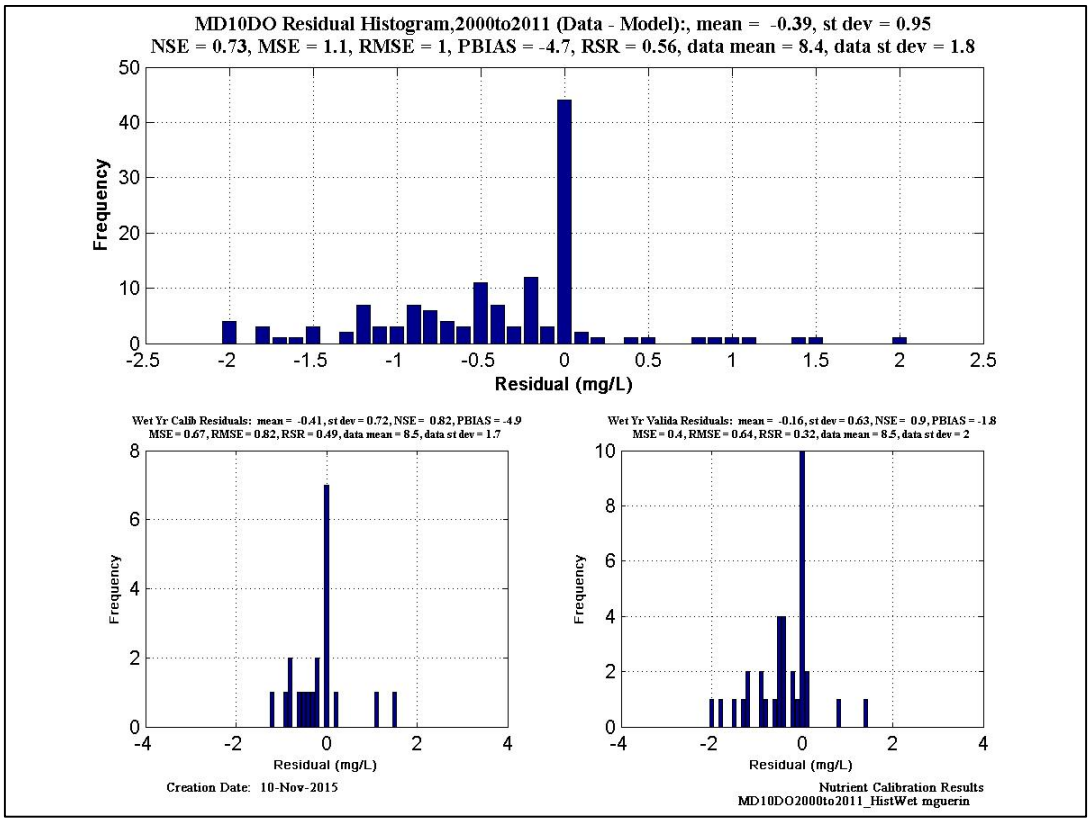

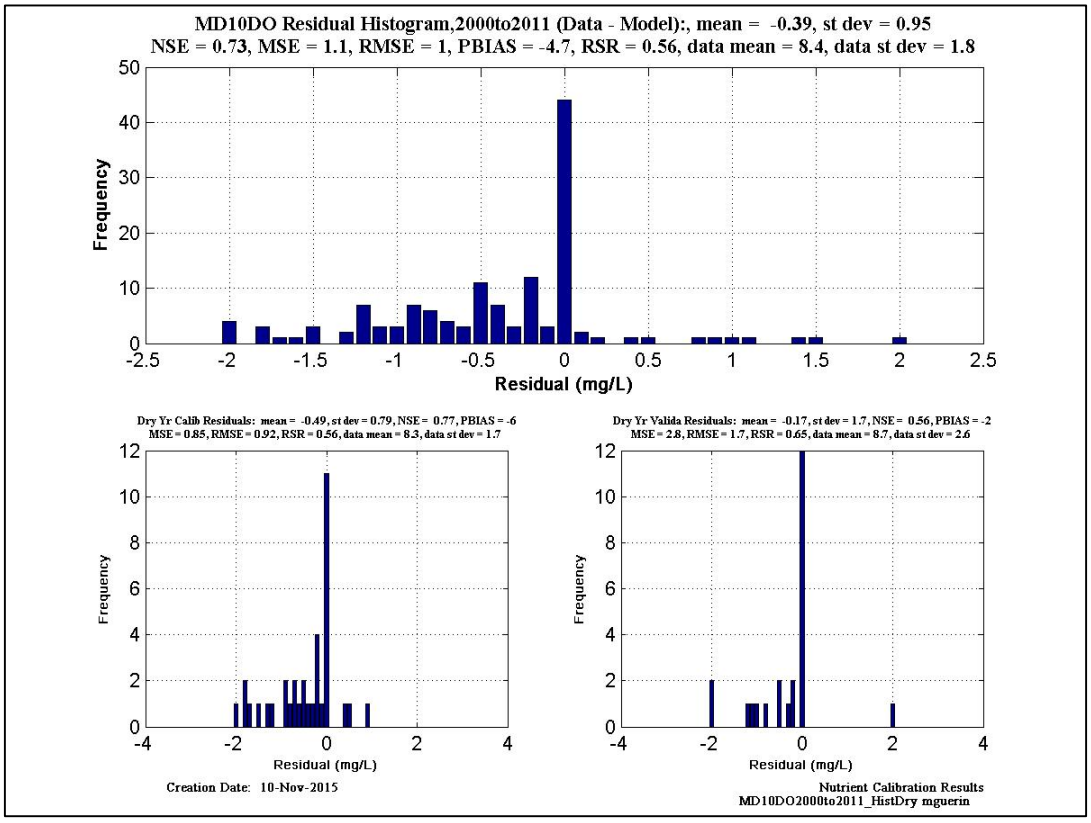

Figure 6-138 DO histogram and statistics at EMP location MD10.

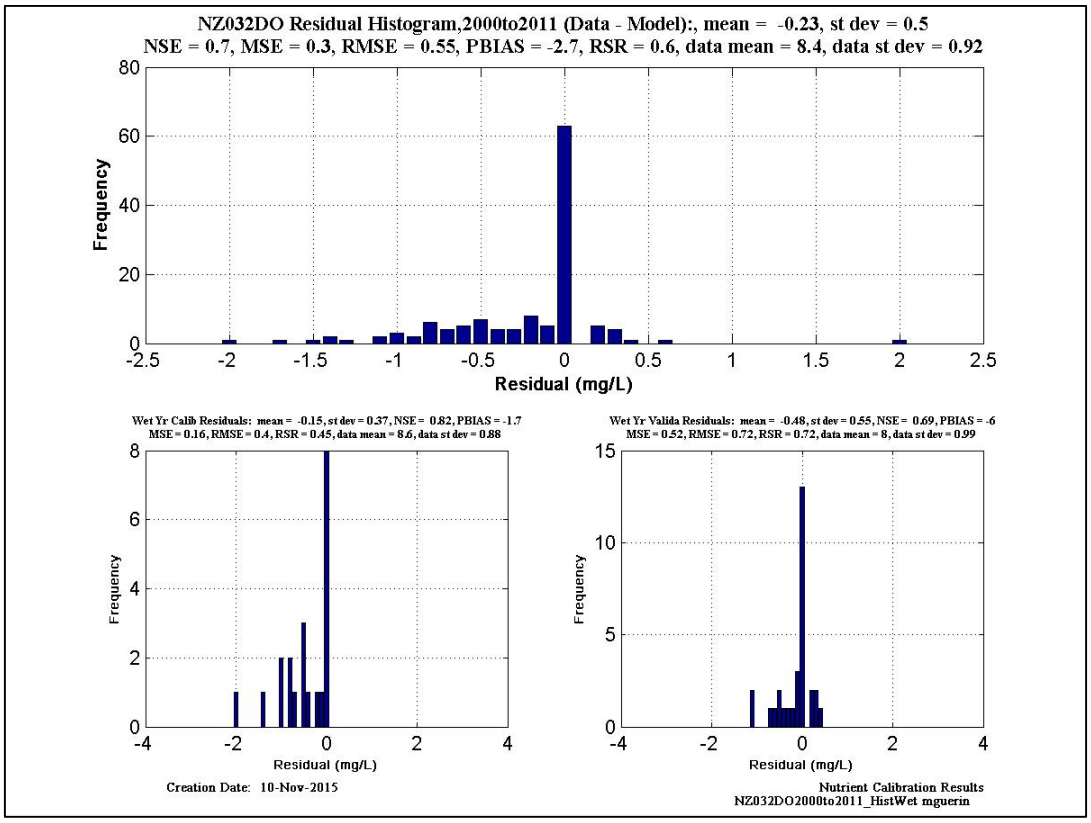

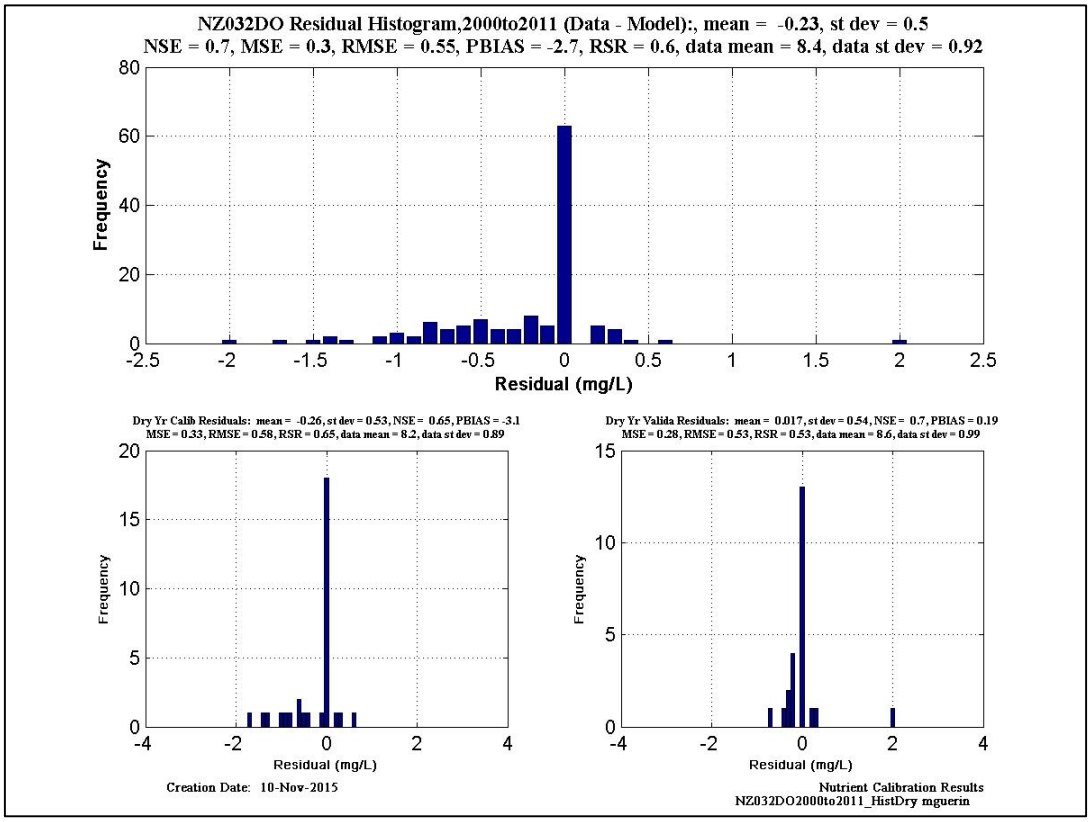

Figure 6-139 DO histogram and statistics at EMP location NZ032.

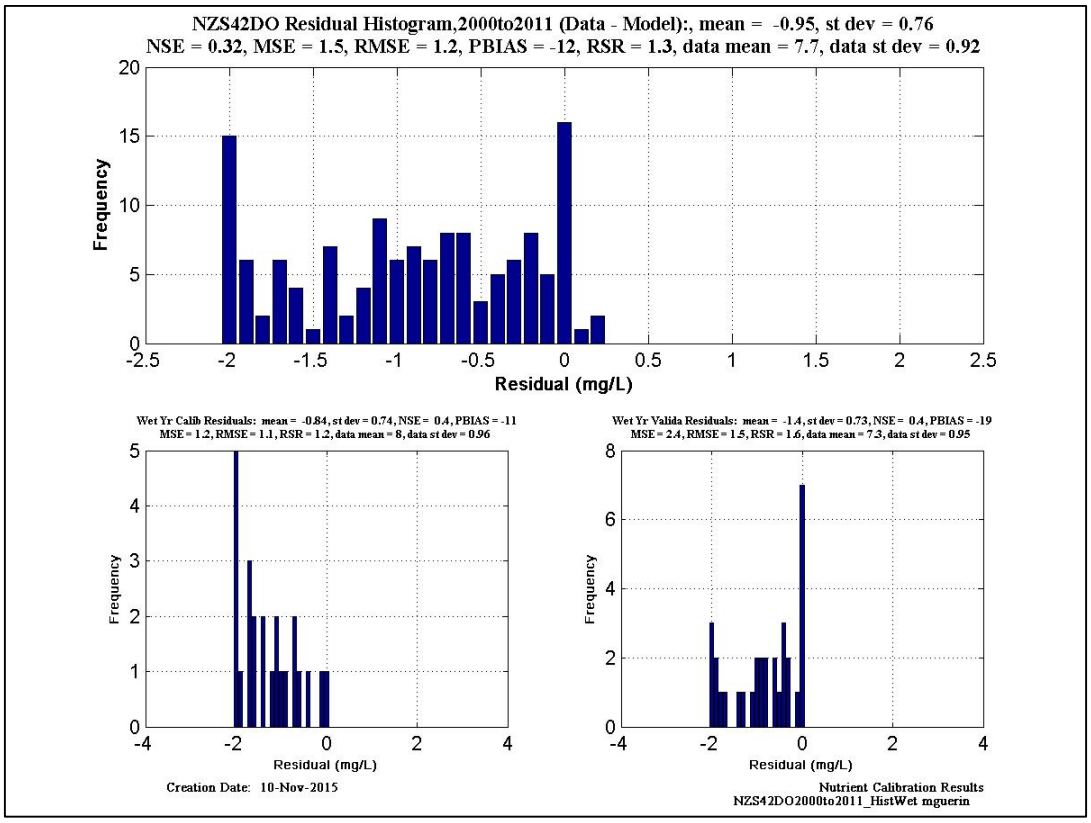

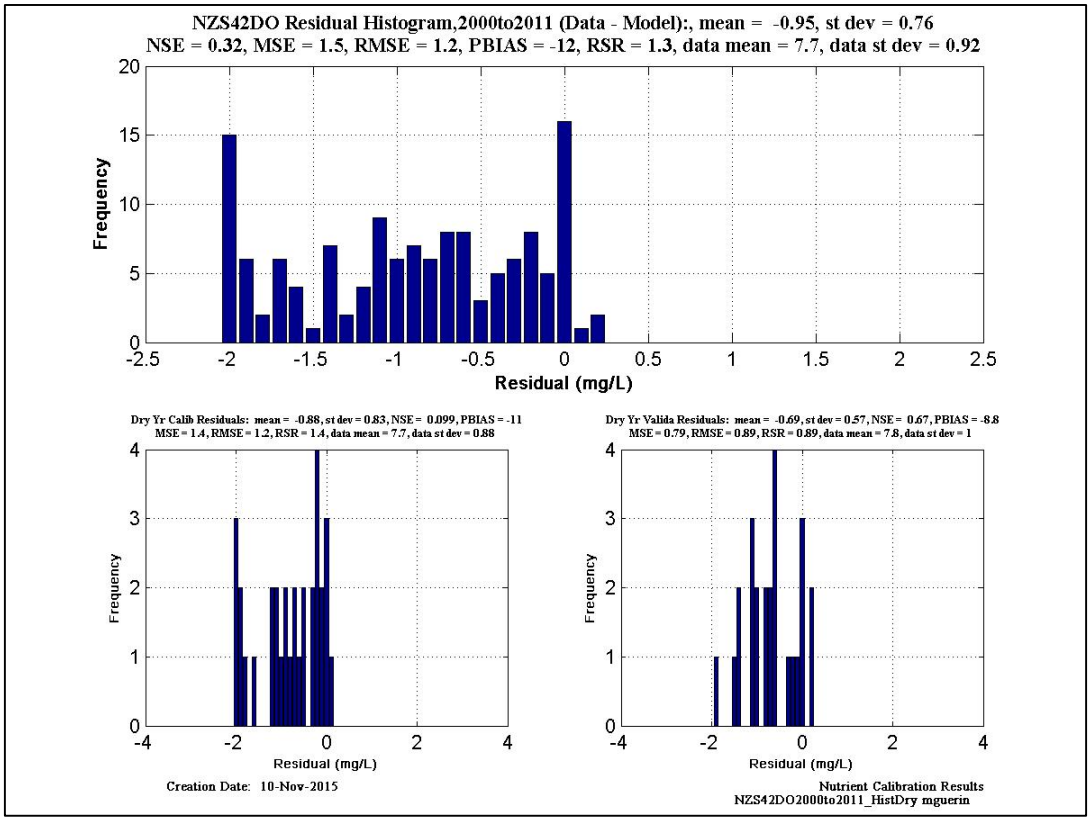

Figure 6-140 DO histogram and statistics at EMP location NZS42.

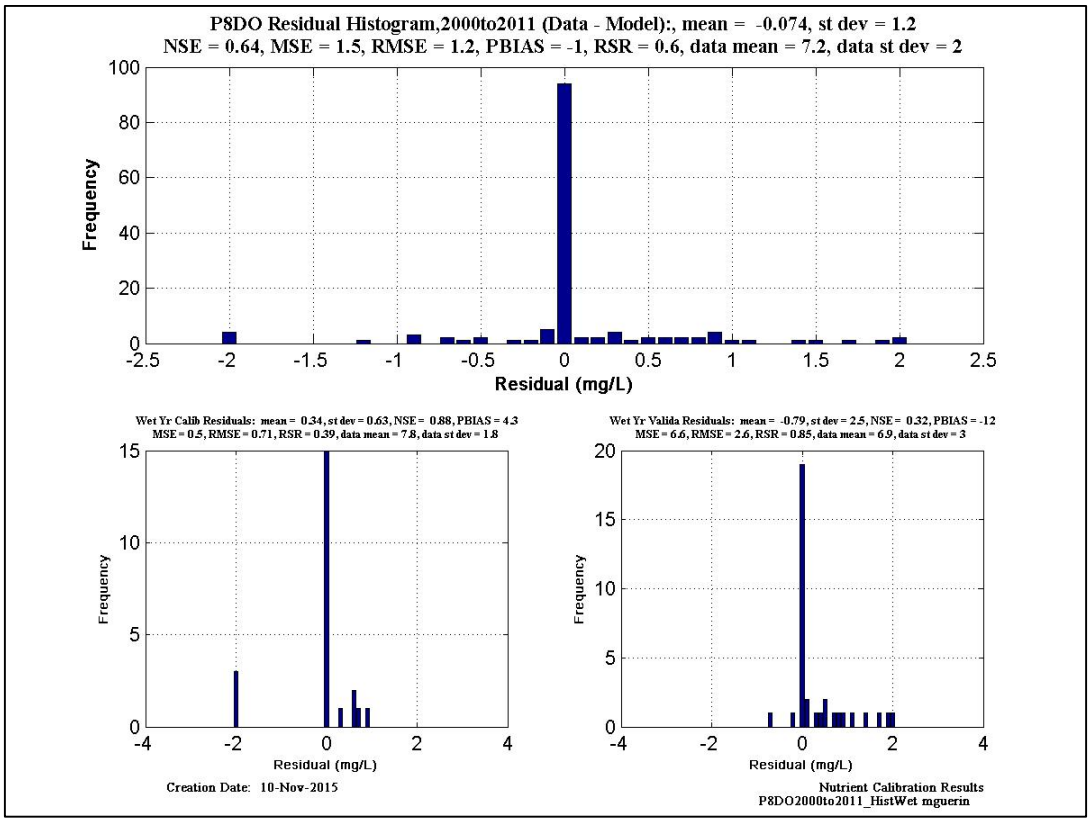

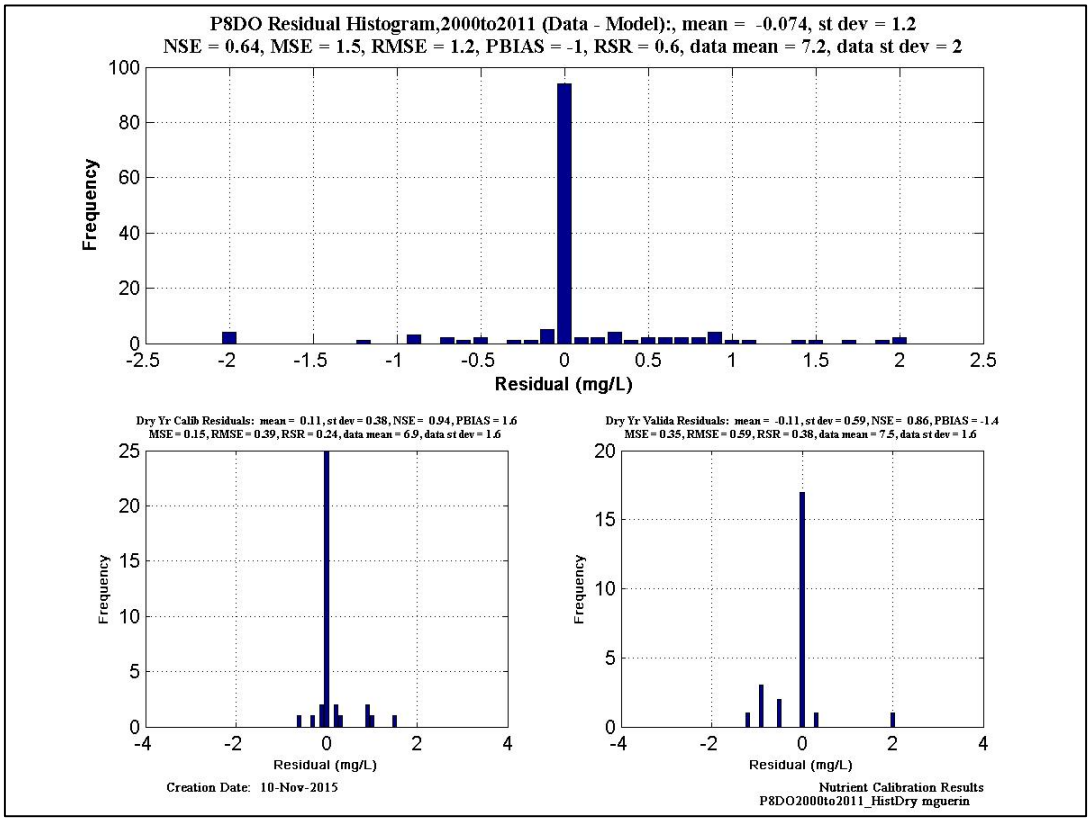

Figure 6-141 DO histogram and statistics at EMP location P8.

6.12.4.3 Statistics for Modeled NH_3-N – EMP Data

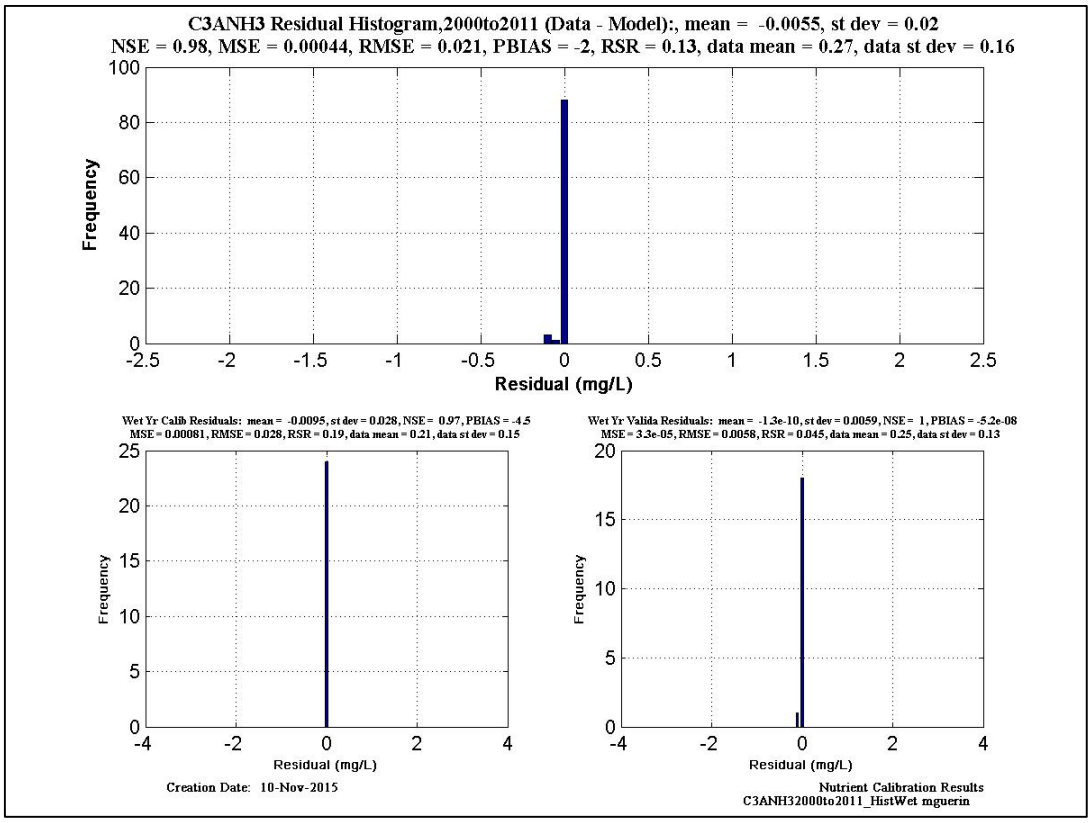

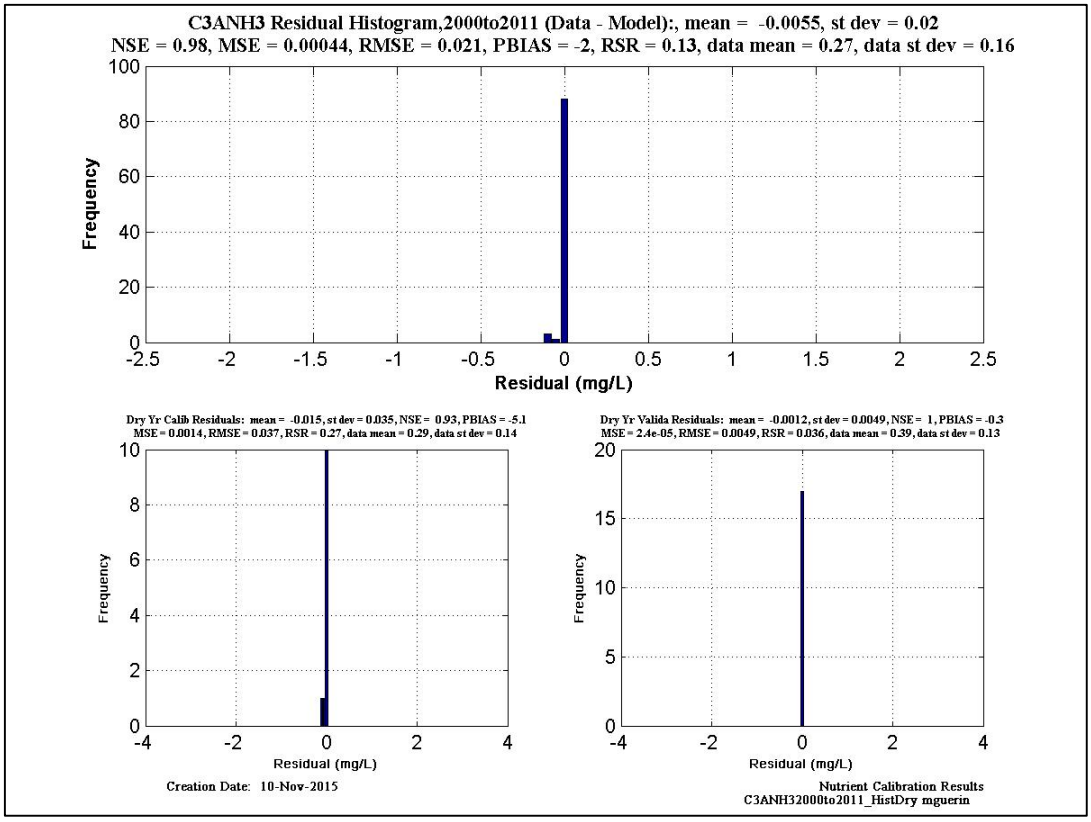

Figure 6-142 NH_3-N histogram and statistics at EMP location C3A.

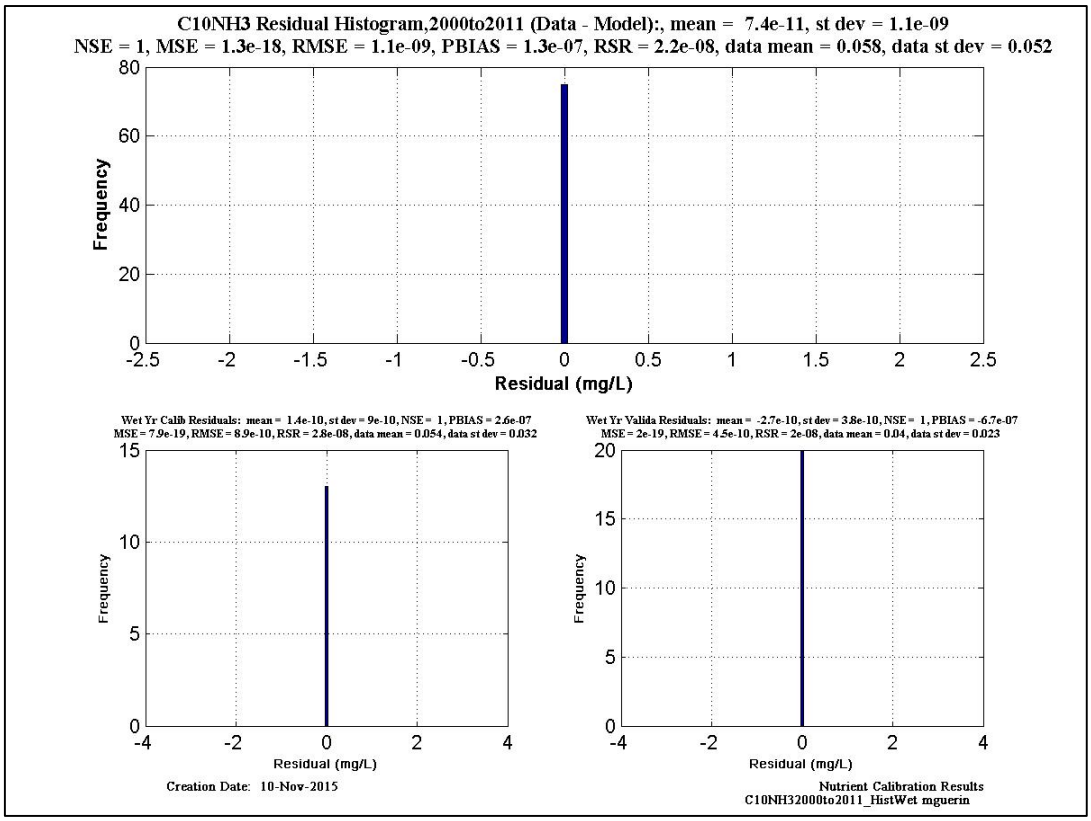

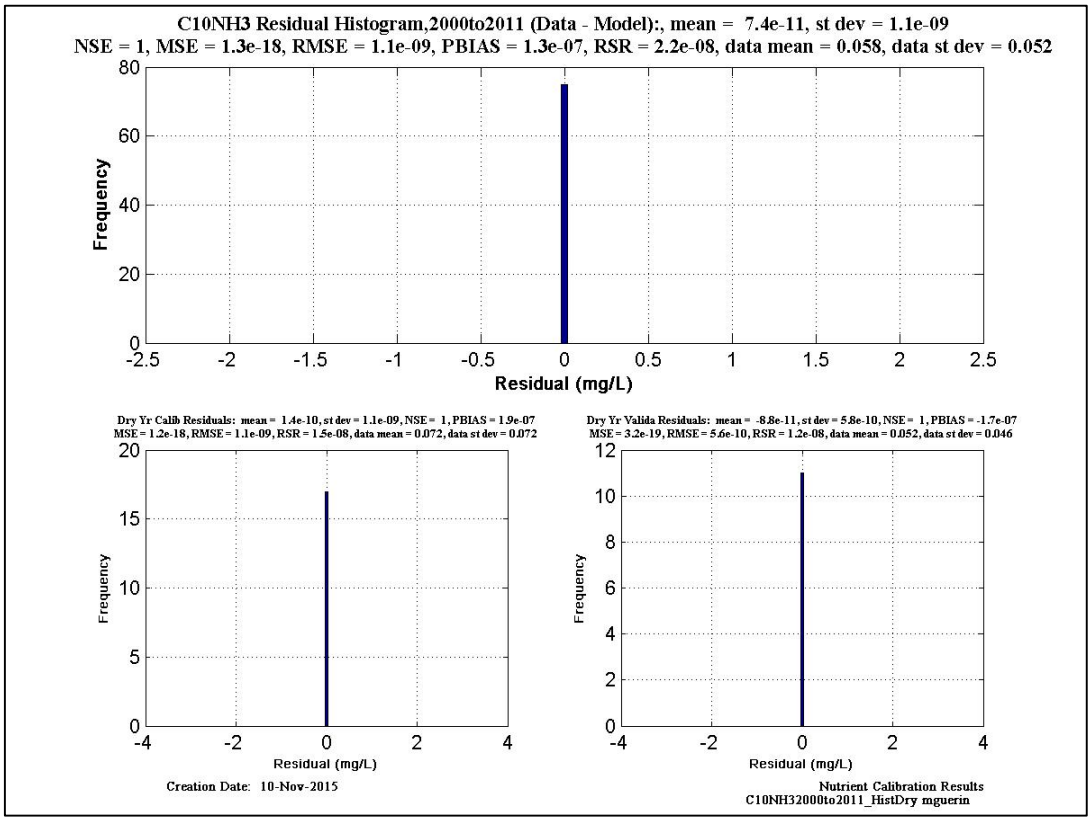

Figure 6-143 NH_3-N histogram and statistics at EMP location C10.

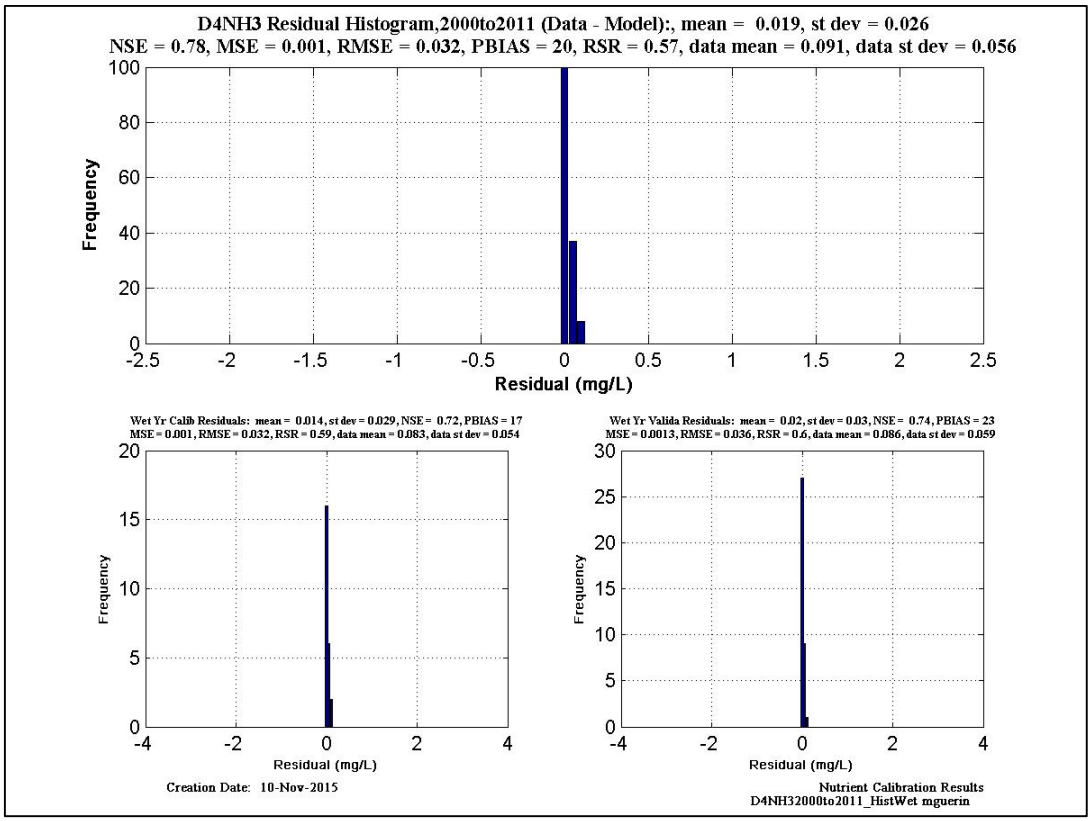

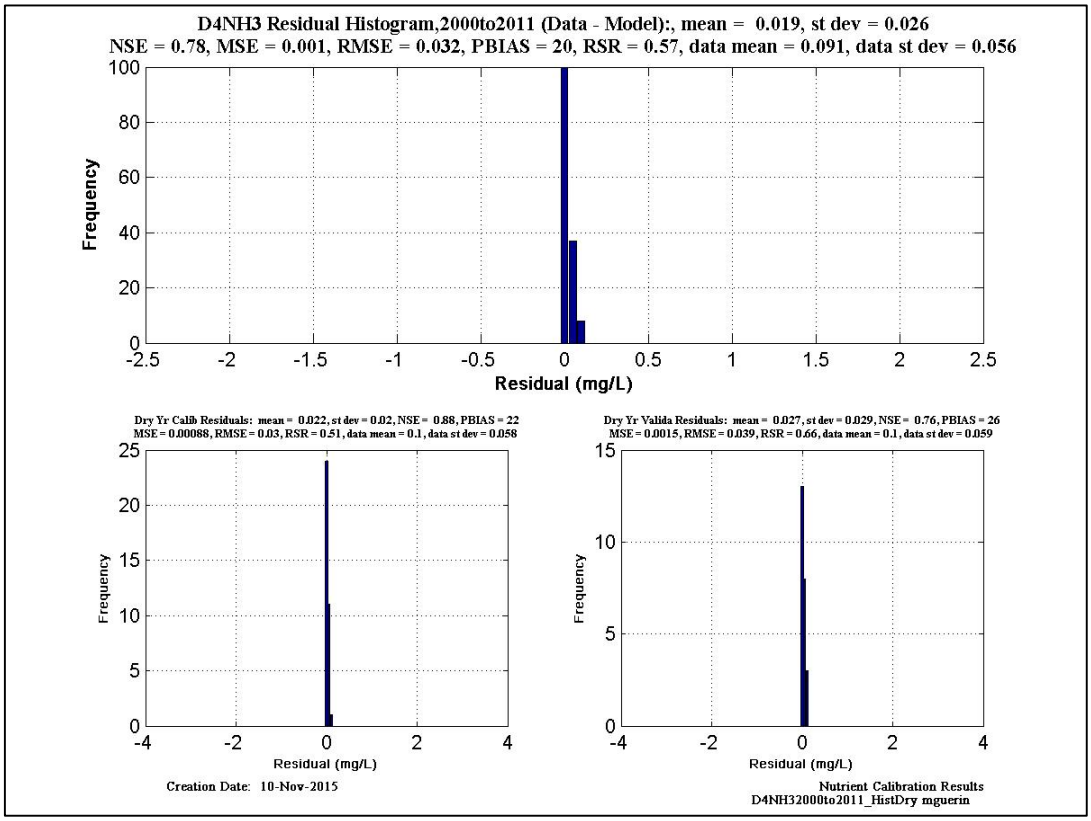

Figure 6-144 NH_3-N histogram and statistics at EMP location D4.

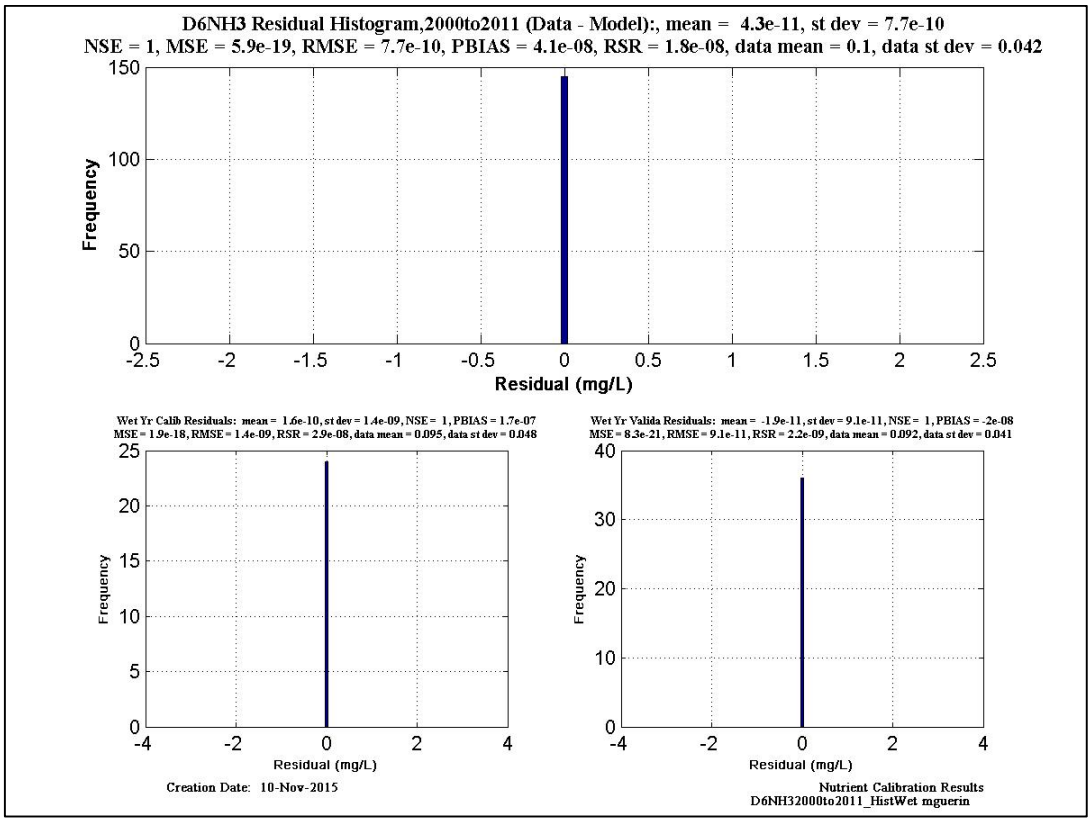

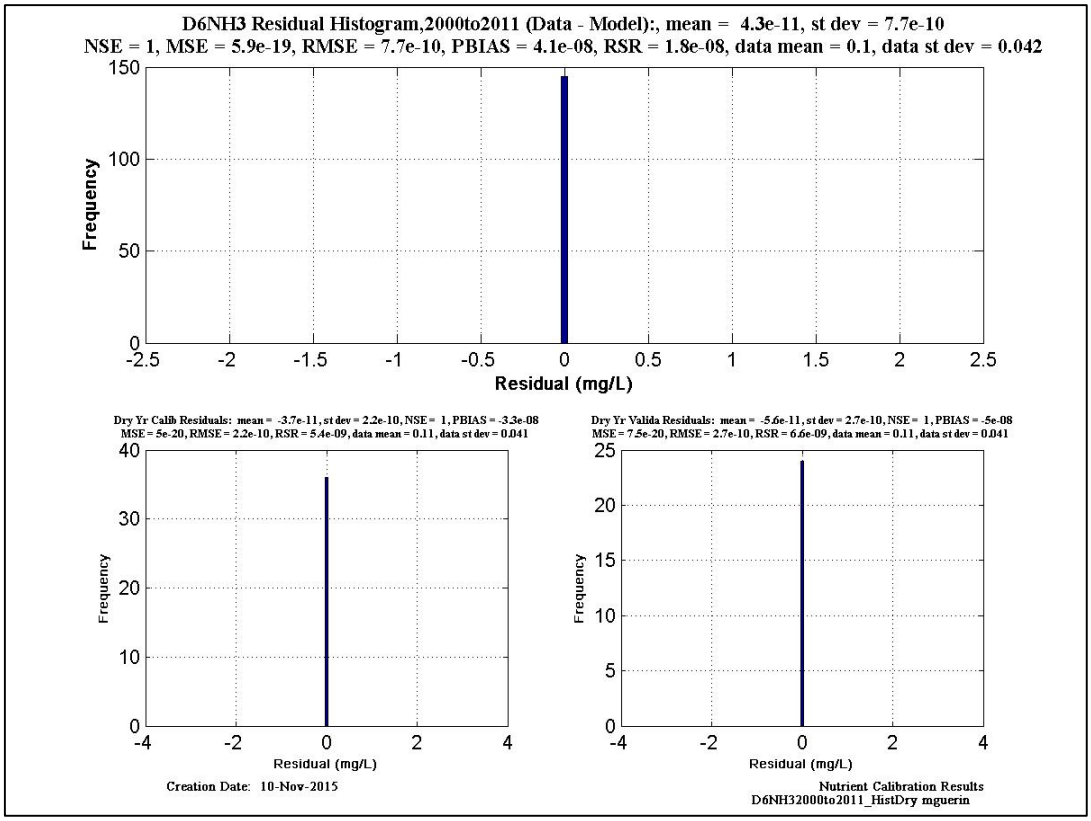

Figure 6-145 NH_3-N histogram and statistics at EMP location D6.

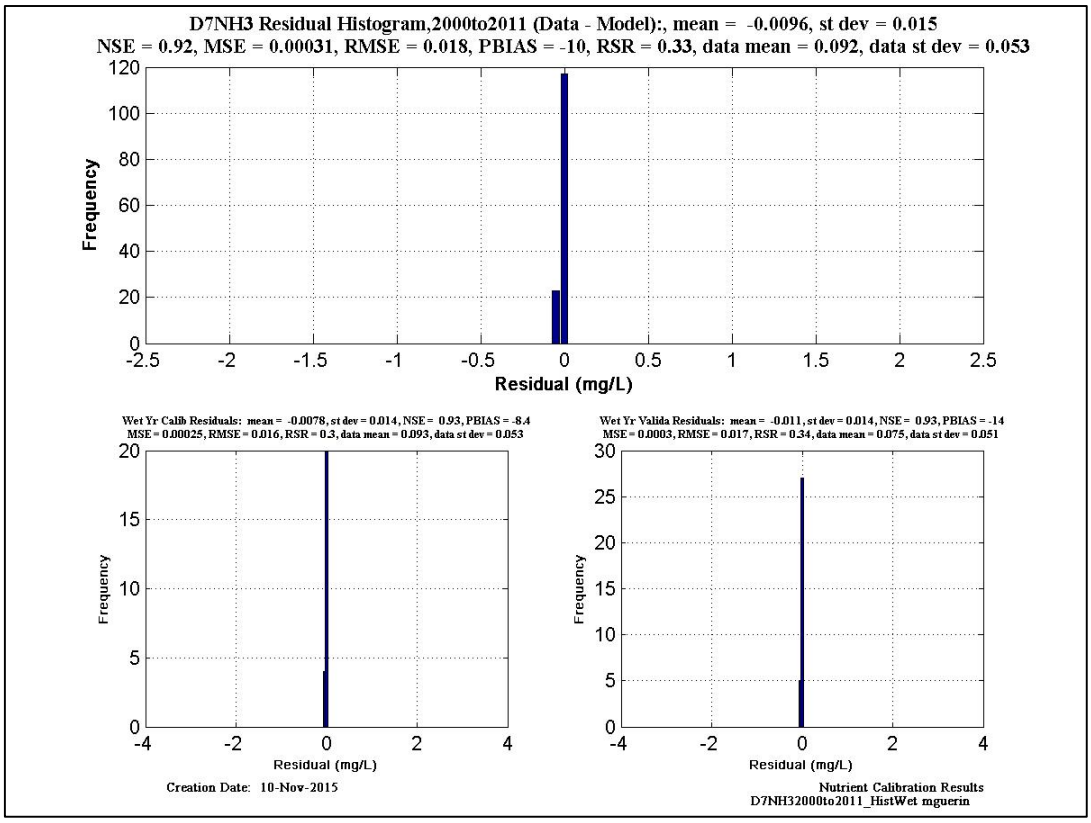

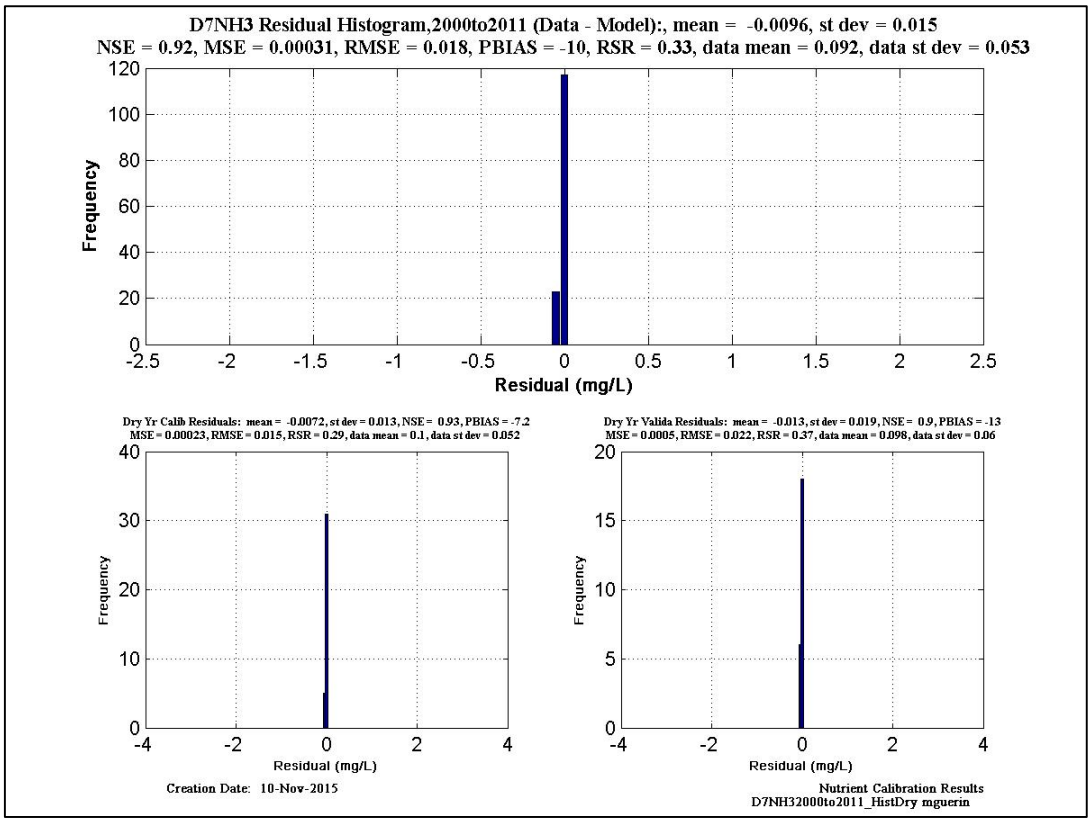

Figure 6-146 NH_3-N histogram and statistics at EMP location D7.

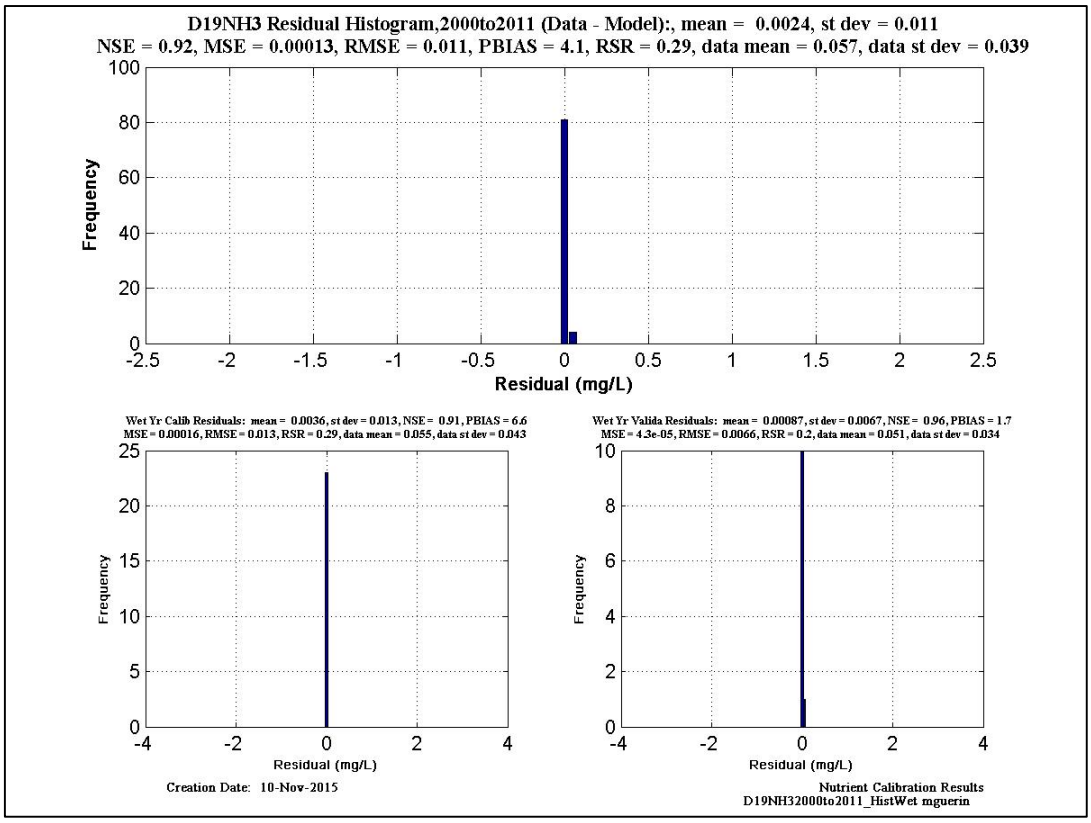

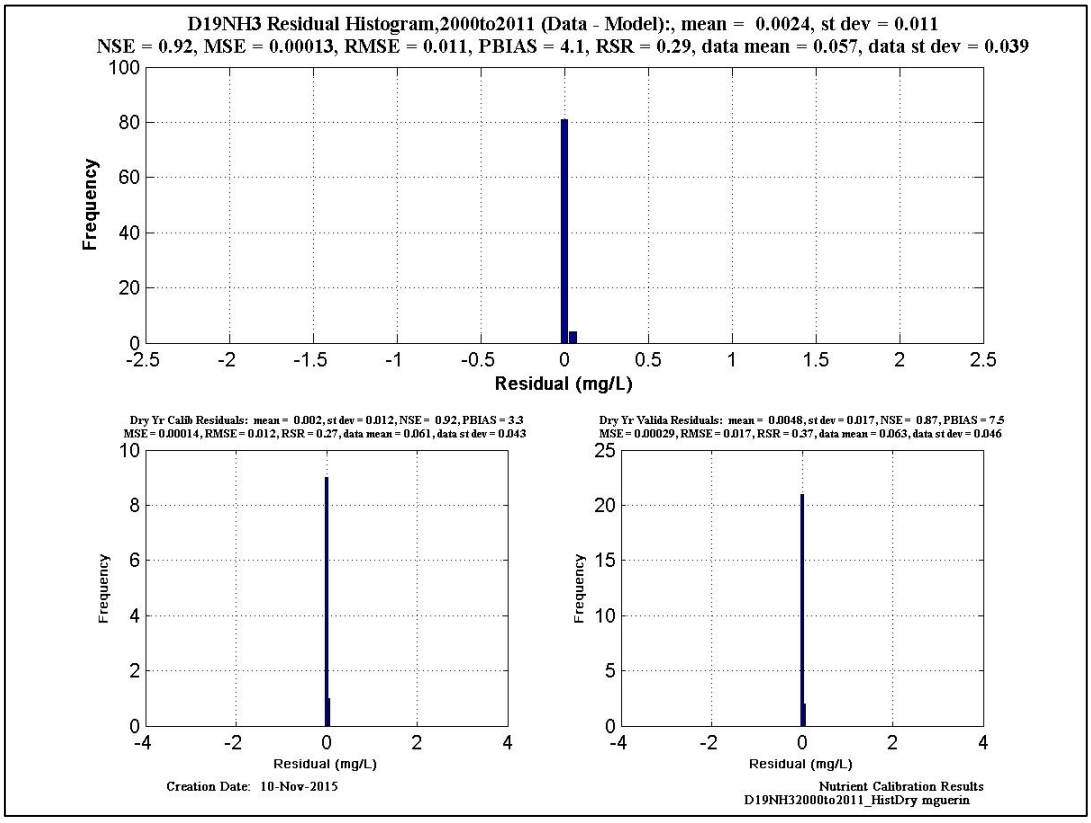

Figure 6-147 NH_3-N histogram and statistics at EMP location D19.

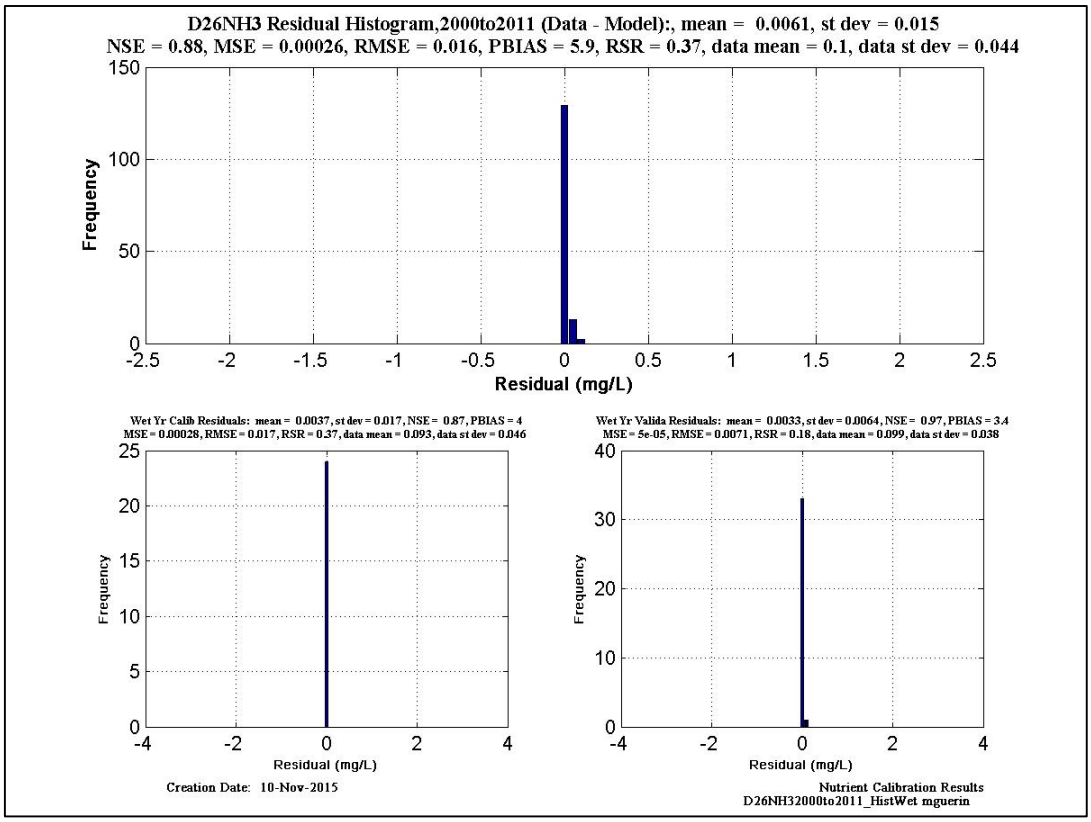

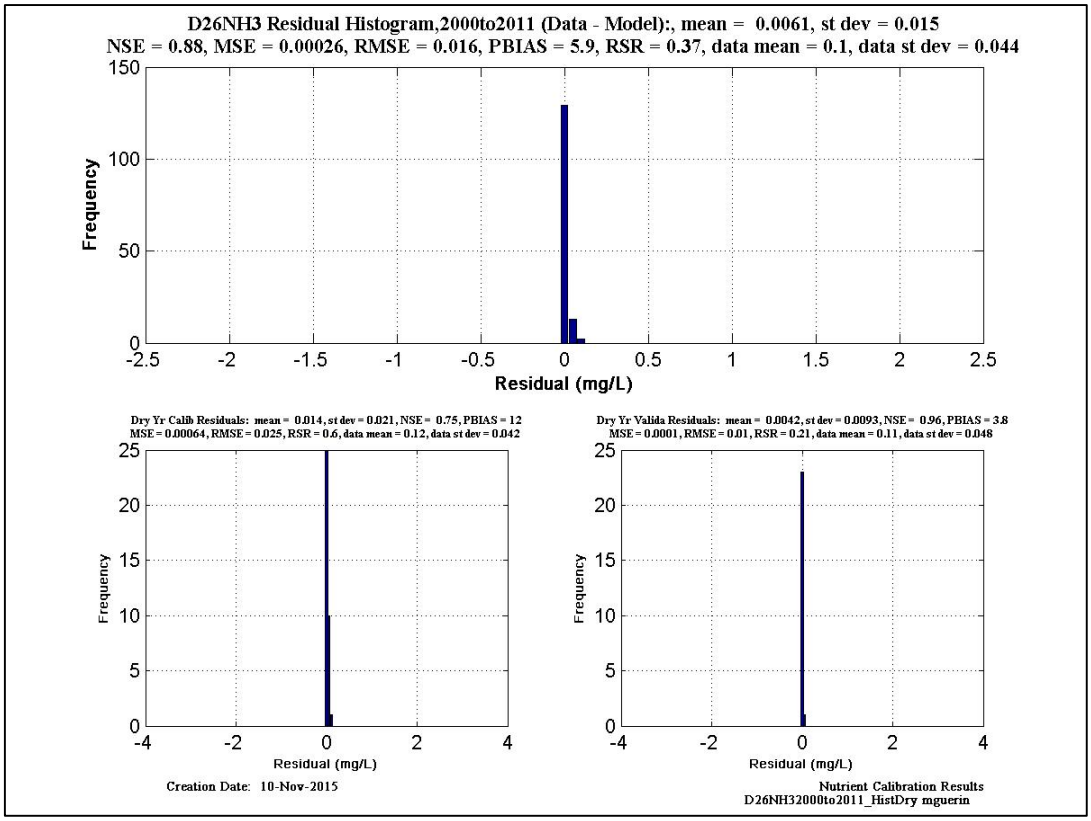

Figure 6-148 NH_3-N histogram and statistics at EMP location D26.

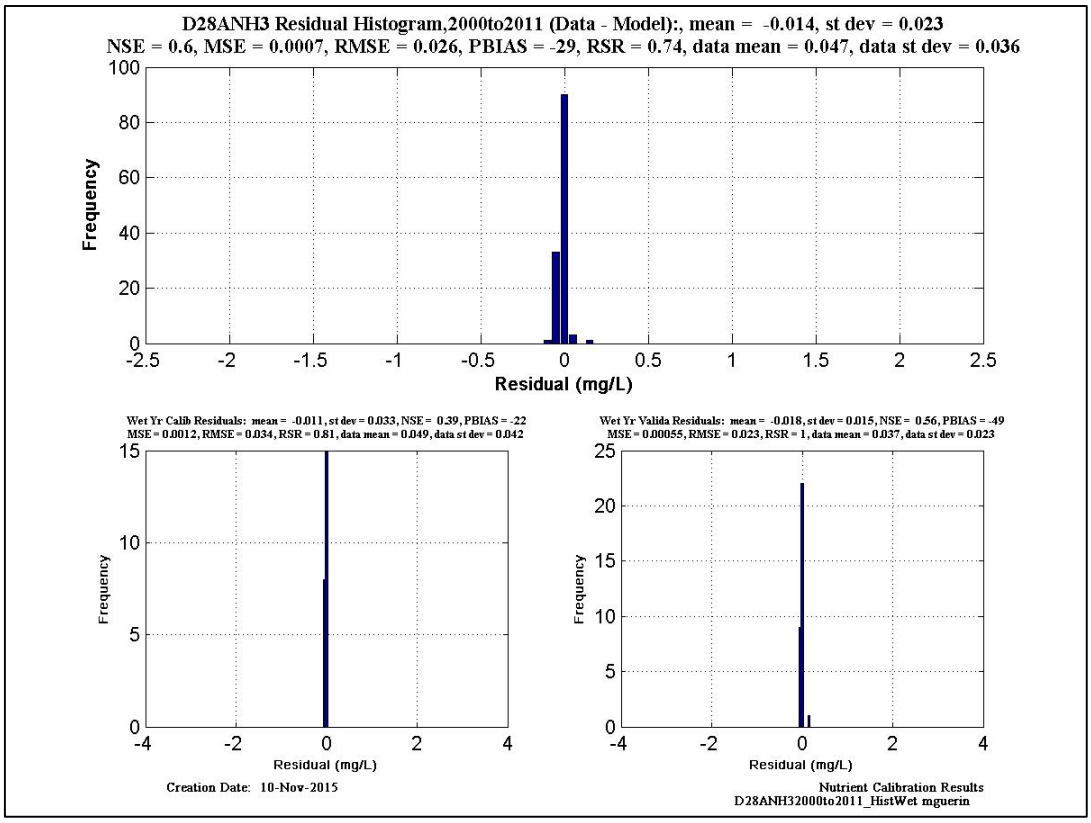

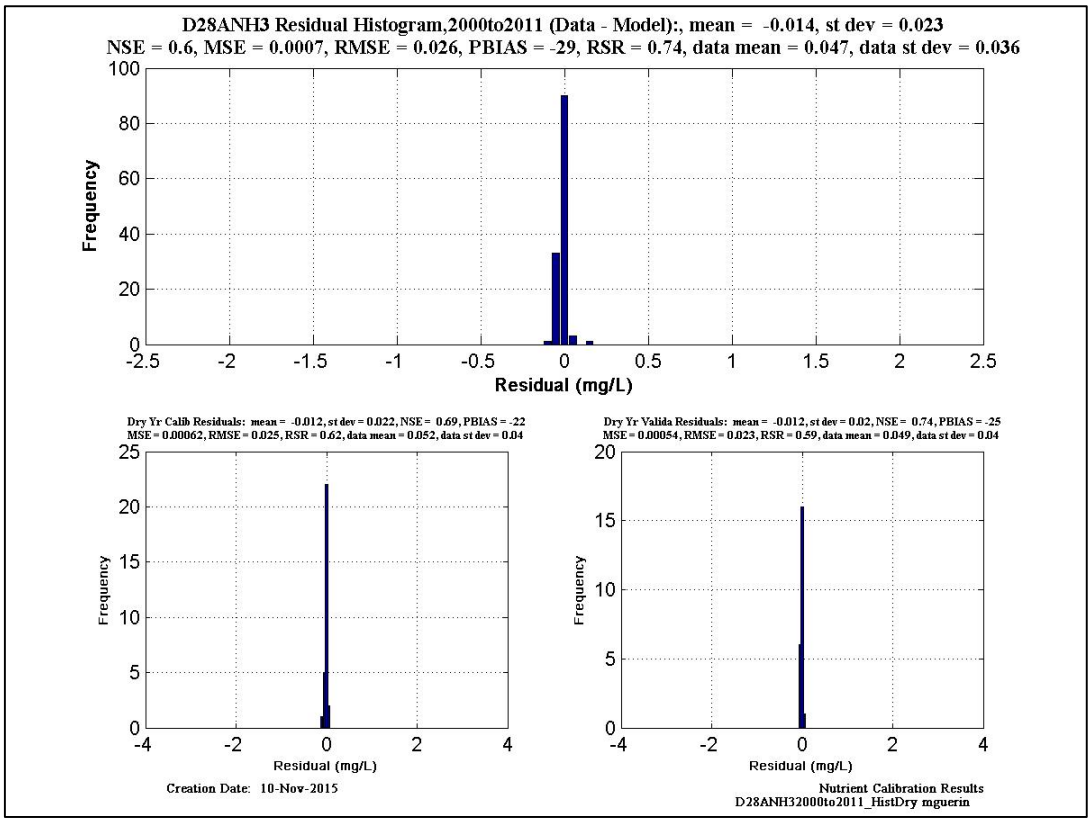

Figure 6-149 NH_3-N histogram and statistics at EMP location D28A.

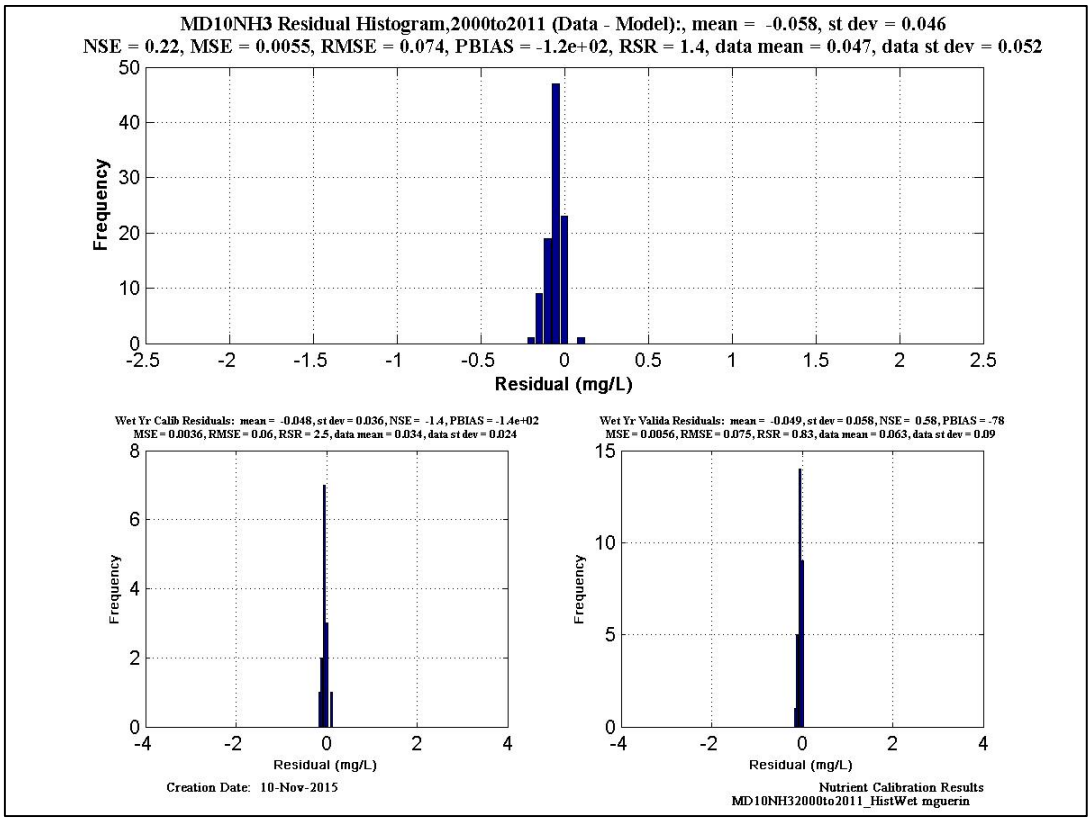

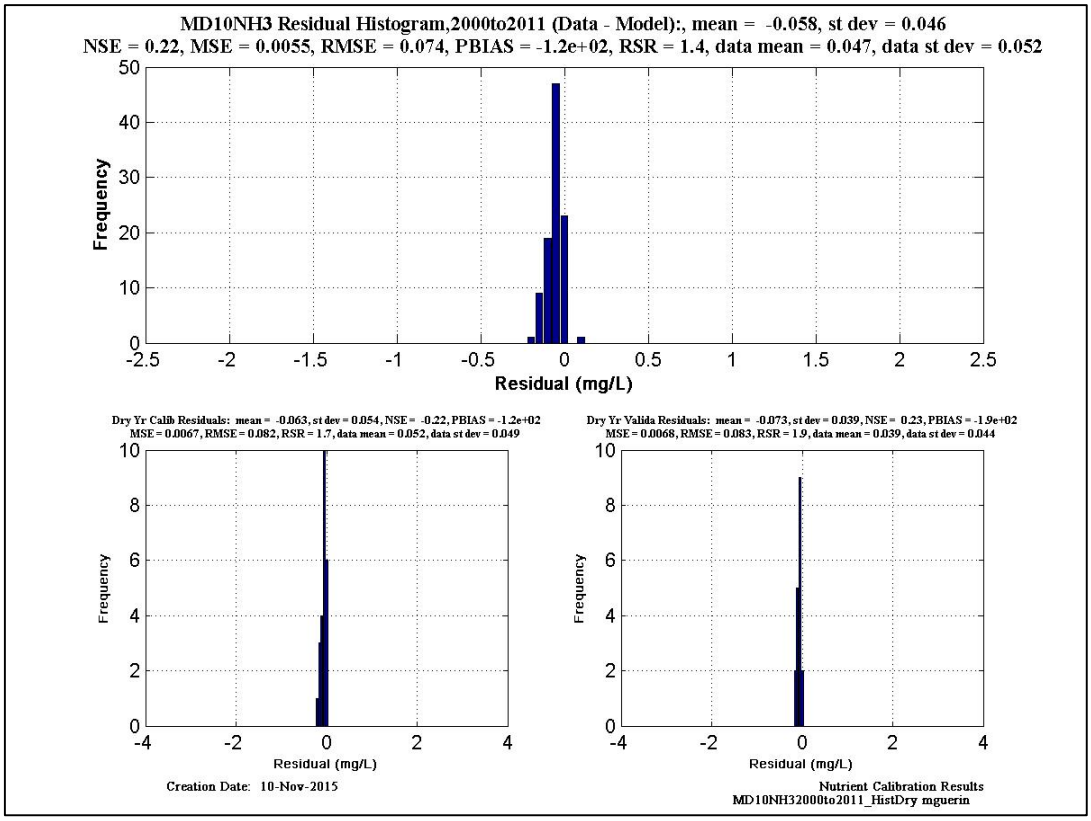

Figure 6-150 NH_3-N histogram and statistics at EMP location MD10.

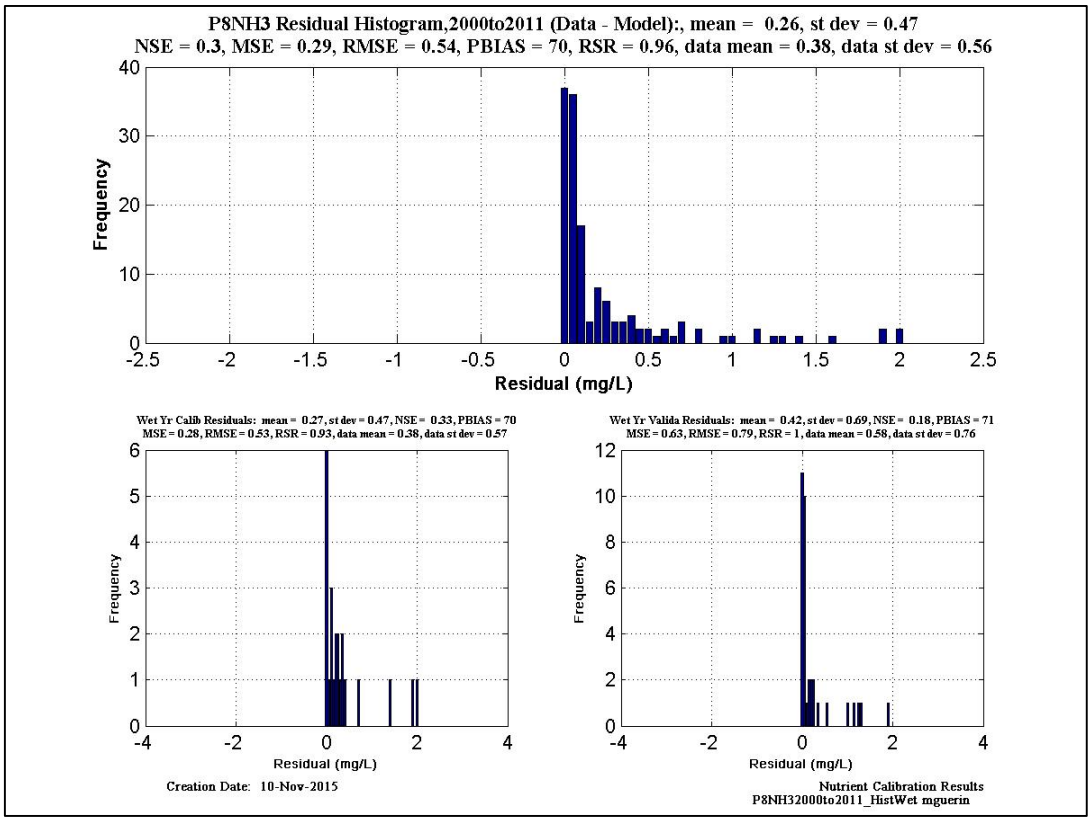

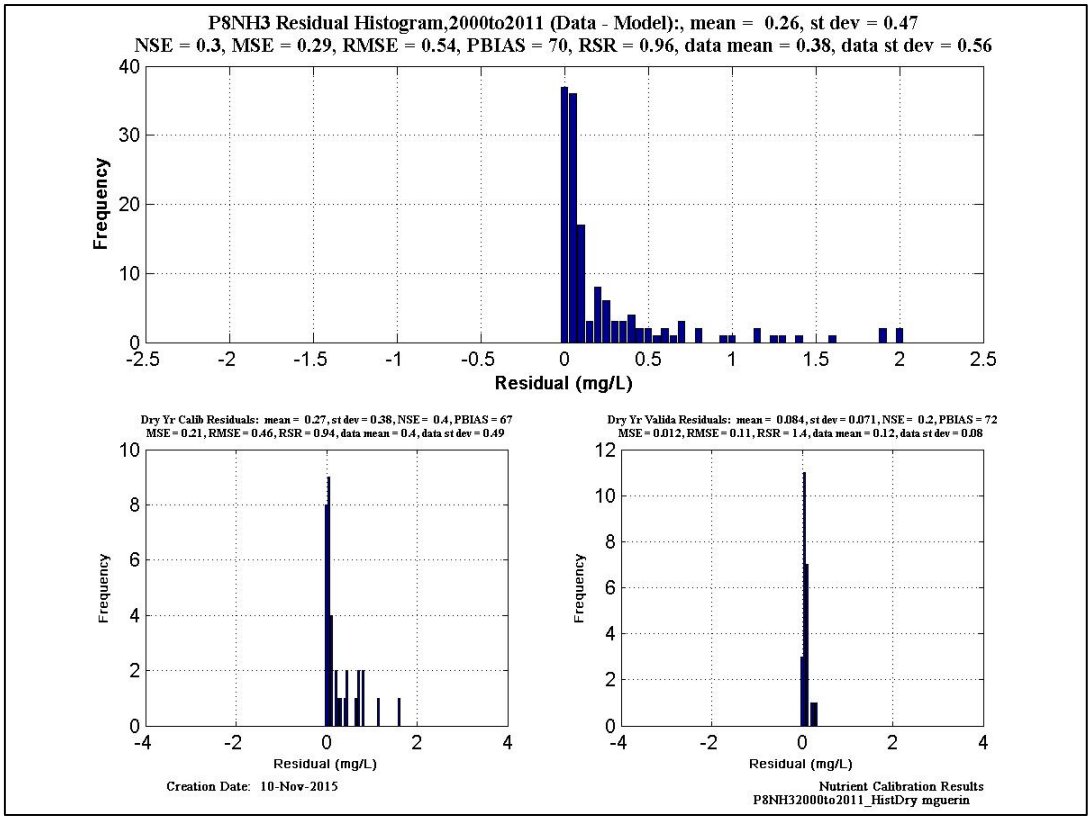

Figure 6-151 NH_3-N histogram and statistics at EMP location P8.

6.12.4.4 Statistics for Modeled NO_3+NO_2-N – EMP Data

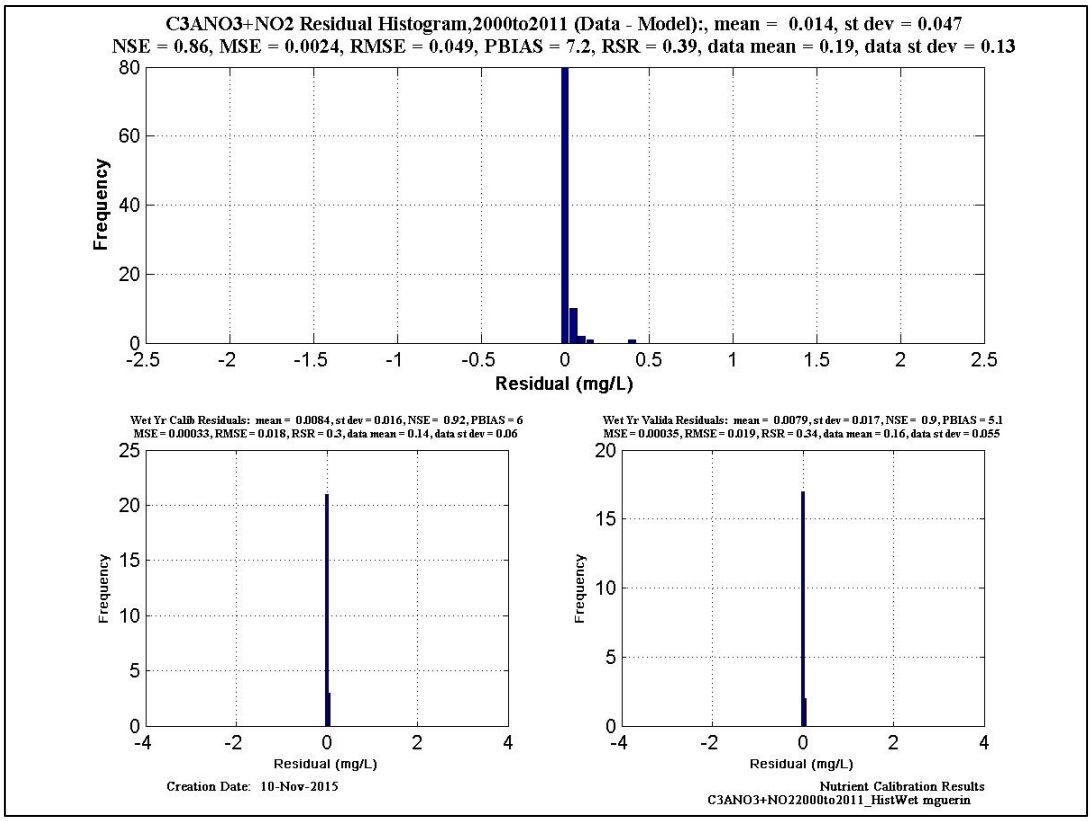

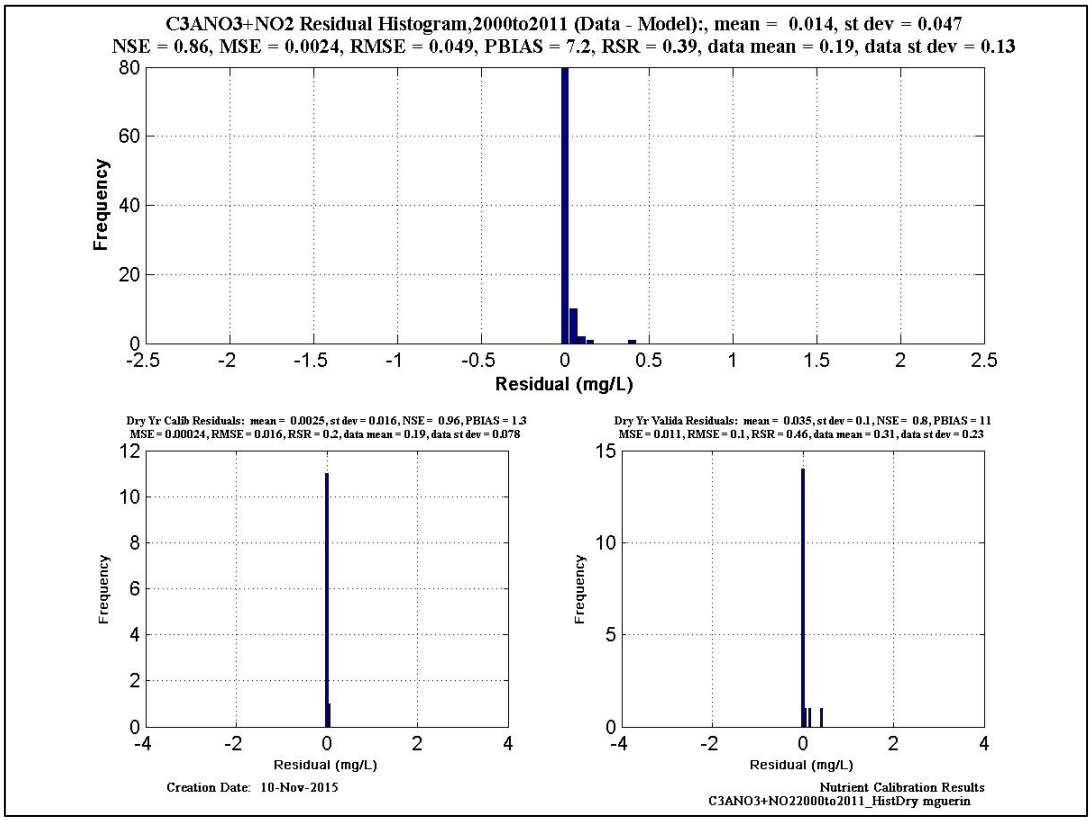

Figure 6-152 NO_3-N histogram and statistics at EMP location C3A.

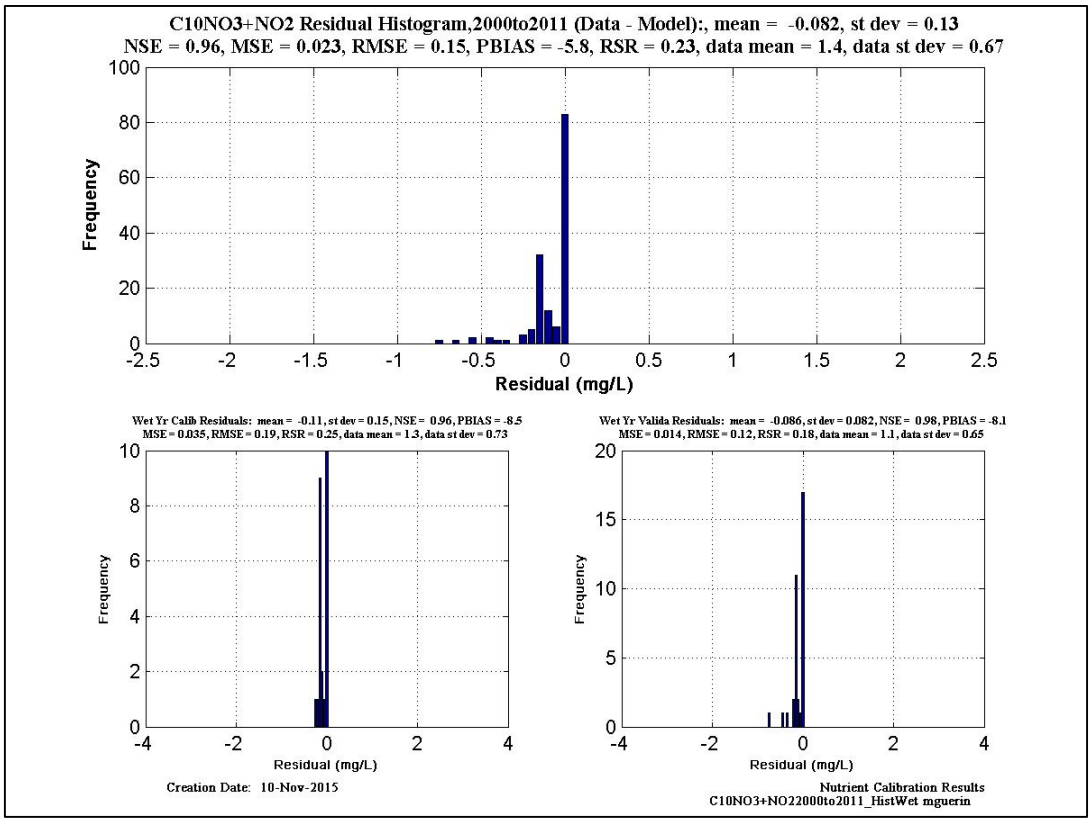

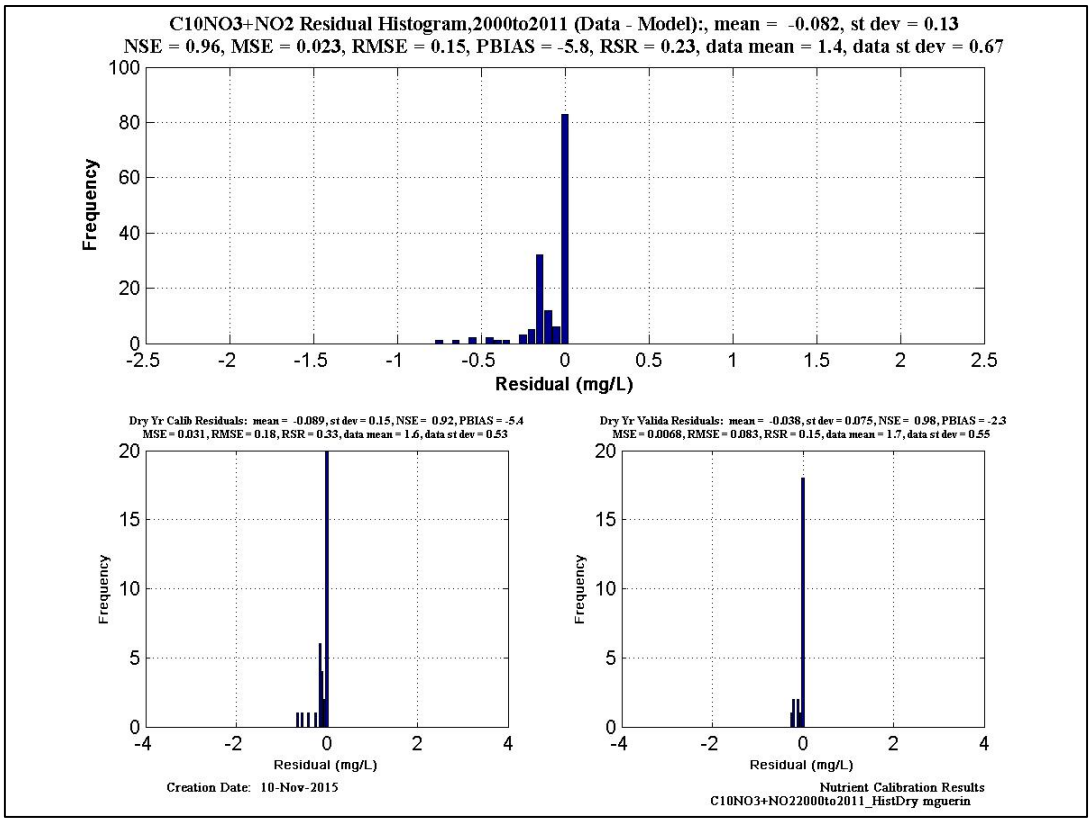

Figure 6-153 NO_3-N histogram and statistics at EMP location C10.

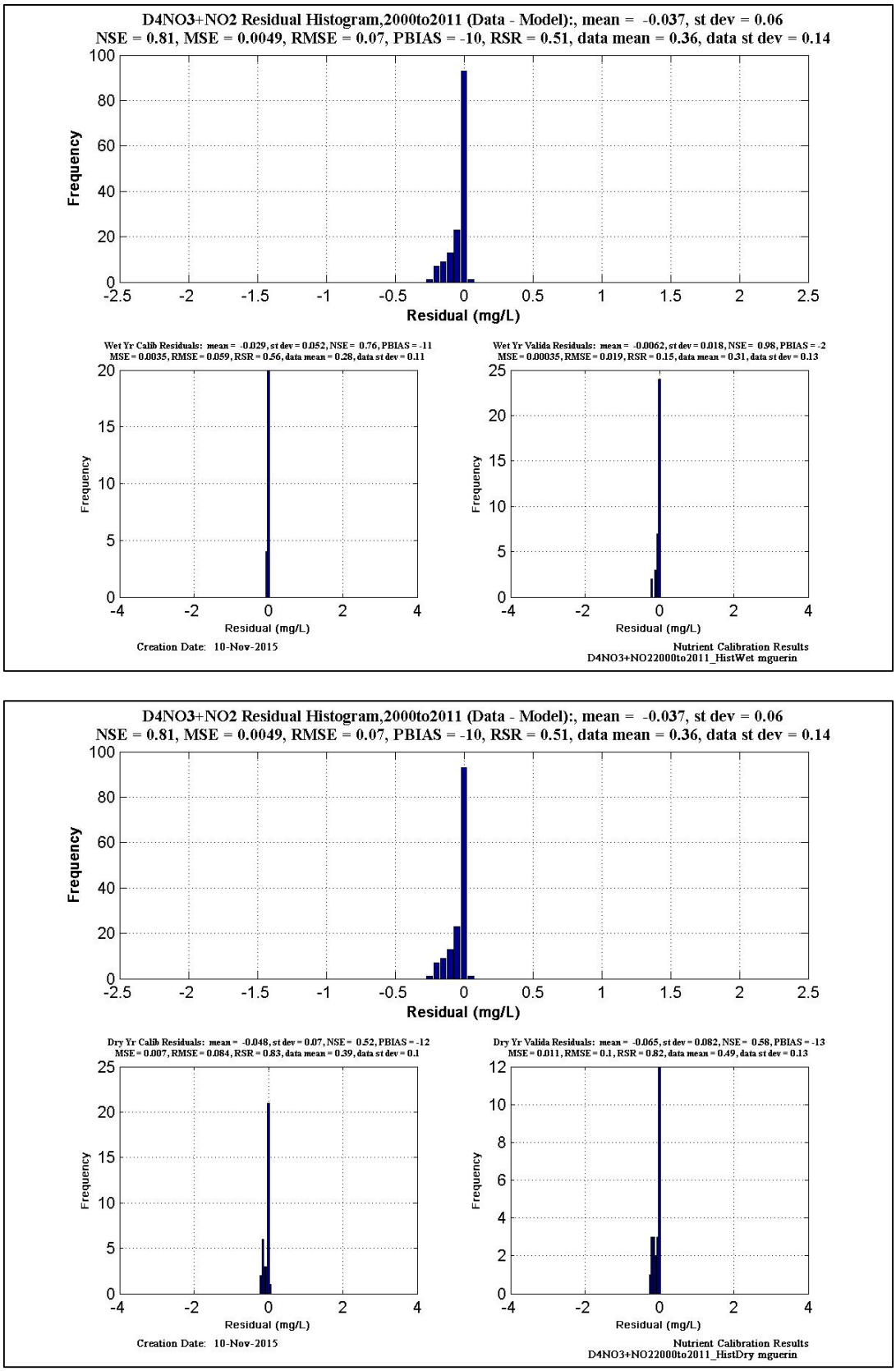

Figure 6-154 NO_3-N histogram and statistics at EMP location D4.

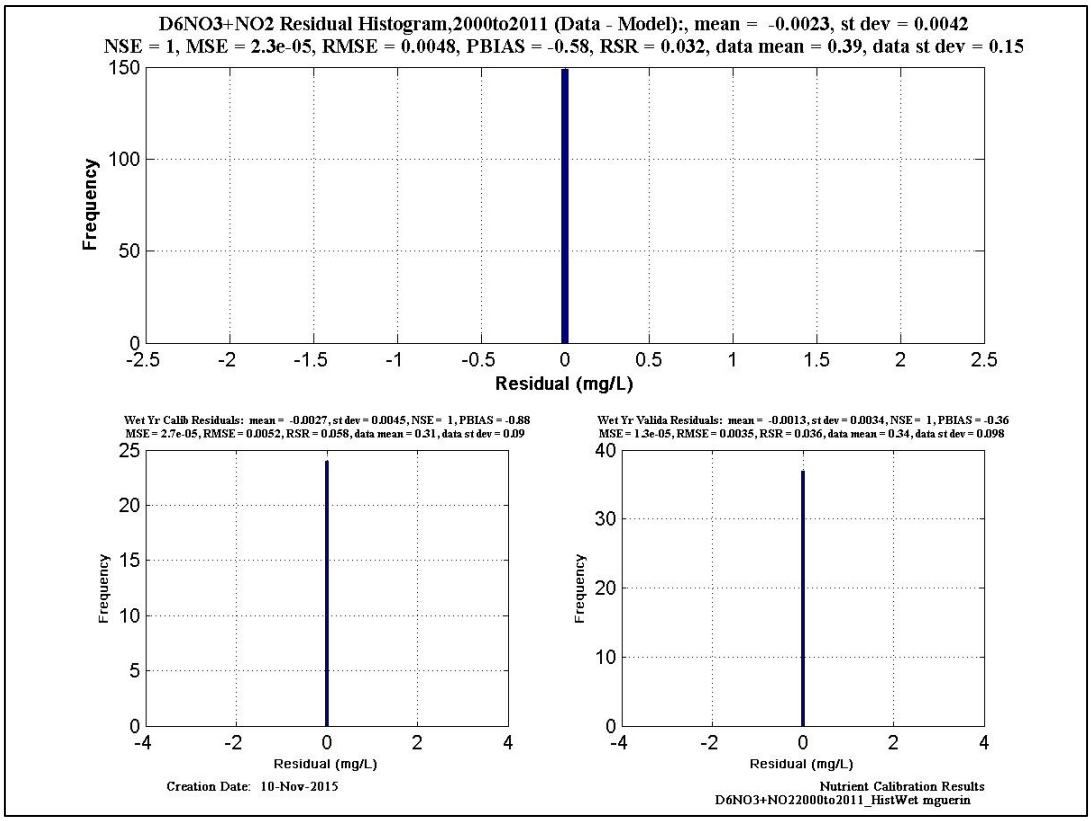

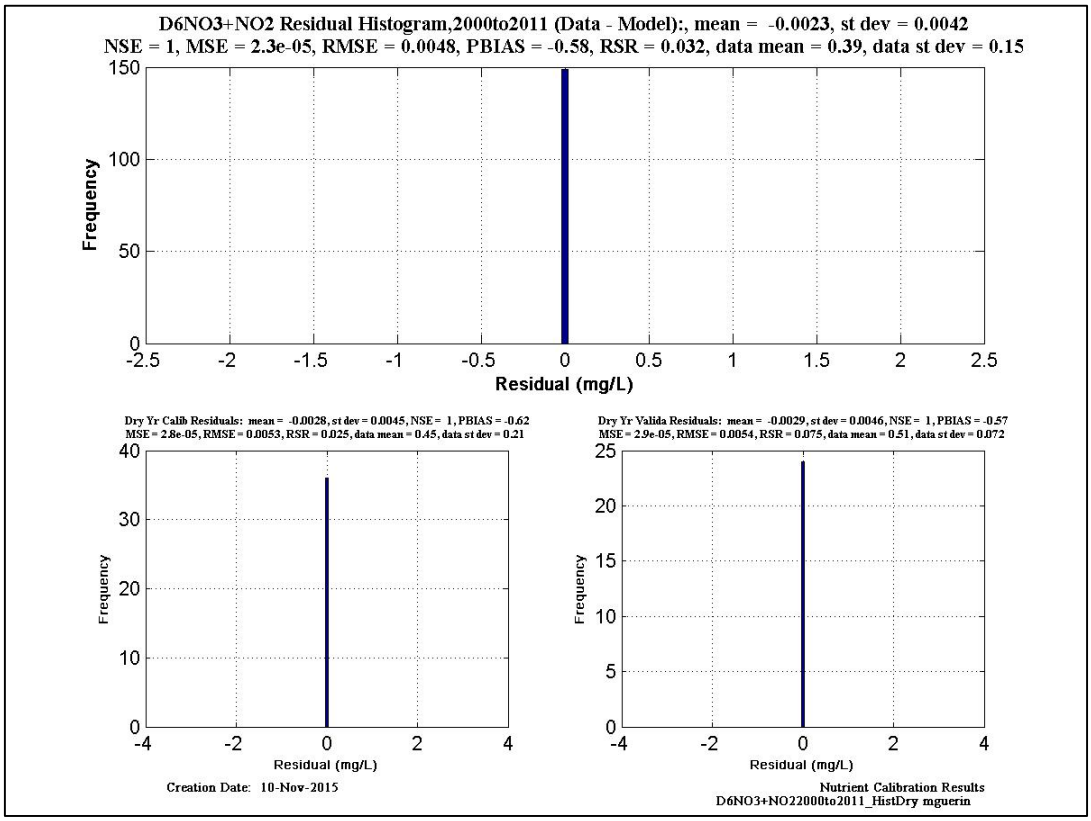

Figure 6-155 NO_3-N histogram and statistics at EMP location D6.

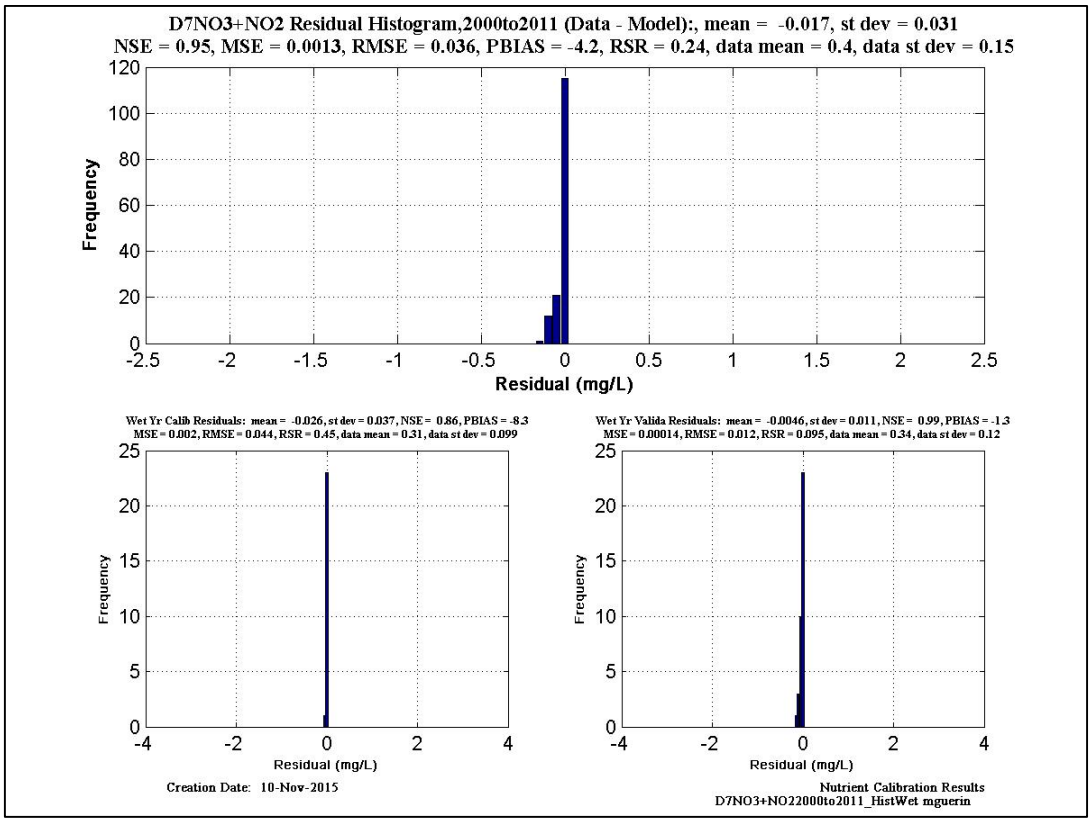

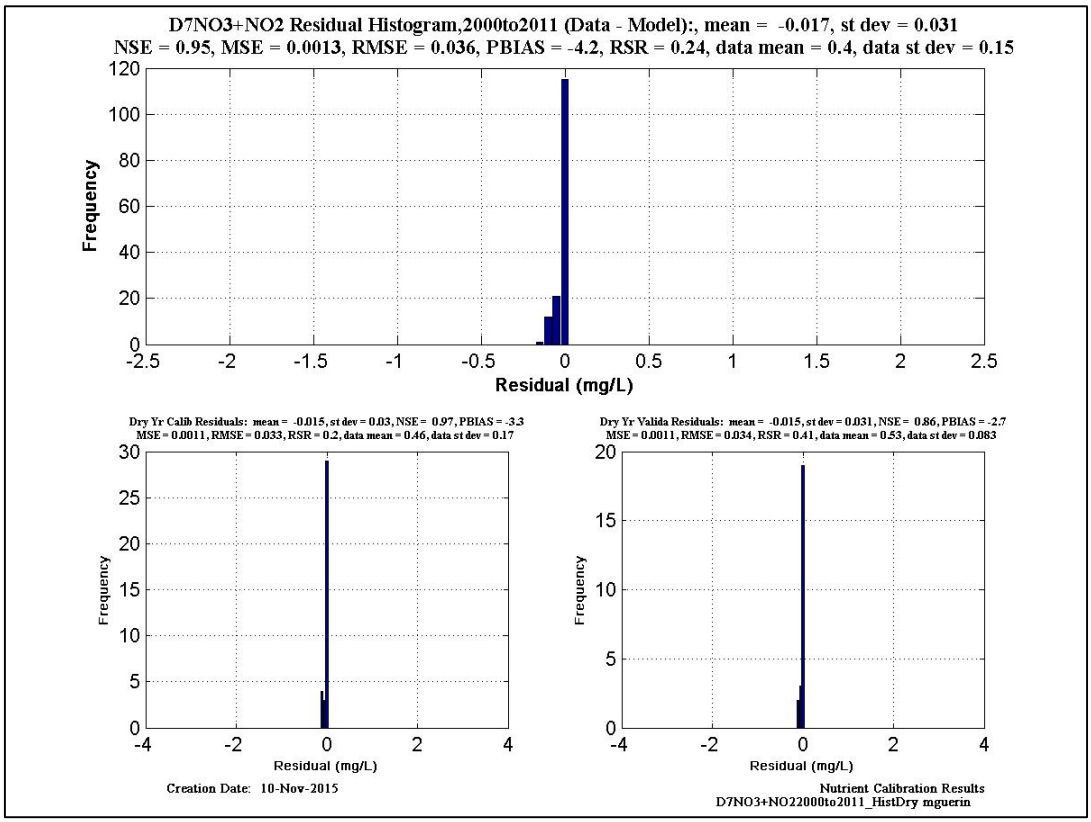

Figure 6-156 NO_3-N histogram and statistics at EMP location D7.

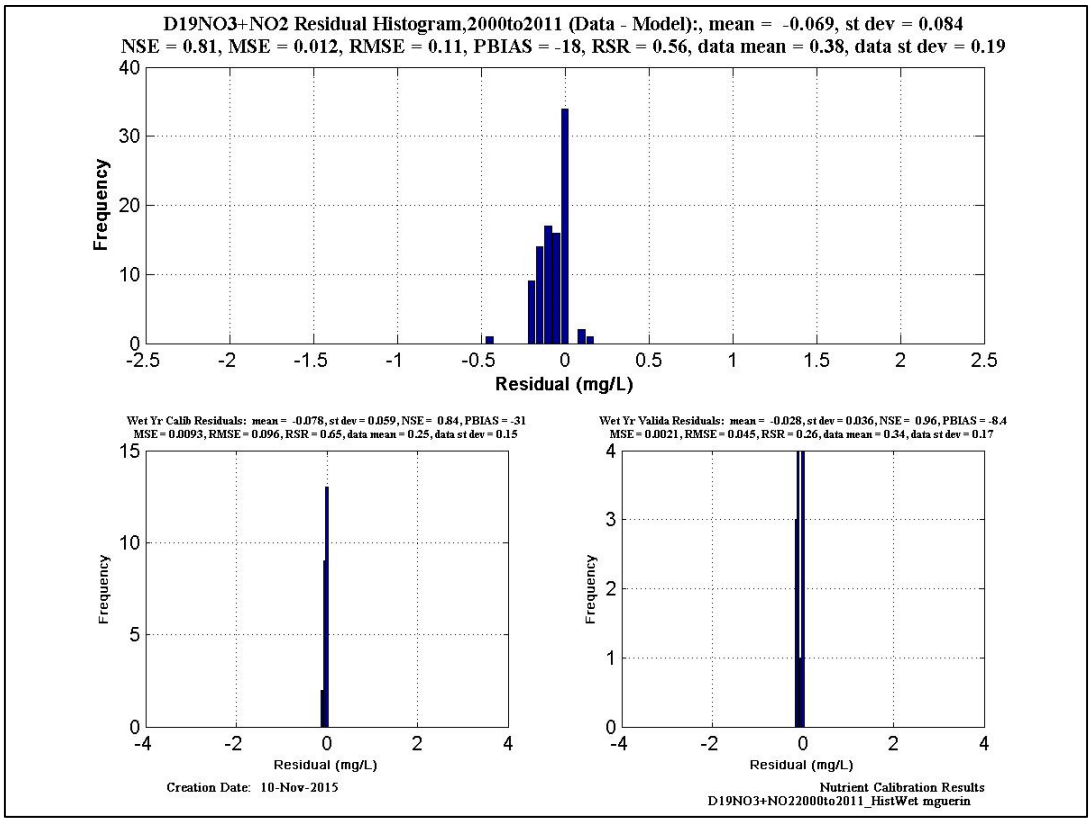

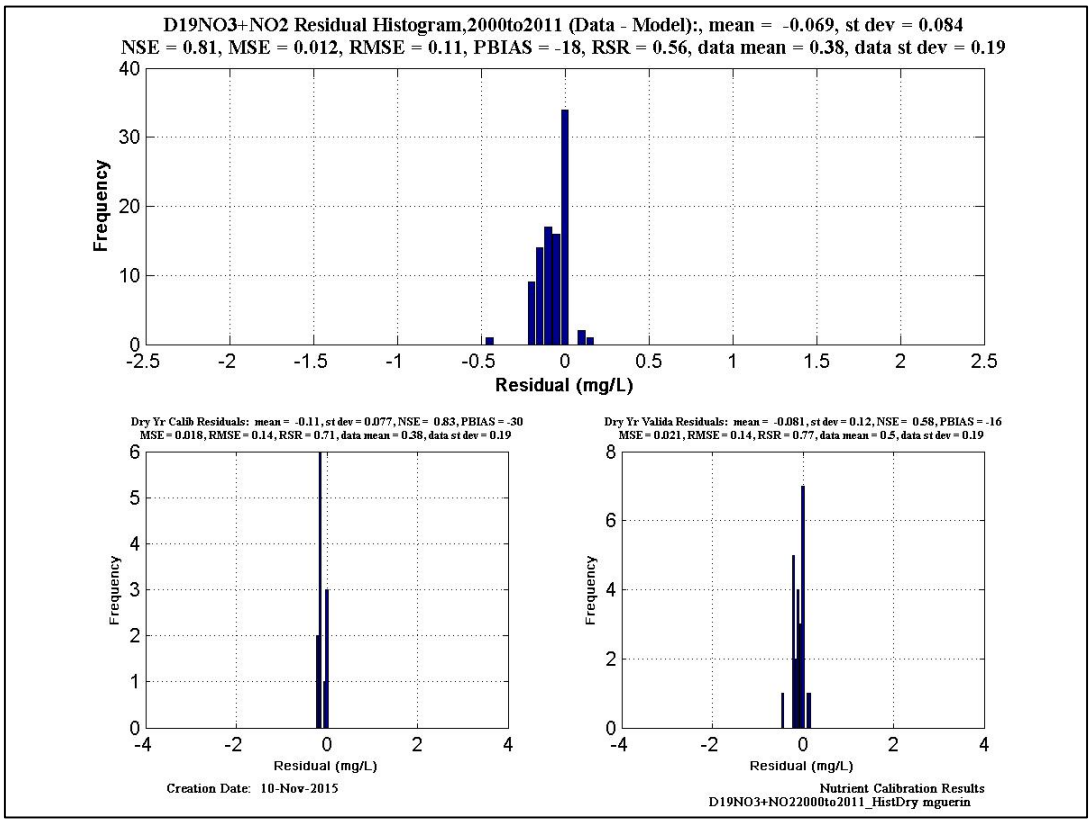

Figure 6-157 NO_3-N histogram and statistics at EMP location D19.

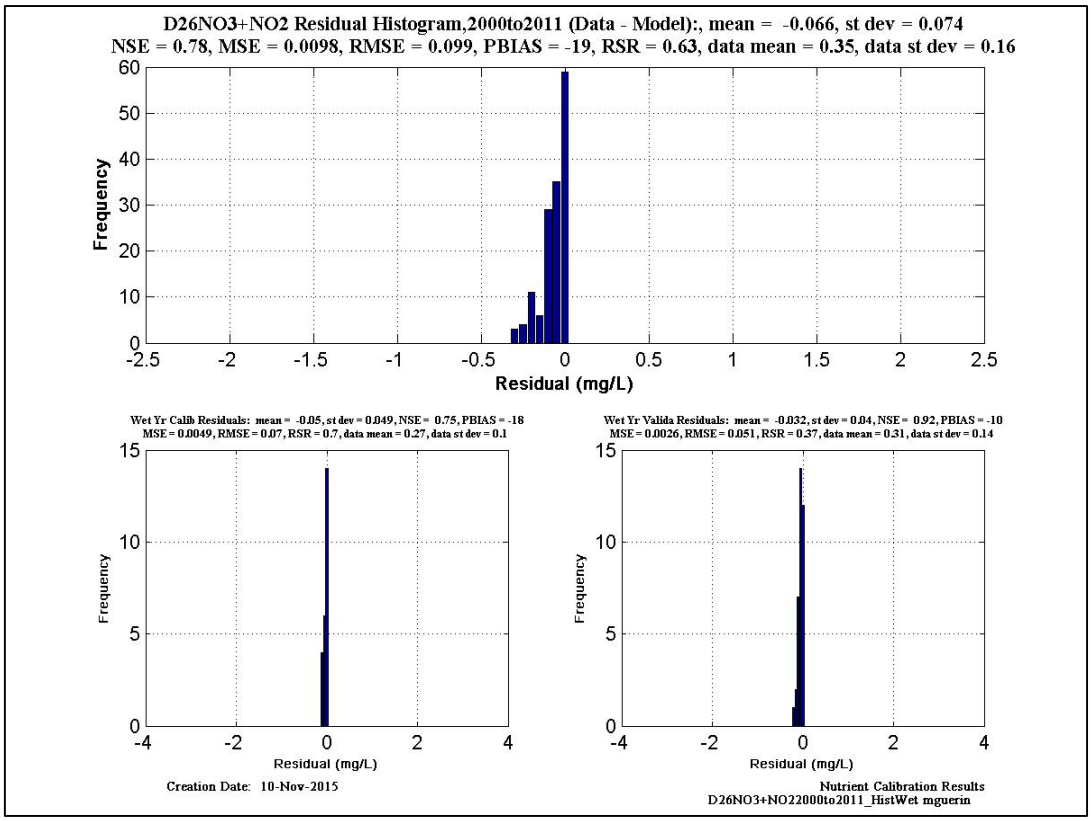

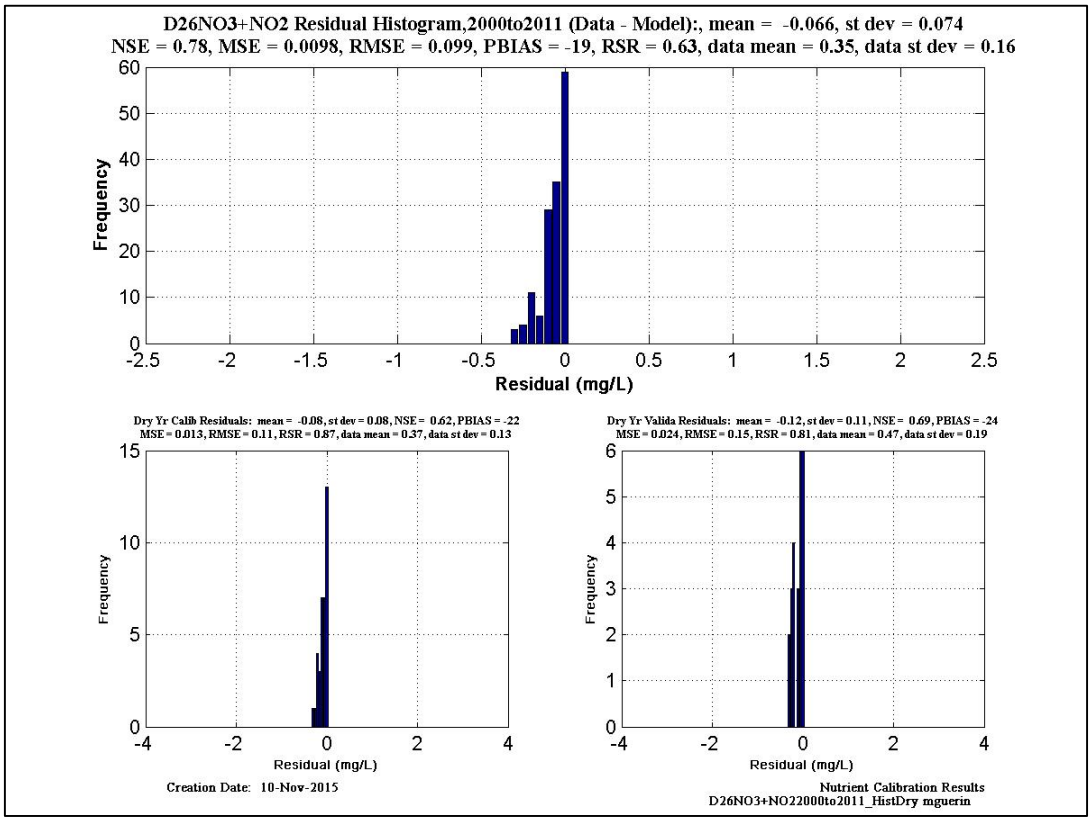

Figure 6-158 NO_3-N histogram and statistics at EMP location D26.

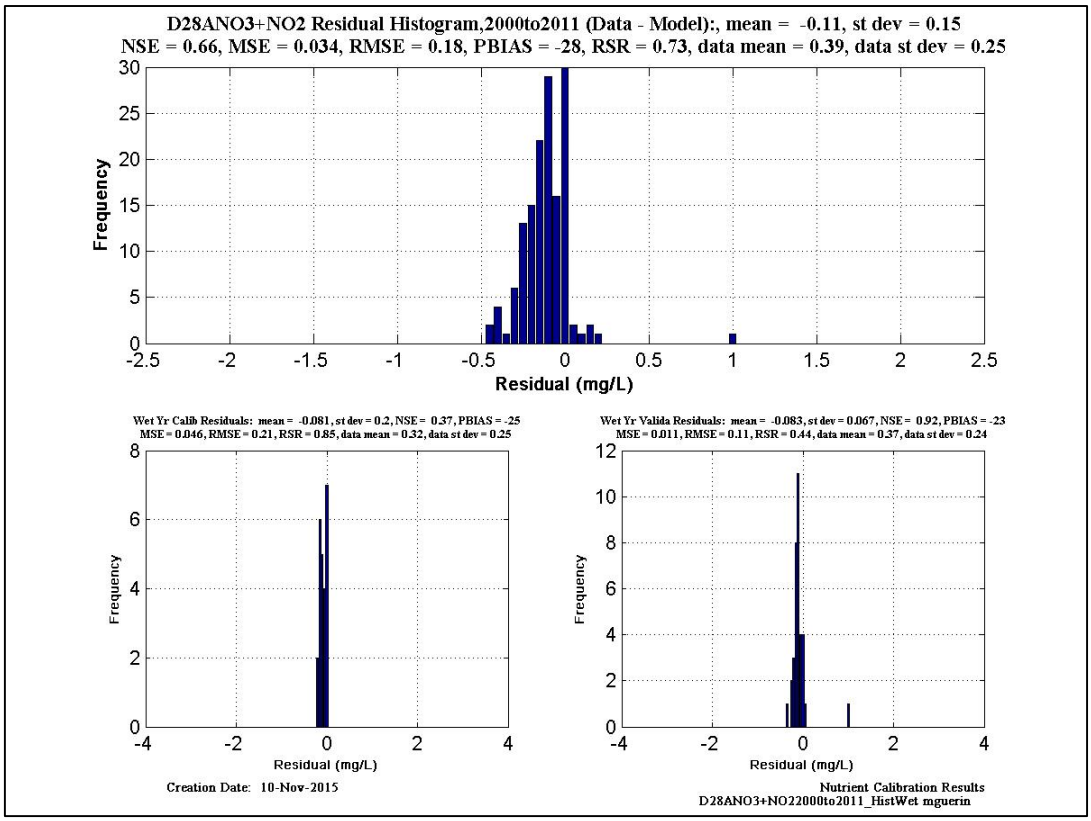

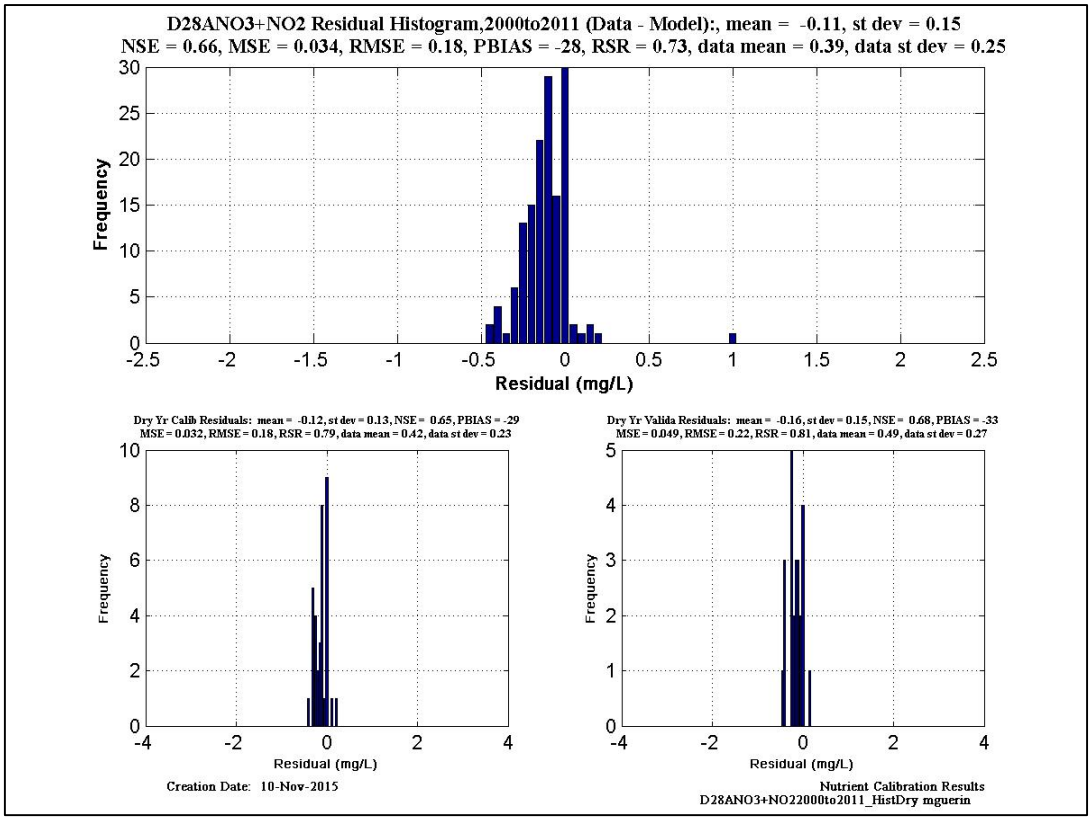

Figure 6-159 NO_3-N histogram and statistics at EMP location D28A.

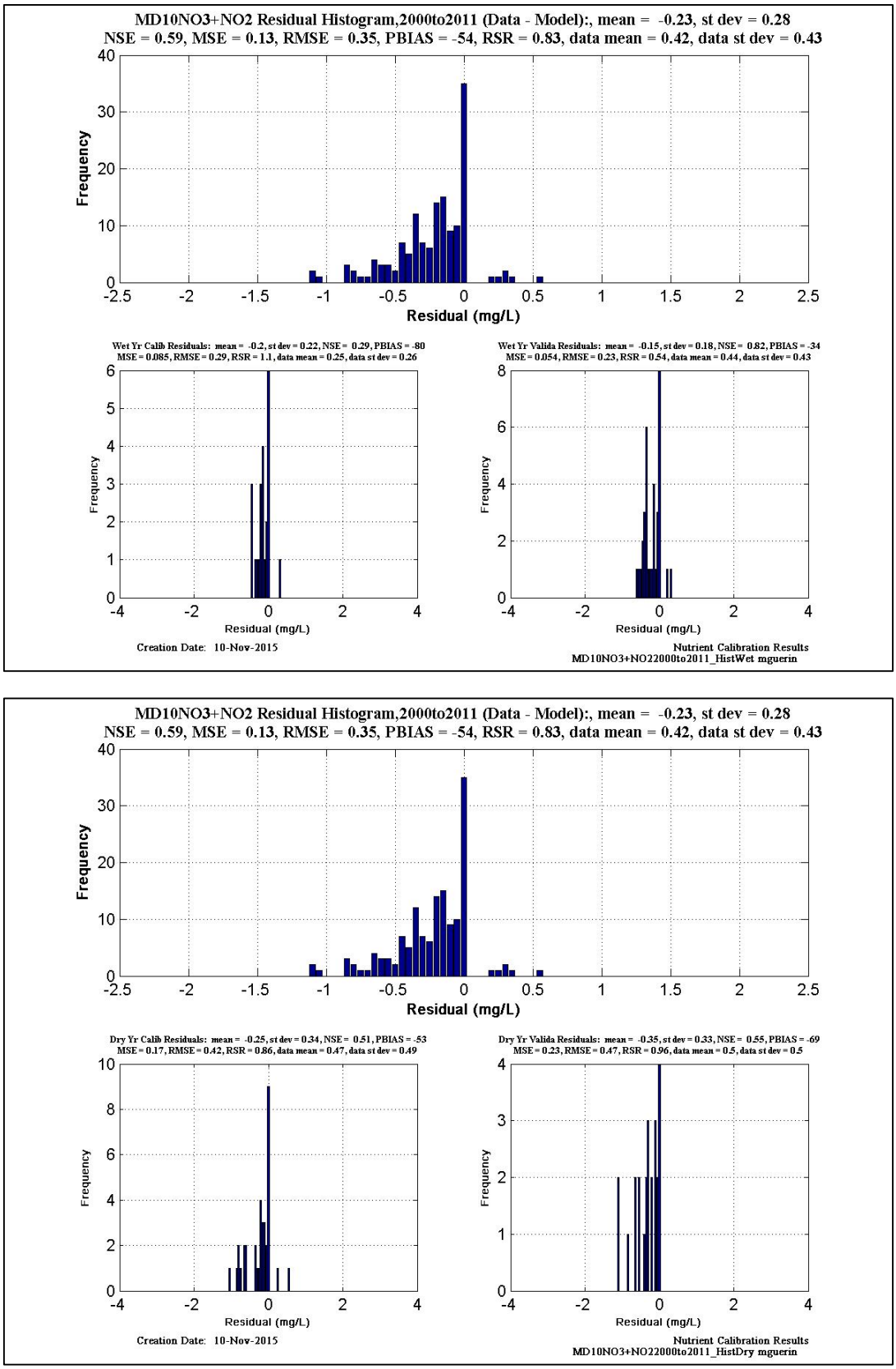

Figure 6-160 NO_3-N histogram and statistics at EMP location MD10.

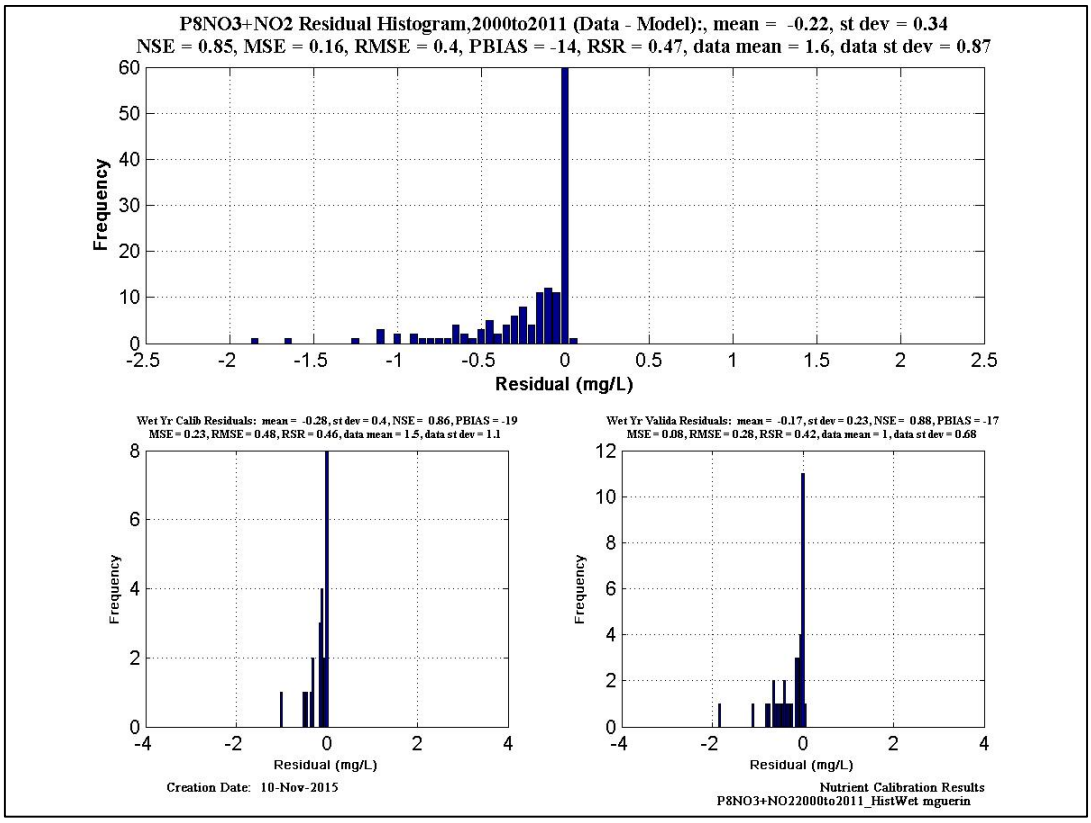

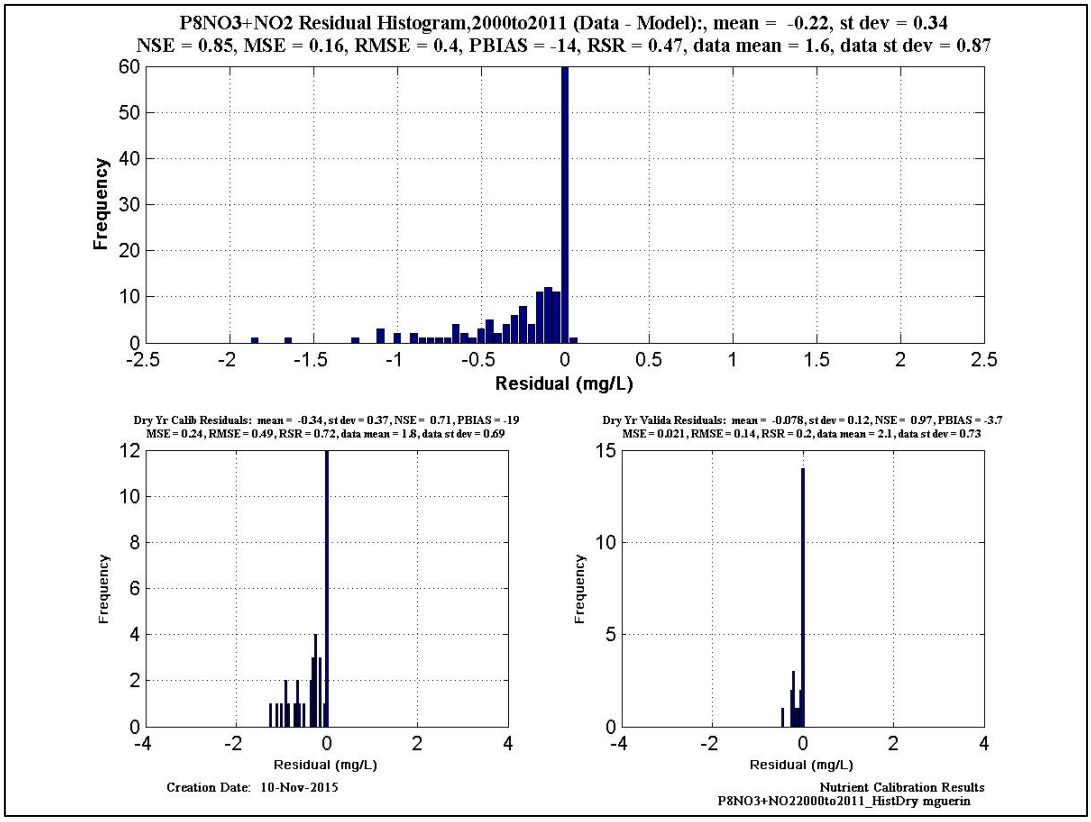

Figure 6-161 NO_3-N histogram and statistics at EMP location P8.

6.12.4.5 Statistics for Modeled Organic-N – EMP Data

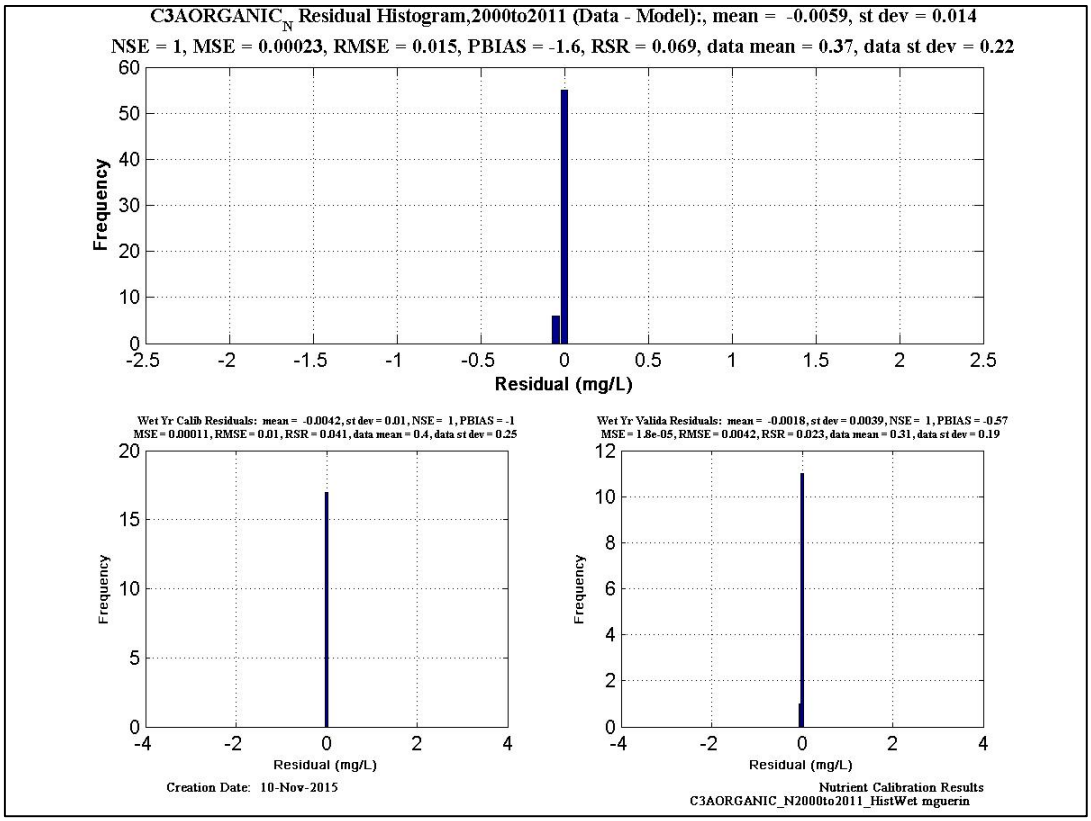

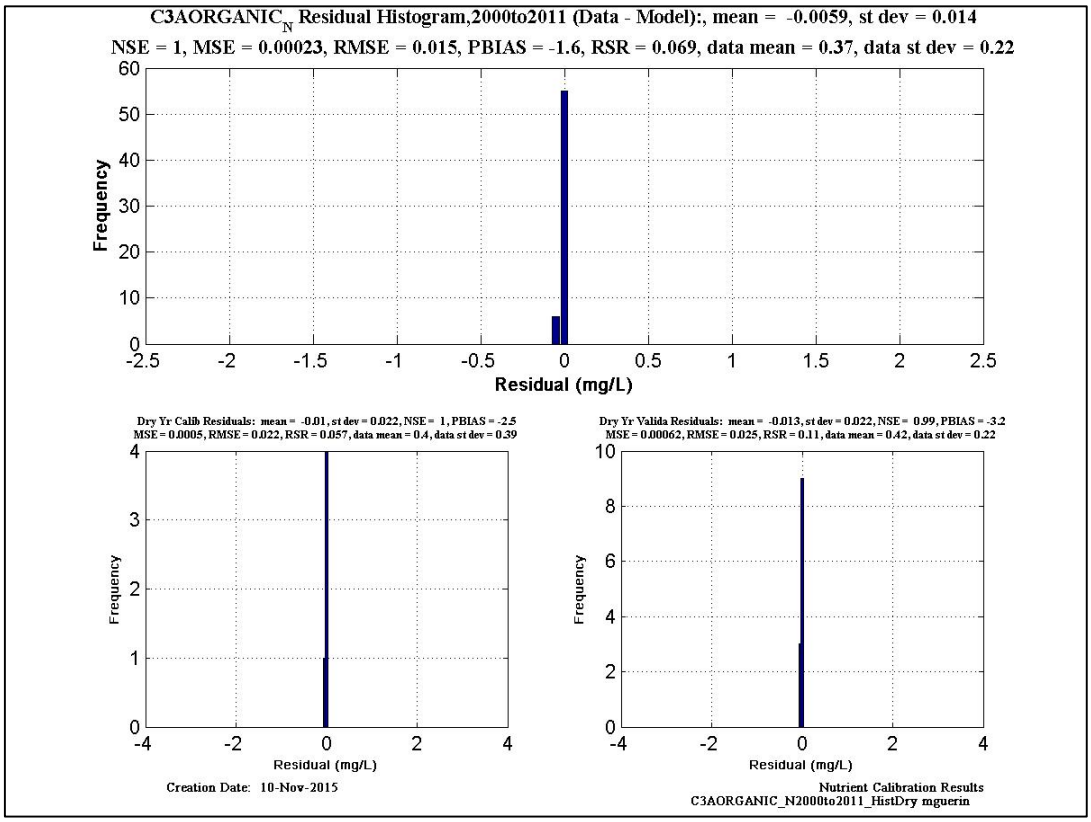

Figure 6-162 Organic-N histogram and statistics at EMP location C3A.

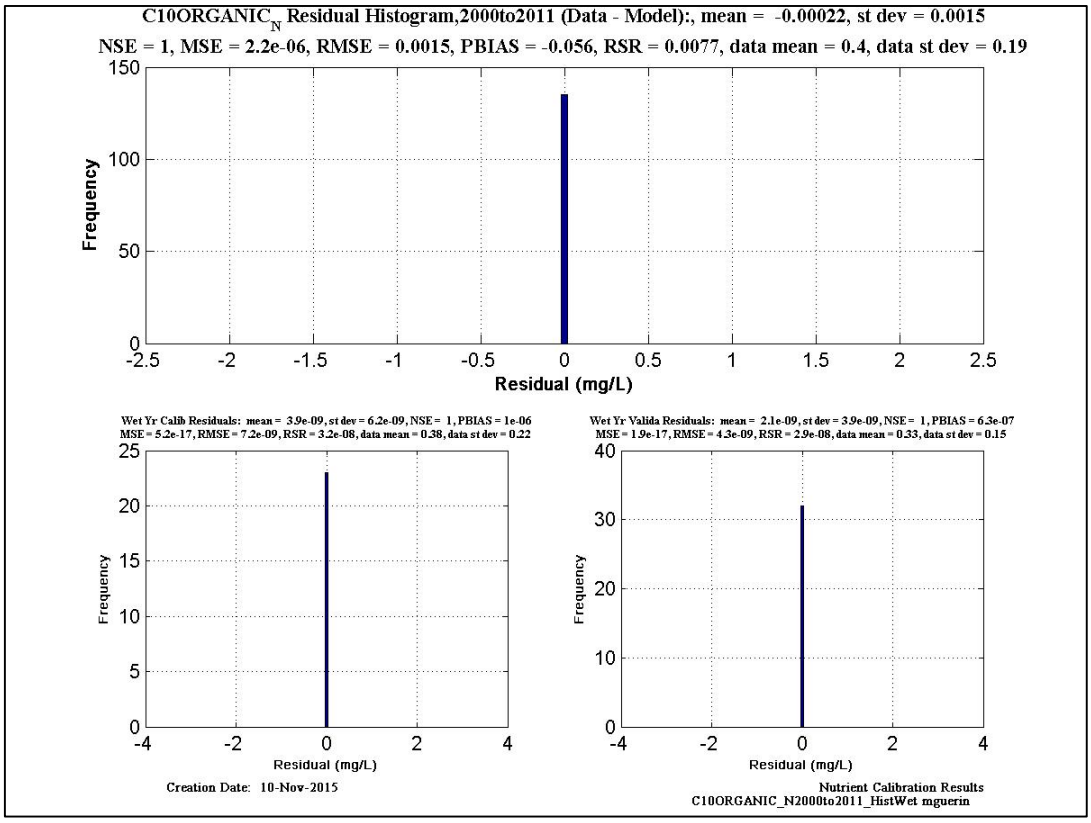

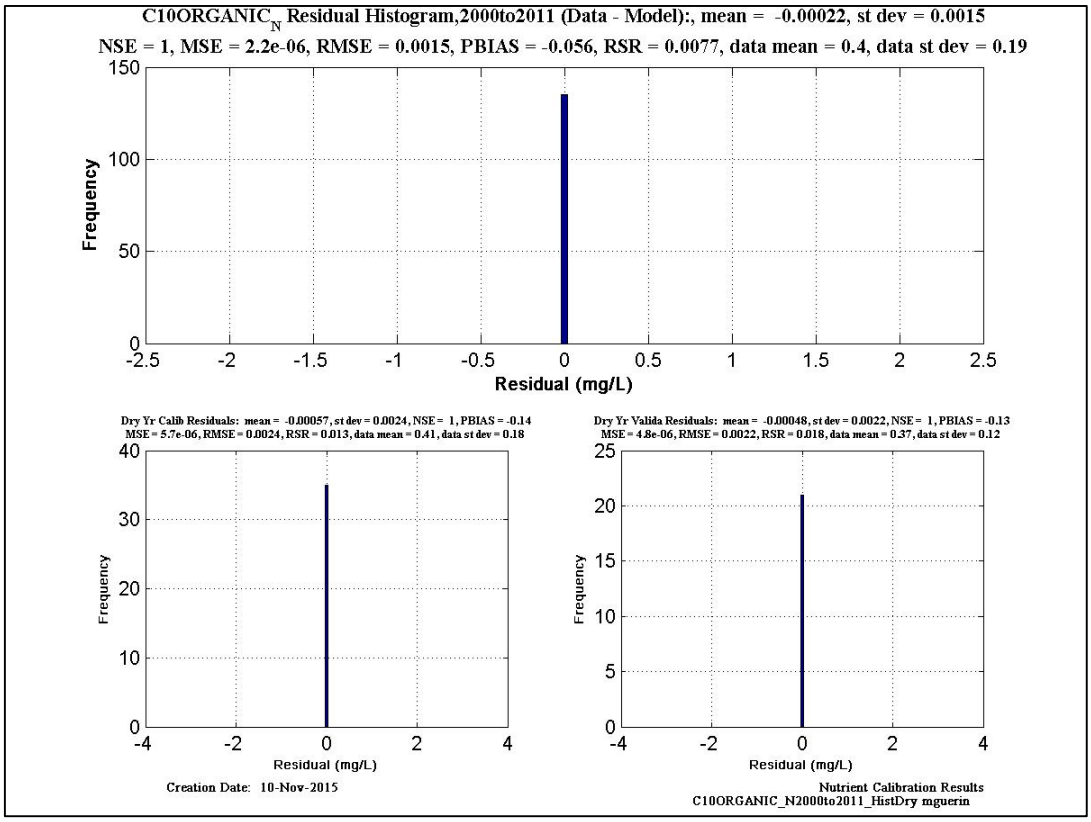

Figure 6-163 Organic-N histogram and statistics at EMP location C10.

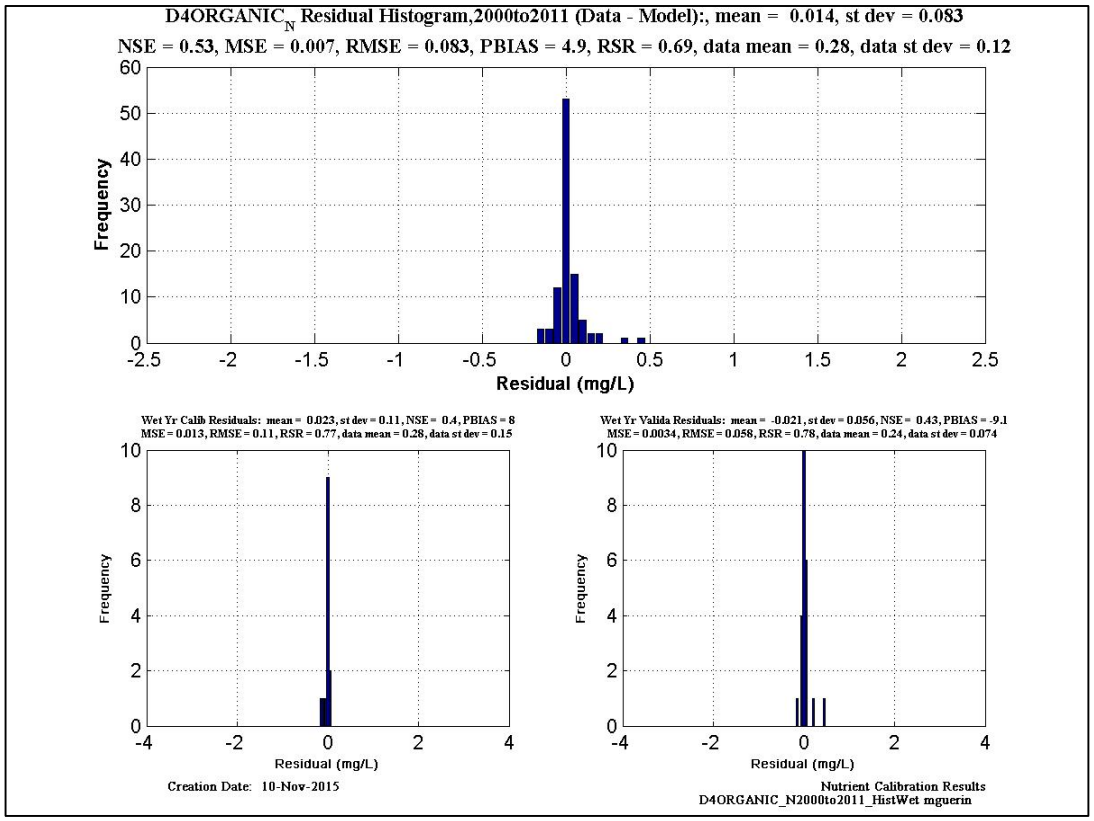

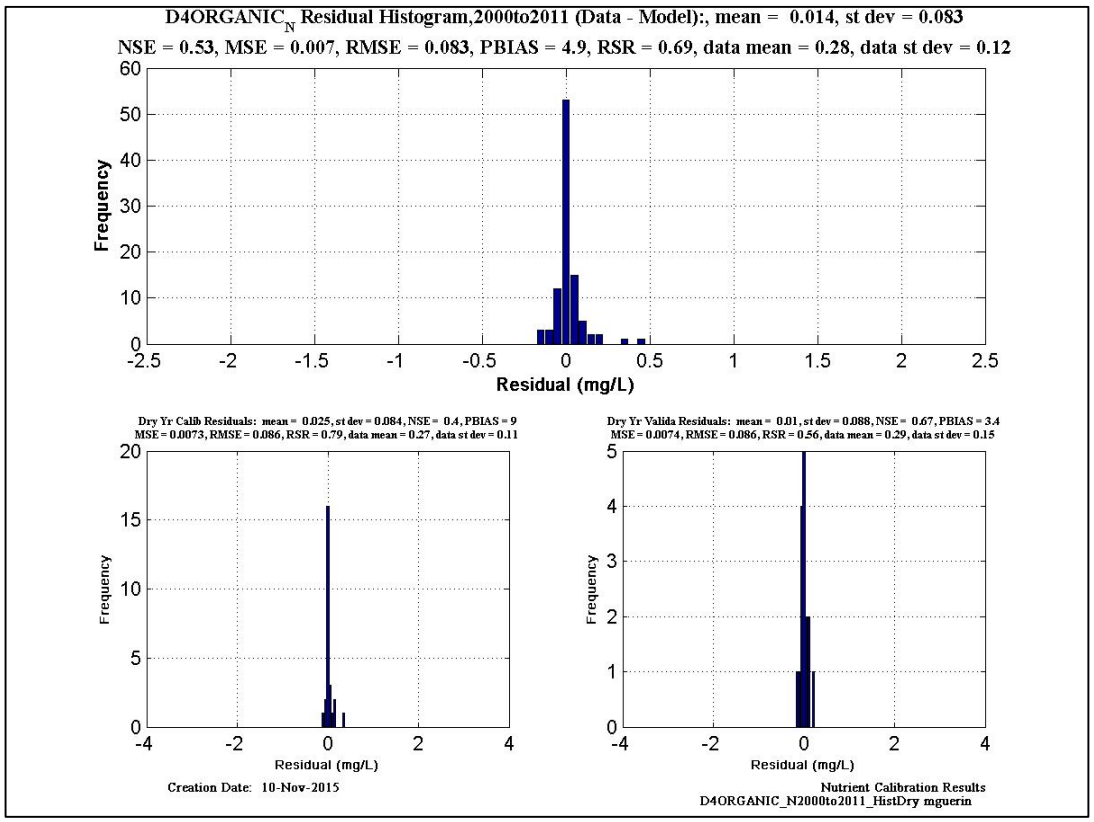

Figure 6-164 Organic-N histogram and statistics at EMP location D4.

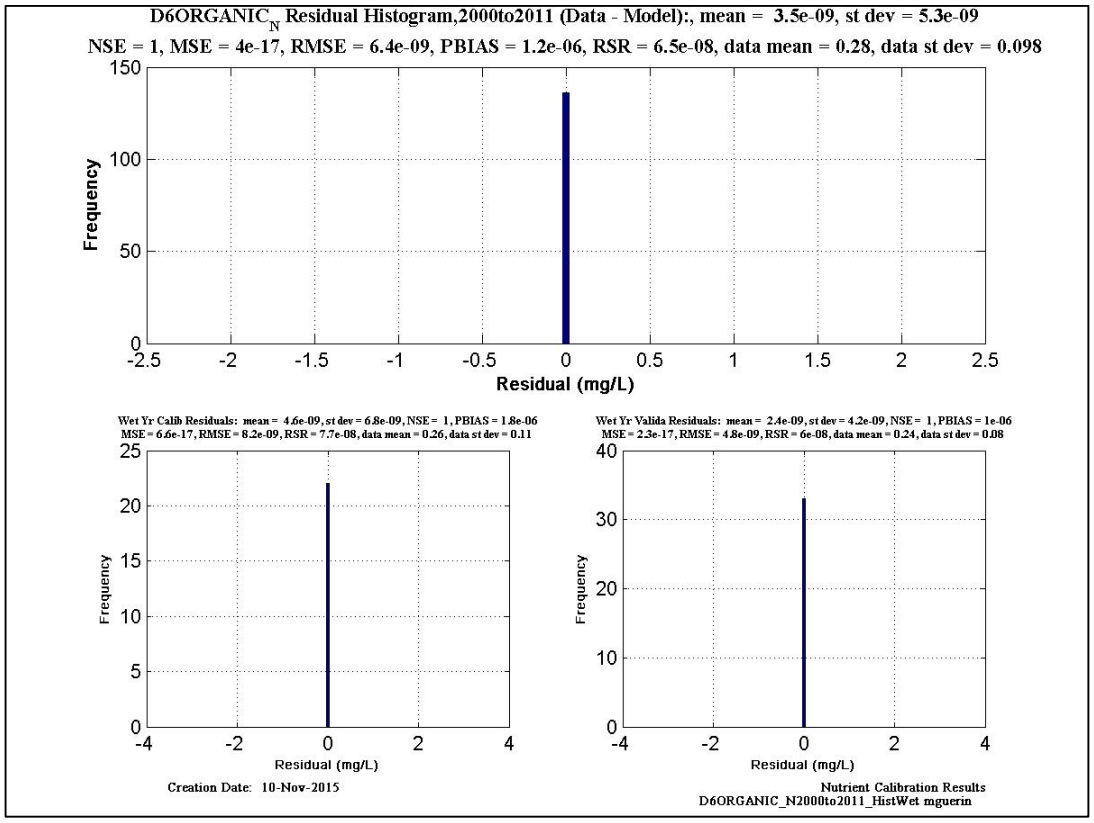

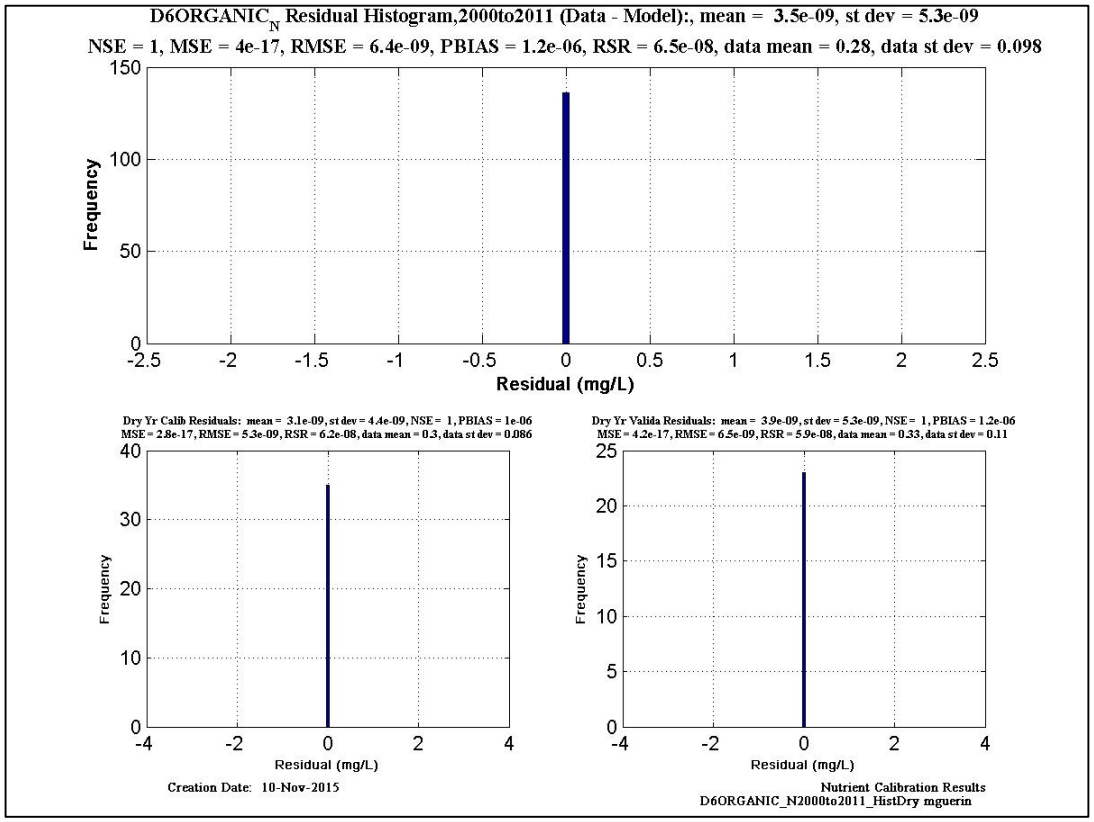

Figure 6-165 Organic-N histogram and statistics at EMP location D6.

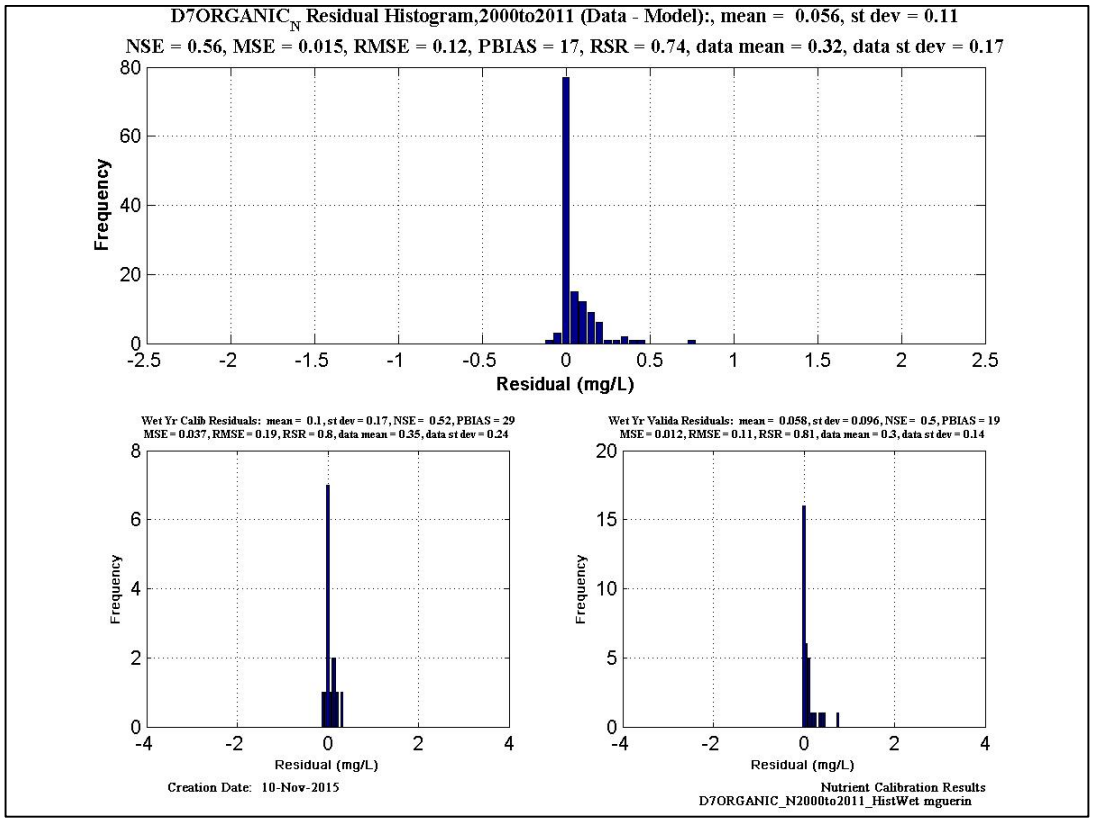

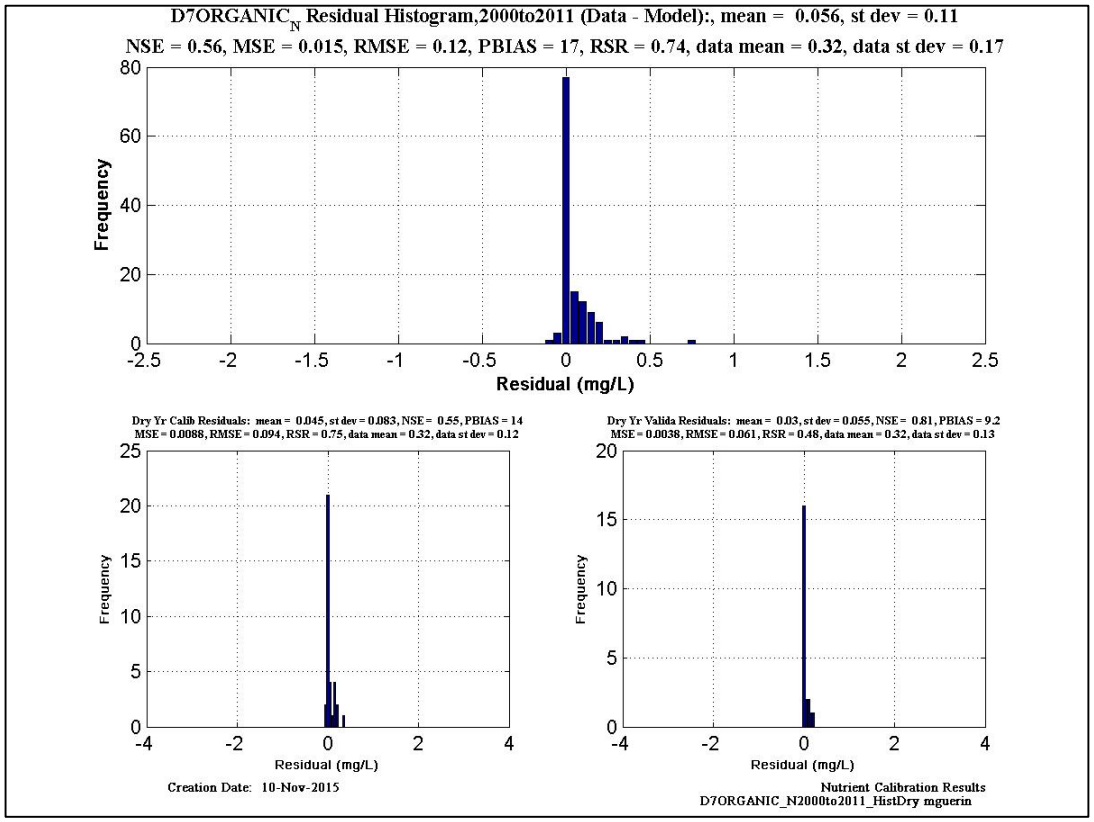

Figure 6-166 Organic-N histogram and statistics at EMP location D7.

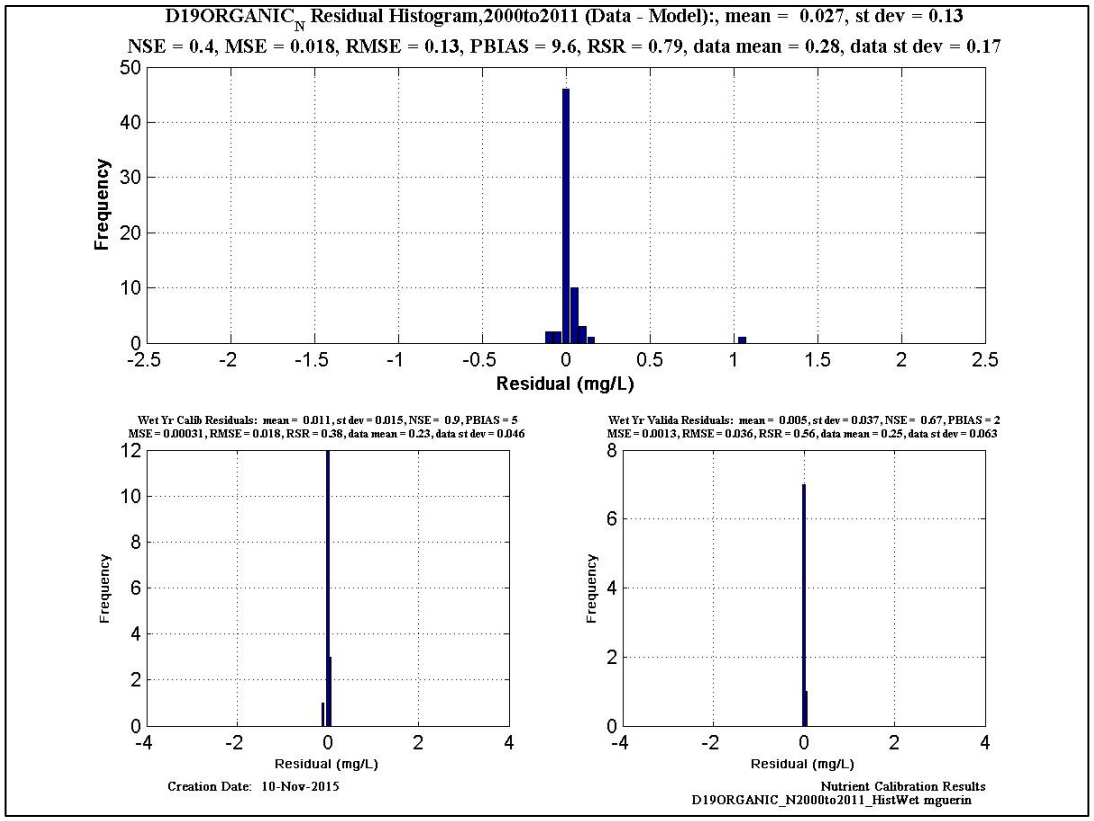

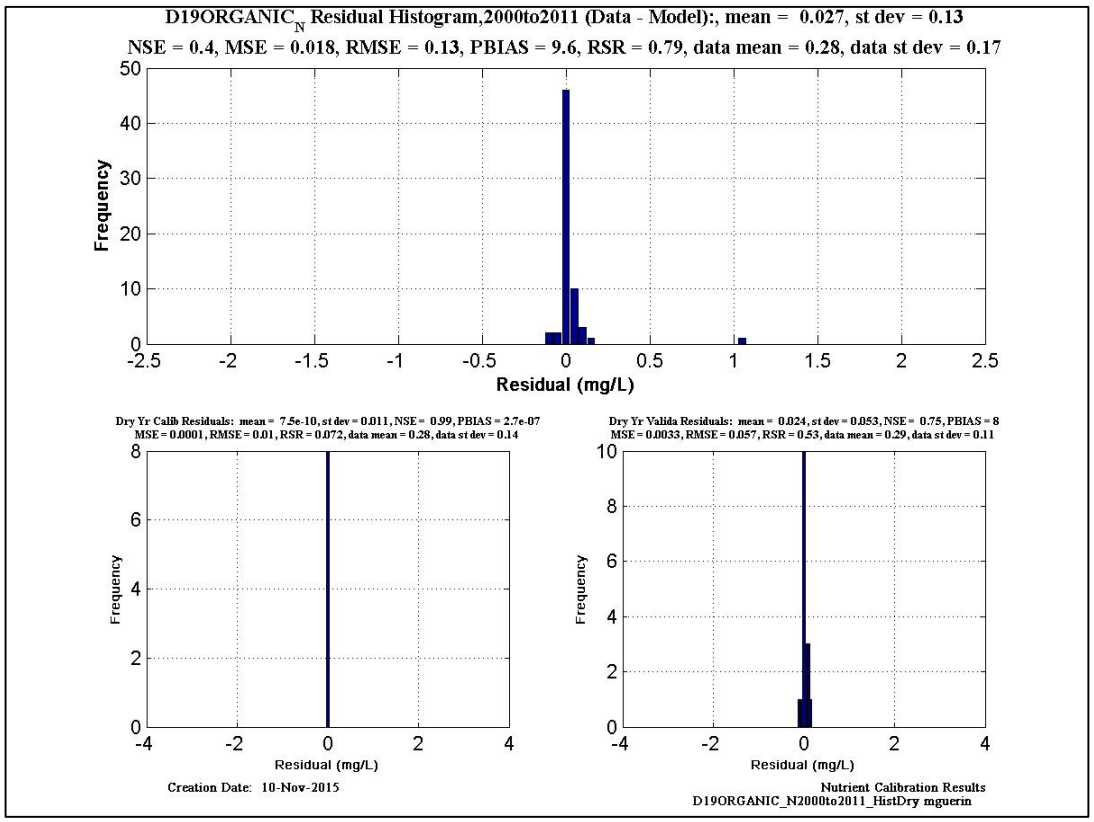

Figure 6-167 Organic-N histogram and statistics at EMP location D19.

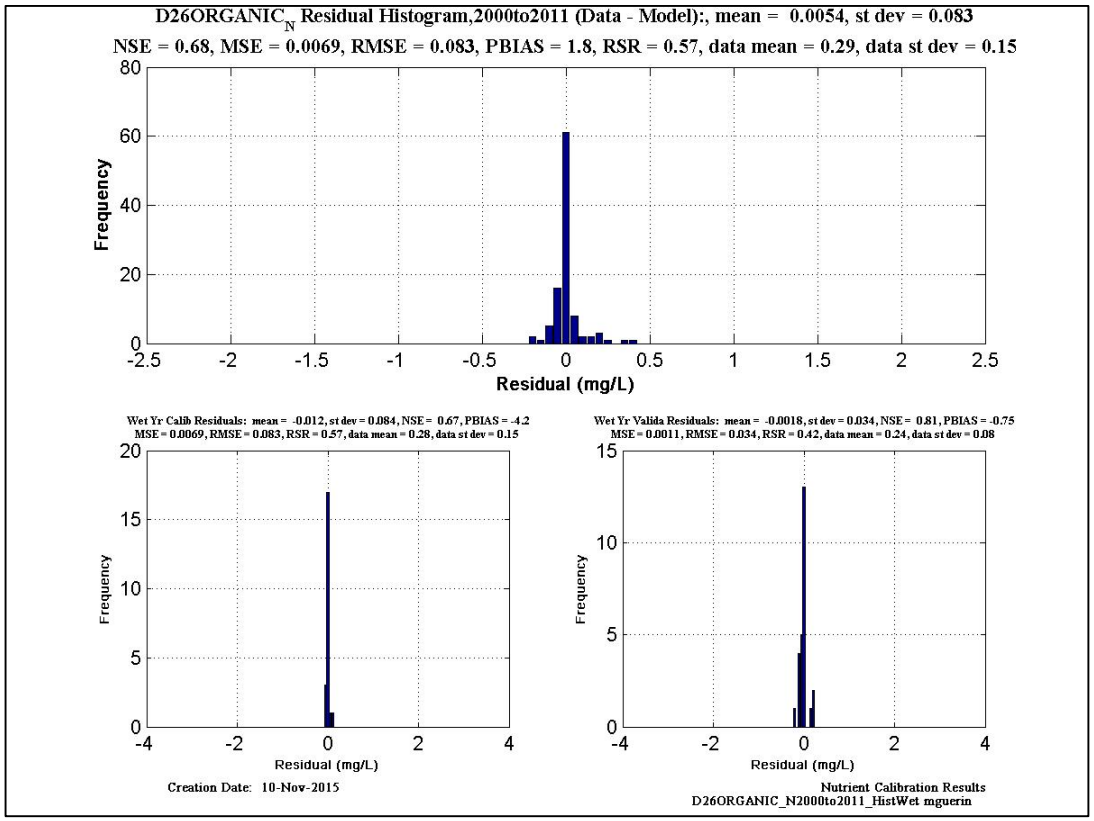

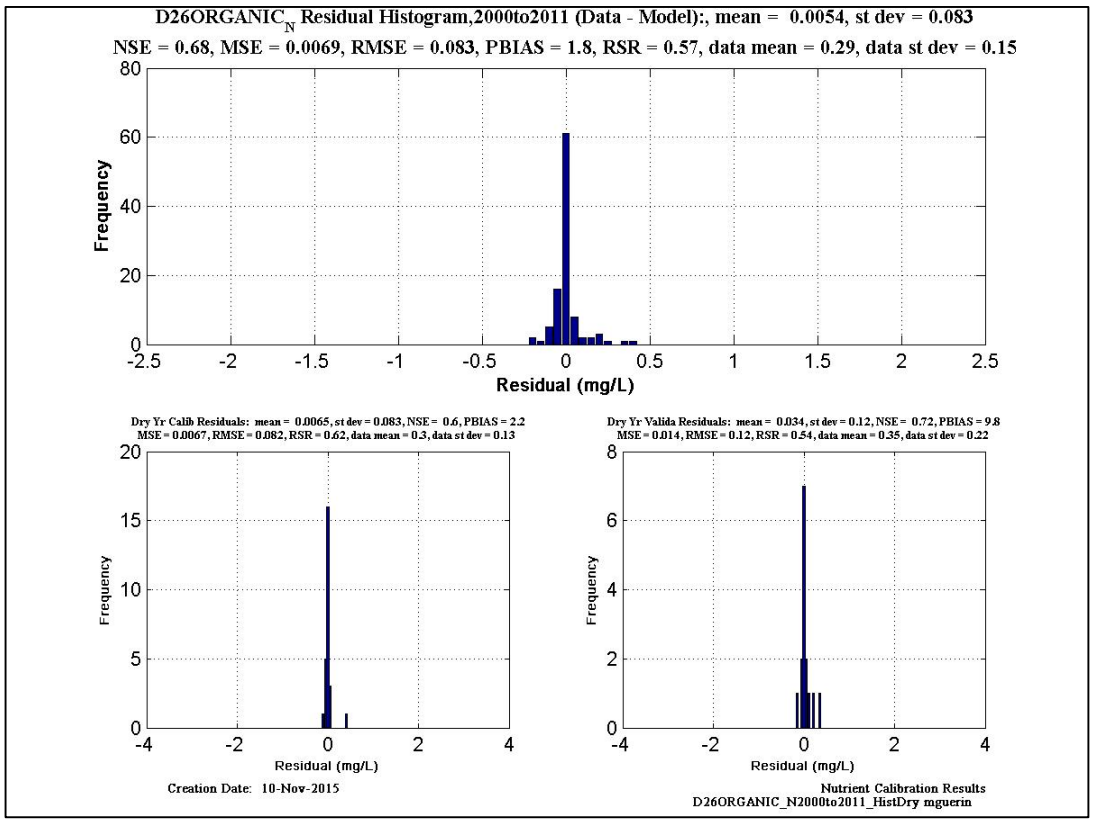

Figure 6-168 Organic-N histogram and statistics at EMP location D26.

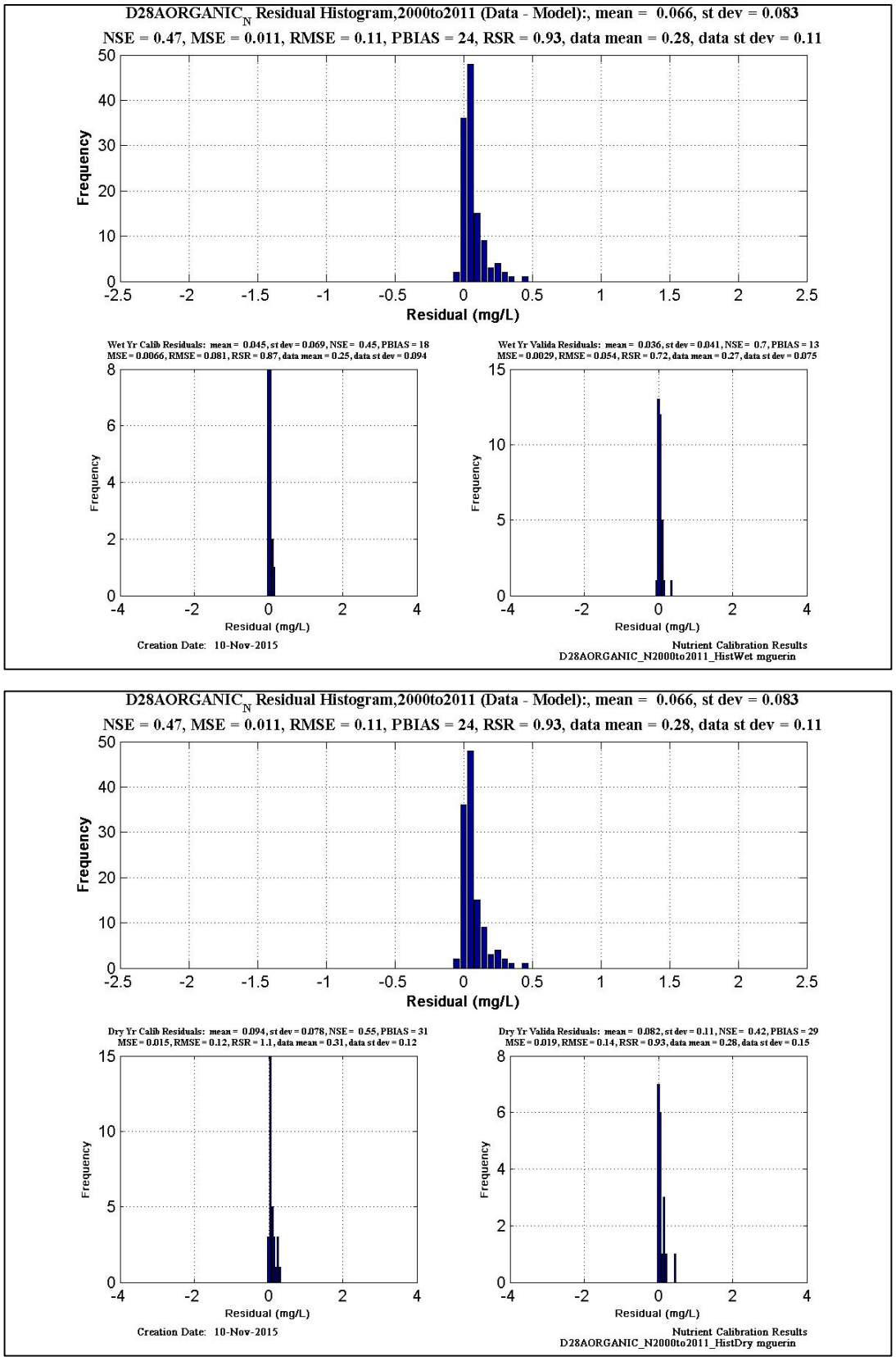

Figure 6-169 Organic-N histogram and statistics at EMP location D28A.

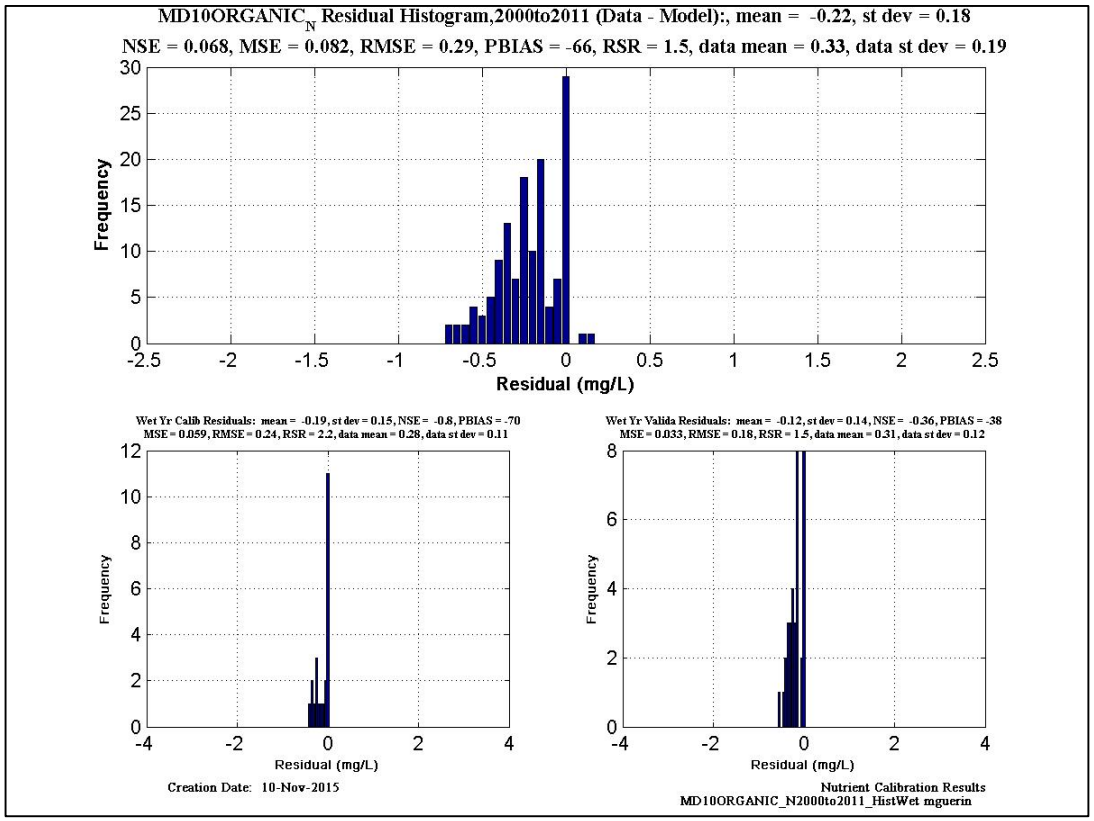

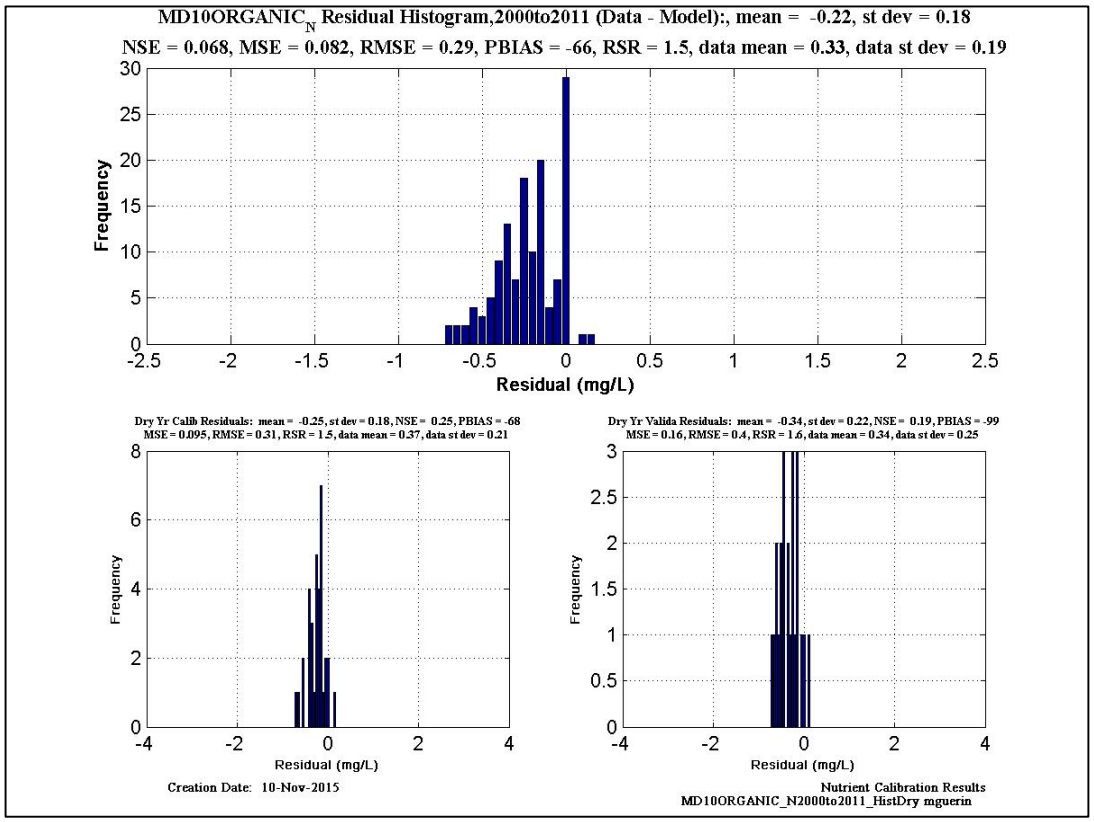

Figure 6-170 Organic-N histogram and statistics at EMP location MD10.

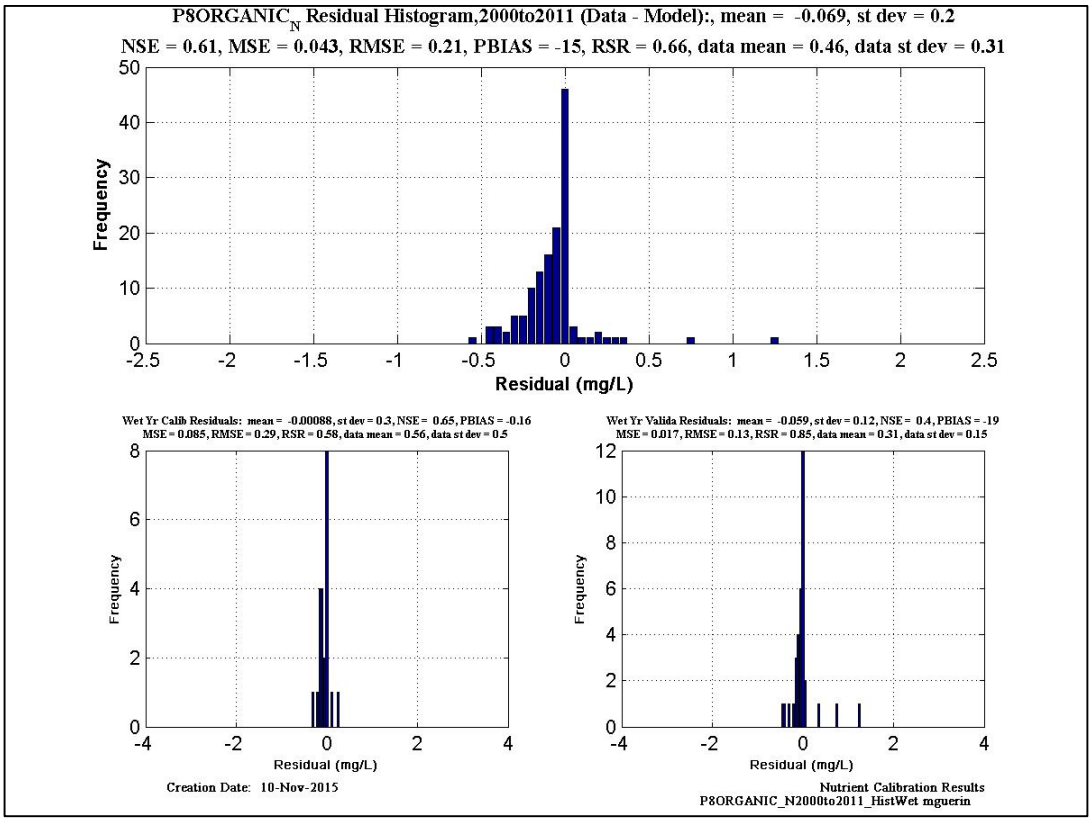

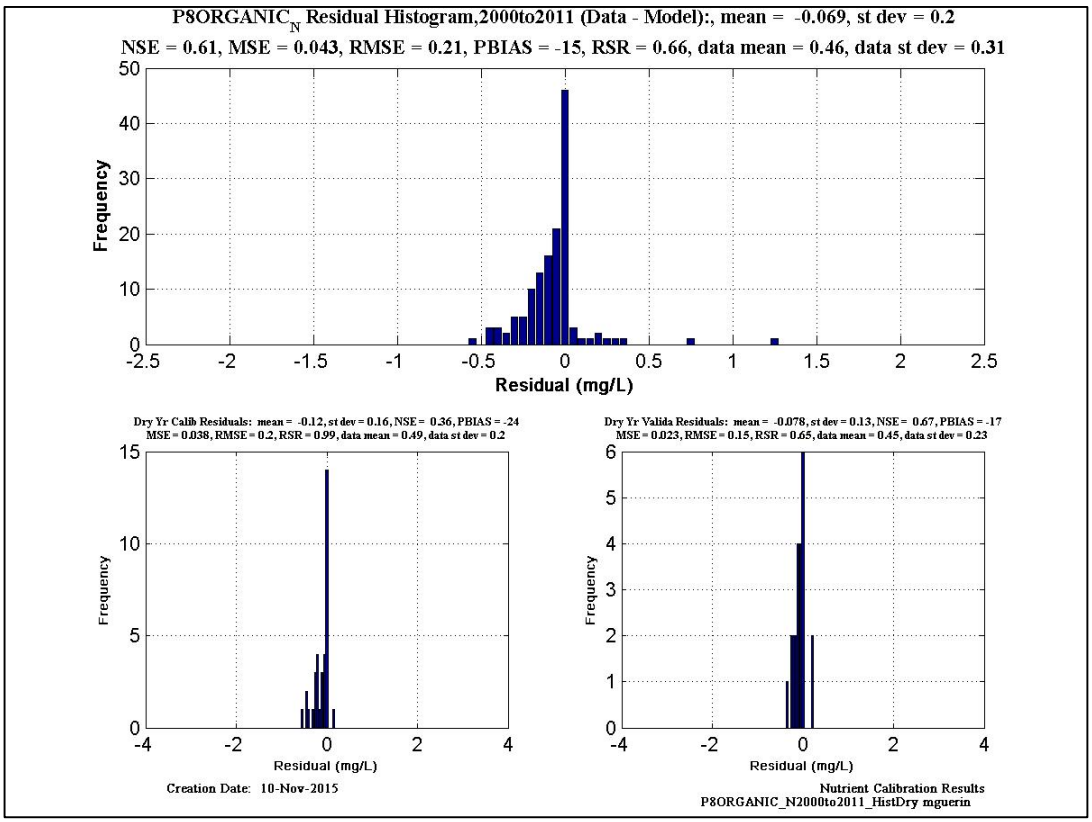

Figure 6-171 Organic-N histogram and statistics at EMP location P8.

6.12.4.6 Statistics for Modeled PO_4-P – EMP Data

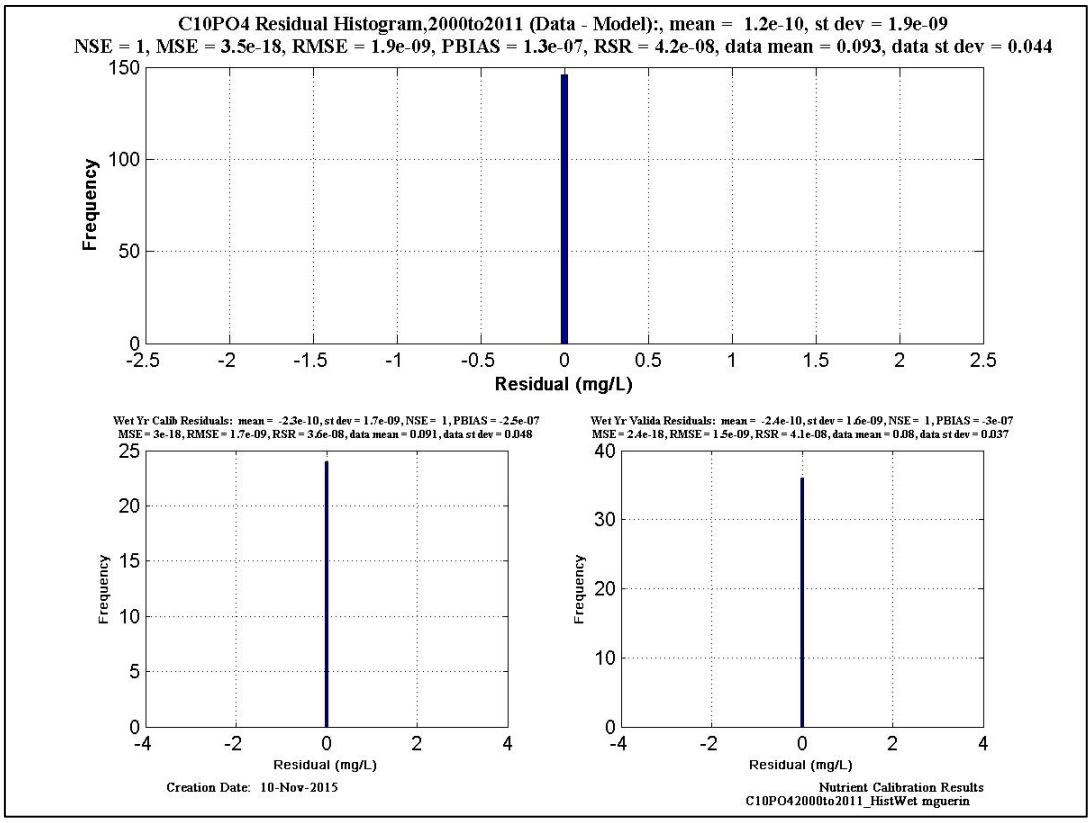

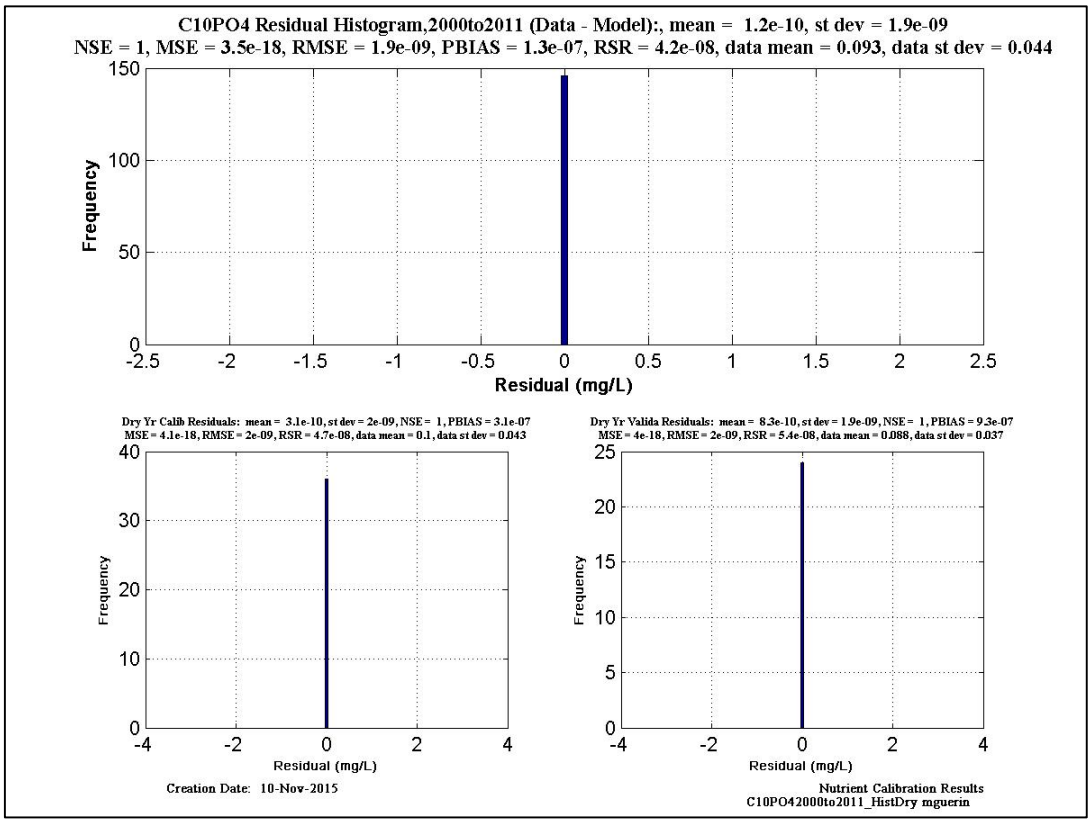

Figure 6-172 PO_4-P histogram and statistics at EMP location C10.

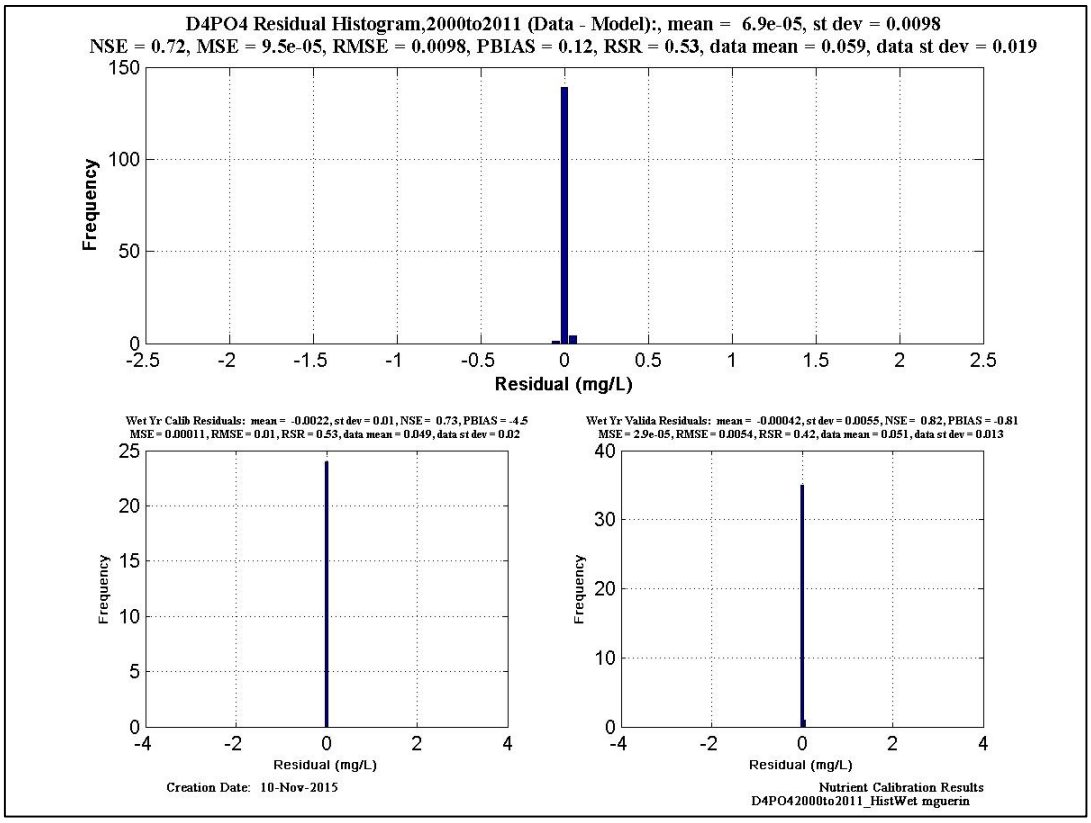

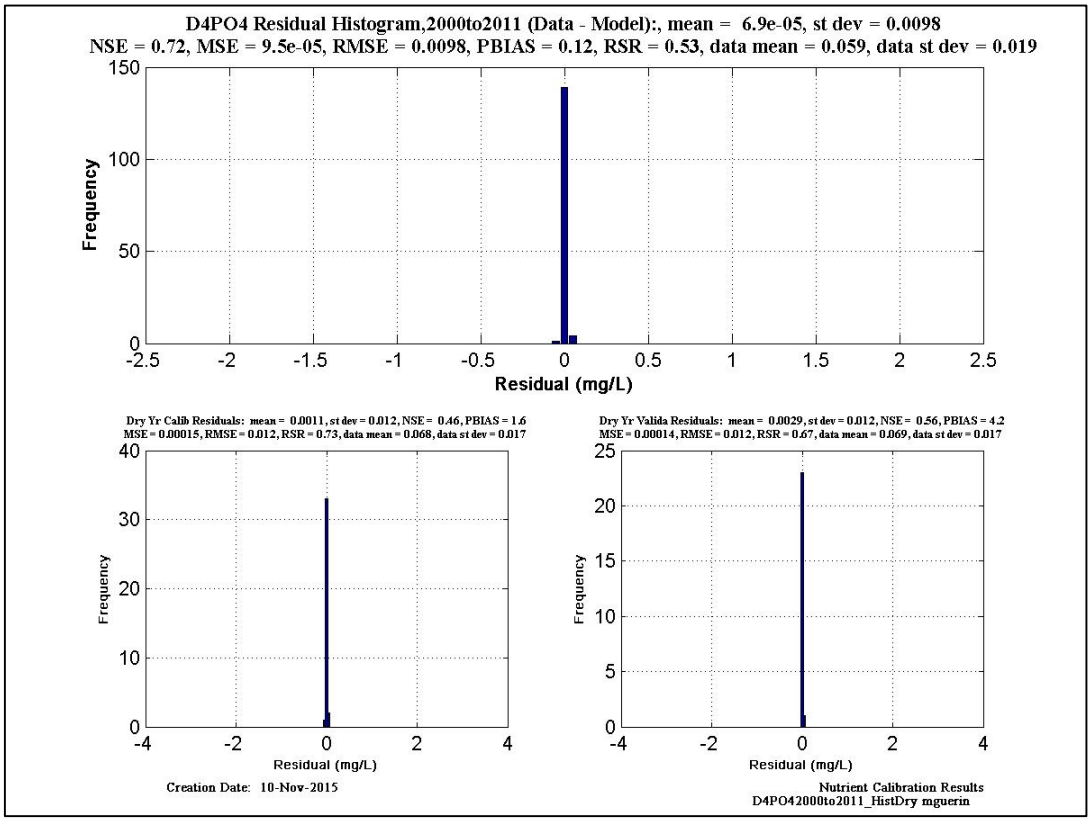

Figure 6-173 PO_4-P histogram and statistics at EMP location D4.

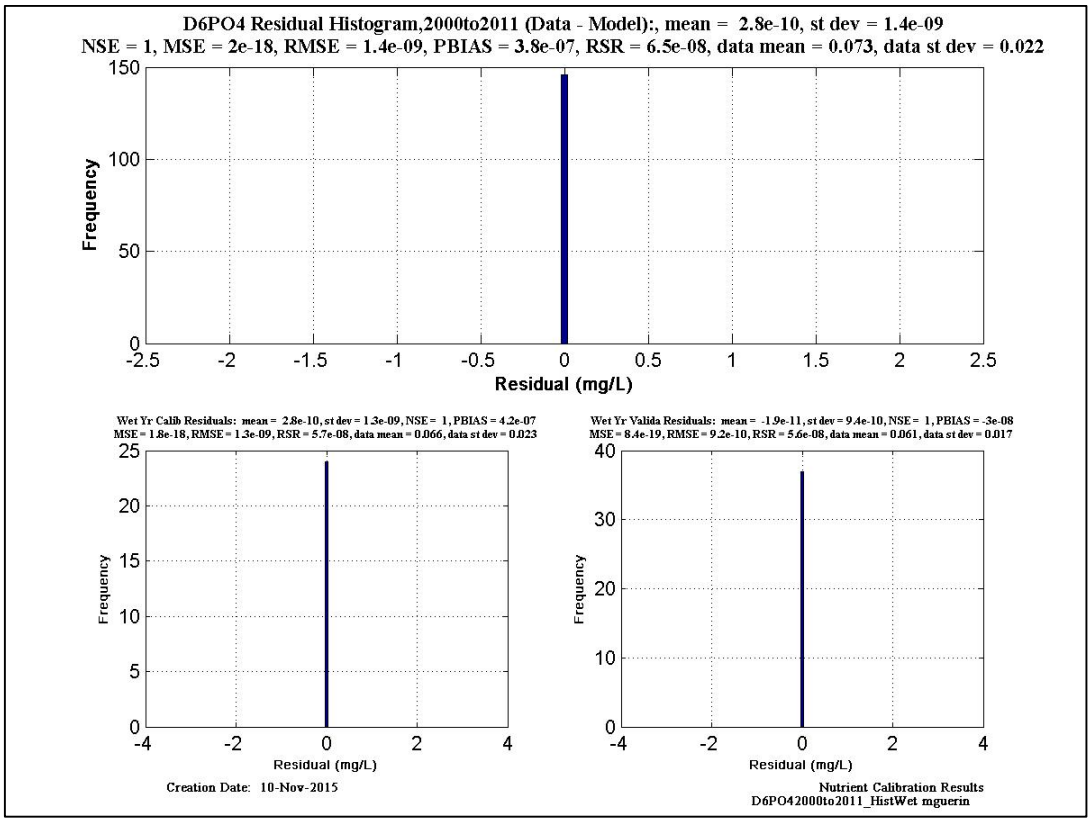

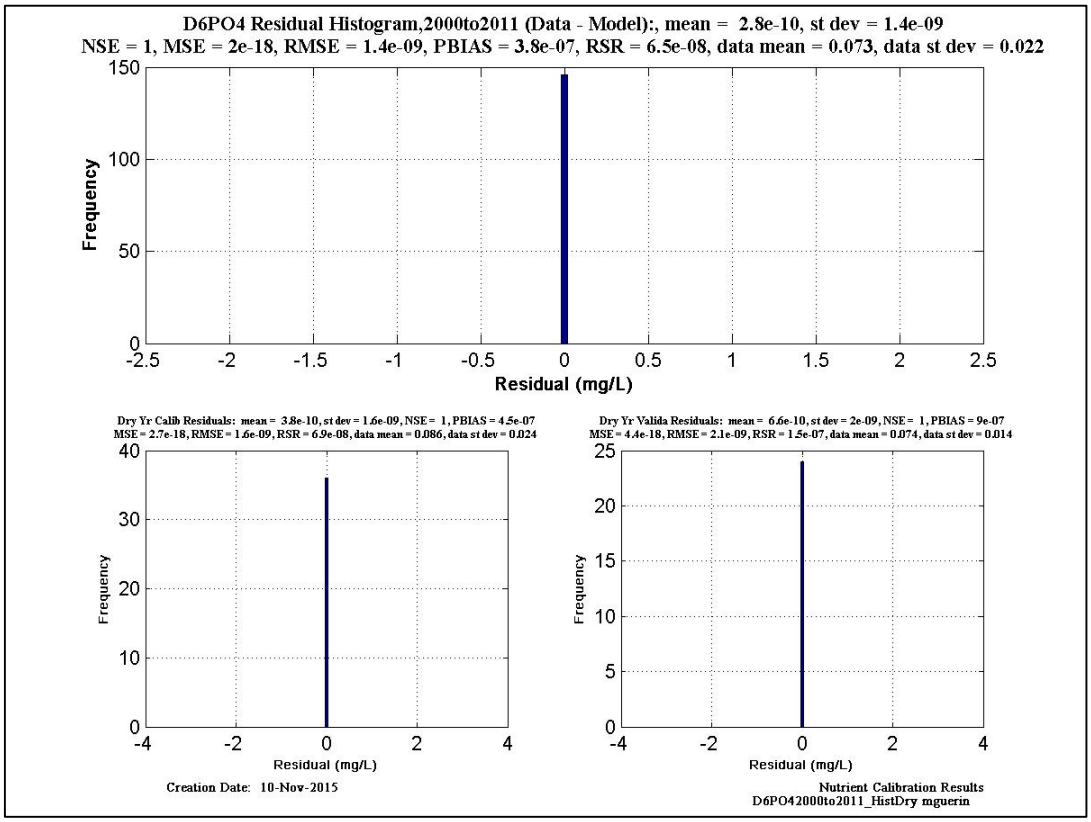

Figure 6-174 PO_4-P histogram and statistics at EMP location D6.

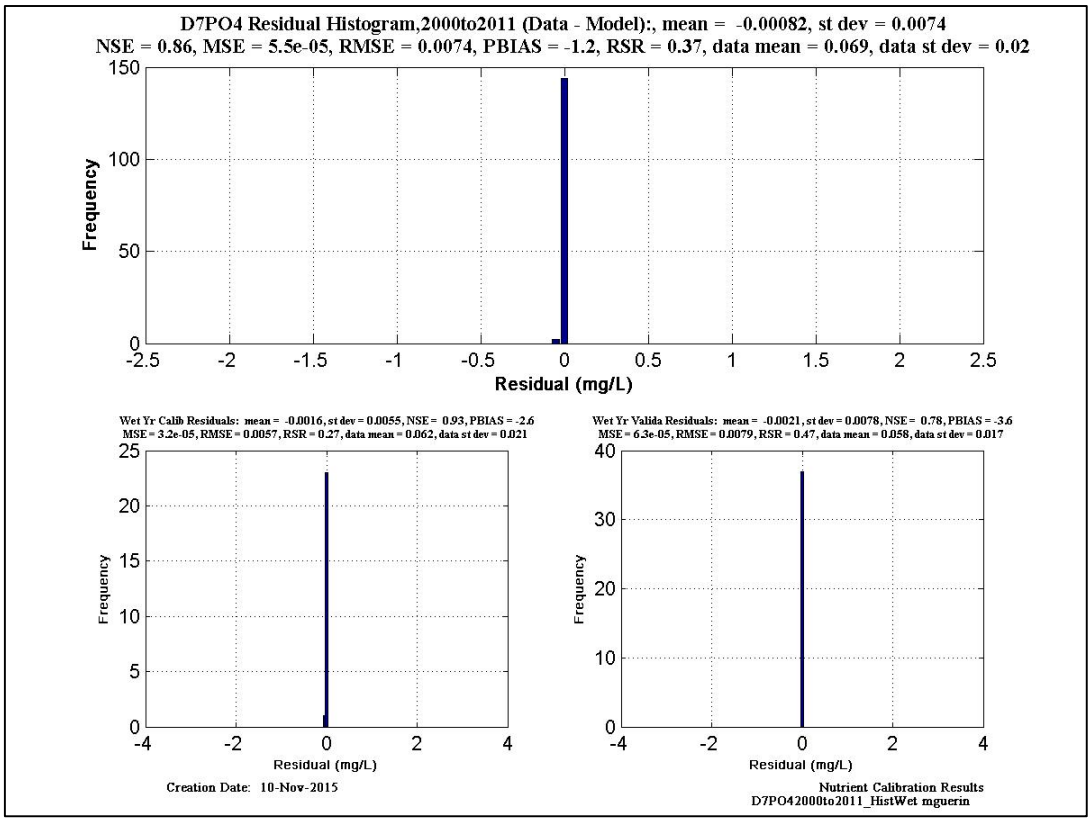

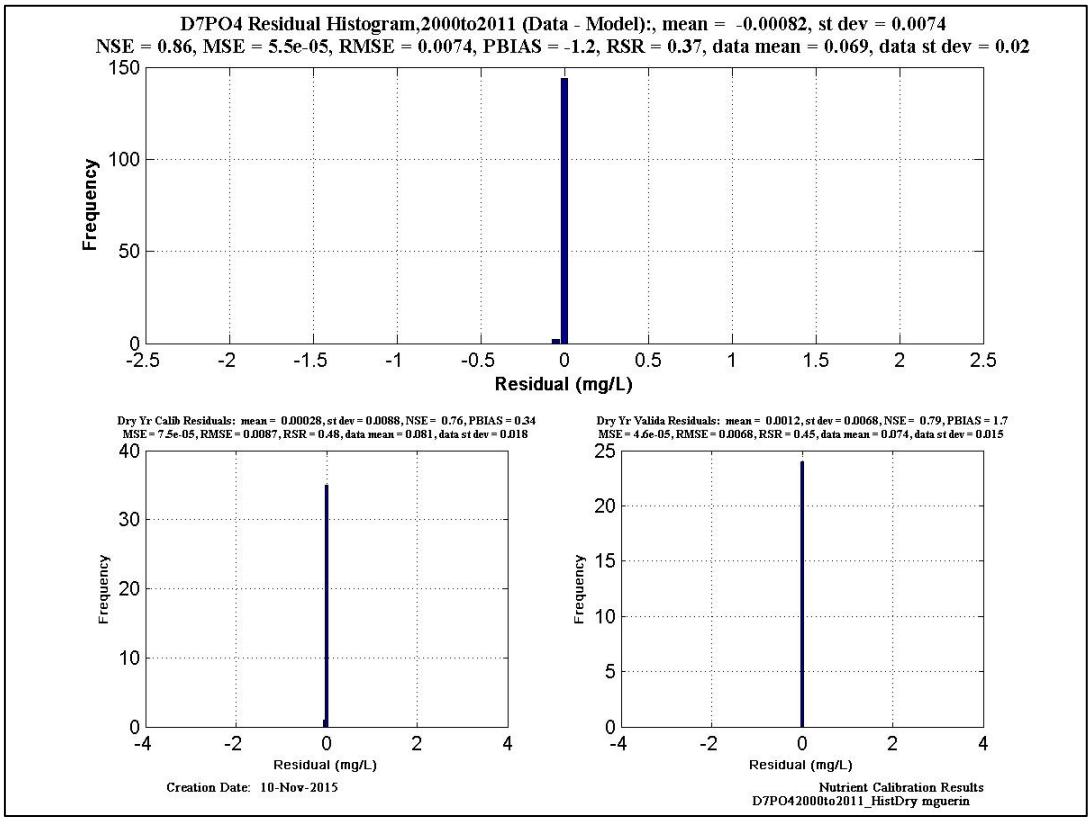

Figure 6-175 PO_4-P histogram and statistics at EMP location D7.

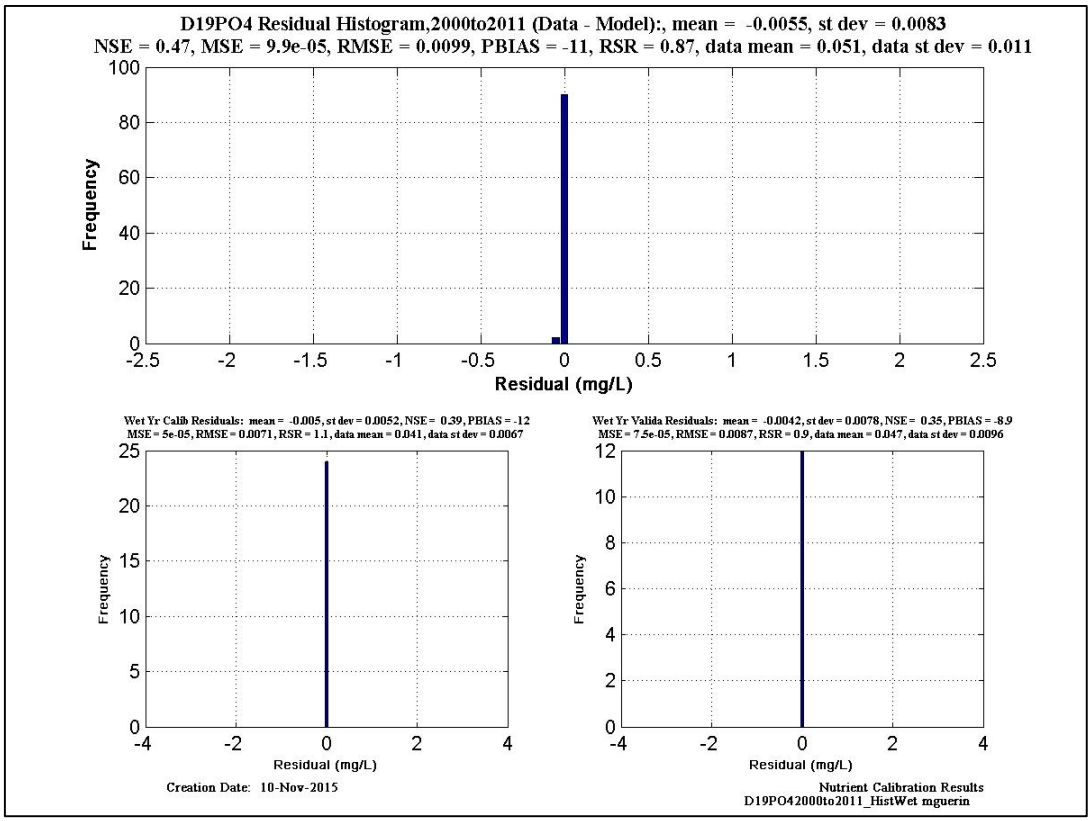

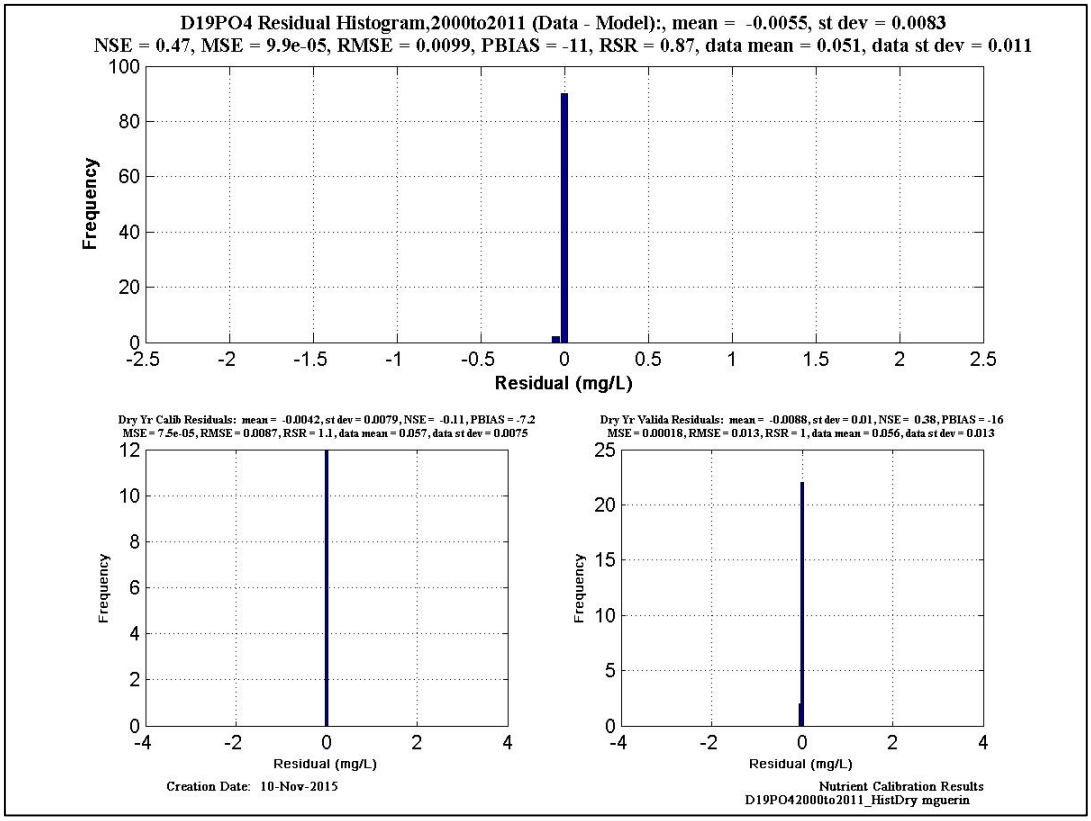

Figure 6-176 PO_4-P histogram and statistics at EMP location D19.

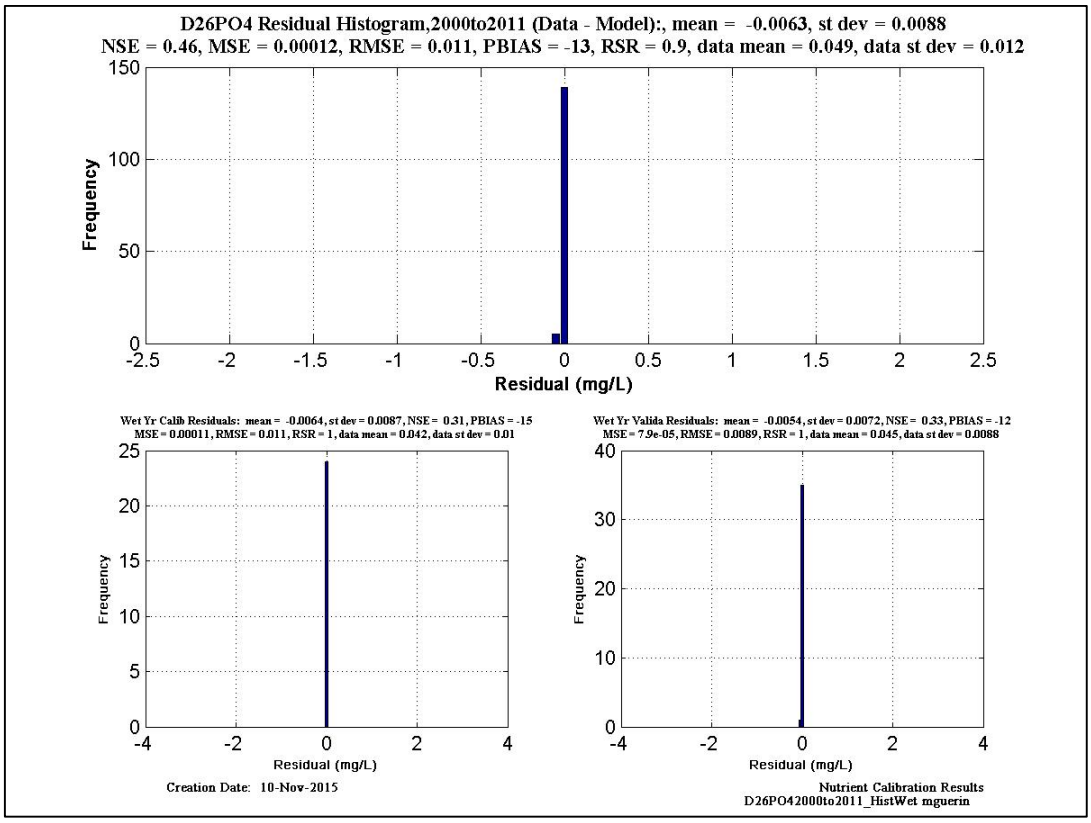

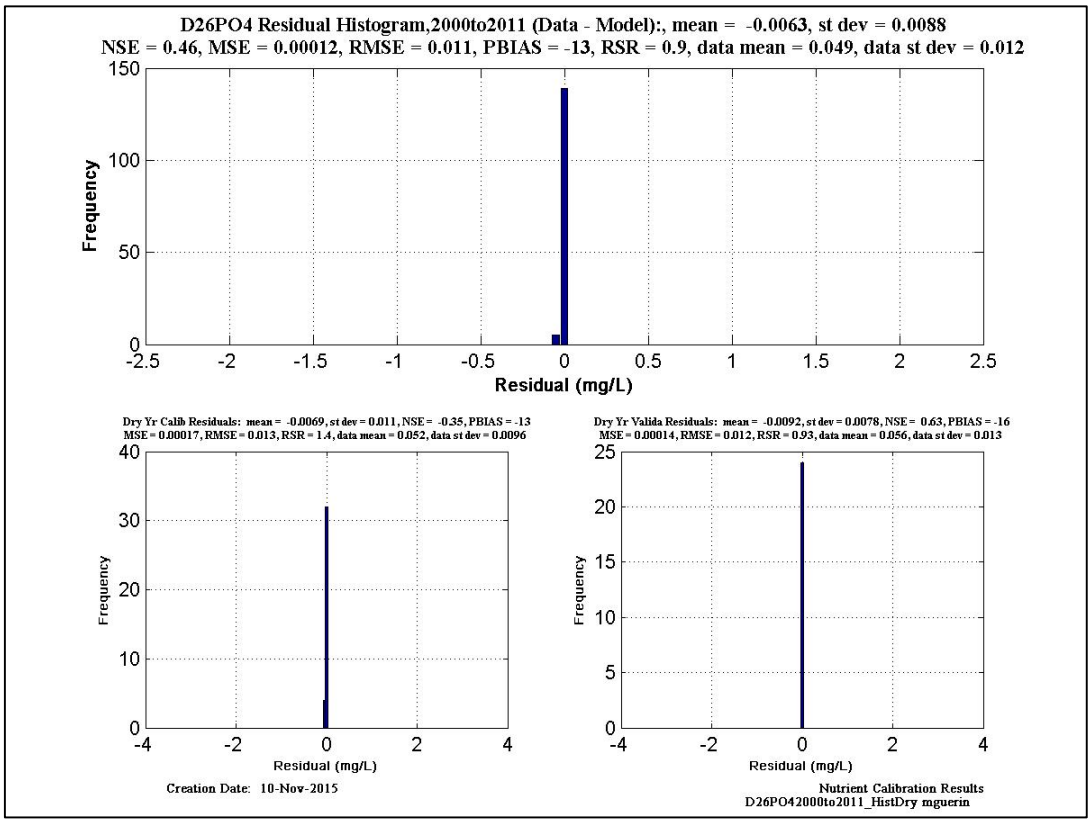

Figure 6-177 PO_4-P histogram and statistics at EMP location D26.

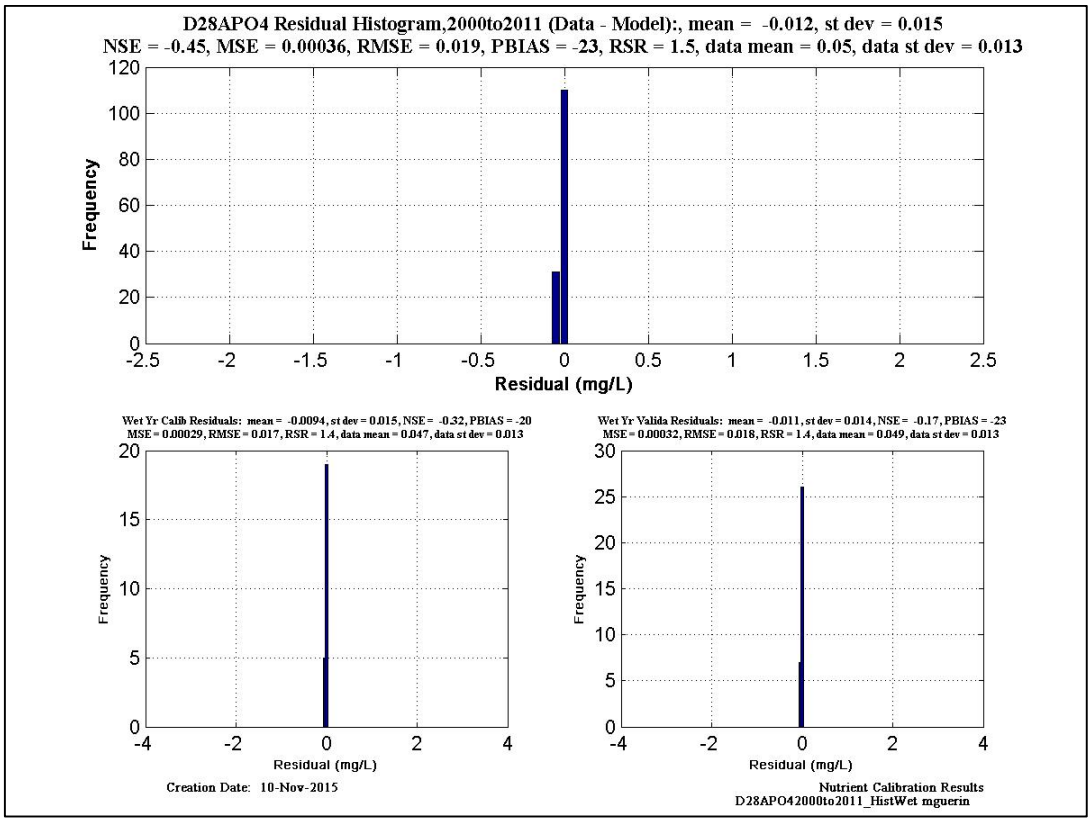

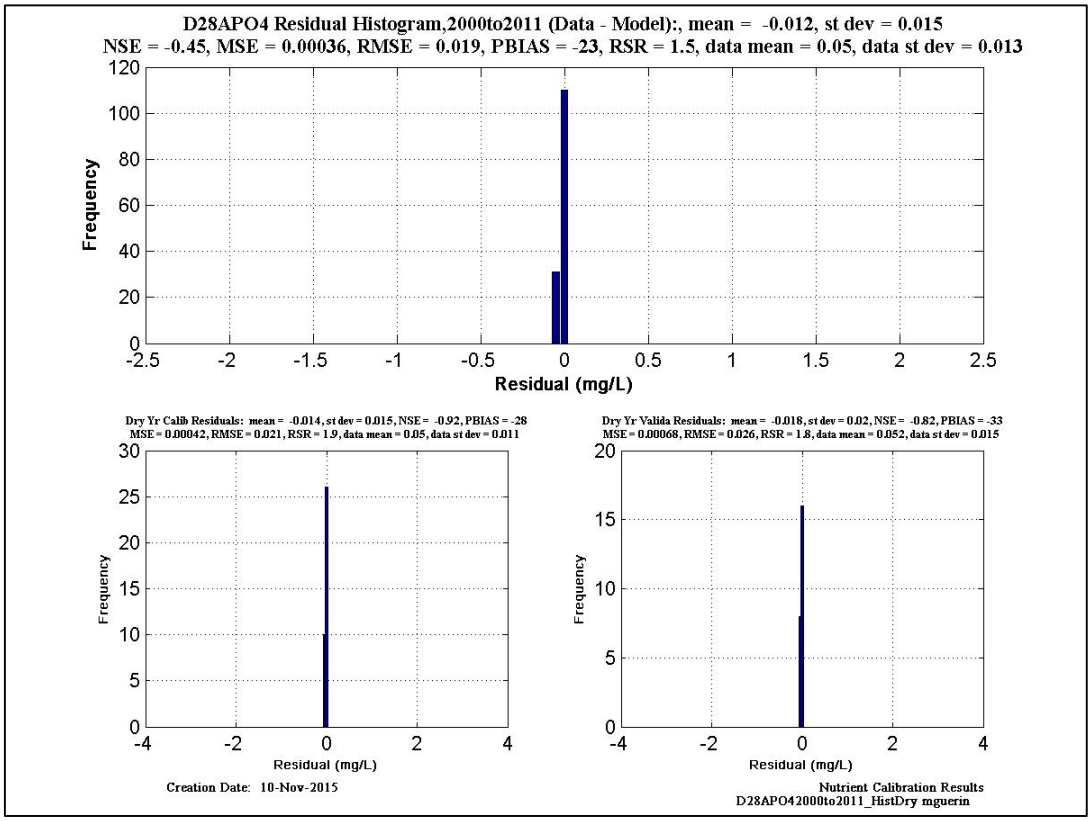

Figure 6-178 PO_4-P histogram and statistics at EMP location D28A.

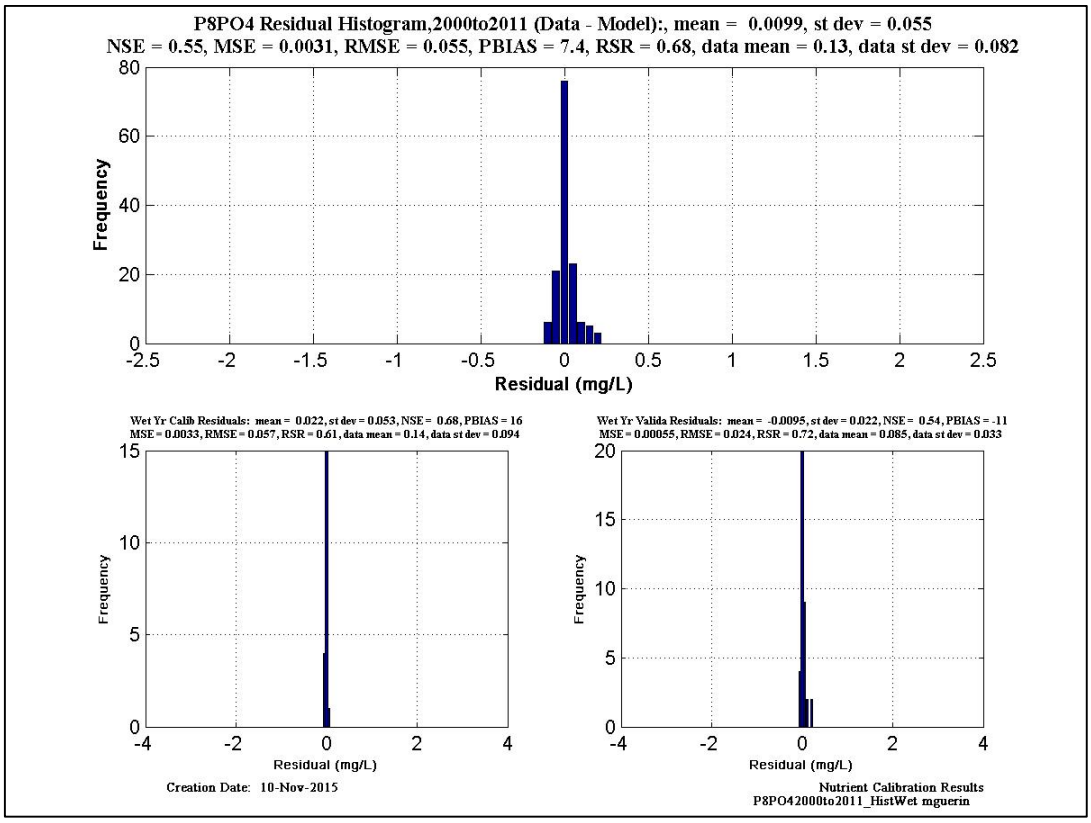

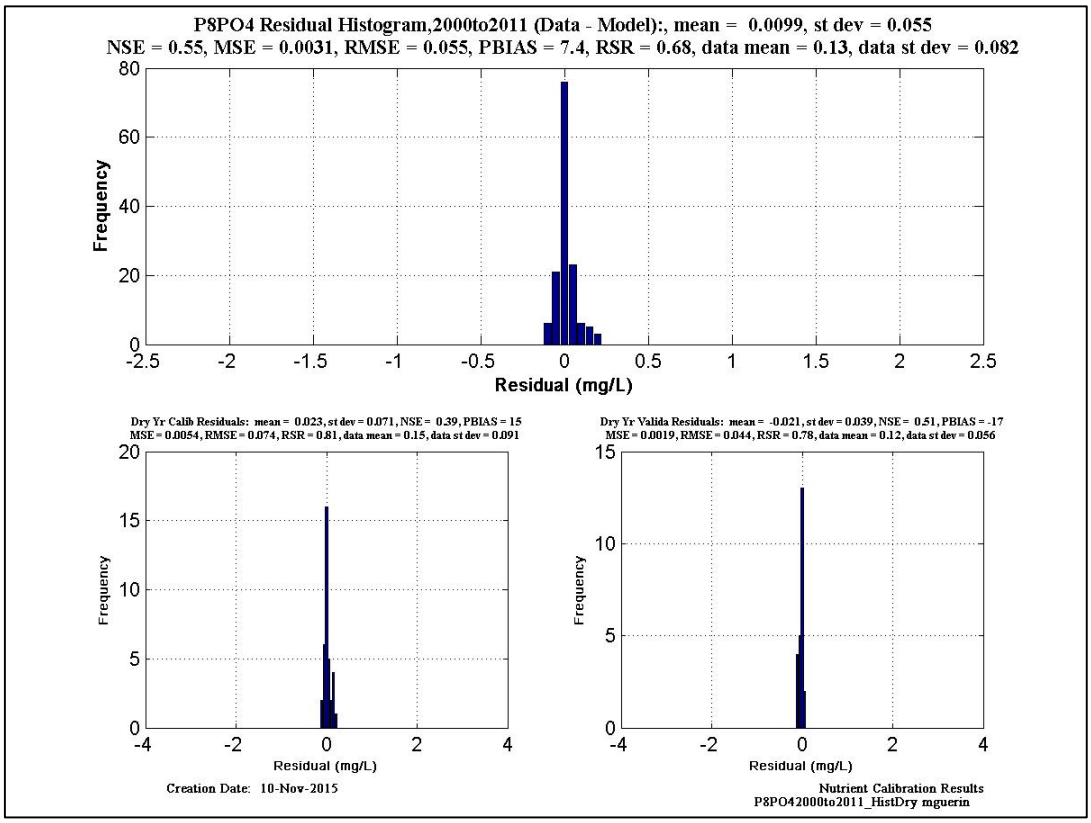

Figure 6-179 PO_4-P histogram and statistics at EMP location P8.